

KINETICS AND EQUILIBRIA
IN
AQUEOUS MEDIA

A Thesis submitted by

PHILIP P. DUCE

for the degree of

DOCTOR OF PHILOSOPHY

in the

FACULTY OF SCIENCE

of the

UNIVERSITY OF LEICESTER

Physical Chemistry Laboratory,
Department of Chemistry,
The University,
LEICESTER. LE1 7RH

August 1982

UMI Number: U334041

All rights reserved

INFORMATION TO ALL USERS

The quality of this reproduction is dependent upon the quality of the copy submitted.

In the unlikely event that the author did not send a complete manuscript and there are missing pages, these will be noted. Also, if material had to be removed, a note will indicate the deletion.



UMI U334041

Published by ProQuest LLC 2015. Copyright in the Dissertation held by the Author.
Microform Edition © ProQuest LLC.

All rights reserved. This work is protected against
unauthorized copying under Title 17, United States Code.



ProQuest LLC
789 East Eisenhower Parkway
P.O. Box 1346
Ann Arbor, MI 48106-1346



THESIS
661213
22.3.83

x752932224

STATEMENT

This thesis is based upon work conducted by the author, in the Department of Chemistry of the University of Leicester, during the period between October 1979 and April 1982.

All the work recorded in this thesis is original unless otherwise acknowledged in the text or by references. This work is not being presented for any other degree.

August 1982

PHILIP DUCE
University of Leicester

ACKNOWLEDGEMENTS

I am indebted to my supervisors, Dr. Mike Blandamer and Dr. John Burgess, for their abundant guidance, assistance, patience and encouragement throughout the period of this research.

I am grateful to Dr. Blandamer, Mr. J. Brivati and Mr. P. Acton for the considerable effort expended in the interfacing and maintenance of the minicomputer system.

Many thanks go to Miss V. Orson-Wright for her excellent and painstaking production of the typescript, and to Mrs. C. A. Crane for drawing most of the diagrams.

The award of a maintenance grant by the Science and Engineering Research Council is acknowledged.

To my Mother

'Now we see but a poor reflection;
then we shall see face to face.
Now I know in part;
then I shall know fully,
even as I am fully known.'

I Cor. xiii : 12

"Science is a very human form of knowledge. We are always at the brink of the known, we always feel forward for what is to be hoped. Every judgement in science stands on the edge of error, and is personal. Science is a tribute to what we can know, although we are fallible."

JACOB BRONOWSKI

CONTENTS

Page No.

Abbreviations

Publications

CHAPTER 1 - Background	1
CHAPTER 2 - Experimental details of collection and analysis of kinetic data.	30
CHAPTER 3 - Solvent effects on the kinetics of redox reactions in transition metal chemistry.	48
CHAPTER 4 - Solvent effects on the mercury(II)-catalysed aquation of chloro-transition metal complexes.	72
CHAPTER 5 - Reactions of anionic iron(II) tris-diimine complexes and diimine ligands with hydroxide and cyanide in aqueous media; kinetics and equilibria.	105
CHAPTER 6 - Initial state and transition state contributions to salt effects on kinetics in inorganic systems.	143
CHAPTER 7 - A re-examination of the solvent effect on the activation parameters for solvolysis of t-butyl chloride in aqueous solution.	181
CHAPTER 8 - Analysis of the temperature dependence of acid dissociation constants in water.	202
APPENDICES 1-6	224
REFERENCES	274

LIGAND ABBREVIATIONS

bdtps	2,4-bis(5,6-diphenyl-1,2,4-triazin-3-yl)pyridine tetrasulphonate
bipy	2,2'-bipyridyl
4CNpy	4-cyanopyridine
C ₂ O ₄	oxalate
dmgH	dimethylglyoximate
en	ethylene diamine
Et ₄ dien	N,N,N'',N'' tetraethyldiethylene triamine (3,9 diethyl-3,6,9-triazaundecane)
5NO ₂ phen	5-nitro-1,10-phenanthroline
phen	1,10-phenanthroline
ppsa (F _z)	3-(2-pyridyl)-5,6-diphenyl-1,2,4-triazine-p,p'- disulphonate ('Ferrozine')
py	pyridine
tu	thiourea

OTHER ABBREVIATIONS

DMSO	dimethylsulphoxide
EtOH	ethanol
i-PrOH	iso-propanol
is	initial state
MeCN	acetonitrile
MeOH	methanol
Nu	nucleophile
TA	typically aqueous
t-BuOH	tertiary-butanol
THF	tetrahydrofuran
TNAN	typically non-aqueous negative
TNAP	typically non-aqueous positive
ts	transition state

PUBLICATIONS

Publication of original work described in this thesis is as follows:

CHAPTER 3 Transition Metal Chem., 7, 10 (1982)

CHAPTER 4 Transition Metal Chem., 7, 183 (1982)
J. Inorg. Nucl. Chem., 43, 173 (1980)

CHAPTER 6 J. Chem. Soc. Dalton, 1809 (1980)
J. Inorg. Nucl. Chem., 43, 3103 (1980)

CHAPTER 7 J. Chem. Soc. Faraday 1, 77, 1999 (1981)

CHAPTER 8 Can. J. Chem., 59, 2845 (1981)
J. Chem. Soc. Faraday 1, 77, 2281 (1981)

CHAPTER 1

BACKGROUND

1.1 INTRODUCTION

The study of inorganic kinetics in binary aqueous media has two objectives. Studies of solvent and salt effects on the kinetics of reactions of known mechanism can lead to an understanding of stabilisation or destabilisation of the various reactants and hence to a rationalisation of reactivity changes in terms of solvation changes. It is also possible to gain an insight into structural properties of solvent systems. Conversely, known medium effects can be used to probe the reaction mechanism. The work in this thesis is largely concerned with the first of these approaches, though the second will be illustrated.

This chapter falls into four sections:

- (i) a description of the properties of water and aqueous mixtures with stress on the latter's thermodynamic properties;
- (ii) a survey of the types of reaction studied;
- (iii) analysis of kinetic data for reactions in solution;
- (iv) a short summary of the information which can emerge from such studies.

1.2 PROPERTIES OF WATER AND MIXED AQUEOUS SOLVENTS

1.2.1 Water

Water is unique among liquids. The literature concerning its experimental and theoretical study is vast and has been effectively reviewed and analysed by Franks.¹ The following comments are essential to subsequent discussion of aqueous solvent systems.

X-ray scattering, spectroscopic and thermodynamic properties confirm that in water a large proportion of the molecules are hydrogen-bonded together in an open, low density arrangement. Regions of water having this structure might be formed as a result of the co-operative nature of

hydrogen bonding. Thus, water might comprise clusters of open, low density hydrogen bonded water molecules, $(\text{H}_2\text{O})_b$, and dense non-hydrogen bonded water molecules $(\text{H}_2\text{O})_d$.² An equilibrium can then be written:



However, X-ray scattering data show that water does not exist as distinct patches of dense and bulky water. Consequently, considerable interest has been shown in interstitial models, where, for example, $(\text{H}_2\text{O})_d$ describes molecules which are guests in the $(\text{H}_2\text{O})_b$ system.

There are several advantages, particularly in the context of aqueous solutions, in representing water using equation [1.1]. Thus, to a first approximation, a solute which increases $(\text{H}_2\text{O})_b$ at the expense of $(\text{H}_2\text{O})_d$ is a structure former; a structure breaker has the opposite effect. The large heat capacity of water can be attributed to the need to 'melt' part of $(\text{H}_2\text{O})_b$ when the temperature is raised.

1.2.2 Chemical potentials

Under conditions of constant temperature and pressure, the appropriate thermodynamic potential function for a closed system is the Gibbs free energy, G . In terms of independent variables we can write

$$G = G [T, p, n_i] \quad \dots [1.2]$$

where T = temperature
 p = pressure
 n_i = no. of moles of component i

The general differential of equation [1.2] is written as follows:

$$dG = \left(\frac{\partial G}{\partial T} \right)_{p, n_i} dT + \left(\frac{\partial G}{\partial p} \right)_{T, n_i} dp + \sum_{j=1}^i \left(\frac{\partial G}{\partial n_j} \right)_{T, p, n_{i \neq j}} dn_j \quad \dots [1.3]$$

The chemical potential, μ , of component j is defined as:

$$\mu_j = \left(\frac{\partial G}{\partial n_j} \right)_{T,p,n_{i \neq j}} \quad \dots [1.4]$$

Hence

$$G = \sum_{j=1}^i n_j \mu_j \quad \dots [1.5]$$

1.2.3 Chemical potentials and composition

(i) Binary aqueous mixtures:

A mixture of two liquid non-electrolytes can be defined as ideal if the chemical potentials obey the following equations:

$$\mu_1 = \mu_1^\bullet + RT \ln x_1 \quad \dots [1.6]$$

$$\mu_2 = \mu_2^\bullet + RT \ln x_2$$

where μ_i^\bullet = the chemical potential of pure i at the same T and p

x_i = mole fraction of component i.

For real mixtures we write

$$\mu_1 = \mu_1^\bullet + RT \ln a_1 \quad \dots [1.7]$$

$$\mu_2 = \mu_2^\bullet + RT \ln a_2$$

Here a_i is the activity, where

$$a_i = x_i f_i \quad \dots [1.8]$$

f_i is the rational activity coefficient, $f_i \rightarrow 1$ as $x_i \rightarrow 1$.

(ii) Solutions:

The component in large excess is called the solvent, component 1.

The component present in small amounts is called the solute, component 2.

Three different equations are used to express the chemical potential of the solvent:

$$a) \quad \mu_1 = \mu_1^\bullet + RT \ln x_1 f_1 \quad \dots [1.9]$$

$$f_1 \rightarrow 1 \text{ as } x_1 \rightarrow 1$$

$$b) \quad \mu_1 = \mu_1^\bullet + g RT \ln x_1 \quad \dots [1.10]$$

rational osmotic coefficient $g=1$ in an ideal solution

$$c) \quad \mu_1 = \mu_1^\circ - \frac{\phi RT m_2 M_1}{1000} \quad \dots [1.11]$$

m_2 = molality of solute

M_1 = relative molecular mass of solvent

ϕ = practical osmotic coefficient = 1 in an ideal solution.

Equations for the chemical potential of a solute are based on a Henry's law type definition. Here we write

$$\mu_2 = \mu_2^\ominus + RT \ln a_2 \quad \dots [1.12]$$

Here the activity, a_2 , is given by

$$a_2 = m_2 \gamma_2$$

where m_2 = molality of the solute

γ_2 = activity coefficient

$\gamma_2 \rightarrow 1$ as $m_2 \rightarrow 0$, i.e. infinite dilution.

μ_2^\ominus is the chemical potential of the solute in a hypothetical solution at the same T and p where $m_2 = 1$ and $\gamma_2 = 1$.

Other Composition Scales can be used:

$$\mu_2 = \mu_2^\ominus + RT \ln c_2 \gamma_2 \quad \dots [1.13]$$

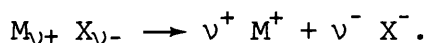
c_2 = concentration, mol dm⁻³ $\gamma_2 \rightarrow 1$ as $c_2 \rightarrow 0$

$$\text{or} \quad \mu_2 = \mu_2^\ominus + RT \ln x_2 f_2^* \quad \dots [1.14]$$

x_2 = mole fraction $f_2^* \rightarrow 1$ as $x_2 \rightarrow 0$.

(iii) Salt solutions:

It is convenient to define an expression for the activity of an electrolyte in terms of the ions into which it dissociates. Consider an electrolyte that dissociates as



We write as a definition

$$a_2 = a_+^{\nu^+} \cdot a_-^{\nu^-} = a_{\pm}^{\nu} \quad \dots [1.15]$$

a_{\pm} , the geometric mean of a_+ and a_- , is called the mean activity of the

ions. We also define individual ionic activity coefficients γ_+ and γ_- by

$$a_+ = \gamma_+ m_+ \quad a_- = \gamma_- m_- \quad \dots [1.16]$$

The experimentally measured activity coefficient is γ_{\pm} , the geometric mean of the individual ionic coefficients, where

$$\gamma_{\pm}^{\nu} = \gamma_+^{\nu_+} \cdot \gamma_-^{\nu_-} \quad \dots [1.17]$$

Equation [1.15] can then be written

$$a_2 = m_+^{\nu_+} \cdot m_-^{\nu_-} \cdot \gamma_+^{\nu_+} \cdot \gamma_-^{\nu_-} \quad \dots [1.18]$$

$$\text{or } a_{\pm} = a^{1/\nu} = \left(m_+^{\nu_+} \cdot m_-^{\nu_-} \cdot \gamma_+^{\nu_+} \cdot \gamma_-^{\nu_-} \right)^{1/\nu}$$

From [1.17] and [1.18] we obtain

$$\gamma_{\pm} = a_{\pm} / \left(m_+^{\nu_+} \cdot m_-^{\nu_-} \right)^{1/\nu} \quad \dots [1.19]$$

For a 1:1 salt of molality m ,

$$m_+ = \nu_+ m \quad \text{and} \quad m_- = \nu_- m.$$

From equation [1.19]

$$a_{\pm} = \gamma_{\pm} (m^2)^{1/2}$$

and from [1.15]

$$a_2 = a_{\pm}^2$$

$$\text{so } a_2 = m^2 \gamma_{\pm}^2$$

Hence, using equation [1.12]

$$\mu_2 = \mu_2^{\ominus} + 2 RT \ln m \gamma_{\pm}$$

1.2.4 Classification and properties of binary aqueous mixtures

Insights into the interactions between the two components in a binary solvent mixture can be obtained by considering the thermodynamic excess functions, X^E . These arise when one considers the mixing of the two components. For one mole of mixture, the Gibbs free energy of mixing at

fixed T and p is given by

$$\Delta_m G = x_1 \mu_1 + x_2 \mu_2 - x_1 \mu_1^\circ - x_2 \mu_2^\circ \quad \dots [1.20]$$

Combining [1.20] with [1.7] and [1.8] we obtain

$$\Delta_m G = RT x_1 \ln x_1 f_1 + RT x_2 \ln x_2 f_2 \quad \dots [1.21]$$

$\Delta_m G$ must be negative for mixing to occur at constant T and p.

It is convenient to define a set of excess functions, X^E , as

$$X^E = \Delta_m X - \Delta_m X (\text{ideal}) \quad \dots [1.22]$$

Then

$$G^E = RT \{x_1 \ln f_1 + x_2 \ln f_2\} \quad \dots [1.23]$$

This is positive or negative depending on the signs of the activity coefficients. Negative values of G^E indicate favourable interactions between the components of the mixture. Non-aqueous-component/water interactions are stronger than water/water interactions. Positive values of G^E indicate intercomponent interactions are weaker than those between two cosolvent molecules or two water molecules.

For an ideal mixture the enthalpy of mixing, $\Delta_m H$, and volume of mixing, $\Delta_m V$, are zero. So for a real mixture the excess functions are simply the mixing functions:

$$H^E = \Delta_m H \quad \dots [1.24]$$

$$V^E = \Delta_m V$$

The excess entropy is calculated from

$$S^E = (H^E - G^E)/T \quad \dots [1.25]$$

On the basis of these properties mixed aqueous solvents can be divided into three classes:

A) "Typically aqueous", TA: $G^E > 0$, $|TS^E| > |H^E|$.

In these cases, mixing is dominated by entropy changes.

B) "Typically non-aqueous": $|H^E| > |TS^E|$.

In these cases, mixing is enthalpy dominated. Two sub-divisions of

this class can be identified:

- (i) $G^E > 0$; TNAP mixtures.
- (ii) $G^E < 0$; TNAN mixtures.

(i) Typically aqueous mixtures

Cosolvents forming TA mixtures with water include monohydric alcohols, acetone, dioxan and tetrahydrofuran. Figure (1.1) shows plots of the excess functions against mole fraction for ethanol-water and t-butanol-water.

The dependence of X^E on mole fraction can be analysed to obtain the corresponding partial molar quantities, $(X_1 - X_1^\bullet)$ and $(X_2 - X_2^\bullet)$. Figure (1.2) shows the variation of the partial molar volumes for some TA systems, and this diagram identifies three types of behaviour:

- a) negative slope at low mole fractions: this implies "structure-making". Water-water interactions are enhanced producing a clathrate¹ type structure around the hydrophobic alkyl group. An exothermic H^E can be identified with this behaviour.
- b) zero slope with $(V_1 - V_1^\bullet)$ negative: no structural effects. The point is reached where the proportion of water in the mixture is insufficient to maintain the clathrate structure.
- c) positive slope: "structure breaking". As x_2 is increased the extended structure is broken down. The tendency for phase separation is most marked at these mole fractions.

Many properties of TA mixtures show extrema and the points at which they occur on the mole fraction scale can act as 'signposts' in the analysis of kinetic results.

(ii) Typically non-aqueous negative mixtures

Cosolvents forming this type of mixture with water include hydrogen

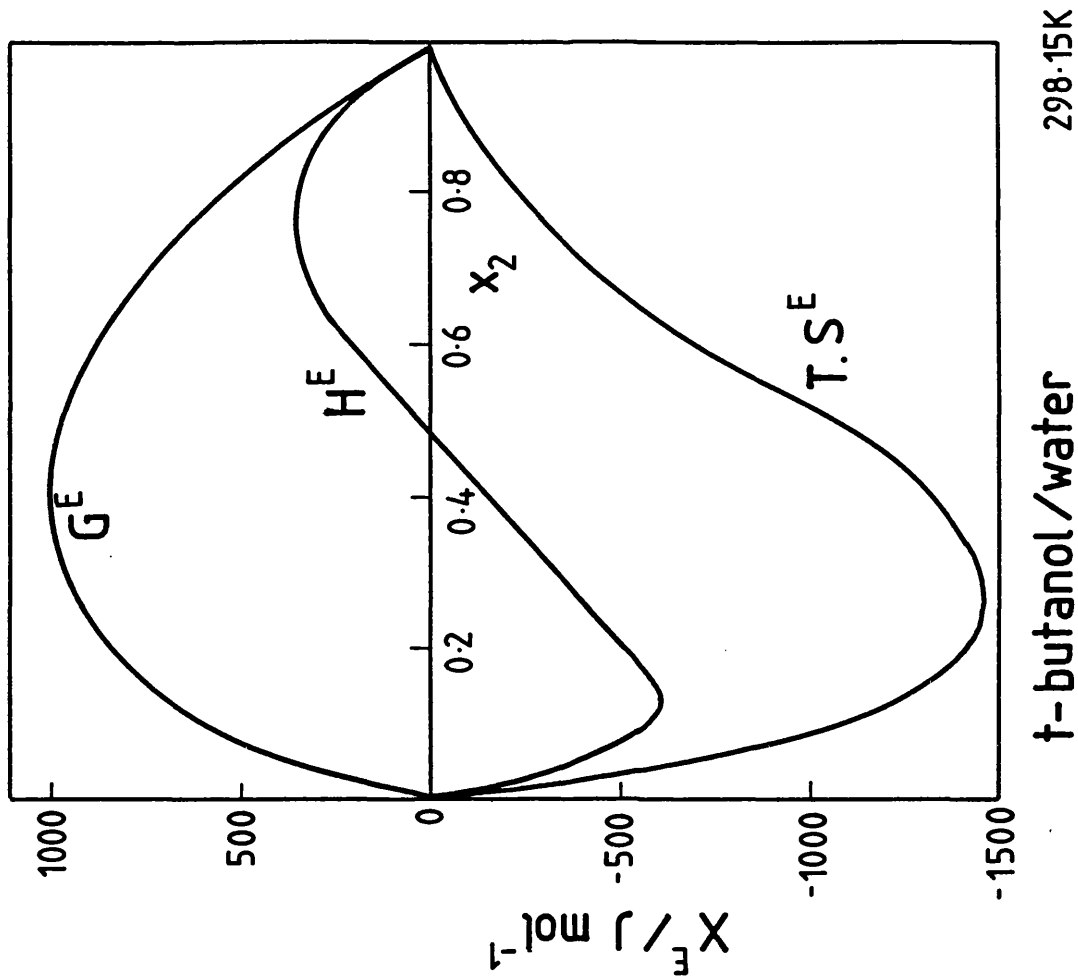
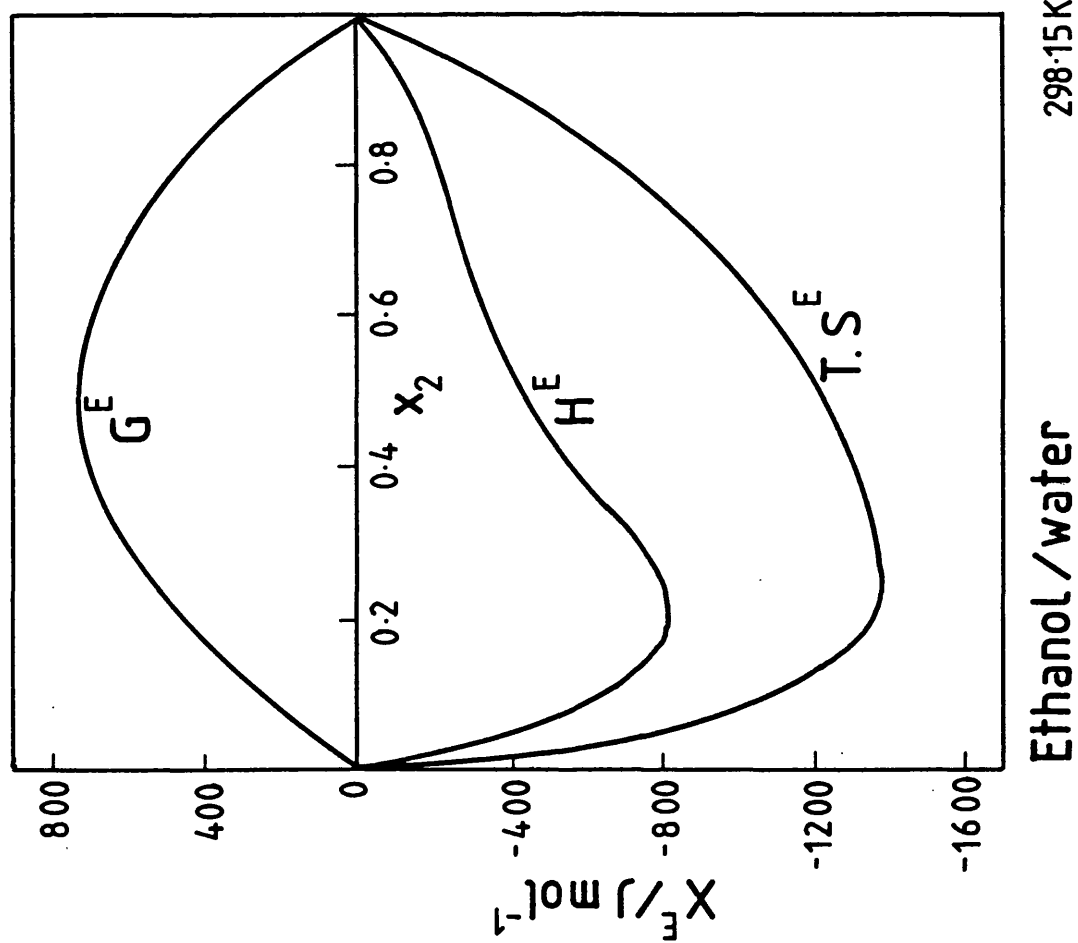


FIGURE (1.1)

Molar excess thermodynamic functions for typically-aqueous mixtures.

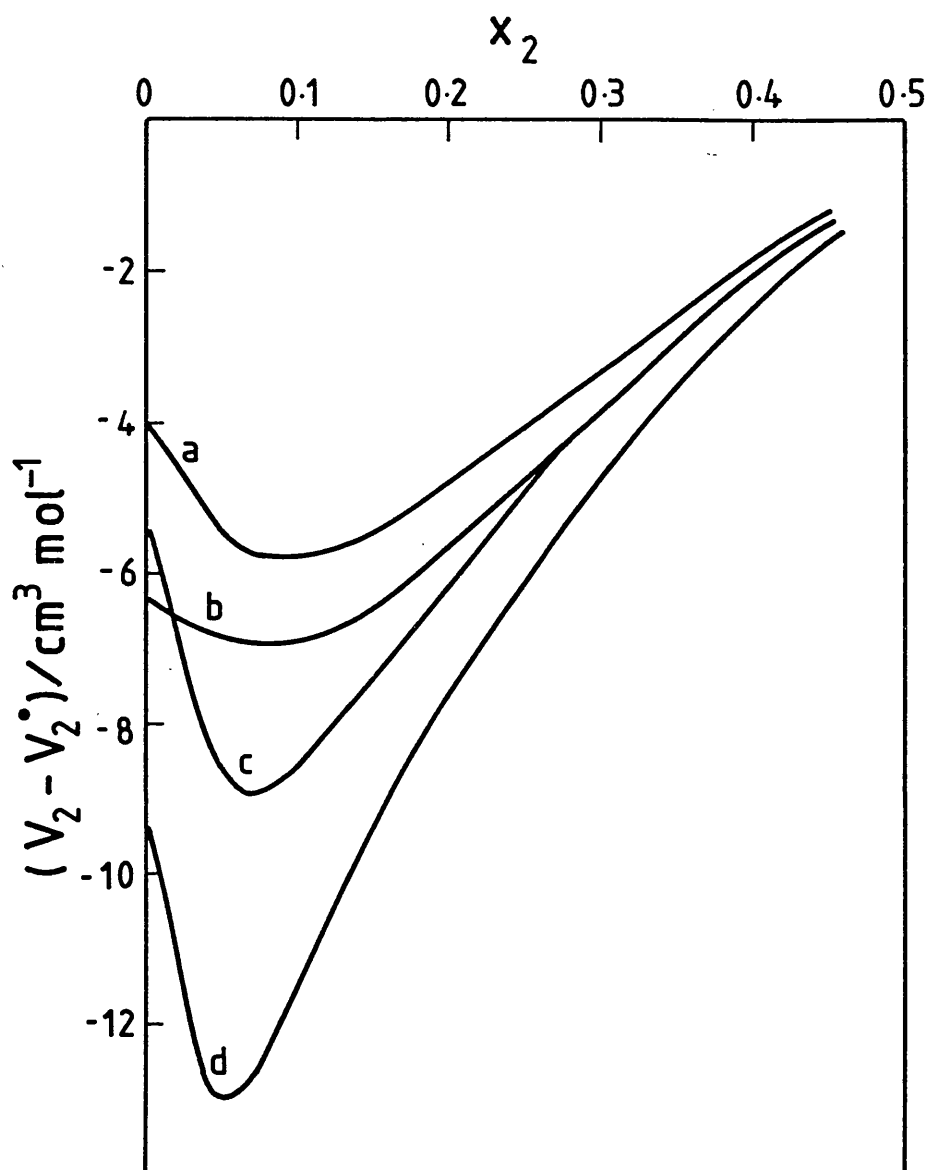


FIGURE (1.2)

Dependence of relative partial molar volume, $(V_2 - V_2^\circ)$ for cosolvents in some TA mixtures as a function of cosolvent mole fraction at 298 K.

(a) ethanol, (b) acetone, (c) n-propanol, (d) t-butanol.

peroxide and dimethyl sulphoxide. Figure (1.3) shows a set of smoothed thermodynamic excess functions for DMSO-water.

For the DMSO-water system all evidence points to extensive inter-component association.

(iii) Typically non-aqueous positive mixtures

A clear example of this type of mixture is provided by acetonitrile-water. At low mole fractions of acetonitrile at 298 K the mixing is exothermic. This does not, however, stem from enhancement of water structure as in TA mixtures. There is no minimum in the partial molar volume of acetonitrile in this region. The overall trend seems to be for this aprotic cosolvent to monotonically disrupt water-water interactions.

1.2.5 Salt solutions as reaction media

Salt solutions are discussed more fully in conjunction with kinetic results in Chapter 6. Here it is noted that added ions drastically modify the water structure in the system under study. With alkali-metal and halide ions, there are intense ion-solvent dipole interactions. With tetra-alkyl ammonium ions the apolar alkyl chains dominate the hydration properties.

Kinetic data should reflect these hydration properties. This is especially true when the reactants are neutral, where dominant charge-charge interactions are absent.

1.3 CONCEPTS OF REACTION MECHANISM

1.3.1 General discussion

In general terms, a reaction in solution between reactants R and R' to form products P and P' may require many steps to complete the trans-

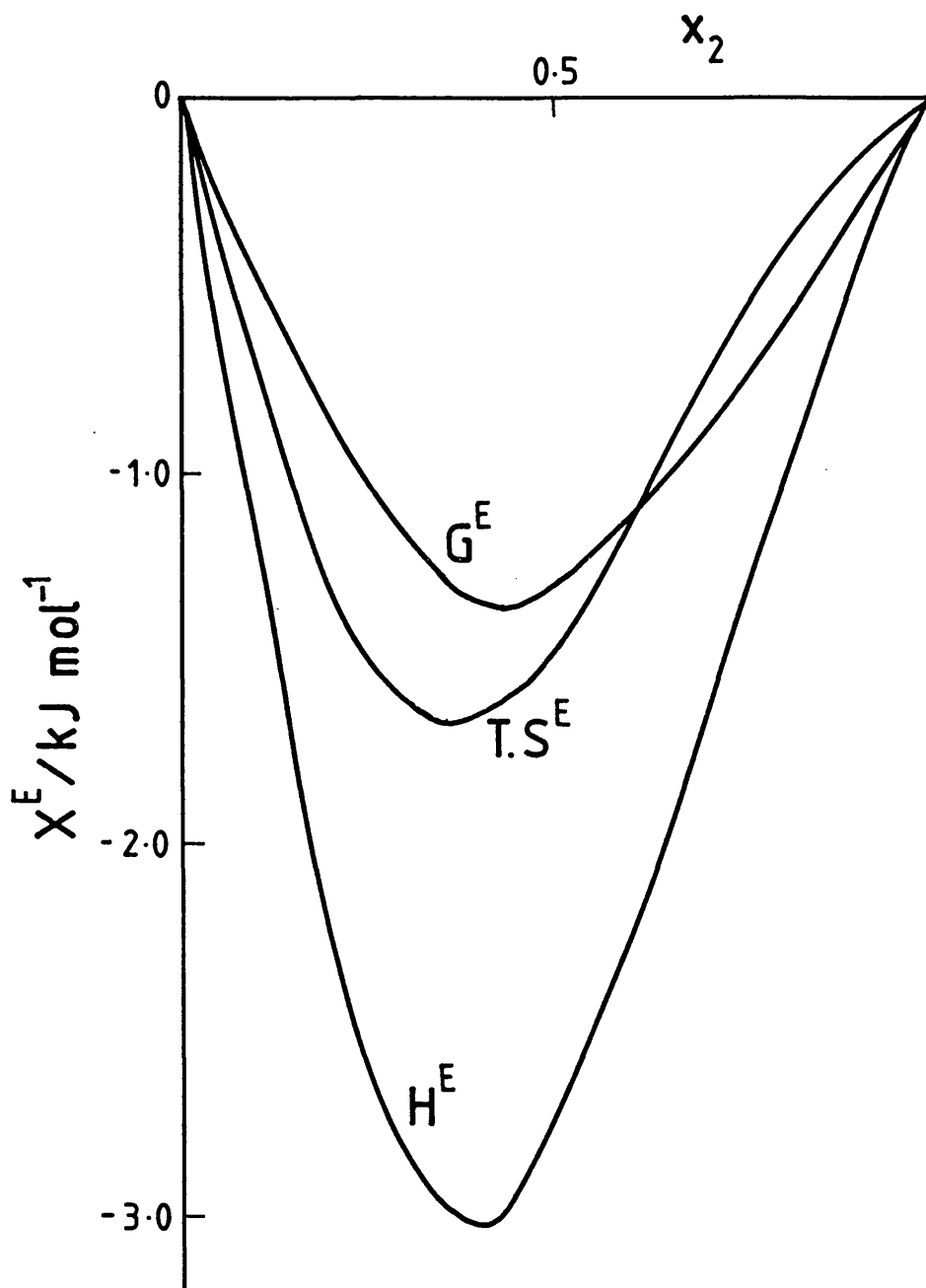


FIGURE (1.3)

Excess thermodynamic functions of mixing for dimethylsulphoxide/water mixtures at 298 K.

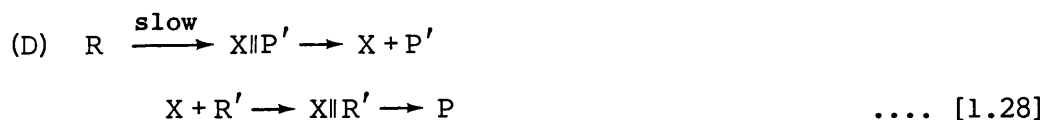
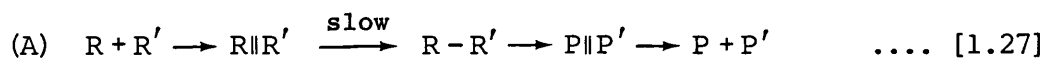
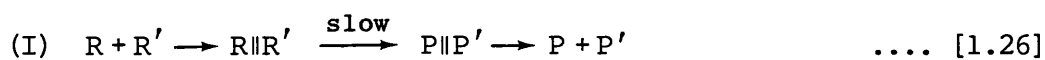
formation. Further, some of these steps may be much faster than others. Often, but not always, one of the steps is much slower than all others such that the speed of that step ultimately determines the form of the overall reaction. The rate law may contain information pertaining to the nature of steps preceding and including the slowest one. The following possibilities can be envisaged;

- (a) R and R' diffuse together to be trapped momentarily in a solvent cavity as an encounter complex, R||R'.
- (b) R and R' smoothly convert to P and P' (within a solvent cavity, P||P').
- (c) R and R' initially convert to a new species, R-R', which subsequently produces P and P'.

For systems where these characterise the slowest step, situation (b) represents an interchange (I) mechanism; situation (c) an associative (A) mechanism; and situation (a) a diffusion controlled process.

There is another possibility. The encounter complex R||R' may not lead to products. Rather, R may unimolecularly dissociate into species P' and X. The intermediate X can either recombine with P' to reform R or, if sufficiently long-lived, diffuse into a solvent cavity with R' and undergo reaction to form P. This situation represents a dissociative (D) mechanism.

The above discussion can be summarised in the following equations:



These concepts can be illustrated by the use of a free energy profile

diagram. The change in the energy of the system is plotted against the reaction coordinate, which represents changes in nuclear co-ordinates and electron distribution as the individual act of reaction progresses.

Figure (1.4) summarizes the differences between I, A and D processes. The dashed curve defines an I process in which reactants are smoothly transformed into products by the formation of a single, unstable 'high' energy chemical species referred to as the *transition state* or *activated complex*. The A and D processes (solid line) involve two steps showing the appearance of two activated complexes, separated along the reaction co-ordinate by a minimum, characteristic of the *intermediate*. The A mechanism describes the formation of the first activated complex by associative activation, in which the reactant $R||R'$ forms a bond creating the intermediate $R-R'$. The second step requires a much smaller activation energy for the conversion of $R-R'$ into product $P||P'$. On the other hand, the D mechanism has a similar energy profile, but the initial step is a dissociative activation, leading to complete fragmentation of R into one of the products (say P'), and a species (intermediate X) of kinetically significant stability. The intermediate rapidly reacts with R' to form the final product P. In contrast to the A mechanism, R' does not play an energetically significant rôle in the D mechanism. With regard to the intimate aspects of an I mechanism, one can visualize a transition state involving considerable fragmentation of R with little progress being made in the formation of the new bond between R and R' , or the converse. Such activation processes are then distinguished as I_d and I_a respectively.

The situation can be summarized as follows;

D = slow unimolecular reaction step. Bond breaking (d)	} produce reactive intermediates
A = slow bimolecular reaction step. Bond making (a)	
I = slow bimolecular reaction step	

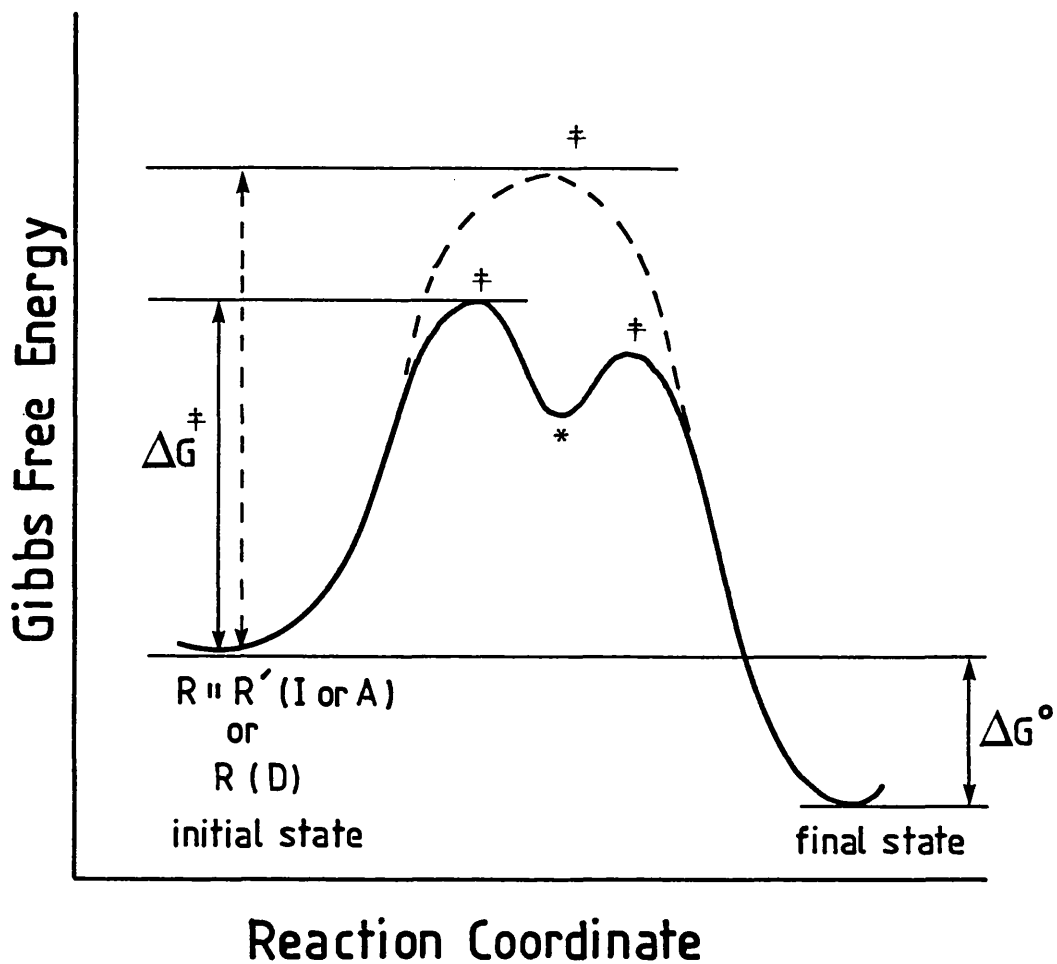


FIGURE (1.4)

Reaction free energy profile illustrating the formation of an intermediate, characteristic of A and D processes (—), and the formation of a transition state, characteristic of an I process (-----).

- ‡ - transition states for A, D and I
- * - intermediate for A or D only
- ΔG° - Gibbs free energy of reaction
- ΔG^\ddagger - Gibbs free energy of activation

I_a = predominantly bond making character	}	no reactive intermediates
I_d = predominantly bond breaking character		

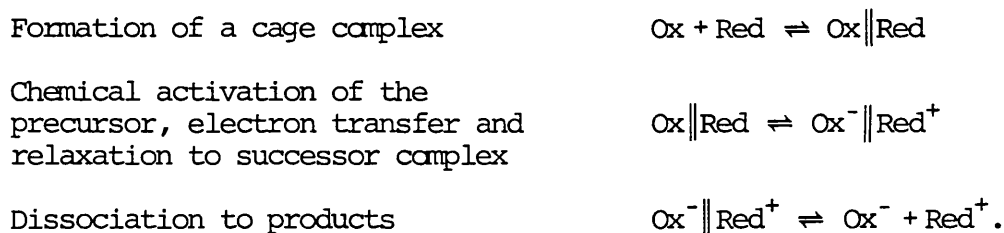
These ideas can be illustrated briefly by the chemistry of systems which are described more fully in subsequent chapters.

1.3.2 Examples

(i) Redox reactions

Electron transfer reactions involving transition metal complexes may occur by either or both of two mechanisms: outer-sphere and inner-sphere.

An outer-sphere mechanism involves electron transfer from reductant to oxidant, with their co-ordination shells or spheres staying intact. Such a mechanism is established when rapid electron transfer occurs between two substitution-inert complexes. The elementary steps involved in the mechanism may be summarised as follows:



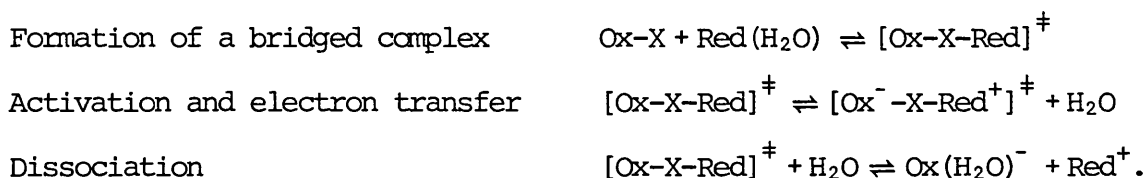
Within the precursor there must be both a reorientation of the oxidant and reductant complexes, and, within those complexes, structural changes that define the chemical activation process for electron transfer.

Solvent reorganisation to accommodate these changes can make an important contribution to the activation free energy. Electron transfer is constrained by the Franck-Condon principle: the time required is very much shorter than the time required for nuclei to change their positions.

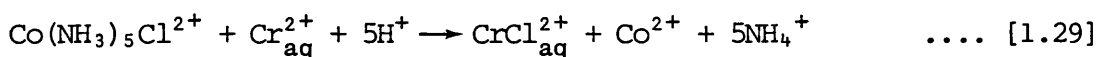
Examples of outer-sphere reactions include the hexachloroiridate(IV) oxidations of iodide and iron(II) phenanthroline complexes. The oxidation of iodide by the 12-tungstocobaltate(III) anion, $CoW_{12}O_{40}^{5-}$, is discussed

in Chapter 3.

Where an inner-sphere mechanism operates, the reductant and oxidant share a ligand in their inner or primary co-ordination spheres, the electron being transferred across a bridging group. The elementary steps in the generalized mechanism are as follows;



This mechanism can be unequivocally demonstrated by experiments using centres of appropriate lability. The classic example is the chromium(II) reduction of the chloropentammine cobalt(III) complex ion;³



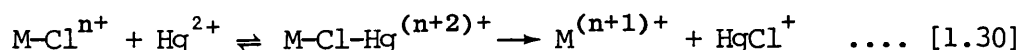
If inert centres are present after electron transfer, the transition state formally becomes an intermediate which may be detected or trapped, e.g. as with the following reactions: $\text{Cr}^{2+}/\text{IrCl}_6^{2-}$, $\text{Fe}(\text{CN})_6^{3-}/\text{Co}(\text{CN})_5^{3-}$.

The inner-sphere reduction of $\text{Co}(\text{NH}_3)_5\text{Cl}^{2+}$ by Fe^{2+} is described in Chapter 3.

Both inner-sphere and outer-sphere mechanisms are classified as I_a processes. Inner-sphere processes with intermediates are A processes.

(iii) Metal-ion catalysed aquation

A well-documented reaction of this type is the mercury(II)-catalysed aquation of chloro-complexes. The general mechanism is



Three types of behaviour are neatly illustrated:

- (i) the dinuclear species can be a transition state in an I_a process, formally resembling the inner-sphere process described above. This

occurs with complexes such as $\text{Co}(\text{NH}_3)_5\text{Cl}^{2+}$ or $\text{Cr}(\text{NH}_3)_5\text{Cl}^{2+}$. The latter system is described in Chapter 4.

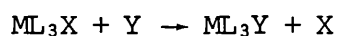
(ii) the dinuclear species may have much greater stability; it now represents an intermediate. The mechanism of reaction is dominated by the dissociation of the intermediate. This is shown by $\text{cis-}[\text{Rh}(\text{en})_2\text{Cl}_2]^+$, described in Chapter 4.

(iii) in intermediate cases, the intermediate exists but is short-lived. The mechanism is A type, illustrated by $\text{trans-}[\text{Rh}(\text{en})_2\text{Cl}_2]^+$, described in Chapter 4.

Catalysed aquation has also been demonstrated for oxalate complexes, e.g. $\text{Cr}(\text{C}_2\text{O}_4)_3^{3-}$, by copper(II) via an I_a mechanism.

(iii) Substitution at d^8 square-planar centres

By far the greatest number of square-planar complexes are formed by Pt(II), Pd(II), Ni(II), Au(III), Rh(I) and Ir(I). For the general reaction



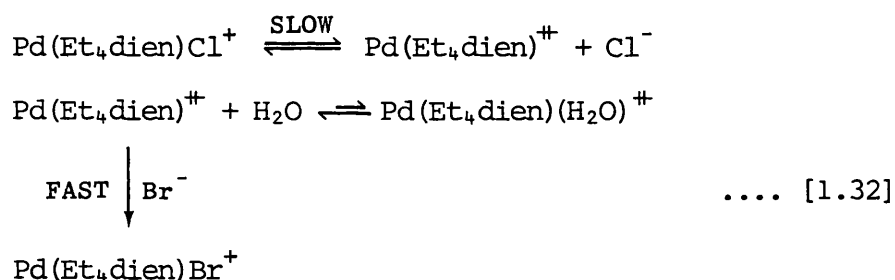
the kinetics and mechanism have been rationalized in terms of two parallel pathways, both involving an A mechanism unless special electronic or steric factors rule this out and a dissociative mechanism arises.

The general rate law has the form

$$-\frac{d}{dt} [\text{ML}_3\text{X}] = (k_s + k_y [\text{Y}]) [\text{ML}_3\text{X}] \quad \dots [1.31]$$

In the k_y pathway the nucleophile Y attacks the metal complex and the reaction passes through a five-coordinate transition state and intermediate, which may have a trigonal-bipyramidal structure. The k_s pathway also involves the formation of such a structure, except that the solvent is the entering group. A great deal of evidence has accumulated for this mechanism.

Reactions of two square-planar centres in salt solutions are described in Chapter 6. The reaction between $\text{cis-}[\text{Pt}(\text{4CNpy})_2\text{Cl}_2]$ and thiourea is a simple substitution reaction at the unhindered Pt(II) centre. The k_s value is effectively zero in these media. Aquation of the $\text{Pd}(\text{Et}_4\text{dien})\text{Cl}^+$ cation is a special dissociative case. The transition state for an associative reaction is more crowded than the initial state, whereas for a dissociative reaction it is less crowded. The latter will therefore be favoured if the initial complex contains bulky ligands. The Et_4dien ligand in the complex blocks the top and bottom of the square plane, making the associative mechanism difficult. Thus for this complex the rate of reaction is independent of the nucleophile concentration. Actually the aquo-complex is unstable and is here scavenged by bromide ions, so the overall mechanism for this complex is as follows:

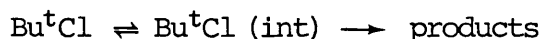


(iv) Miscellaneous systems

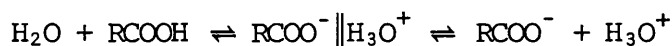
In the reactions of iron(II) tris-diimine complexes with H^+ , OH^- and CN^- the formal mechanisms are riddled with pre-equilibria and alternative pathways. However, in many cases, these schemes reduce to A mechanisms with the intermediates being formed by initial attack of the nucleophile at the coordinated ligands. This subject will be discussed more fully in the appropriate chapter.

In the later chapters describing analysis of data using computer-based procedures, the consequences of treating the solvolysis of t-butyl chloride as a D process are explored with particular regard to derived

temperature coefficients of the rate constants. Thus the mechanistic basis is



as opposed to the original Ingold³² S_N1/I_d assignment. Closely related to this is an analysis of acid dissociation constants using the following mechanism:



1.4 ANALYSIS OF MEDIUM EFFECTS ON REACTIVITY

1.4.1 General discussion

Solvation changes affect the chemical potentials of the initial state and the transition state of a reaction. In general these solvation changes will cause a change in reaction rate which may be considerable.

If the Gibbs free energy of activation of a certain reaction in a reference medium (usually water) is ΔG_1^\ddagger and in a different medium is ΔG_2^\ddagger then:

$$\delta_m \Delta G^\ddagger = \Delta G_2^\ddagger - \Delta G_1^\ddagger \quad \dots [1.33]$$

Here δ_m is the medium operator.

Transition state theory⁴ provides the link between a rate constant (which describes an irreversible process) and ΔG^\ddagger (which can be treated using the principles of reversible thermodynamics);

$$k_r = \left(\frac{kT}{h} \right) \cdot \exp(-\Delta G^\ddagger/RT) \cdot (c^\ominus)^{(1-m)} \quad \dots [1.34]$$

k_r = rate constant, h = Planck's constant,

k = Boltzmann's constant, m = molecularity

c^\ominus = concentration in the standard state to which the thermodynamic parameters refer.

From [1.33] and [1.34]

$$\delta_m \Delta G^\ddagger = -RT \ln \left(\frac{k_{r2}}{k_{r1}} \right) \quad \dots [1.35]$$

In general ΔG^\ddagger is the difference between the chemical potentials of the transition state and reactants in their solution standard states:

$$\Delta G^\ddagger = \mu^\ddagger - \sum_{i=3}^n \mu_i^\ominus \quad \dots [1.36]$$

Hence the dependence of ΔG^\ddagger on solvent can be described in terms of the dependence of chemical potentials on solvent using the medium operator:

$$\delta_m \Delta G^\ddagger = \delta_m \mu^\ddagger - \sum_{i=3}^n \delta_m \mu_i^\ominus \quad [1.37]$$

If both $\delta_m \Delta G^\ddagger$ and $\delta_m \mu_1^\ominus$ are known for a first order reaction, $\delta_m \mu^\ddagger$ can be calculated directly from [1.37]. If the experiment is repeated over a wide range of solvent composition, a plot can be constructed showing the dependence of the three quantities $\delta_m \Delta G^\ddagger$, $\delta_m \mu_1^\ominus$ and $\delta_m \mu^\ddagger$ on composition. When the reaction is second order the corresponding plot shows $\delta_m \Delta G^\ddagger$, $\delta_m \mu_1^\ominus$, $\delta_m \mu_2^\ominus$ and $\delta_m \mu^\ddagger$; it is useful to include $\delta_m \mu^\ominus$ (initial state) (which is $\delta_m \mu_1^\ominus + \delta_m \mu_2^\ominus$).

These plots show at a glance the essential features of the medium effect on the reaction kinetics.

In all the work described in this thesis, the quantities $\delta_m \mu_i^\ominus$ are derived from solubility data.

1.4.2 Initial state trends and solubility data

Consider two saturated solutions of a compound, each in equilibrium with the solid material. The chemical potentials of the solutes and solid must be equal:

$$\begin{aligned} \mu_2 (\text{solid compound}) &= \mu_2 (\text{solid in solution I}) \\ \mu_2 (\text{solid compound}) &= \mu_2 (\text{solid in solution II}) \end{aligned} \quad \dots [1.38]$$

Solvent I is the reference solvent (usually water).

For a solute in solution

$$\mu_2 = \mu_2^\ominus + RT \ln m_2 f_2 \quad \dots [1.39]$$

μ_2^\ominus is the chemical potential of the solute in its solution standard state.

f_2 is an activity coefficient such that $f_2 \rightarrow 1$ as $m_2 \rightarrow 0$.

In this type of analysis, the definition of the standard state is important. If a second order rate constant is given in units of $\text{dm}^3 \text{mol}^{-1} \text{s}^{-1}$, then the relevant standard state is the hypothetical solution where the concentration of each reactant is 1.0mol dm^{-3} and f_2 is unity.

If the solubility in solution I is $S(\text{I}) \text{mol dm}^{-3}$ and in solution II is $S(\text{II}) \text{mol dm}^{-3}$, then

$$\begin{aligned} \mu_2(\text{I}) &= \mu_2^\ominus(\text{I}) + RT \ln S(\text{I}) f_2(\text{I}) \\ \mu_2(\text{II}) &= \mu_2^\ominus(\text{II}) + RT \ln S(\text{II}) f_2(\text{II}) \end{aligned} \quad \dots [1.40]$$

From [1.38]:

$$\mu_2^\ominus(\text{I}) + RT \ln S(\text{I}) f_2(\text{I}) = \mu_2^\ominus(\text{II}) + RT \ln S(\text{II}) f_2(\text{II}) \quad \dots [1.41]$$

Rearrangement gives

$$\mu_2^\ominus(\text{II}) - \mu_2^\ominus(\text{I}) = -RT \ln \left[\frac{S(\text{II}) f_2(\text{II})}{S(\text{I}) f_2(\text{I})} \right] \quad \dots [1.42]$$

$$\text{Since } \delta_m \mu_2^\ominus = \mu_2^\ominus(\text{II}) - \mu_2^\ominus(\text{I}) \quad \dots [1.43]$$

Then:

$$\delta_m \mu_2^\ominus = -RT \ln \left[\frac{S(\text{II}) f_2(\text{II})}{S(\text{I}) f_2(\text{I})} \right] \quad \dots [1.44]$$

The usually reasonable assumption is made that the ratio of activity coefficients $f_2(\text{II})/f_2(\text{I})$ is unity. Thus [1.44] gives the required quantity solely in terms of experimental solubility data.

Different authors use different standard states and scales (mole fraction, molality, molarity). Ben-Naim has commented on the suitability

of the molar scale.⁵ Fortunately inter-scale conversion is arithmetically simple.⁶

The above analysis applies to uncharged solutes. For ionic compounds, the same analysis applies to obtain $\delta_{m\mu}^{\ominus}$ (salt) except S is replaced by the solubility product, K_{sp} . However, for the analysis of kinetic data, the required parameter is the contribution of the individual ions. We need estimates of single ion transfer parameters. Obtaining these parameters is beset with problems and the following section presents a review of this subject to set the stage for discussion in later chapters.

1.4.3 Single ion thermodynamic properties

There is no experiment by which the absolute free energy of transfer of a single ionic species from one solvent to another may be determined. In general, each method used in deriving such quantities rests on an extra thermodynamic assumption. These methods fall into two fundamental types:

- (i) The transfer is analysed in terms of electrical interactions between ion and solvent. Here the solvent is often characterised by its dielectric properties, so

$$\delta_{m\mu}^{\ominus}(\text{ion}) = f(\Delta\epsilon_r), \quad \text{where } \epsilon_r \text{ is the relative permittivity of the solvent.}$$

- (ii) The assumption is made that certain large ions are lightly enough solvated for an anion and cation of similar size and exterior to have equal transfer parameters, i.e.

$$\delta_{m\mu}^{\ominus}(M^+) = \delta_{m\mu}^{\ominus}(X^-) = \frac{1}{2}\delta_{m\mu}^{\ominus}(MX) \quad \dots [1.45]$$

When a value has been obtained for one ion, the rest can be obtained by combination with values for the salts.

Wells has analysed ion-solvent interactions using a modification of the Born model and arbitrary assumptions concerning primary solvation

shells of ions to obtain a value for $\delta_{m\mu}^{\ominus}(\text{H}^+)$ and hence values for simple anions and cations for a relatively large number of cosolvent mixtures up to 50% w/w.⁷⁻¹³ De Ligny and co-workers have also used a Born model, taking account of quadrupole interactions and orientation of solvent molecules to obtain sets of transfer parameters over the whole mole fraction range of organic cosolvent (e.g. ref. 14).

The arbitrary assignment $\delta_{mX}^{\ominus}(\text{Me}_4\text{N}^+) = 0$ where X is μ , H or S was used by Abraham.¹⁵ Being unsatisfactory for aqueous mixtures this method has been superceded.

One of the first methods of obtaining single ion values assumed that $\delta_{mX}^{\ominus}(\text{K}^+) = \delta_{mX}^{\ominus}(\text{Cl}^-)$. This method is still used in some studies, e.g. in highly acidic media where other species (see below) are unstable.

In the equality assumption large organic ions of the type R_4N^+ and BR_4^- are used as reference ions. The most commonly used examples are Ph_4As^+ and BPh_4^- . Cox has used these for an analysis of transfer parameters for non-aqueous¹⁶ and mixed-aqueous¹⁷ solvents (acetonitrile/water, DMSO/water). Recently Abraham has extended this work to include methanol/water mixtures. Similar, though less widely used versions of this approach include the assumption that the Gibbs free energy of transfer of tri-isoamylbutylammonium tetraphenylboronate can be equally divided: using this method Popovych and Dill¹⁸ have reported single ion values for transfer into ethanol/water mixtures.

Redox linked assumptions based on the ferrocene-ferrocinium¹⁹ cation and the bisbiphenylchromium²⁰ couples have also been employed.

In a very different approach Parsons^{21,22} has used the measurement of surface potentials at interfaces to obtain $\delta_{m\mu}^{\ominus}(\text{Cl}^-)$ for several aqueous mixtures.

Extrapolation methods based on the Born equation have had a limited

application. In one example $\delta_{m\mu}^{\ominus}(M^+Cl^-)$ is plotted against reciprocal cation radius and the intercept of the fitted straight line as $1/r_i \rightarrow 0$ is taken as $\delta_{m\mu}^{\ominus}(Cl^-)$.²³

All estimated transfer parameters involving mixed-aqueous solvents up to 1976 have been tabulated.²⁴ Although many are available, it is noteworthy that transfer parameters involving non-aqueous solvents are considerably more extensive (e.g. ref. 25); this reflects the fact that binary aqueous mixtures are rather more complex systems.

It is not surprising that with differing approaches, the reported values usually disagree, often markedly. However, for e.g. $\delta_{m\mu}^{\ominus}(Cl^-)$, Wells and de Ligny agree very closely, after appropriate scale conversion, in methanol-water mixtures up to 40% v/v methanol.

For the requirements of initial state/transition state dissections, there often exists only one appropriate set of values for the required mixture. The work in this thesis largely uses the set given by Wells. The problem with Wells' approach is that it is based on an assumed model for solvation of the proton in water and water-methanol mixtures. Bearing in mind the proton's unique nature among cations, this ion is probably the most difficult for understanding and modelling its solvation. There is also some controversy over the solution thermodynamics involved. The Born analysis used by de Ligny starts with large cations, e.g. Cs^+ .

Both Wells and de Ligny together only report parameters for Gibbs free energy changes. In contrast, Cox and Abraham also tabulate parameters for enthalpy and entropy changes, but only for a limited range of mixtures.

Initial state-transition state analyses of ionic inorganic reactions will improve as estimates of single ion values improve. It is likely that future adjustments will make a difference to actual values but not, however, to the overall patterns which emerge from the analysis. Forward

looking development includes the beginnings of inroads into transition metal cations, e.g. via solubilities of iodates and an analysis of iron(II)-tris diimine complex formation, and the possibility of using the $\text{Cr}(\text{C}_2\text{O}_4)(\text{H}_2\text{O})_4^+/\text{Cr}(\text{C}_2\text{O}_4)_2(\text{H}_2\text{O})_2^-$ pair as a hydrophilic counterpart to the hydrophobic $\text{R}_4\text{N}^+/\text{R}_4\text{B}^-$ type splits.

1.4.4 Transition state theory in perspective

In transition state theory, the quantity ΔG^\ddagger (equation [1.34]) is expressed as

$$\Delta G^\ddagger = -RT \ln \left\{ K^\ddagger / (C^\ominus)^{(1-m)} \right\} \quad \dots [1.46]$$

where K^\ddagger is the equilibrium constant (in terms of concentrations) for



This is not a stable equilibrium because the transition state lies at a saddle point rather than a minimum of the potential energy profile.

Although the equilibrium hypothesis is ultimately untenable, there is probably little error in treating the equilibrium by ordinary thermodynamic or statistical methods, even when the activation energy is very low.²⁶ It must be remembered, however, that ΔG^\ddagger is applicable on the molecular scale whereas a true thermodynamic quantity like ΔG^\ominus is applicable at the bulk level. [A statistical formulation of the theory is given in the literature which does not involve recourse to the equilibrium hypothesis.²⁷]

In the context of solvent effects, the equilibrium condition means that the organization of the solvent around the solute changes reversibly from that determined by the initial state to that determined by the transition state. In addition these solvent cospheres²⁸ are in equilibrium with the bulk solvent.²⁹ Consequently it is implied that activation is sufficiently slow to allow this equilibrium to be maintained at all

stages. However, it is not difficult to imagine that the key process in a reaction is sufficiently rapid for the reorganization of solvent in the cospheres to lag behind the equilibrium structure; the solvent may 'catch up' with the solute on the product side of the energy maximum. This irreversible activation negates characterisation of the transition state by a chemical potential.

Another factor to consider is the possibility that the position of the transition state along the reaction coordinate varies with solvent: evidence for this is that solvent variation can cause a change in mechanism.³⁰

In spite of these aspects, transition state theory provides a useful entry point into the analysis of solvent effects. Substantial progress can be made as long as the quantities obtained are used with care. This applies particularly to related and derived parameters³¹ such as ΔH^\ddagger , ΔS^\ddagger , ΔC_p^\ddagger , and ΔV^\ddagger .

1.5 A SUMMARY OF INITIAL STATE/TRANSITION STATE DISSECTIONS

The results of solvent effect on reactivity are illustrated in Table (1.1). This shows the relative importance of initial state and transition state solvation changes, indicates the dominant influences, covers substitution and redox reactions and puts inorganic complexes into the context of sp-block elements and organic chemistry (cf. ref. 29). Some reactions fit into the general pattern for organic reactions established by Ingold,³² which is based on simple electrostatic considerations. Others, however, cannot be accommodated and this is due to the variety of ligands and their accompanying solute-solvent interactions.

Solvent effects on reactivity may show more dramatic variations with solvent in mixed-aqueous media than in organic solvents. The hydrophobic

TABLE (1.1)

A Summary of Initial State/Transition State Dissections
(ΔG unless otherwise indicated)

REACTION	RELATIVE IMPORTANCE OF INITIAL STATE AND TRANSITION STATE SOLVATION CHANGES		REF.
t-BuCl solvolysis (ΔH)	is > ts	is, ts trends opposed ^a	33
C ₆ H ₅ CH ₂ Cl solvolysis (ΔV)	is > ts		34
Finkelstein CH ₃ I + Cl ⁻	is > ts	Cl ⁻ transfer dominant	35
Menschutkin Me ₃ N + MeI	is » ts		36
Me ₃ N + p-O ₂ NC ₆ H ₄ CH ₂ Cl	is < ts		36
Et ₄ Sn + HgCl ₂ (also ΔH)	is > ts	is, ts trends parallel	37
R ₄ Pb + I ₂	is ~ ts		38
Pt(bipy)Cl ₂ + tu	is » ts	} is, ts trends parallel	39
Pt(4CNpy) ₂ Cl ₂ + tu	is > ts		40
Fe(bipy) ₃ ²⁺ + CN ⁻	is ~ ts	bipy solvation dominates is and ts	41
Co(NH ₃) ₅ Cl ²⁺ + Hg [#]	is ~ ts	} all reactant trends parallel cf. charges is → ts	42
ReCl ₆ ²⁻ + Hg [#]	is > ts		
IrCl ₆ ²⁻ + I ⁻ , catechol	is < ts		43
Fe(phen) ₃ ²⁺ + S ₂ O ₈ ²⁻	is > ts	reactant solvation trends opposed: Fe(II) > S ₂ O ₈ ²⁻	44
Fe(bipy) ₂ CN ₂ + S ₂ O ₈ ²⁻	is « ts	reactant solvation trends equal and opposite	45

^a See also Chapter 7

or hydrophilic character of the solute is a more important consideration in structurally complex mixed-aqueous media than in organic solvents. When water itself is used as a reference solvent, which is the case in Table (1.1) and the work in this thesis, the kinetic consequences can be particularly striking.

CHAPTER 2

EXPERIMENTAL DETAILS OF COLLECTION
AND ANALYSIS OF KINETIC DATA

2.1 INTRODUCTION

This chapter describes how kinetic data were measured. The spectrophotometric apparatus used to collect these data and the methods of analysing them are described.

For the work in this thesis, two experimental procedures were employed:

- (i) data collection by paper-tape logging and subsequent computer analysis;
- (ii) 'real time' data collection and analysis using a minicomputer.

The description of the method and mathematics of (i) provides the background to the principles of method (ii).

Appendix 1 provides more details concerning computer programs and outputs.

2.2 RATE CONSTANTS AND OBSERVABLES

All rate constants in the work presented in subsequent chapters are overall first or second order, but all were measured under first-order conditions.

Consider a reaction that proceeds to completion in which the concentration of only one reactant, A, changes appreciably during the reaction.

This may arise because

- (1) there is only one reactant A involved;
- (2) all other possible reactants are in much larger concentration than A;
- (3) the concentration of one of the other reactants is held constant by buffering, or is constantly replenished, e.g. a catalyst.

We are concerned with cases (1) and (2).

Attention needs only to be focussed on the change of concentration of

A as the reaction proceeds. In general

$$-\frac{d}{dt} [A] = k [A]^a \quad \dots [2.1]$$

A first-order dependence occurs when $a=1$. This is extremely common and forms the bulk of reported kinetic studies, as is the case in this thesis. The rate of loss of the reactant A decreases as the concentration of A decreases. The differential form of [2.1] leads to several equivalent integrated expressions, e.g.

$$[A]_t = [A]_o \exp(-kt) \quad \dots [2.2]$$

$$\ln \frac{[A]_o}{[A]_t} = kt \quad \dots [2.3]$$

Also $-\frac{d}{dt} \ln [A]_t = k \quad \dots [2.4]$

$[A]_o$ = initial concentration of A.

$[A]_t$ = concentration of A at time t.

k = rate constant under the given conditions of T, p, $[X_i]$.

A quantity characteristic of a first-order reaction is $t_{1/2}$, the half-life of the reaction, which is the value of t when $[A]_t = [A]_o/2$ or $[A]_{t+t_{1/2}} = [A]_t/2$. So

$$t_{1/2} = \frac{\ln 2}{k} \quad \dots [2.5]$$

$t_{1/2}$ is constant over the complete first-order reaction.

In case (2) above, the observed first-order rate constant will vary with the concentrations of the other reactants and enables the determination of the second order rate constant for a bimolecular reaction by the use of an ISOLATION METHOD. Values of the observed first-order rate constant for reaction of A are measured for several different concentrations of B, e.g. 100×, 200× and 300× excess over the concentration of A. These values of k_{obs} will differ and the dependence of k_{obs} on [B] will

reveal the order with respect to B.

A common pattern which emerges is a straight line of the form

$$k_{\text{obs}} = k_1 + k_2 [\text{B}] \quad \dots [2.6]$$

k_1 - first-order B-independent path.

k_2 - second-order path: $\text{A} + \text{B} \rightarrow \text{P}$.

This type of behaviour is illustrated, for example, in chapter 3 (redox) and chapter 6 (substitution at square planar d^8 complexes). In certain systems k_1 can be small or effectively zero. More complex dependences can emerge, e.g. for mercury(II)-catalysed aquation (chapter 4).

Errors in pseudo first-order rate constants arising from the small variation in B for a given excess as the reaction proceeds have been conveniently plotted.¹ An excess of B as low as 25× can be satisfactory: hundred-fold excesses are usually used.

Concentrations and absorbances

The optical density or absorbance D arising from a single chemical species A in solution is related to its concentration by the Beer-Lambert law:

$$D = \log_{10} \frac{I_0}{I_t} = \epsilon_{\lambda} \cdot \ell \cdot [\text{A}] \quad \dots [2.7]$$

I_0, I_t ; intensities of incident and transmitted light at wavelength λ .

ϵ_{λ} = molar extinction coefficient at wavelength λ .

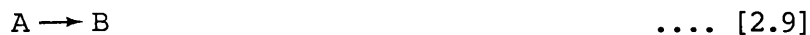
ℓ = light path / cm.

$[\text{A}]$ = concentration of species A / mol dm^{-3} .

This law is obeyed strictly only for monochromatic light and in dilute solution of A. Mixtures of species usually give additive absorbances:

$$\frac{D}{\ell} = \epsilon_{\text{A}} [\text{A}] + \epsilon_{\text{B}} [\text{B}] + \dots \quad \dots [2.8]$$

Thus it is possible to analyse concentration changes from absorbance changes in the mixture. Absorbance changes can be used directly to measure rate constants. Consider the first-order reaction



Omitting brackets to denote concentrations, we find:

$$\text{At zero time,} \quad D_0 = \epsilon_A A_0 + \epsilon_B B_0 \quad \dots [2.10]$$

$$\text{At time } t, \quad D_t = \epsilon_A A_t + \epsilon_B B_t \quad \dots [2.11]$$

$$\text{At infinite } t, \quad D_\infty = \epsilon_B B_\infty = \epsilon_B (A_0 + B_0) = \epsilon_B (A_t + B_t) \quad \dots [2.12]$$

(complete reaction)

Therefore

$$A_0 = \frac{(D_0 - D_\infty)}{\epsilon_A - \epsilon_B} \quad A_t = \frac{(D_t - D_\infty)}{\epsilon_A - \epsilon_B} \quad \dots [2.13]$$

$$\frac{\ln A_t}{A_0} = \ln \frac{(D_0 - D_\infty)}{(D_t - D_\infty)} = kt \quad \dots [2.14]$$

A semilog plot of $\ln (D_t - D_\infty)$ vs. t is linear with slope $-k$.

Visible and ultraviolet monitoring is particularly useful because few, if any, reactions of transition metal complexes are unaccompanied by absorption changes in these regions. The visible region is advantageous in that added electrolytes, etc., are usually transparent. However, extinction coefficients in the ultraviolet are often much higher than in the visible and a smaller concentration gives a comparable absorbance change.

The use of equation [2.14] to obtain rate constants is discussed in more detail in section 2.4.

2.3 SPECTROPHOTOMETRIC APPARATUS

2.3.1 Instruments

Absorbance measurements were made using Pye Unicam SP800 and SP1800 spectrophotometers. These are double beam instruments which measured

directly the logarithmic ratio of the reference and sample beam intensities.

The SP800 was equipped with a chart recorder and could be used to produce a continuous scan spectrum within the range $14500 - 50000 \text{ cm}^{-1}$ (approx. 690 - 200 nm). This scan could be repeated immediately after the first was completed, or at intervals of up to 15 minutes. Thus the SP800 was generally used in the initial stages of a kinetic study, to assess the suitability and nature of absorbance changes, to check for any isosbestic points and to select a wavelength at which to monitor the reaction routinely.

Single wavelength monitoring and data logging could be performed using either instrument. Generally, the SP1800 was used, being the superior. The linearity and correctness of absorbance scales, and optics of both instruments were examined and checked in the course of the studies. The correctness of wavelength scales was checked periodically with didymium filters.

2.3.2 Thermostatting and cell composition

Both spectrophotometers were equipped to hold three sample (and three reference) cells in a thermostatted cell block which could be moved automatically to place each cell as selected in the light beam. The fourth space in the block was used to hold a cell in which was placed the probe of a Hewlett-Packard quartz thermometer. This probe, calibrated periodically against a platinum resistance thermometer, allowed the temperature of the solutions in the cells to be measured accurately (digital display) to 0.01 K at all times during the kinetic run. The temperature of the solutions in the cells was maintained by pumping water from a large thermostatted tank through the cell housing. The water in the tank was maintained at the required temperature by a contact heater

and a flow of cold water or cooled ethylene glycol-water in coils in the tank.

1 cm silica UV/visible cells of greater than 3 cm³ capacity were used. Cells were made up with reagents to a total volume of 3 cm³. Stock solutions of reagents were prepared such that when all components had been pipetted into the cell and mixed, the required in-cell concentrations of solutes and composition of cosolvent were obtained. In an alternative, less used method, a few drops of concentrated reagent (usually complex) were added to a filled cell containing the reaction medium.

2.3.3 Paper tape data-logging with the SP1800

The analogue output from the spectrophotometer was connected via a data-logging interface to a Solartron digital voltmeter which presented the absorbance in digital form on a display. The interface was also connected to a clock: these two components provided accurately timed pulses at intervals from 2 to 2¹² seconds. The pulse interval was set manually to obtain an optimum number of data points during the first 2½ half-lives of the reaction. For a time interval of less than 64 seconds only single-cell runs could be performed: the cell block required approximately one minute to complete the successive monitoring of three cells. The shortest time step used in fast single-cell runs was 2 seconds.

The output from the digital voltmeter was fed to a recorder drive unit which transmitted the series of digits from the voltmeter to a Facit paper tape punch. The punch recorded the information in ASCII code on 8-track paper tape. The complete system is shown in Figure (2.1).

A routine kinetic run using the data-logging system will now be described. The machine and associated electronics were given time to stabilize after switching on, and the cell block was allowed to reach and maintain the required temperature.

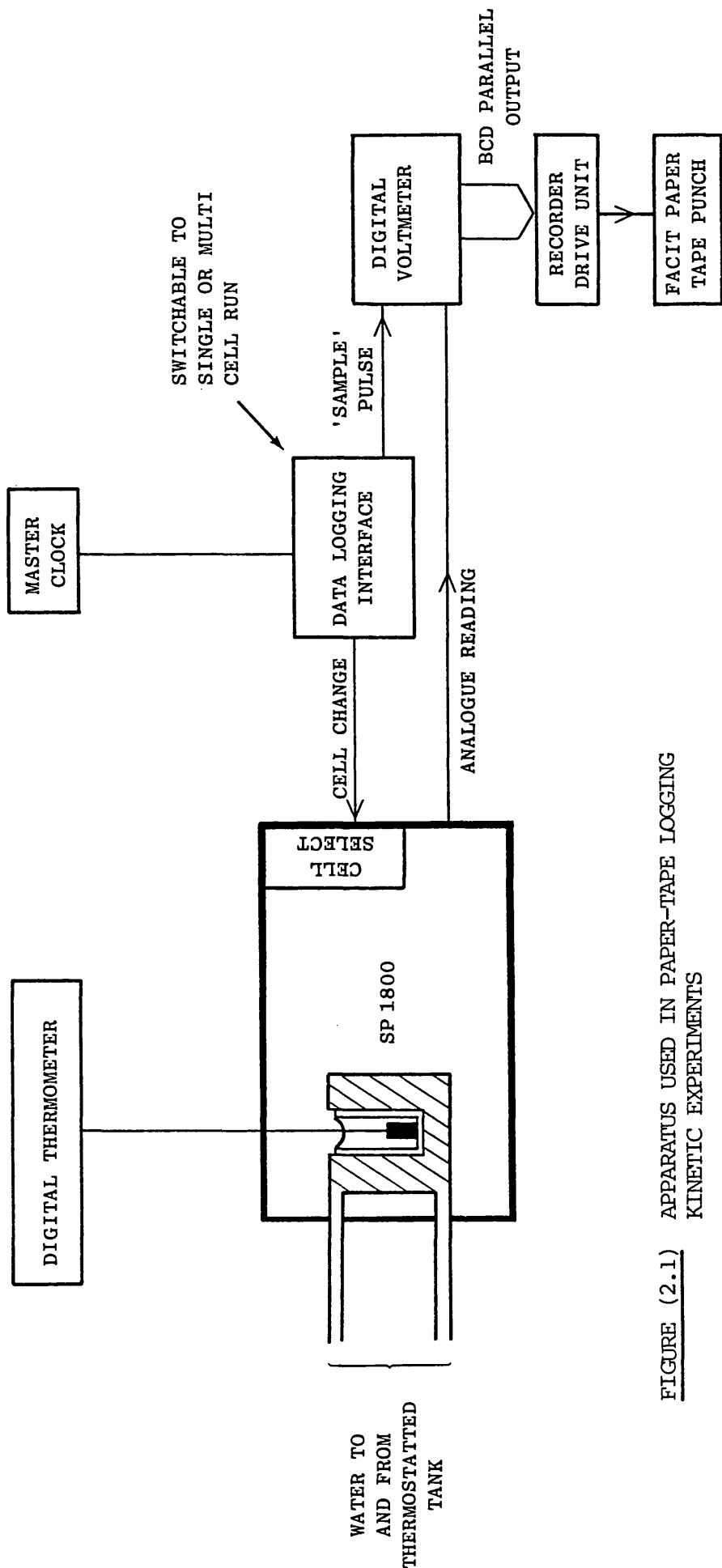


FIGURE (2.1) APPARATUS USED IN PAPER-TAPE LOGGING KINETIC EXPERIMENTS

The reaction cell or cells were made up with the appropriate reagents except one - usually a small volume of solution containing the complex. The cells, previously cleaned with a concentrated hydrochloric acid/acetone solution followed by washing with methanol and allowed to dry (and periodic thorough cleaning with concentrated nitric acid), were placed in the cell block and allowed to equilibrate for at least ten minutes. Often in single cell runs other cells could be equilibrated concurrently. A cell containing the outstanding reagent was also thermostatted in the same manner. Reference cells were not normally needed or used. The sample beam was zeroed against air.

Before beginning the run, three numbers were manually punched onto the paper tape: a run identification number, the number of cells and the time step in seconds. The latter two were necessary for the subsequent computer analysis.

To commence the run, the remaining aliquot of reagent was added to the cell(s) from the equilibrated supply. Each cell was stoppered and inverted several times to ensure thorough mixing, and then replaced in the cell block. Readings were commenced by a single switch on the data logging interface. Absorbances were recorded on the paper tape (values between 0 and 2.0 were recorded as five-digit numbers between 0 to 20000).

Each run was followed for at least $2\frac{1}{2}$ half-lives: this duration enabled the computer program used in subsequent data analysis to calculate a good infinity value, and also ensured that differences between readings in the later stages of the run were larger than the error in the reading.

The run was terminated by returning the switch on the data logging interface to its original position. The number 99999 was manually punched on the tape - a terminator flag for the computer program.

The FORTRAN computer program (for the University CDC Cyber 73) used

for the analysis is described and listed elsewhere.² The underlying method will now be discussed because this also lies at the core of the minicomputer system which superceded the paper tape logging procedure.

2.4 ANALYSIS OF ABSORBANCE DATA

The method used for analysis of absorbance data is based on a Newton-Raphson non-linear least squares procedure suggested by Moore.³ It enables calculation of a first order rate constant when neither the absorbances at times $t=0$ or $t=\infty$ are known. It is an improvement on Guggenheim's method,⁴ where well-spaced, constant time intervals are needed.

Rearranging equation [2.14] and writing P for D we obtain

$$P = P_{\infty} + (P_0 - P_{\infty}) e^{-kt} \quad \dots [2.15]$$

P_0 = initial absorbance; P = absorbance at time t ;

P_{∞} = final absorbance; k = rate constant

For n observations, we wish to minimize the sum of the squares of the errors, as in

$$SQ = \sum_{i=1}^n [P_i^{obs} - P_i^{calc}]^2 \quad \dots [2.16]$$

Equation [2.15] is of the form $P=f(t)$ so we expand equation [2.15] as a Taylor series, truncating second and higher differentials;

$$f(t) = f_0(t) + \left(\frac{\partial f_0}{\partial P_0}\right)\Delta P_0 + \left(\frac{\partial f_0}{\partial P_{\infty}}\right)\Delta P_{\infty} + \left(\frac{\partial f_0}{\partial k}\right)\Delta k \quad \dots [2.17]$$

$f_0(t)$ is the calculated absorbance using some initial estimates of the three parameters we wish to find. When all the data for a run are available, as in paper tape analysis, these estimates can be obtained as follows:

$$\begin{aligned}
P_0 &\approx \text{first reading} \\
k &\approx 2/t_n \quad \dots [2.18] \\
P_\infty &\approx 1.25 P_n - 0.25 P_0
\end{aligned}$$

In real time analysis, the estimates must be supplied at the start of the run: they can be reasonably guessed from repeat scan experiments and/or previous kinetic runs.

These estimates form the starting point for an iterative process which calculates ΔP_0 , ΔP_∞ and Δk : these are the correctors from the initial values to better estimates. We need to solve equation [2.17]. For each data point we write

$$\begin{aligned}
\delta &= P_i^{\text{obs}} - P_i^{\text{calc}} \\
\therefore \delta &= P_i^{\text{obs}} - f_0(t) - \left(\frac{\partial f_0}{\partial P_0}\right)\Delta P_0 - \left(\frac{\partial f_0}{\partial P_\infty}\right)\Delta P_\infty - \left(\frac{\partial f_0}{\partial k}\right)\Delta k \\
\therefore \delta &= E_i - \left(\frac{\partial f_0}{\partial P_0}\right)\Delta P_0 - \left(\frac{\partial f_0}{\partial P_\infty}\right)\Delta P_\infty - \left(\frac{\partial f_0}{\partial k}\right)\Delta k \quad \dots [2.19]
\end{aligned}$$

E_i = deviation between observed absorbance and calculated value.

For minimization of $\sum_{i=1}^n \delta^2$ with respect to ΔP_0 , ΔP_∞ and Δk we have the condition

$$0 = \frac{\partial}{\partial \Delta P_0} \sum \delta_i^2 = 2 \sum \delta_i \left(\frac{\partial \delta_i}{\partial \Delta P_0}\right) ; \text{ so from [2.19] } \sum \delta_i \left(\frac{\partial f_0}{\partial P_0}\right) = 0$$

$$\text{Similarly } \sum \delta_i \left(\frac{\partial f_0}{\partial P_\infty}\right) = 0 \quad \dots [2.20]$$

$$\sum \delta_i \left(\frac{\partial f_0}{\partial k}\right) = 0$$

Substitution of [2.19] into [2.20] and rearrangement gives the three normal equations:

$$\sum_{i=1}^n \left(\frac{\partial f_0}{\partial P_0}\right)^2 \Delta P_0 + \sum_{i=1}^n \left(\frac{\partial f_0}{\partial P_\infty}\right)\left(\frac{\partial f_0}{\partial P_0}\right)\Delta P_\infty + \sum_{i=1}^n \left(\frac{\partial f_0}{\partial k}\right)\left(\frac{\partial f_0}{\partial P_0}\right)\Delta k = \sum_{i=1}^n E_i \left(\frac{\partial f_0}{\partial P_0}\right)$$

$$\sum_{i=1}^n \left(\frac{\partial f_0}{\partial P_0} \right) \left(\frac{\partial f_0}{\partial P_\infty} \right) \Delta P_0 + \sum_{i=1}^n \left(\frac{\partial f_0}{\partial P_\infty} \right)^2 \Delta P_\infty + \sum_{i=1}^n \left(\frac{\partial f_0}{\partial k} \right) \left(\frac{\partial f_0}{\partial P_\infty} \right) \Delta k = \sum_{i=1}^n E_i \left(\frac{\partial f_0}{\partial P_\infty} \right)$$

$$\sum_{i=1}^n \left(\frac{\partial f_0}{\partial P_0} \right) \left(\frac{\partial f_0}{\partial k} \right) \Delta P_0 + \sum_{i=1}^n \left(\frac{\partial f_0}{\partial P_\infty} \right) \left(\frac{\partial f_0}{\partial k} \right) \Delta P_\infty + \sum_{i=1}^n \left(\frac{\partial f_0}{\partial k} \right)^2 \Delta k = \sum_{i=1}^n E_i \left(\frac{\partial f_0}{\partial k} \right)$$

.... [2.21]

The partial derivatives can be written and calculated as follows:

From [2.15]

$$\left(\frac{\partial f_0}{\partial P_0} \right)_{P_\infty, k} = e^{-kt} \quad \left(\frac{\partial f_0}{\partial P_\infty} \right)_{P_0, k} = 1 - e^{-kt} \quad \left(\frac{\partial f_0}{\partial k} \right)_{P_0, P_\infty} = t(P_\infty - P_0) e^{-kt}$$

.... [2.22]

Thus with a given set of estimates equations [2.21] can be solved (by matrix inversion) to yield ΔP_0 , ΔP_∞ and Δk . The estimates are then updated, e.g:

$$k \text{ (improved)} = k \text{ (previous)} + \Delta k \quad \text{.... [2.23]}$$

and the calculation is repeated. This is continued until $\sum_{i=1}^n E_i^2$ converges to its smallest value (an appropriate test compares the value in successive cycles).

The final result is therefore the three required parameters P_0 , P_∞ and k . Standard deviations on these parameters can be estimated from the covariance matrix⁵ generated in solving the normal equations.

2.5 "ON-LINE" KINETICS WITH THE SP1800

2.5.1 Apparatus

The apparatus used for interactive kinetic studies is shown in Fig. (2.2). The SP1800 spectrophotometer was connected directly to the 'home-built' MIKE interface (MIKE = Microprocessor Instrumentation of Kinetic

JESS INTERFACE LOOKS LIKE A FACIT PUNCH TO THE LINE DRIVER. CONVERTS SIGNAL TO FORM REQUIRED BY COMPUTER. ALL DATA TRANSFER IS UNDER 'HANDSHAKE' CONTROL BY COMPUTER.

CELL CONTROL. 2-POSITION SWITCH FOR SINGLE OR MULTI CELL RUN

(2), (9) - PERIPHERAL DEVICE IDENTIFICATION USED BY THE PROGRAM

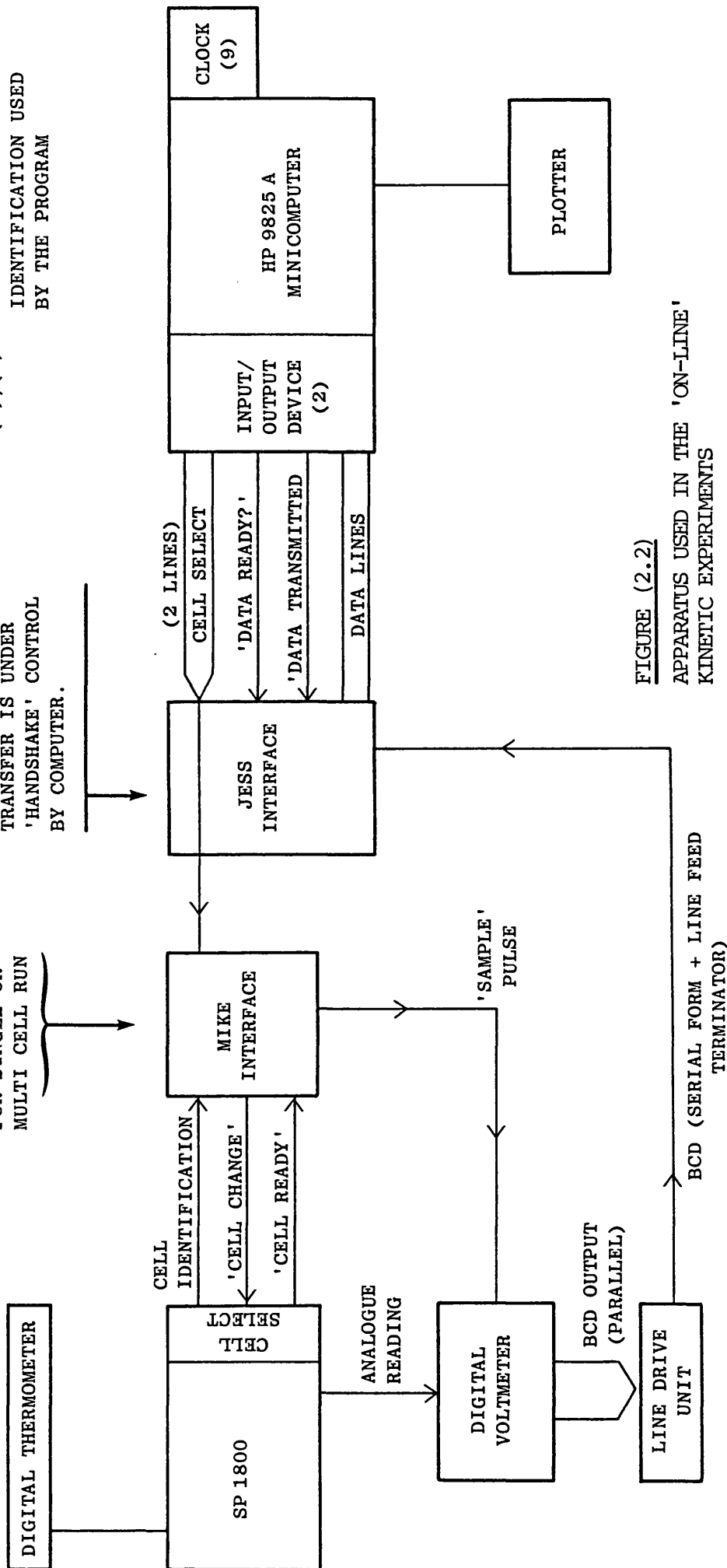


FIGURE (2.2)
APPARATUS USED IN THE 'ON-LINE'
KINETIC EXPERIMENTS

Experiments) which, in turn, was linked via a home-built data logging ('JESS') interface to a Hewlett-Packard 9825A minicomputer.

The computer incorporated 24 K bytes of RAM, three advanced-programming ROM modules, input/output interfaces and a real-time clock. It was also connected to a HP 7245A plotter. The whole system was under the control of the computer.

The MIKE interface was the key communication device between computer and spectrophotometer. The computer supplied a 'cell select' binary number, to call one of the four possible cells, coded as follows:

```
cell 1 = 0 0
cell 2 = 0 1
cell 3 = 1 0
cell 4 = 1 1
```

The MIKE interface compared the cell requested with the cell currently located in the light beam of the spectrophotometer using the 'cell identification' and 'cell ready' lines from the SP1800. The 'cell ready' signal indicated that a cell was accurately positioned and that a reading could be taken. If the 'cell selected' and 'cell ready' signals were not the same, the 'cell change' line to the spectrophotometer was activated to move the cell block until the correct cell was positioned.

At this stage, the interface activated the digital voltmeter to record the absorbance of the cell in position using the 'sample' line. To allow the pointer of the analogue meter in the SP1800 to come to rest after a cell change, a one-and-a-half second delay between the 'cell ready' and 'sample' pulses was introduced via MIKE interface hardware. For single cell kinetics a delay was not necessary so the interface was switchable for single- or multi- cell running.

The absorbance reading of a given cell was presented at the JESS interface. This interface was continually interrogated by the computer.

When a reading was available, the computer accepted it and returned a 'data transmitted' pulse to clear the interface in readiness for more data.

2.5.2 Kinetic experiments

A program for interactive control of kinetic experiments was written (Hewlett-Packard BASIC) by Dr. M. J. Blandamer. This program is documented in Appendix 1.

The program was stored on a data tape cartridge and loaded into the computer at the start of a series of kinetic runs.

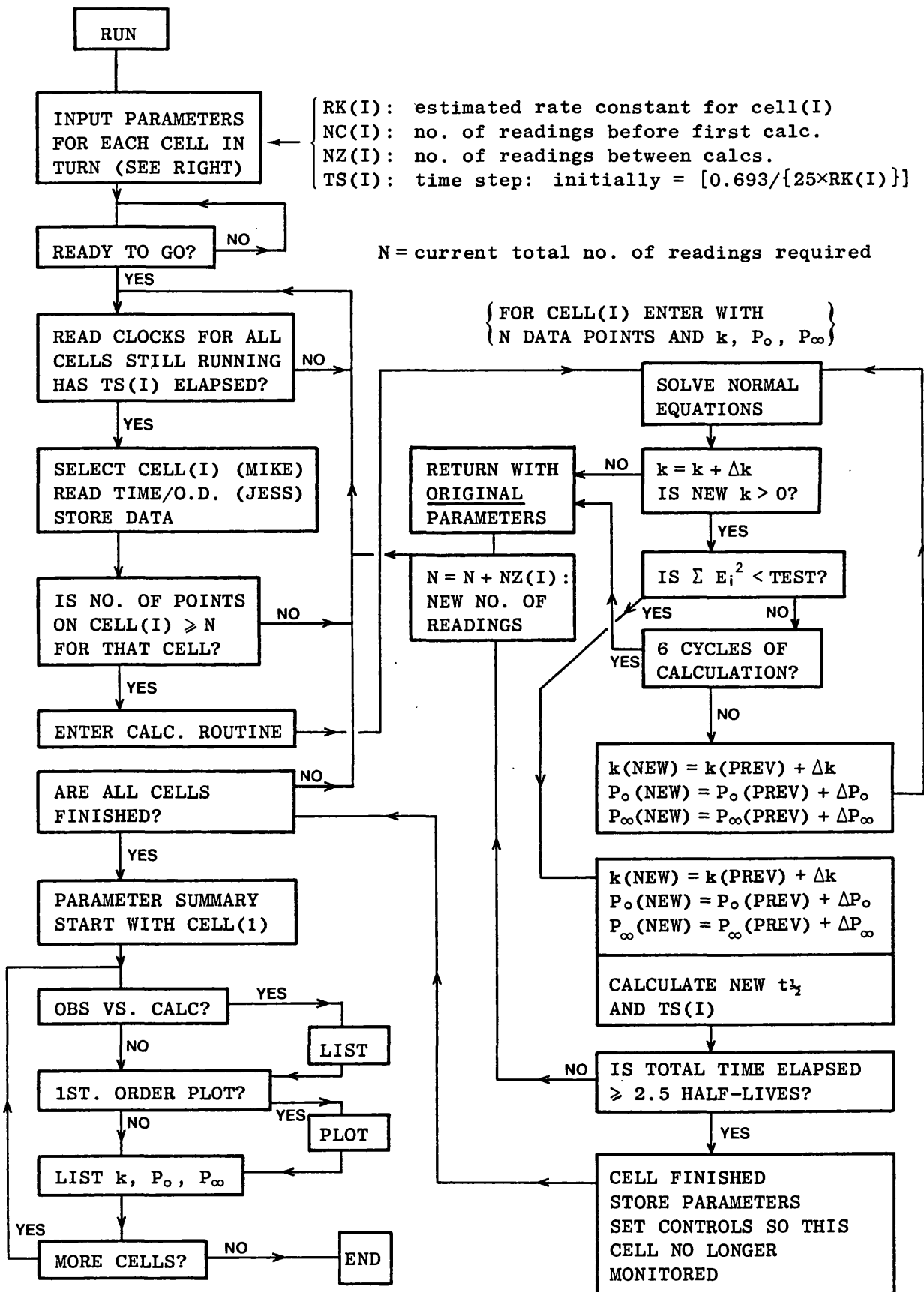
The spectrophotometer was thermostatted and cells prepared as described in section 2.3.

The program was initiated by typing 'RUN', and run identification data were entered. The program requested the number of cells in the run and the estimates of the run parameters for each cell. An initial time step for readings was calculated from the estimated rate constant. A choice was available for the number of readings to be taken on each cell before a calculation of the rate constant was attempted, and for the number of readings between successive calculations.

The program awaited a command to begin monitoring and reading the cells. The remaining reagent was added to the cells to initiate reaction, the analogue meter of the spectrophotometer was allowed to settle and the monitoring was initiated by one keystroke at the computer. The program took over complete control of the experiment. This control is summarized in flow-diagram form in Figure (2.3). The thermal printer output from the computer recorded labelled time and absorbance data for each cell; the results of the iterations at the calculation stages and final rate constants when cells had run for at least $2\frac{1}{2}$ half-lives. The LED display also showed time and absorbance at the point when the readings were

FIGURE (2.3)

FLOW DIAGRAM FOR MINICOMPUTER CONTROL OF KINETIC EXPERIMENTS



actually taken, and displayed a 'please do not touch' message between readings to indicate a run was in progress.

When all cells had run for at least $2\frac{1}{2}$ half-lives and satisfactory rate constants had been obtained, a parameter summary was presented, with the option of first-order plots of the form of equation [2.14]. Another run could be initiated in the same manner.

Typical computer outputs are listed in Appendix 1.

2.5.3 Comments and problems

The minicomputer system described in the last system was used for the routine accumulation of kinetic data for a chemical system which had been previously characterised and which was 'well-behaved'. Under these conditions, the measurement of first-order rate constants was efficient and largely trouble free.

Some care was needed in supplying the initial parameter estimates. A poor P_0 or P_∞ guess could drive the least-squares analysis away from minimization, usually with the result that a negative rate constant was obtained. The accumulation of additional data points generally did not rectify this, in which case the run was aborted. A bad initial estimate of the rate constant could also have undesirable results since the initial time step between readings was calculated from this number. A low guess meant that fast changes at the beginning of a run were missed. A high guess caused too many readings to be taken too soon, resulting in a set of data which did not really reflect the true kinetic profile. In this case, a negative rate constant was usually obtained initially, but further data accumulation did allow minimization.

Occasionally the digital voltmeter gave a 'spurious' reading, e.g. 1.9999, which usually prevented minimization and so caused run abortion. An attempt was made to introduce a 'check point' routine into the program,

but this would not overcome a hardware failure.

On rare occasions in a perfectly good run, the data minimization could become 'stuck' in a local minimum rather than the global one, giving a negative rate constant.

Baffling results could occur if a multi-cell run was attempted with the MIKE interface set for a single cell run!

The on-line analysis was especially powerful when second-order plots were being generated, as the data points (k_{obs} vs. nucleophile concentration) were available almost immediately the particular run was finished. Any dubious results could be spotted straight away when the rate pattern emerged.

CHAPTER 3

SOLVENT EFFECTS ON THE KINETICS OF REDOX
REACTIONS IN TRANSITION METAL CHEMISTRY

3.1 INITIAL STATE AND TRANSITION STATE SOLVATION EFFECTS IN THE 12-TUNGSTOCOBALTATE(III) OXIDATION OF IODIDE IN BINARY AQUEOUS MIXTURES

3.1.1 Introduction

Dissection of solvent effects on reactivity into initial state and transition state contributions has been completed for a variety of substitution reactions, as illustrated by Table (1.1). For these reactions, initial state effects either dominate or are comparable in magnitude to transition state effects.

Extension of this type of analysis into the area of redox chemistry began recently with a study of the peroxodisulphate oxidations of the $\text{Fe}(\text{phen})_3^{2+}$ cation¹ and of $\text{Fe}(\text{bipy})_2\text{CN}_2$.² For both these reactions the effect of solvent variation was much greater on the chemical potential of the transition state than the chemical potential of the initial state. Therefore, transition state effects dominate reactivity trends, in contrast to the situation for substitution reactions.

A problem with peroxodisulphate oxidation reactions is the possibility of radical formation in binary aqueous solvent mixtures. Redox reactions between one-electron oxidants and one-electron reductants would be preferable.

In Chapter 1 two possible mechanisms by which a redox reaction may occur were described: inner-sphere and outer-sphere. For the purposes of determining reactivity trends an outer-sphere mechanism is preferred because of its simplicity. Investigation of an inner-sphere reaction would be interesting because the mechanism combines a substitution step with a redox step and Section 3.2 reports a preliminary study of one example.

A reaction in which both reactants change their oxidation states by one and which is known to proceed by an outer-sphere mechanism is that

between the hexachloroiridate(IV) ion and iodide ion. An analysis of solvation effects for this reaction³ clearly indicates that transition state chemical potential changes dominate reactivity trends, as in the above examples.

This section reports an extension of this work for the 12-tungsto-cobaltate anions $[\text{CoW}_{12}\text{O}_{40}]^{5-}$ and $[\text{CoW}_{12}\text{O}_{40}]^{6-}$. These complexes contain cobalt(III) and cobalt(II) respectively. The encapsulated cobalt atom is substitution inert and in the same octahedral environment in both species.⁴ Thus the cobalt(III) anion, $[\text{CoW}_{12}\text{O}_{40}]^{5-}$, should act as an outer-sphere oxidant, and this has been demonstrated in a recent kinetic study involving benzenediols.⁵ Here the outer-sphere nature of the process was supported by conformance to the Marcus cross-relationship.⁶ Outer-sphere electron transfer has also been demonstrated for 12-tungsto-cobaltate oxidation of the vanadyl cation and of iodide.⁷ The kinetics of the oxidation of iodide in binary aqueous solvent mixtures with an initial state/transition state dissection on reactivity is reported here.

3.1.2 Experimental

$\text{K}_5[\text{CoW}_{12}\text{O}_{40}]\cdot 2\text{OH}_2\text{O}$ was prepared by Baker and McCutcheon's method.⁴ The yellow compound is slowly reduced to the dark green cobalt(II) analogue on exposure to light, so the compound and its solutions were kept in the dark. Solutions were also frozen between periods of use.

Because the electron transfer reaction was very fast, very low concentrations of reactants were used to make the kinetics accessible by the conventional technique at 298 K. Initial concentrations of 12-tungsto-cobaltate(III) were in the range 3 to 9×10^{-5} mol dm⁻³. When iodide concentration was in the range 1.5 to 6×10^{-3} mol dm⁻³ first-order kinetics were observed. The iodide was present as the potassium salt (AnalaR) and a constant ionic strength was maintained with potassium

chloride (AnalaR). Organic cosolvents were purified where necessary by established procedures.

Absorbance data were collected using the paper-tape logging apparatus described in Chapter 2. Rate constants were derived from $+d[I_2]/dt$ monitored at 345 nm. Their numerical values were therefore one half of rate constants corresponding to $-d[CoW_{12}O_{40}^{5-}]/dt$, since the redox step produces iodine atoms.

Solubility data for $K_5[CoW_{12}O_{40}]$ were obtained from the absorbances of diluted samples taken from saturated solutions of the salt in the appropriate binary aqueous mixtures. $\epsilon = 1150 \text{ dm}^3 \text{ mol}^{-1} \text{ cm}^{-1}$ at 388 nm.⁵

3.1.3 Results and discussion

The 12-tungstocobaltate(III) oxidation of iodide followed first order kinetics under large excess of iodide for at least three half-lives in all the conditions investigated. Observed first-order rate constants are reported in Table (3.1). They are consistent with the following rate law:

$$+\frac{d}{dt} [I_2] = \{k_1 + k_2 [I^-]\} [CoW_{12}O_{40}^{5-}] \quad \dots [3.1]$$

The k_2 term of this rate law can be confidently assigned to outer-sphere electron transfer between the two reactants.⁷ The nature of the reaction pathway giving rise to the (minor) k_1 term is not so obvious. By analogy with, for example, peroxodisulphate oxidation of iron(II) phenanthroline complexes⁸ this term can be assigned to a rapid redox step following a rate-determining dissociative step involving only the 12-tungstocobaltate(III). However, it proved difficult to obtain convincing evidence to support this hypothesis. Several other potential redox or substitution reactions of 12-tungstocobaltate(III) were sought, for example reactions with bromide, hexacyanoferrate(II), nickel(II), EDTA and hydroxide. Of

TABLE (3.1)

Observed first-order rate constants, k_{obs} , and derived rate constants k_1 and k_2 (defined in equation [3.1]) for 12-tungstocobaltate(III) oxidation of iodide in water and in binary aqueous mixtures at 298.2 K. Constant ionic strength = 0.0060 mol dm⁻³.

[KI]/mol dm ⁻³ :	0.0015	0.0020	0.0030	0.0040	0.0045	0.0050	0.0060	$10^2 k_1/s^{-1}$	$k_2 \pm \sigma^b$ dm ³ mol ⁻¹ s ⁻¹
SOLVENT ^a	$10^2 k_{\text{obs}}/s^{-1}$								
H ₂ O	2.0	2.4	3.5	4.4	4.9	6.4	0.5	0.5	9.8 ± 0.1
MeOH	0.60	0.75	1.06	1.36	1.68	0.14	0.14	0.14	3.1 ± 0.1
40%	0.23	0.28	0.37	0.50	0.59	0.70	0.06	0.06	1.1 ± 0.02
MeCN	0.63	1.04	1.74	2.8	3.6	~3 ^c			
DMSO	0.48	0.56	0.68	0.77	0.85	0.29	0.29	0.29	0.95 ± 0.04
30%	0.13	0.20	0.26	0.31	0.38	0.01	0.01	0.01	0.60 ± 0.02
40%	0.023	0.029	0.037	0.049	0.072	0.006	0.006	0.006	0.11 ± 0.004
60%				0.004					

^a Compositions of binary aqueous mixtures are given by volume before mixing.

^b Quoted values for σ are standard errors.

^c Approximate value only as the k_{obs} vs. $[I^-]$ plot is somewhat curved.

these, rates could only be measured satisfactorily for the reaction with hydroxide in water. Observed first-order rate constants are reported in Table (3.2). Solubility difficulties precluded the collection of rate data for binary aqueous solvent mixtures. The rate law for reaction with hydroxide, equation [3.2], is analogous to that for the reaction with iodide, equation [3.1]. The values of k_1 and k_1' are equal within experimental uncertainty, indicating a common rate determining dissociative pathway.

$$-\frac{d}{dt} [\text{CoW}_{12}\text{O}_{40}^{5-}] = \{k_1' + k_2' [\text{OH}^-]\} [\text{CoW}_{12}\text{O}_{40}^{5-}] \quad \dots [3.2]$$

Although there have been many kinetic studies of heteropolytungstates and related compounds,⁹ no data for dissociation or base hydrolysis of the 12-tungstocobaltate(III) anion could be found. However, the rate law for base hydrolysis of the analogous $[\text{SiW}_{12}\text{O}_{40}]^{4-}$ anion is similar to equation [3.2].¹⁰

The prime concern of the experiments was the k_2 term of equation [3.1], which represents the electron transfer process. The first comment to make is that these rates decrease markedly on adding organic cosolvents to the aqueous reaction medium (Table 3.1). This pattern follows that established for e.g. peroxodisulphate oxidation of iodide^{11,12} or of low-spin iron(II) diimine complexes,¹ and hexachloroiridate(IV) oxidation of iodide.³ We wish to apportion these rate decreases between chemical potential changes arising from solvation changes for each reactant and the transition state. In order to do this we need to estimate Gibbs free energies of transfer for the iodide and 12-tungstocobaltate(III) ions from water into the binary aqueous solvent mixtures used in the kinetic investigation.

Gibbs free energies of transfer for the iodide ion have been published for all the solvent mixtures studied here. Some interpolation of values

TABLE (3.2)

Mean observed^a first-order rate constants, k_{obs} , and derived rate constants k_1' and k_2' (defined in equation [3.2]) for reaction of 12-tungstocobaltate(III) with hydroxide in aqueous solution at 298.2 K.

[KOH]/mol dm ⁻³	0.025	0.050	0.075	0.100	k_2'	
SOLVENT	$10^2 k_{obs}/s^{-1}$				$10^2 k_1'/s^{-1}$ dm ³ mol ⁻¹ s ⁻¹	
H ₂ O	0.8	1.2	1.4	1.8	0.5	0.13 ± 0.01

^a Reaction monitored at 274 nm (shoulder of allowed UV band of complex).

and changes of units were needed to obtain values for $\delta_{m\mu}^{\ominus}(\text{I}^-)$ on the molar scale at the particular solvent compositions in which the kinetic results were obtained. Two sets of values for transfer to aqueous methanol are available, by Wells¹³ and de Ligny and co-workers,¹⁴ both based on calculations of the Born type. Values for transfer into aqueous acetonitrile¹⁵ and into aqueous dimethyl sulphoxide¹⁶ are based on the $\delta_{m\mu}^{\ominus}(\text{AsPh}_4^+) = \delta_{m\mu}^{\ominus}(\text{BPh}_4^-)$ assumption.¹⁷

Gibbs free energies of transfer are not available for the 12-tungstocobaltate anion, and therefore these have been estimated by solubility measurements on the potassium salt and the use of published values for $\delta_{m\mu}^{\ominus}(\text{K}^+)$. Values of $\delta_{m\mu}^{\ominus}(\text{K}_5[\text{CoW}_{12}\text{O}_{40}])$ were calculated directly from the measured solubilities. In splitting these values into cation and anion components, negligible ion pairing is assumed. Although the anion has a charge of 5-, it is large, and estimates for K_{ip} from theoretical equations or from extrapolation of known K_{ip} values¹⁸ suggest that there will be only a few per cent of ion-pairs in any of the solvent media used here. This will have only a very small effect on ion transfer values, introducing an uncertainty which is negligible in comparison with other uncertainties in the analysis of solvent effects on reactivity. The estimates for $\delta_{m\mu}^{\ominus}(\text{CoW}_{12}\text{O}_{40}^{5-})$ are shown in Table (3.3), which includes the values and sources used for $\delta_{m\mu}^{\ominus}(\text{K}^+)$.

From the kinetic data [k_2 values from Table (3.1)] values for $\delta_{m\Delta G}^{\ddagger}$ can be calculated. Although specific cation effects have been reported on the rate of 12-tungstocobaltate(III) oxidation of iodide in aqueous solution,⁷ these effects do not operate at the low concentrations used in the experiments described here. From the $\delta_{m\Delta G}^{\ddagger}$ values and $\delta_{m\mu}^{\ominus}$ (initial state) estimates, values of $\delta_{m\mu}^{\ddagger}$ can be calculated. These calculations are shown in Table (3.3) which incorporates different sets of values for $\delta_{m\mu}^{\ominus}$ (ion)

TABLE (3.3)

Dissection of solvent effects on reactivity into initial state and transition state contributions for the 12-tungstocobaltate(III) ^a oxidation of iodide at 298.2 K. All transfer quantities are from water on the molar scale.

Cosolvent % v/v	MeOH		DMSO		MeCN 40
	20	40	20	40	
$k_2/\text{dm}^3 \text{ mol}^{-1} \text{ s}^{-1}$ ^b	3.1	1.1	0.95	0.60	~3
$\therefore \delta_m \Delta G^\ddagger / \text{kJ mol}^{-1}$	+2.9	+5.5	+5.8	+6.9	~+3
$\text{solv.} (K_5 [\text{Co}^{\text{III}}]) / \text{mol dm}^{-3} \text{ } \ominus$	0.092	0.062	0.077	0.074	0.080
$\therefore \delta_m \mu^\ominus (K_5 [\text{Co}^{\text{III}}]) / \text{kJ mol}^{-1}$	+0.8	+6.7	+3.4	+3.9	+2.8
$5\delta_m \mu^\ominus (K^+) / \text{kJ mol}^{-1}$	+4.5 ^d	-1.5 ^e	-1.5 ^f	-4.0 ^f	+2.1 ^g
$\therefore \delta_m \mu^\ominus ([\text{Co}^{\text{III}}]) / \text{kJ mol}^{-1}$	-3.7	+2.3	+4.9	+7.9	+0.7
$\delta_m \mu^\ominus (I^-) / \text{kJ mol}^{-1}$	+1.6 ^d	+1.6 ^e	+0.5 ^f	+1.2 ^f	+0.8 ^g
$\therefore \delta_m \mu^\ominus (\text{initial state}) / \text{kJ mol}^{-1}$	-2.1	+3.9	+5.4	+9.1	+1.5
$\therefore \delta_m \mu^\ddagger / \text{kJ mol}^{-1}$	+0.7	+6.8	+11.2	+16.0	~+5
		+21.8		+29.8	

^a Abbreviated here to $[\text{Co}^{\text{III}}]$; ^b $k_2 = 9.8 \text{ dm}^3 \text{ mol}^{-1} \text{ s}^{-1}$ in water; ^c solubility in water = $0.097 \text{ mol dm}^{-3}$; ^d from Ref. (13); ^e from Ref. (14); ^f from Ref. (16); ^g from Ref. (15).

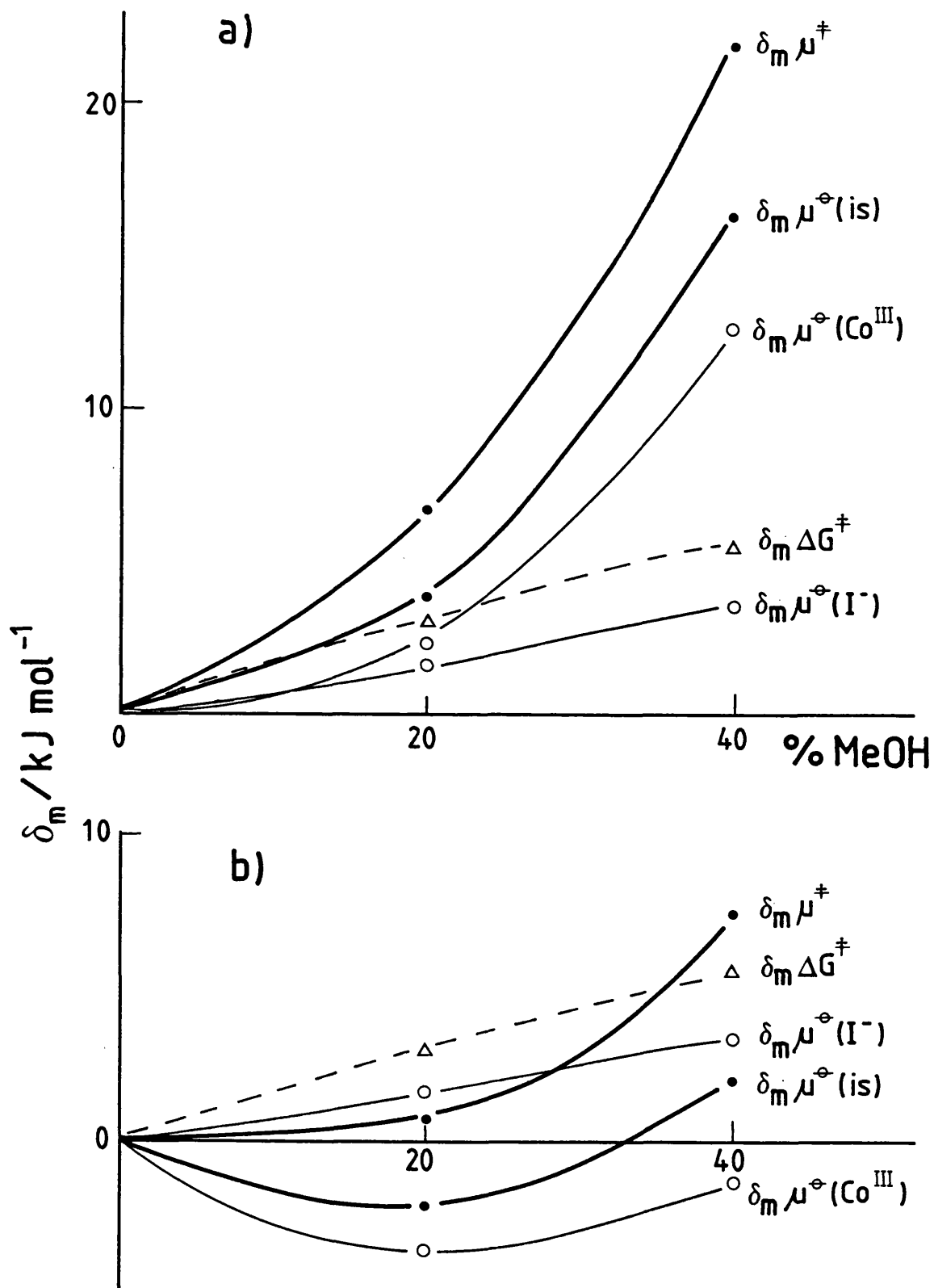
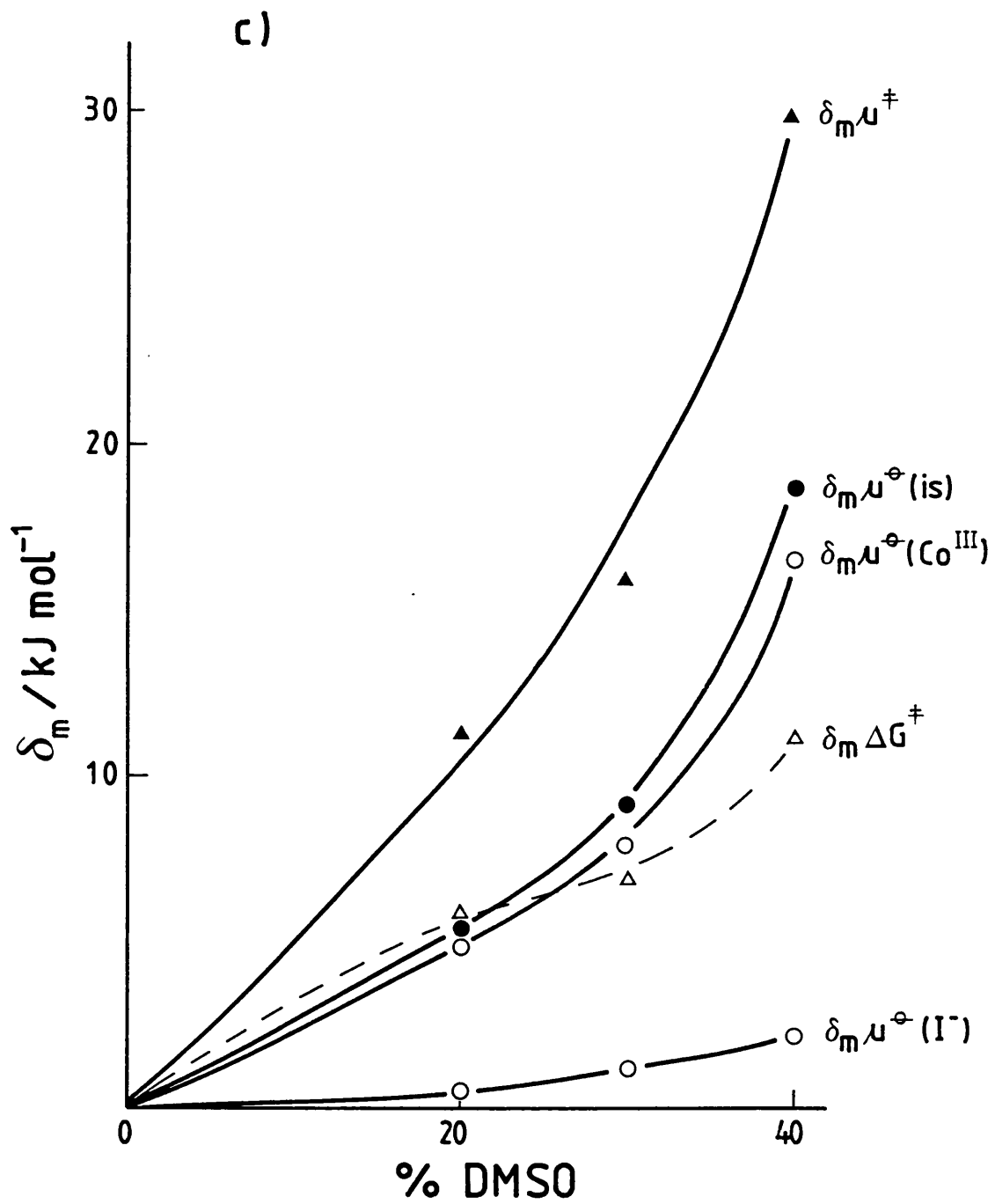


FIGURE (3.1)

Initial state and transition state contributions to solvent effects on reactivity for 12-tungstocobaltate(III) oxidation if iodide in (a) and (b), aqueous methanol and (c), aqueous DMSO at 298 K.

Single ion assumptions: (a) de Ligny, ref. 14, (b) Wells, ref. 13, (c) Cox, ref. 15.



where these are given. The dissection of solvent effects into initial state and transition state components set out in Table (3.3) is illustrated diagrammatically in Figure (3.1).

A general pattern emerges, though the detailed picture depends somewhat on the nature of the organic cosolvent and of the single ion assumptions used. In all cases, the transition state is destabilized on transfer from water into mixed aqueous solvents, while the initial state is destabilized to a smaller extent or even slightly stabilized. This behaviour is similar to that found for the hexachloroiridate(IV)-iodide and -catechol reactions³ and peroxodisulphate oxidation of $\text{Fe}(\text{bipy})_2(\text{CN})_2$ ². However, this pattern does not apply in all redox reactions. In the peroxodisulphate oxidation of $\text{Fe}(\text{phen})_3$ ²⁺ in aqueous methanol and in aqueous DMSO, the initial state is markedly stabilized while the transition state is slightly stabilized on transfer from water.¹ In the bromide-bromate reaction, for which kinetic data are available in several aqueous ethanol mixtures,¹⁹ it seems likely that both initial and transition states are considerably destabilized on transfer from water, with the transition state slightly less destabilized than the initial state.

Figure (3.1a) probably gives a better representation of solvation changes than Figure (3.1b) especially with regard to the 12-tungsto-cobaltate(III) anion. Figure (3.1b), which uses Wells' single ion values, shows this anion as being stabilized on transfer from water to 20% by volume methanol-water. This is surprising in view of the fact that solvent structure-making is at a maximum in this region of methanol-water solvent composition; it is difficult to expect more favourable dissolution of the large cobalt (and iodide) anions into this enhanced structure than into water itself. Figure (3.1b) is more acceptable in this respect.

This section is concluded with a brief consideration of solvent effects

TABLE (3.4)

Dissection of solvent effects on reactivity into initial state and transition state contributions for dissociation of the 12-tungstocobaltate(III) anion, at 298.2 K.
 All transfer quantities are from water, on the molar scale.

Cosolvent % v/v	MeOH			DMSO		
	20	30	40	20	30	40
$10^4 k_1/s^{-1}$ ^a	14	1	6	29	1	0.6
$\therefore \delta_m \Delta G^\ddagger / kJ mol^{-1}$	+3.2		+5.3	+1.4	+9.7	+11.0
$\delta_m \mu^\ominus$ (initial state) / $kJ mol^{-1}$ ^b	-3.7	+2.3	-1.3	+4.9	+7.9	+16.6
$\therefore \delta_m \mu^\ddagger / kJ mol^{-1}$ ^c	-0.5	+5.5	+4.0	+6	+17	+27

^a From Table (3.1); ^b $\delta_m \mu^\ominus$ ([CoIII]) from Table (3.3) (q.v. for single ion assumptions);

^c a dissociative mechanism is assumed. An associative hydrolysis mechanism would only make a small difference (up to about 1 kJ mol⁻¹) to these $\delta_m \mu^\ddagger$ estimates.

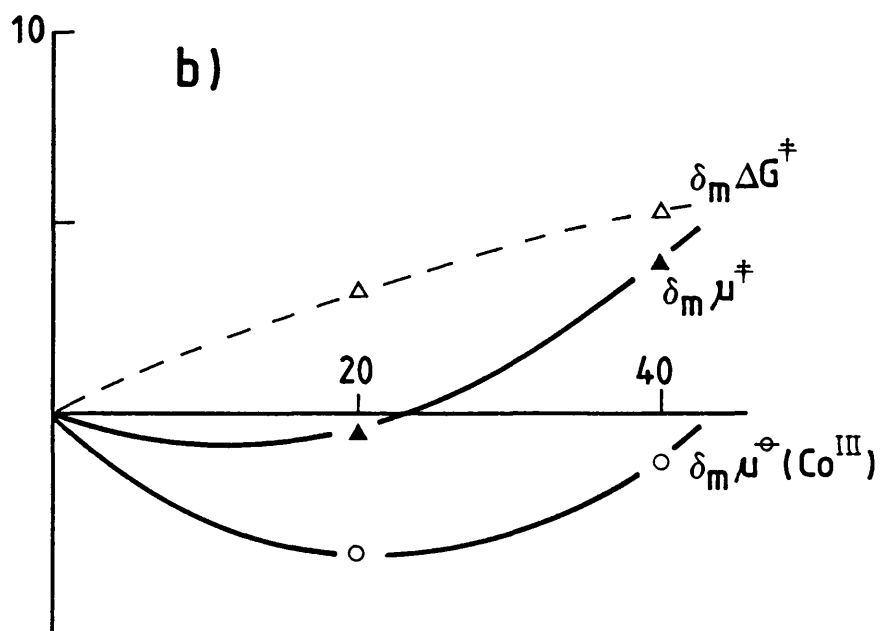
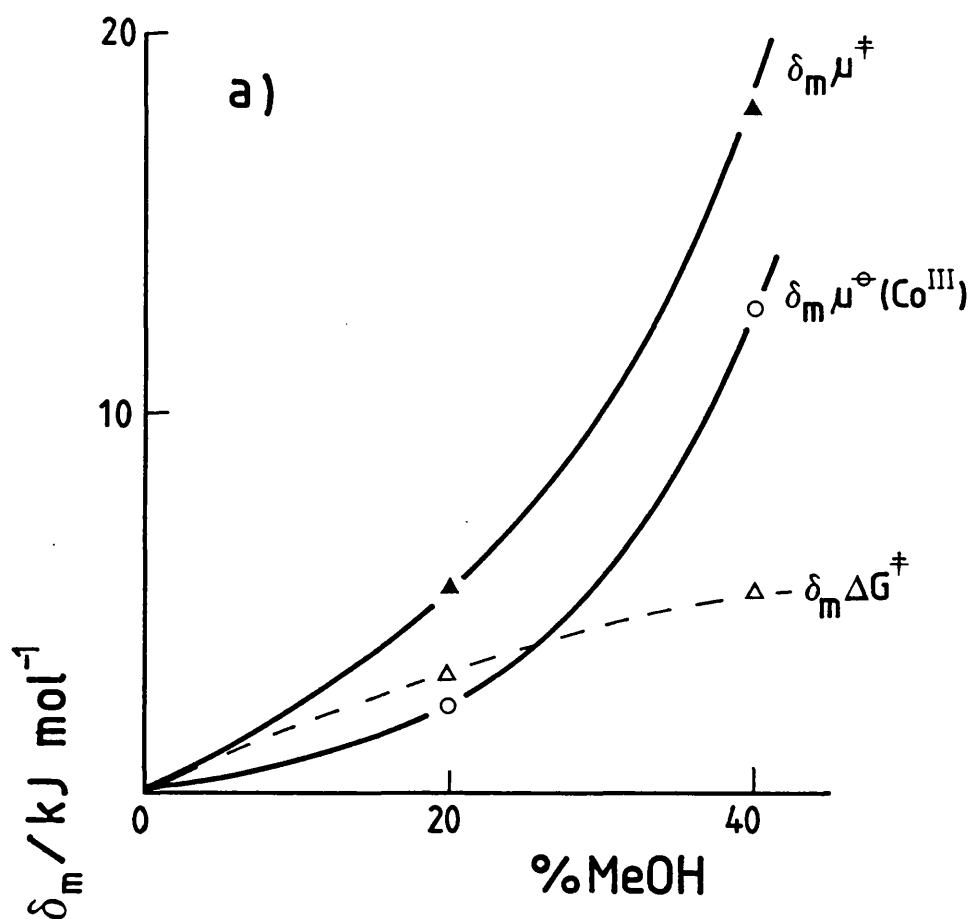
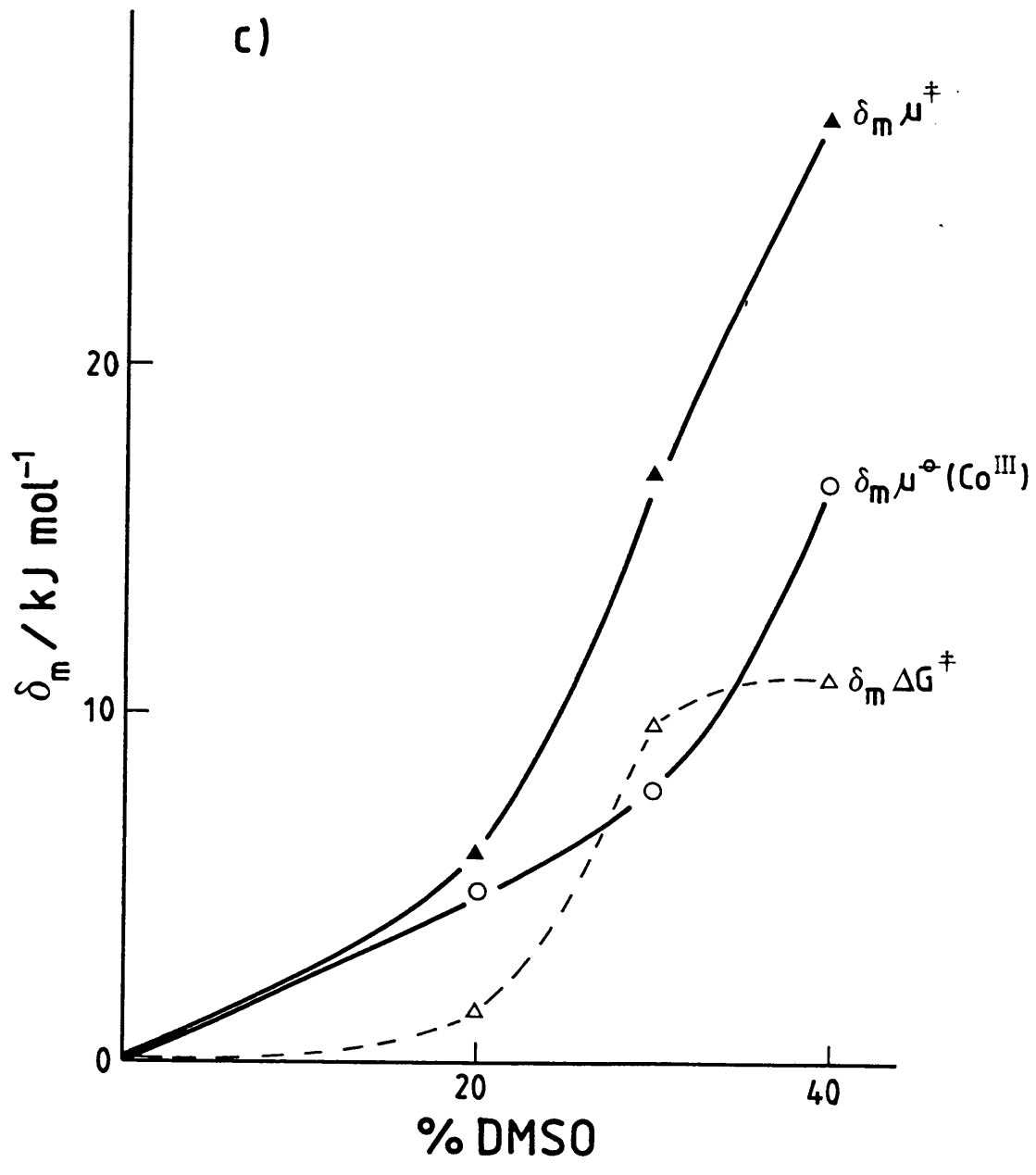


FIGURE (3.2)

Initial state and transition state contributions to solvent effects on reactivity for the dissociation of the 12-tungstocobaltate(III) anion in (a) and (b), aqueous methanol and (c), aqueous DMSO at 298 K.

Single ion assumptions used are as in Figure (3.1) caption.



on 12-tungstocobaltate(III) dissociation, the k_1 term of equation [3.1]. The k_1 values in Table (3.1) are approximate as they represent small intercepts. Nevertheless, it is clear that k_1 decreases markedly as the proportion of organic cosolvent increases. A plot of $\log_{10} k_1$ against solvent Y values²⁰ is not a good straight line, but there is a trend corresponding to a slope, \underline{m} , of the order of unity. This is much larger than \underline{m} values reported for other inorganic substitutions.²¹ This unusually large value may be due to the very hydrophilic nature of leaving group and non-leaving moiety, both having oxygen-atom peripheries. An initial state - transition state dissection of solvent effects (Table 3.4, Figure 3.2) shows that the transition state is probably destabilised even more than the initial state on transfer from water into the mixed solvents. The situation for transfer to aqueous methanol is confused by the differences arising from the different single ion assumptions involved. However, Wells's approach leads to the conclusion that the reactivity trend is attributable almost entirely to initial state stabilisation, which seems unlikely here.

3.2 A PRELIMINARY STUDY OF SOLVENT EFFECTS ON AN INNER-SPHERE REDOX REACTION

3.2.1 Introduction

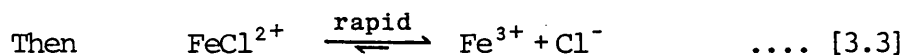
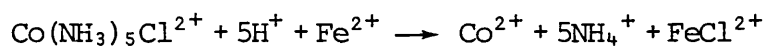
Dissection of the effect of solvent on the rate of an inner-sphere redox reaction is an interesting and important project in the context of the work described in this thesis. Because an inner-sphere mechanism involves both a redox and a substitution step the relative importance of initial state and transition state contributions will depend to a large extent on the relative contributions to the speed of the reaction from each step of the mechanism. The substitution step is probably the slowest step of the inner-sphere pathway (when persistent intermediates are not

formed) so it may well be that for reactions proceeding by this mechanism initial state solvation trends dominate the reactivity pattern.

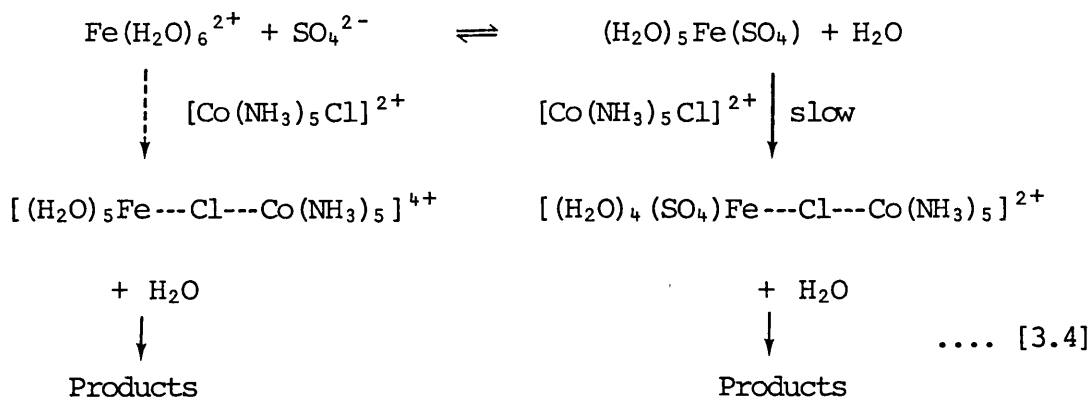
An obvious example of an inner sphere process is the chromium(II) reduction of the $\text{Co}(\text{NH}_3)_5\text{Cl}^{2+}$ cation²² (see equation [1.29]). However, this reaction is too fast to be followed by conventional spectroscopic techniques, and because chromium(II) is air-sensitive the reaction must be carried out under an inert atmosphere using degassed solvents. Calculation of $\delta_{\text{m}\mu}^{\ominus}(\text{Cr}^{2+})$ is also difficult because of the lack of background knowledge concerning single ion transfer parameters for transition metal cations. The Cr^{2+} ion would reduce counter-anions such as ClO_4^- or IO_3^- .

The reduction of the $\text{Co}(\text{NH}_3)_5\text{Cl}^{2+}$ cation by iron(II) has been shown to proceed via the expected inner sphere mechanism from an analysis of volumes of activation.²³ The reaction has been studied where the iron(II) is introduced as the perchlorate salt^{23,24} and as iron(II) ammonium sulphate.²⁵

For iron(II) perchlorate, the reaction proceeds via a straightforward inner-sphere mechanism:



For iron(II) ammonium sulphate, the second-order rate constant and volume of activation are significantly larger. These results have been discussed²⁵ in terms of a rapid pre-equilibrium between iron(II) and sulphate ions which is established before the rate-determining inner sphere step. This step proceeds predominantly via the iron(II) sulphato-complex:



In this section, second-order rate constants are reported for the reduction of $[\text{Co}(\text{NH}_3)_5\text{Cl}]^{2+}$ by iron(II) perchlorate and iron(II) ammonium sulphate in water and in aqueous methanol. Dissection of the solvent effect on the reactivity is discussed for the reaction with iron(II) in perchlorate medium.

3.2.2 Experimental

$[\text{Co}(\text{NH}_3)_5\text{Cl}]\text{Cl}_2$ was prepared by an established method.²⁶ Kinetic data were obtained using the minicomputer-controlled apparatus.

Iron(II) perchlorate was prepared from iron wire and 60% perchloric acid (B.D.H.). In the kinetic runs, the initial concentration of iron(II) was 0.5 mol dm^{-3} (ionic strength = 1.5 mol dm^{-3}), and of $[\text{Co}(\text{NH}_3)_5\text{Cl}]^{2+}$ was ca. $5 \times 10^{-3} \text{ mol dm}^{-3}$. These concentrations were used in each solvent mixture. The reaction was monitored at 535 nm.

Iron(II) ammonium sulphate (AnalaR) was used as supplied. The initial concentration of iron(II) was 0.1 mol dm^{-3} (ionic strength = 0.7 mol dm^{-3}) and of $[\text{Co}(\text{NH}_3)_5\text{Cl}]^{2+}$ was ca. $2 \times 10^{-3} \text{ mol dm}^{-3}$. Fresh stock solutions of iron(II) were made up approximately every hour. The reaction was monitored at 340 or 350 nm.

3.2.3 Results and discussion

Reduction of $[\text{Co}(\text{NH}_3)_5\text{Cl}]^{2+}$ by iron(II) perchlorate followed first-

order kinetics for at least $2\frac{1}{2}$ half-lives in each solvent. The repeat scan spectrum showed an isosbestic point at 365 nm. The absorbance at 535 nm for the complex decreased with time and a new band grew at 333 nm corresponding to FeCl^{2+} . Derived second-order rate constants are reported in Table (3.5). The value for reaction in water is in agreement with the literature value.²⁴ The rate constant increased as the proportion of organic cosolvent increased.

Reduction of $[\text{Co}(\text{NH}_3)_5\text{Cl}]^{2+}$ by iron(II) ammonium sulphate also followed first-order kinetics for at least $2\frac{1}{2}$ half-lives in each solvent. The value in water is in excellent agreement with that given in reference 25. Derived second-order rate constants are reported in Table (3.6). The rate constant increased markedly as the proportion of organic cosolvent increased.

As can be seen from Tables (3.5) and (3.6), the effect of added methanol on the second-order rate constant is greater for the iron(II) ammonium sulphate system than for the iron(II) perchlorate system. Presumably this is a result of solvent effects on the pre-equilibrium, where two charged species produce a neutral species. The ions will be destabilised as methanol is added to the system and the equilibrium will be displaced to the right. This enhances reactivity via the predominant pathway.

For the iron(II) perchlorate system, an initial state - transition state dissection of reactivity trends has been carried out. Estimates of $\delta_{\text{m}}\mu^\ominus(\text{Fe}^{2+})$ from water into methanol-water mixtures have been made using formation constant data for the $[\text{Fe}(\text{phen})_3]^{2+}$ cation.²⁷ The exceptional stability of iron(II) complexes of this type provides a unique opportunity for obtaining single-ion transfer parameters for a transition metal aquo-cation.

TABLE (3.5)

Second-order rate constants for the reduction of $[\text{Co}(\text{NH}_3)_5\text{Cl}]^{2+}$ by iron(II) perchlorate in water and methanol-water mixtures at 298.2 K, with a dissection of the solvent effect on reactivity into initial state and transition state contributions.

Solvent ^a	Water	% Methanol		
		20	30	40
$10^3 k_2 / \text{dm}^3 \text{ mol}^{-1} \text{ s}^{-1}$	1.19 ^b	1.85 ^b	2.09 ^b	
$\therefore \delta_m \Delta G^\ddagger / \text{kJ mol}^{-1}$		-1.09	-1.40	
$\delta_m \mu^\ominus([\text{Co}(\text{NH}_3)_5\text{Cl}]\text{Cl}_2) / \text{kJ mol}^{-1}$		+4.68 ^c		+9.32 ^c
$2\delta_m \mu^\ominus(\text{Cl}^-) / \text{kJ mol}^{-1}$		+4.8 ^d		+11.6 ^d
$\therefore \delta_m \mu^\ominus([\text{Co}(\text{NH}_3)_5\text{Cl}]^{2+}) / \text{kJ mol}^{-1}$		-0.12		-2.28
$\delta_m \mu^\ominus(\text{Fe}^{2+}) / \text{kJ mol}^{-1}$		+1.7 ^e		+2.0 ^e
$\therefore \delta_m \mu^\ominus(\text{initial state}) / \text{kJ mol}^{-1}$		+1.58	+1.0 ^f	-0.28
$\therefore \delta_m \mu^\ddagger / \text{kJ mol}^{-1}$		+0.49	-0.40	

^a solvent compositions by volume before mixing;

^b $k_2 = k_{\text{obs}} / [\text{Fe}^{2+}]$. $[\text{Fe}^{2+}] = 0.5 \text{ mol dm}^{-3}$;

^c from solubility data;

^d ref. 13 (Wells);

^e ref. 27;

^f interpolated.

All transfer quantities are on the molar scale.

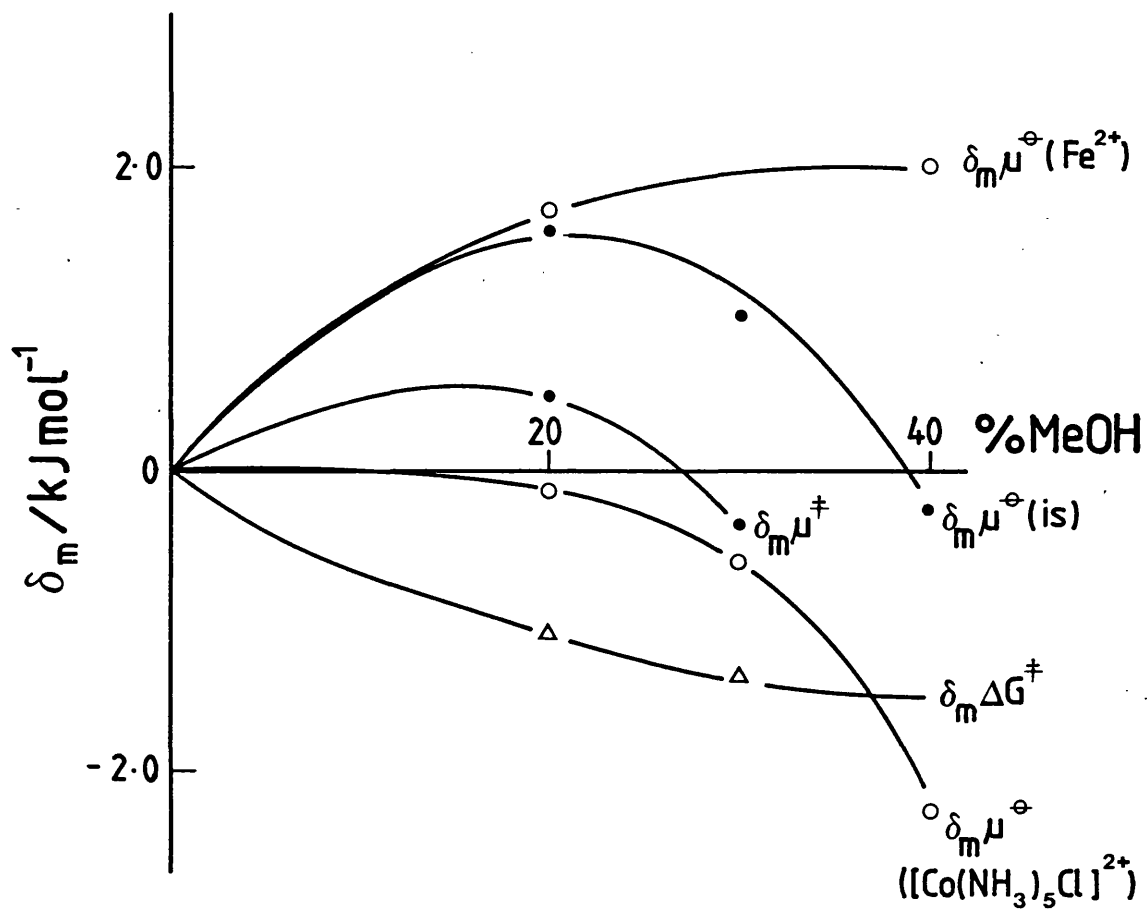


FIGURE (3.3)

Initial state and transition state contributions to solvent effect on reactivity for iron(II) reduction of $[\text{Co}(\text{NH}_3)_5\text{Cl}]^{2+}$ in aqueous methanol at 298.2 K.

TABLE (3.5)

Mean second-order rate constants for the reduction of $[\text{Co}(\text{NH}_3)_5\text{Cl}]^{2+}$ by iron(II) ammonium sulphate in water and methanol-water mixtures at 298.2 K, with solvent effect on reactivity in terms of the transfer function $\delta_m\Delta G^\ddagger$.

Solvent ^a	Water	% Methanol	
		20	40
$10^3 k_2/\text{dm}^3 \text{ mol}^{-1} \text{ s}^{-1}$	8.69 ^b	25.2 ^b	61.4 ^b
$\therefore \delta_m\Delta G^\ddagger/\text{kJ mol}^{-1}$		-2.63	-4.85

^a solvent compositions by volume before mixing

^b $k_2 = k_{\text{obs}}/[\text{Fe}^{2+}]$. $[\text{Fe}^{2+}] = 0.1 \text{ mol dm}^{-3}$.

The dissection of solvent effect on reactivity is shown in Table (3.5) and illustrated in Figure (3.3). With reference to this Figure, the pattern of relative solvation changes for the initial and transition states is probably correct. However, it is difficult to visualise the negligible change in the chemical potential of the $[\text{Co}(\text{NH}_3)_5\text{Cl}]^{2+}$ cation arising from the values used for $\delta_{m\mu}^\ominus(\text{Cl}^-)$, especially on comparison with the behaviour in ethanol-water mixtures where this cation is considerably destabilised.²⁸ Wells' values for $\delta_{m\mu}^\ominus(\text{Cl}^-)$ must be used here for compatibility with the derivation of $\delta_{m\mu}^\ominus(\text{Fe}^{2+})$. If values for $\delta_{m\mu}^\ominus(\text{Cl}^-)$ were taken from the set produced recently for methanol-water by Abraham,²⁹ then the resulting pattern would show the initial state, and therefore the transition state in this case, to be destabilised considerably, the latter to a smaller extent than the former. [Chapter 4 contains a more detailed

comparison of the results obtained when two different sets of single-ion values are used in conjunction with the same kinetic data.]

This situation may be compared with that for mercury(II)-catalysed aquation of the $[\text{Co}(\text{NH}_3)_5\text{Cl}]^{2+}$ cation, which is a similar process with the Hg^{2+} cation bonding at the chloride instead of the Fe^{2+} cation. Here a very small change in rate on passing from water to ethanol-water mixtures is attributed to comparable destabilisation of both initial and transition states. The difference in behaviour between the iron(II) and mercury(II) reactions must therefore be largely assigned to some difference in solvation characteristics of these ions.

In the inner sphere reduction by iron(II), a significant contribution to the volume of activation ($+8 \text{ cm}^3 \text{ mol}^{-1}$ ²³) is the release of coordinated and electrostricted water from the Fe^{2+} cation in the formation of the bridged intermediate. This electrostriction will cause the initial state to be more sensitive to changes in the solvent environment than the transition state, where the electrostriction will have been removed. In these terms, the initial and transition states for the Hg^{2+} case show similar sensitivity to solvation changes (volume of activation = $+2 \text{ cm}^3 \text{ mol}^{-1}$ ²³).

To summarise, these initial experiments have probably justified the expectation that initial state effects predominate in an inner sphere redox mechanism involving ions of like charge. This is in contrast to the case for the outer sphere redox mechanisms discussed previously, where transition state effects predominate. The discussion in this section has also illustrated how additional information such as volume of activation can help to rationalise solvation changes.

There are several reports of kinetic studies of inner sphere redox reactions in mixed aqueous solvents in the literature. Initial state -

transition state dissections of these data are mainly hindered by lack of information concerning free energies of transfer of the required reductant cation into the required solvent mixture. Once this information is available, systems which could be analysed include:

- (i) $[\text{Co}(\text{NH}_3)_5\text{Br}]^{2+}/\text{Fe}^{2+}$ in ethanol-water, propanol-water and butanol-water;³⁰
- (ii) $[\text{Co}(\text{NH}_3)_5\text{X}]^{2+}/\text{Fe}^{2+}$ in DMSO-water (X = F, Cl, Br);³¹
- (iii) $[\text{Co}(\text{en})_3]^{3+}/\text{Cr}^{2+}$ and V^{2+} in ethanol-water and DMF-water.³²

The iron(II) reduction of $[\text{Co}(\text{C}_2\text{O}_4)_3]^{3-}$ has been characterised³³ and under pseudo first-order conditions would have rates accessible by the slowest stopped-flow techniques. As the complex is readily prepared, this system would seem a likely candidate for study in methanol-water solvent mixtures.

The reference to mercury(II)-catalysed aquation in this section provides a link with Chapter 4, where this subject is discussed more fully.

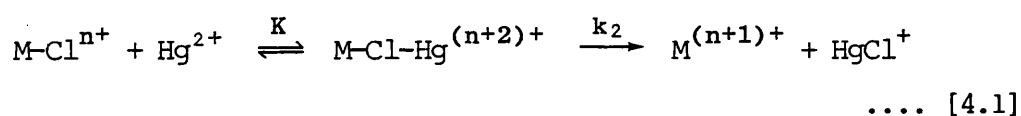
CHAPTER 4

SOLVENT EFFECTS ON THE MERCURY (II)-CATALYSED
AQUATION OF CHLORO-TRANSITION METAL COMPLEXES

4.1 INTRODUCTION

This chapter reports an examination of solvent effects on reactivity in one example of metal-ion catalysed aquation of transition metal complexes. This account includes a brief comparison of the results of initial state-transition state dissections of the reactivities when single-ion transfer parameters based on differing extrathermodynamic assumptions are used.

Analysis of solvent effects on inorganic systems in the manner described in this thesis is more readily carried out on bimolecular than on unimolecular reactions, due to technical reasons connected with the collection of required rate and thermodynamic data. There are relatively few examples of bimolecular substitution reactions of octahedral complexes. A well-documented reaction of this type is the mercury(II)-catalysed aquation of chloro-complexes.^{1,2} Though dissociative as far as the central metal ion is concerned, these reactions are in fact bimolecular S_E2 processes at the coordinated chloride:



As discussed in Chapter 1 the dinuclear M-Cl-Hg⁽ⁿ⁺²⁾⁺ species in equation [4.1] may be either a genuine intermediate or the transition state for a one-step S_E2 process. The general dependence of k_{obs} (Hg²⁺ in large excess) on mercury(II) concentration is shown in Figure (4.1). When M-Cl-Hg⁽ⁿ⁺²⁾⁺ is a transition state, second-order kinetic behaviour is observed (region A in the figure). When this dinuclear species has much greater stability, being formed rapidly and completely from reactants, k_{obs} is constant (region C in the figure). In intermediate circumstances, plots of k_{obs} against [Hg²⁺] are curved (region B in the figure). All

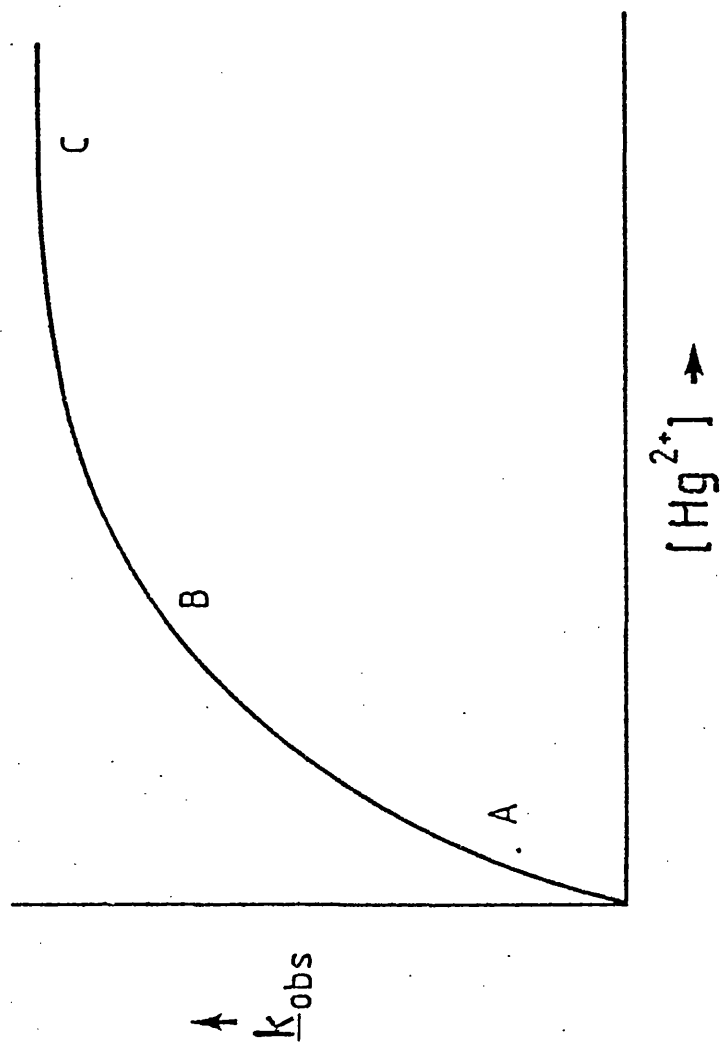


FIGURE (4.1)

General diagram of the variation of observed first-order rate constant, k_{obs} , for mercury(II)-catalysed aquation of chloro-complexes on mercury(II) concentration [large excess].

three types of kinetic behaviour have been reported for this type of reaction in aqueous solution. Initial state - transition state analyses on reactions of the first type involving $[\text{Co}(\text{NH}_3)_5\text{Cl}]^{2+}$ and $[\text{ReCl}_6]^{2-}$ have been reported.³ A partial analysis of an organic solvolysis exhibiting an intermediate has been carried out for the mercury(II)-catalysed solvolysis of the anti-inflammatory agent fenclorac (α -3-dichloro-4-cyclohexylbenzene-acetic acid).⁴

This chapter describes the results of the investigation of two rhodium complexes and two chromium complexes in this context.

(i) $\text{trans-}[\text{Rh}(\text{en})_2\text{Cl}_2]^+$: this complex exhibits 'type B' behaviour.

The solvent dependence of K and k_2 is established, and the results are analysed as far as possible into solvent effects on reactants, intermediate and transition state.

(ii) $\text{cis-}[\text{Rh}(\text{en})_2\text{Cl}_2]^+$: this complex exhibits 'type C' kinetic behaviour. An analysis of kinetic results for reaction in water and aqueous methanol is given.

(iii) $[\text{Cr}(\text{NH}_3)_5\text{Cl}]^{2+}$, $[\text{Cr}(\text{NH}_3)_4(\text{H}_2\text{O})\text{Cl}]^{2+}$: these complexes exhibit 'type A' behaviour. Results of initial state - transition state dissections of reactivity in mixed solvents are compared with those for $[\text{Co}(\text{NH}_3)_5\text{Cl}]^{2+}$.

4.2 EXPERIMENTAL

(i) $\text{trans-}[\text{Rh}(\text{en})_2\text{Cl}_2]^+$:

$\text{trans-}[\text{Rh}(\text{en})_2\text{Cl}_2]\text{NO}_3$ was prepared by a published method.⁶ Solutions of mercury(II) nitrate were prepared by dissolving mercury(II) oxide (May & Baker) in the required volume of concentrated nitric acid and made up to give a stock solution of $1.5 \text{ mol dm}^{-3} \text{ Hg}(\text{NO}_3)_2$ in 0.67 mol dm^{-3} nitric acid. Acidic conditions were used to prevent polymerisation or

hydrolysis of the mercury(II). Ionic strengths were maintained using a similar stock solution of magnesium nitrate.

The run conditions were as follows:

- (a) initial concentration of complex: $1.8 \times 10^{-3} \text{ mol dm}^{-3}$
- (b) $[\text{Hg}^{++}]$ range: 0.08 to 0.75 mol dm^{-3}
- (c) constant nitric acid concentration: 0.33 mol dm^{-3}
- (d) overall constant ionic strength: 2.58 mol dm^{-3} .

Kinetic runs were monitored at 420 nm. Rate constants were obtained from absorbance data (paper-tape logged) over at least $2\frac{1}{2}$ half-lives. Solubility data were obtained for $\text{trans-}[\text{Rh}(\text{en})_2\text{Cl}_2]\text{ClO}_4$. This was prepared by the addition of a saturated solution of the nitrate salt to a concentrated aqueous solution of sodium perchlorate. Concentrations of the rhodium complex were obtained from spectrophotometric measurements ($\epsilon = 1510$ at 240 nm^7) of saturated solutions of the perchlorate salt in the required solvent mixtures.

Values of $\delta_{\text{ml}}^{\ominus}(\text{ClO}_4^-)$ for acetonitrile-water mixtures were obtained from solubilities of potassium perchlorate. These were measured by atomic absorption spectroscopy of diluted samples from saturated solutions.

(ii) $\text{cis-}[\text{Rh}(\text{en})_2\text{Cl}_2]^+$:

The $\text{cis}[\text{Rh}(\text{en})_2\text{Cl}_2]^+$ cation was obtained from its chloride salt, prepared from rhodium trichloride via $[\text{Rh}(\text{en})_2(\text{C}_2\text{O}_4)]\text{ClO}_4 \cdot \frac{1}{2}\text{H}_2\text{O}$.⁵ Solutions containing mercury(II) were prepared by dissolving an appropriate weight of mercury(II) oxide (May & Baker) in aqueous perchloric acid (2.0 mol dm^{-3}). Ionic strengths were maintained at 0.36 mol dm^{-3} by the use of calcium perchlorate.

Kinetic data were obtained using the paper-tape logging apparatus. The initial concentration of the rhodium complex was $4.0 \times 10^{-3} \text{ mol dm}^{-3}$. Repeat-scan spectra showed excellent isosbestic points at 305 and 332 nm.

Rate constants were calculated from absorbance changes at 350 nm monitored over at least $2\frac{1}{2}$ half-lives.

(iii) Chromium complexes:

$[\text{Cr}(\text{NH}_3)_5\text{Cl}]\text{Cl}_2$,⁸ *cis*- $[\text{Cr}(\text{NH}_3)_4(\text{OH}_2)\text{Cl}]\text{Cl}_2$ ⁹ and *cis*- $[\text{Cr}(\text{NH}_3)_4(\text{OH}_2)\text{Cl}]\text{SO}_4$ ⁹ were prepared by published methods. Mercury(II) perchlorate was AnalaR material used as supplied. Ionic strengths were maintained with magnesium perchlorate.

Kinetic data were obtained using the minicomputer controlled apparatus described in Chapter 2. Runs were monitored at 250 nm for $[\text{Cr}(\text{NH}_3)_5\text{Cl}]^{2+}$ and at 400 nm for $[\text{Cr}(\text{NH}_3)_4(\text{OH}_2)\text{Cl}]^{2+}$. For the latter, the sulphate salt could be used for monitoring in the visible region. The chloride salts of the cations could not be used to monitor the reactions in the visible region of the spectrum, as at the concentrations required for a reasonable absorbance change, anionic chloride reacts with a significant proportion of the added mercury(II). However, these reactions could be monitored in the ultraviolet region because the much higher molar extinction coefficients for these absorptions meant that the chloride salts of $[\text{Cr}(\text{NH}_3)_5\text{Cl}]^{2+}$ and $[\text{Cr}(\text{NH}_3)_4(\text{OH}_2)\text{Cl}]^{2+}$ could be used; the ratio of anionic chloride to added mercury(II) concentrations was negligibly small.

Solubilities of the chloride salts were obtained by spectrophotometric measurements^{10,11,12,13,14} of suitably diluted saturated solutions. These solutions were kept in the dark and equilibration times were kept short enough to avoid significant aquation of the chromium(III) complexes.

4.3 RESULTS AND DISCUSSION

(i) $\text{trans}-[\text{Rh}(\text{en})_2\text{Cl}_2]^+$:

Aquation of the $\text{trans}-[\text{Rh}(\text{en})_2\text{Cl}_2]^+$ cation in the presence of a large excess of mercury(II) followed first-order kinetics (for at least

2½ half-lives) in water and in all the binary aqueous solvent mixtures. The removal of the second chloride does not make a detectable contribution to the kinetics under these conditions. [In the aquation of these chloro-complexes in the absence of mercury(II), the reaction for removal of the first chloride does not go to completion, and the second chloride may not be removed at all. In the presence of mercury(II), the removal of the first chloride goes to completion and the second chloride may be removed, though approximately one thousand times slower than the first.]

Observed first-order rate constants are reported in Table (4.1). The variation of k_{obs} with mercury(II) concentration and with solvent composition is summarized in Figure (4.2). Clearly all the plots in this Figure correspond to the situation where there is a persistent binuclear intermediate of significant stability [Figure (4.1), region B]. Spontaneous aquation is very much slower¹⁰ than mercury(II) catalysed aquation, and makes no contribution to observed rates in the work described here.

Plots of $1/k_{obs}$ against $1/[Hg^{2+}]$ are linear, as expected for a mechanism of the type shown in equation [4.1] above. The equivalent empirical relationship for the dependence of k_{obs} on $[Hg^{2+}]$ is

$$k_{obs} = \frac{[Hg^{2+}]}{B + A[Hg^{2+}]} \quad \dots [4.2]$$

where A and B are constants. It may be shown (Appendix 2) that the empirical constants in equation [4.1] are related to the parameters in equation [4.2] as follows:

$$1/B = k_2 K \quad ; \quad A/B = K \quad \dots [4.3]$$

So

$$k_{obs} = \frac{k_2 K [Hg^{2+}]}{1 + K [Hg^{2+}]} \quad \dots [4.4]$$

Equation [4.2] was fitted to each data set for k_{obs} against $[Hg^{2+}]$ using

TABLE (4.1)

Observed first-order rate constants, k_{obs} , derived equilibrium constants, K , and dissociation rate constants, k_2 , for the binuclear intermediate (equation [4.1]) for mercury(II) catalysed aquation of the trans-[Rh(en)₂Cl₂]⁺ cation at 298.2 K in water and in binary aqueous solvent mixtures

[Hg ²⁺] mol dm ⁻³	10 ⁴ $k_{\text{obs}}/\text{s}^{-1}$ -						
	water	10	% methanol		% ethanol		% acetonitrile
			30	40	40	20	40
0.08	1.57						
0.10	2.08	2.80	3.48	4.57	5.39	2.37	3.13
0.15	2.81	3.83		6.50	6.78	3.43	4.65
0.20	3.75		6.48	7.91	8.47	4.42	5.51
0.25	4.94	6.01	7.67	8.97	10.2	5.77	6.62
0.35	6.09	7.50	9.81	11.2	11.9	7.25	7.84
0.40	6.40	8.09	10.8	12.1	13.0	7.73	8.89
0.50	8.07	9.58	12.3	13.1	15.0	9.71	10.1
0.60	9.30	10.2		14.7	15.7	10.2	11.1
0.75	10.7	11.8	14.1	16.7	17.2	10.9	11.9
10 ⁴ k_2/s^{-1}	32 ± 3	23 ± 1	25 ± 1	27 ± 1	27 ± 1	24 ± 2	21 ± 1
$K/\text{dm}^3 \text{ mol}^{-1}$	0.66 ± 0.03	1.4 ± 0.1	1.8 ± 0.1	2.0 ± 0.1	2.3 ± 0.1	1.2 ± 0.05	1.8 ± 0.1

Solvent compositions by volume before mixing.

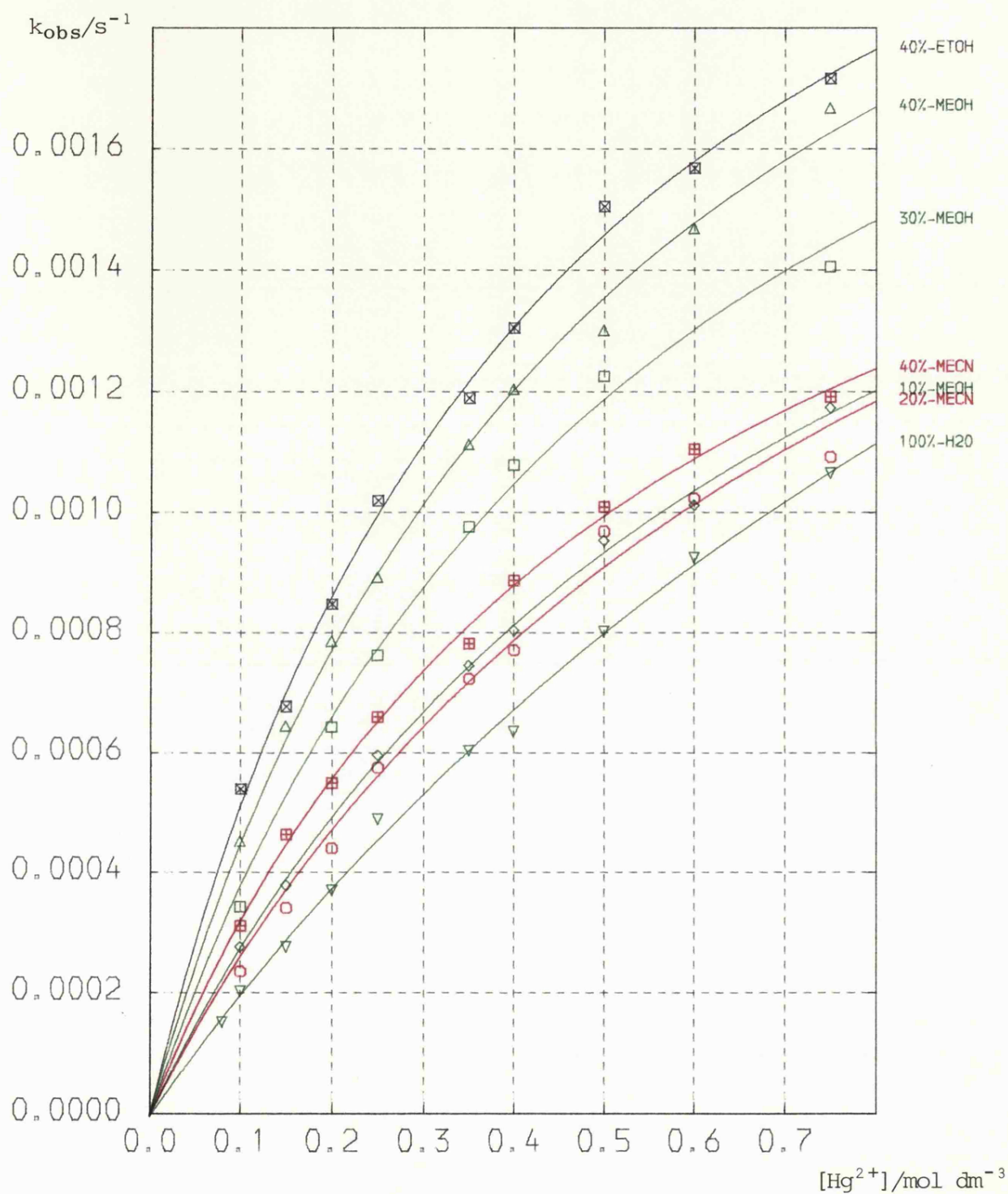


FIGURE (4.2)

Dependence of observed first-order rate constants for mercury(II)-catalysed aquation of $trans-[Rh(en)_2Cl_2]^+$ on mercury(II) concentration in water and in binary aqueous solvent mixtures at 298 K.

the Newton-Raphson iterative non-linear least squares technique,¹⁵ taking the parameters obtained from the reciprocal plot as starting values. The solid curves in Figure (4.2) are the resulting calculated dependences. The data fitting was achieved by the use of a computer program (FORTRAN, for the CDC Cyber 73 computer at Leicester University) which is listed and documented in Appendix 2. Thus values for K and k_2 in each solvent mixture were obtained from the kinetic data. These values are listed in Table (4.1) and their dependence on solvent composition is illustrated in Figure (4.3).

In order to calculate Gibbs free energies of transfer of the binuclear intermediate, and of the transition state for aquation of this intermediate, Gibbs free energies of transfer of the Hg^{2+} cation and of the trans- $[\text{Rh}(\text{en})_2\text{Cl}_2]^+$ cation from water to the solvent mixtures used need to be estimated. Some data were available, but many values have had to be derived in this work. Solubilities and ancillary data are reported in Table (4.2).

Figure (4.3) shows that the variation of the equilibrium constant for interaction of mercury(II) with trans- $[\text{Rh}(\text{en})_2\text{Cl}_2]^+$ (K of equation [4.1]) with solvent composition is not large. However, addition of increasing amounts of organic cosolvent does increase K significantly. Values of k_2 for dissociation of the binuclear intermediate are also hardly affected by medium composition; there is no clear pattern in the small changes found. This very low sensitivity of rate constant to solvent composition may be compared with that reported in the analogous fenclorac system.⁴ Such low sensitivity of rate constant when HgCl^+ is the leaving group contrasts dramatically with the large variations when Cl^- is the leaving group, in inorganic (e.g. chlorocobalt(III) complexes³) and even more in organic (e.g. t-butyl chloride or adamantyl chloride) solvolysis in mixed

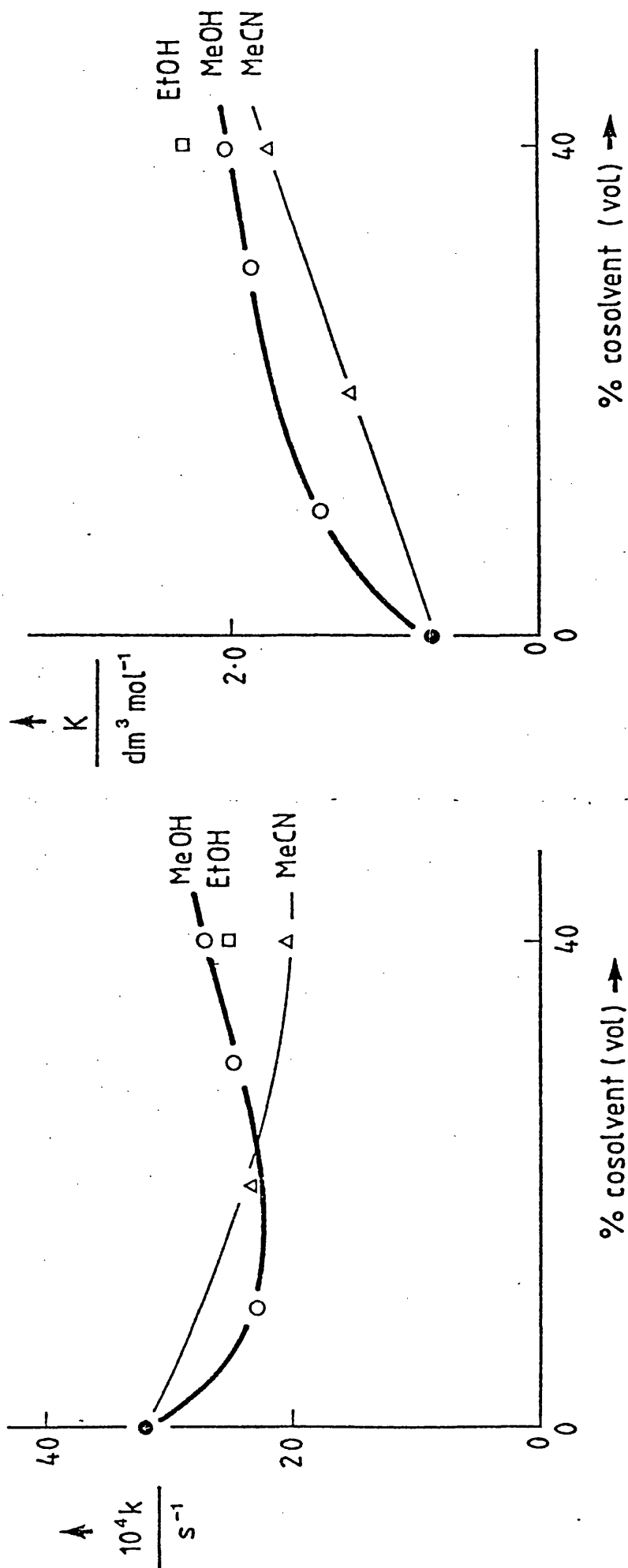


FIGURE (4.3)

Dependence of K and k_2 (equation [4.1]) on solvent composition for mercury(II)-catalysed aquation of the $\text{trans-}[\text{Rh}(\text{en})_2\text{Cl}_2]^+$ cation.

TABLE (4.2)

Solubilities of trans-[Rh(en)₂Cl₂]ClO₄ and Gibbs free energies of transfer of the trans-[Rh(en)₂Cl₂]⁺ cation; Gibbs free energies of transfer of Hg²⁺.
 [All values on the molar scale at 298.2 K]

	water	% methanol			% acetonitrile	
		10	30	40	20	40
10 ² soly [Rh] ^a ClO ₄ /mol dm ⁻³	1.27	1.08	1.04	1.02	1.99	3.86
∴ δ _m μ [⊖] ([Rh]ClO ₄)/kJ mol ⁻¹		+0.8	+1.0	+1.1	-2.2	-5.5
δ _m μ [⊖] (ClO ₄ ⁻)/kJ mol ⁻¹		+0.5 ^b	+1.8 ^b	+2.7 ^b	-1.6	-3.0
∴ δ _m μ ([Rh] ⁺)/kJ mol ⁻¹		+0.3	-0.8	-1.6	-0.6	-2.5
10 ² soly KClO ₄ /mol dm ⁻³	14.1				18.9	23.8
∴ δ _m μ [⊖] (KClO ₄)/kJ mol ⁻¹					-1.5	-2.6
δ _m μ [⊖] (K ⁺)/kJ mol ⁻¹ ^c					+0.1	+0.4
∴ δ _m μ [⊖] (ClO ₄ ⁻)/kJ mol ⁻¹					-1.6	-3.0
δ _m μ [⊖] (Hg ²⁺)/kJ mol ⁻¹ ^b		+3.2	+6.6	+6.9	+12.4	+22.3

^a [Rh] ≡ trans-[Rh(en)₂Cl₂]⁺; ^b ref. 16; ^c ref. 17.

aqueous media.¹⁸ Relative sensitivities may be expressed in terms of Grunwald-Winstein m values¹⁸ (see Appendix 6) where for t-butyl chloride m is, by definition, 1.0. For chlorocobalt(III) complexes m is about 0.3,¹⁹ and for mercury(II)-catalysed aquation of fenclorac m is 0.08.²⁰

The reactivity patterns for the $\text{trans-}[\text{Rh}(\text{en})_2\text{Cl}_2]^+$ cation on changing solvation characteristics for reactants, intermediate and transition state are shown in Table (4.3) and Figure (4.4). The binuclear intermediate is destabilised on transfer from water into the aqueous mixtures. However, it is less destabilised than the rhodium(III) complex and Hg^{2+} taken separately. It may be that the greater volume of the binuclear intermediate offsets its 3+ charge; the electric field intensity around a 3+ species of this size will be less than that round a monoatomic Hg^{2+} ion. It is the unfavourable transfer of this cation that dominates the reactants' free energy changes. The binuclear intermediate here is analogous to the transition state for the apparently one-step mercury(II)-catalysed aquation of the corresponding cobalt(III) complex, $\text{trans-Co}(\text{en})_2\text{Cl}_2^+$. The Gibbs free energies of transfer of the rhodium-mercury binuclear intermediate would be expected to be similar to those for the cobalt-mercury transition state: Table (4.4) shows that this is indeed the case.

It was remarked earlier that solvent variation has only a small effect on the rate of loss of the HgCl^+ leaving group in the k_2 stage of equation [4.1]. This is a consequence of the transition state for this step being destabilised by a comparable amount to the binuclear intermediate [Figure (4.4) and Table (4.3)]. In the dissociation of the binuclear intermediate formed between $\text{cis-}[\text{Rh}(\text{en})_2\text{Cl}_2]^+$ and Hg^{2+} , discussed below, the binuclear intermediate for $\text{trans-}[\text{Rh}(\text{en})_2\text{Cl}_2]^+$ is used as a model for the initial state in that reaction.

TABLE (4.3)

Dissection of solvent effects on mercury(II)-catalysed aquation of the trans-[Rh(en)₂Cl₂]⁺ cation into initial state, intermediate and transition state components. [All transfer quantities are in kJ mol⁻¹ on the molar scale at 298.2 K]

	% methanol			% ethanol		% acetonitrile	
	10	30	40	40		20	40
$\delta_{m\mu}^{\ominus}(\text{is})^a$	+3.5	+5.8	+5.3	+17 ^{b,c}		+11.9	+19.9
$\delta_m\Delta G^{\ominus}(\text{for K})$	-1.9	-2.5	-2.8	-3.1		-1.5	-2.5
$\therefore \delta_{m\mu}^{\ominus}(\text{intermediate})$	+1.6	+3.3	+2.6	+14		+10.4	+17.4
$\delta_m\Delta G^{\ddagger}$	+0.8	+0.6	+0.4	+0.4		+0.7	+1.0
$\therefore \delta_{m\mu}^{\ddagger}(\text{k}_2 \text{ step})$	+2.4	+3.9	+3.0	+14		+11.1	+18.4

^a is = [Rh(en)₂Cl₂]⁺ + Hg²⁺.

^b A value of +1.0 kJ mol⁻¹ has been used for $\delta_{m\mu}^{\ominus}[\text{Rh}(\text{en})_2\text{Cl}_2^{\ddagger}]$ here, which value has been taken the same as that estimated for the analogous cobalt(III) cation from published solubility data.²⁵ This assumption is correct within 0.4 kJ mol⁻¹ for transfer of the cations into aqueous methanol.

^c $\delta_{m\mu}^{\ominus}(\text{Hg}^{2+}) = +16 \text{ kJ mol}^{-1}$.¹⁶

FIGURE (4.4)

Initial state - binuclear intermediate - transition state analysis of solvent effects on reactivity for mercury(II)-catalysed aquation of the trans-[Rh(en)₂Cl₂]⁺ cation in (a) aqueous methanol and (b) aqueous acetonitrile, at 298.2 K.

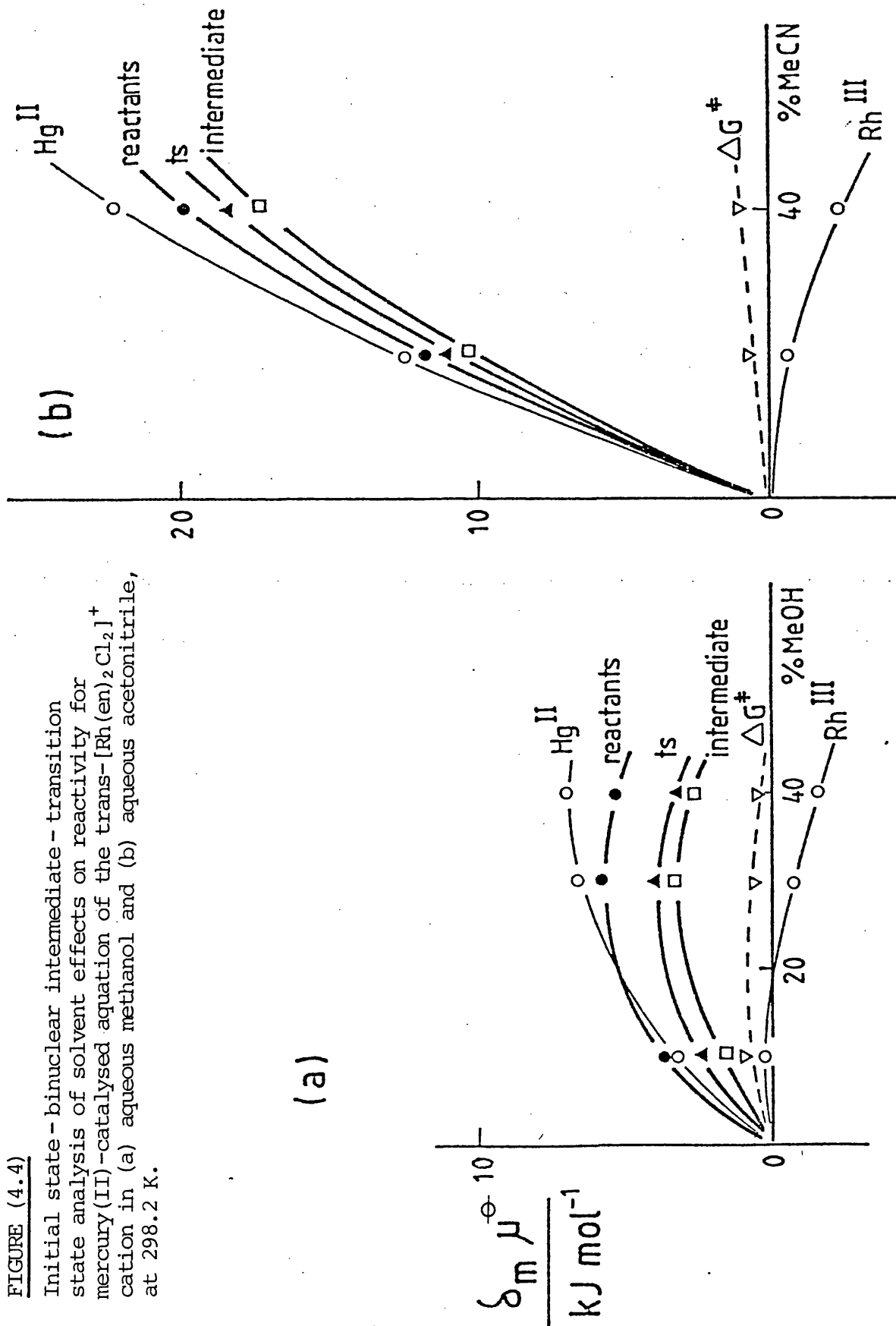


TABLE (4.4)

Comparison of Gibbs free energies of transfer of the binuclear intermediate in the $\text{trans-}[\text{Rh}(\text{en})_2\text{Cl}_2]^+$ plus Hg^{2+} reaction and of the transition state for the $\text{trans-}[\text{Co}(\text{en})_2\text{Cl}_2]^+$ plus Hg^{2+} reaction.
[kJ mol⁻¹; molar scale; 298.2 K]

	% methanol 10 30	% ethanol 40
Rh-Hg intermediate	+1.6 +3.3	+14 ^a
Co-Hg transition state	+2.8 +5.9	+17.8 ^b

^a From Table (4.3).

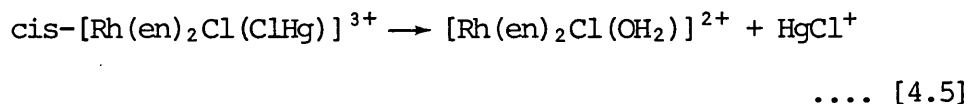
^b From ref. 3.

(ii) cis-[Rh(en)₂Cl₂]⁺:

The mercury(II) catalysed aquation of the cation follows a kinetic pattern corresponding to a stable and long-lived intermediate, thus showing the same behaviour as the cis-[Co(en)₂Cl₂]⁺ cation.²¹ The observed first-order rate constants with mercury(II) in large excess do not vary with mercury(II) concentration over the range 0.06-0.18 mol dm⁻³. The average k_{obs} values in water and methanol-water mixtures are reported in Table (4.5). These values correspond to the k₂ step in equation [4.1]. The intermediate [Rh-Cl-Hg]³⁺ species must be rapidly and completely formed.

The marked difference between the kinetic patterns for the mercury(II) catalysis of aquation of cis-[Rh(en)₂Cl₂]⁺ and trans-[Co(en)₂Cl₂]⁺²¹ or trans-[Rh(en)₂Cl₂]⁺ (above) can be rationalised on the basis of stereochemistry. The value of K in equation [4.1] is much larger in cis-dichloro-complexes than in trans-dichloro-complexes. This situation may be compared with, for example, the much greater importance of acid catalysis in aquation of hexafluoro- or cis-difluoro-complexes than in aquation of trans-difluoro-complexes,²² or with the significant rôle played by double bridging in the chromium(II) reduction of cis-, but not of trans-[Co(NH₃)₄(N₃)₂]⁺ and its tetra-ammine analogues.²³

Thus the reaction on which the initial state - transition state analysis of solvent effects is to be carried out is:



with a transition state [Cl(en)₂Rh---ClHg]^{‡3+}. In order to achieve the desired dissection, the transfer chemical potential of the initial state, δ_{mμ}[⊖](Rh-Cl-Hg) and of the Gibbs free energy of activation, ΔG[‡], are needed. The latter is directly calculable from the kinetic results. The

former is not directly available, as it would prove difficult to measure solubilities of a salt of the $\text{cis-}[\text{Rh}(\text{en})_2\text{Cl}(\text{ClHg})]^{3+}$ cation. However, this species is closely related to $\text{trans-}[\text{Rh}(\text{en})_2\text{Cl}(\text{ClHg})]^{3+}$ for which transfer data are available from the analysis described in the previous section. The analysis of solvent effects on reactivity is shown in Table (4.5) and Figure (4.5a). The dominant feature is the relatively small effect of solvent, especially on the rates of aquation. The smallness of effects is brought out by comparison with solvolysis of the PtCl_4^{2-} anion,²⁴ where rate constants, initial states and transition states are markedly affected by solvent variation (Figure 4.5b). One reason for the different behaviour is the difference in leaving group; leaving chloride ion is considerably more solvated and therefore stabilised in water-rich solvent media, whereas the HgCl^+ leaving group may well be similarly solvated in the three solvent mixtures. Also the square planar Pt(II) complex is likely to be more sensitive to solvent environment than the larger, octahedral, Rh(III) intermediate.

TABLE (4.5)

The dissection of solvent effects on the kinetics of dissociation of the $\text{cis-}[\text{Rh}(\text{en})_2\text{Cl}(\text{ClHg})]^{3+}$ intermediate in aqueous methanol into initial state and transition state components at 298.2 K on the molar scale

	% methanol (by volume)		
	0	20	40
$10^4 k_2/\text{s}^{-1}$	3.0	2.0	2.0
$\therefore \delta_m \Delta G^\ddagger / \text{kJ mol}^{-1}$		+1.0	+1.0
$\delta_m \mu^\ominus(\text{is}) / \text{kJ mol}^{-1} \text{ }^{\text{a}}$		+2.7 ^b	+2.6
$\therefore \delta_m \mu^\ddagger / \text{kJ mol}^{-1}$		+3.7	+3.6

^a From Table (4.3); ^b interpolated.

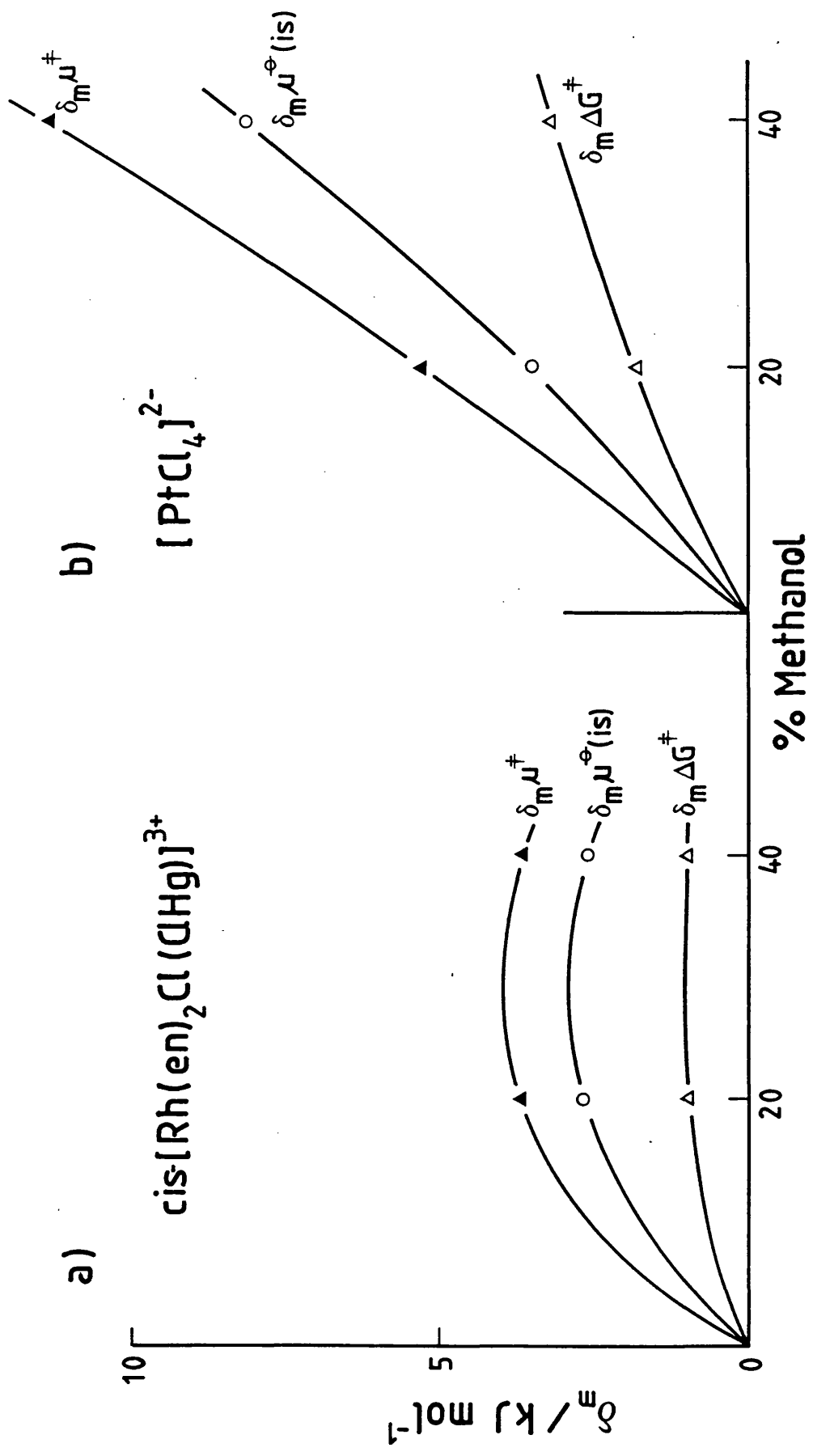


FIGURE (4.5)
 Initial state and transition state contributions to solvent effects on reactivity for aquation of
 (a) the $\text{cis}[\text{Rh}(\text{en})_2\text{Cl}(\text{ClHg})]^{3+}$ cation and (b) the $[\text{PtCl}_4]^{2-}$ anion for comparison.

(iii) Chromium complexes:

Aquation of the $[\text{Cr}(\text{NH}_3)_5\text{Cl}]^{2+}$ and $\text{cis-}[\text{Cr}(\text{NH}_3)_4(\text{OH}_2)\text{Cl}]^{2+}$ cations in the presence of a large excess of mercury(II) follows first-order kinetics over at least $2\frac{1}{2}$ half-lives in water and in the binary aqueous mixtures. The nature of the products, $[\text{Cr}(\text{NH}_3)_5(\text{OH}_2)]^{3+}$,¹¹ and $\text{cis-}[\text{Cr}(\text{NH}_3)_4(\text{OH}_2)_2]^{3+}$ ^{12,13} was confirmed by their visible absorption spectra; retention of configuration in mercury(II)-catalysed aquation of $\text{cis-}[\text{Cr}(\text{NH}_3)_4(\text{OH}_2)\text{Cl}]^{2+}$ in water has been established.¹⁴ Spontaneous aquation of chloro-chromium(III) complexes does not always go to completion;²⁶ mercury(II)-catalysed aquation is very much more likely to result in complete reaction. Observed first-order rate constants are reported in Table (4.6). In contrast to $\text{trans-}[\text{Rh}(\text{en})_2\text{Cl}_2]^+$, but in common with $[\text{Co}(\text{NH}_3)_5\text{Cl}]^{2+}$, plots of k_{obs} against mercury(II) concentration are linear, at least over the range of concentrations used in this work. Values for the respective second-order rate constants are included in Table (4.6). The rate constant for reaction in water, $0.053 \text{ dm}^3 \text{ mol}^{-1} \text{ s}^{-1}$, compares satisfactorily with that estimated²⁷ for 298.2 K, $0.087 \text{ dm}^3 \text{ mol}^{-1} \text{ s}^{-1}$, from published kinetic data.²⁸ The value in this work was obtained at a lower ionic strength than that used in the earlier work, and it is known that the k_2 value for mercury(II)-catalysed aquation of $[\text{Co}(\text{NH}_3)_5\text{Cl}]^{2+}$ decreases markedly as ionic strength decreases.²⁷ There is no intercept of the k_{obs} against $[\text{Hg}^{2+}]$ plots on the rate constant axis, because both for $[\text{Cr}(\text{NH}_3)_5\text{Cl}]^{2+}$ ¹¹ and for $\text{cis-}[\text{Cr}(\text{NH}_3)_4(\text{OH}_2)\text{Cl}]^{2+}$ ^{12,14} spontaneous rates of aquation are very much lower than the mercury(II)-catalysed rates reported here. Solubilities required for the derivation of transfer parameters are reported in Table (4.7).

TABLE (4.6)

Observed first-order rate constants, k_{obs} , and derived second-order rate constants, k_2 , with their standard errors, σ , for mercury(II)-catalysed aquation of the $[\text{Cr}(\text{NH}_3)_5\text{Cl}]^{2+}$ and $[\text{Cr}(\text{NH}_3)_4(\text{OH}_2)\text{Cl}]^{2+}$ cations, in water and in binary aqueous solvent mixtures at 298.2 K and a constant ionic strength of 0.13 mol dm^{-3} . [Solvent compositions are by volume before mixing]

complex	solvent	$10^3 k_{obs}/\text{s}^{-1}$ [Hg^{2+}]/ mol dm^{-3}					$10^3 k_2 \pm \sigma$ $\text{dm}^3 \text{ mol}^{-1} \text{ s}^{-1}$
		0.020	0.029	0.039	0.049	0.059	
$[\text{Cr}(\text{NH}_3)_5\text{Cl}]^{2+}$	water	1.4	2.0	2.6	3.3	55 ± 5	
	23.3% MeOH	1.7	2.5	2.9	3.6	61 ± 5	
	34.5% MeOH	3.0	4.6	5.2	6.6	114 ± 13	
	46.6% MeOH	3.3	5.5	6.9	9.6	203 ± 17	
	46.6% MeCN	1.8	2.2	2.9	3.6	61 ± 5	
cis- $[\text{Cr}(\text{NH}_3)_4(\text{OH})_2\text{Cl}]^{2+}$	water	2.9	3.8	5.3	7.0	147 ± 7	
	23.3% MeOH	3.4	4.6	7.5	9.2	204 ± 12	
	34.5% MeOH	4.4	6.6	8.6	10.3	199 ± 7	
	46.6% EtOH	6.3	9.6	11.7	13.4	218 ± 22	
	46.6% MeCN	2.2	4.2	5.4	7.1	168 ± 8	

TABLE (4.7)

Spectrophotometrically-determined solubilities of $[\text{Cr}(\text{NH}_3)_5\text{Cl}]\text{Cl}_2$
and of $\text{cis-}[\text{Cr}(\text{NH}_3)_4(\text{OH}_2)\text{Cl}]\text{Cl}_2$ in water and binary aqueous
solvent mixtures at 298.2 K

Solvent	Solubilities/mol dm ⁻³	
	$[\text{Cr}(\text{NH}_3)_5\text{Cl}]\text{Cl}_2$	$\text{cis-}[\text{Cr}(\text{NH}_3)_4(\text{OH}_2)\text{Cl}]\text{Cl}_2$
Water	0.0297 ^a	0.184 ^b
23.3% MeOH	0.016	0.135
34.5% MeOH	0.010	0.052
46.6% MeOH	0.0064	
46.6% EtOH		0.079

^a i.e. 0.73g per 100g solution: cf. ref. [14] value of 0.65g per 100g of water at 289 K;

^b i.e. 4.6g per 100g solution: cf. ref. [14] value of 6.3g per 100g of water at 288 K.

Rate constants for mercury(II)-catalysed aquation of these two chloro-chromium(III) complexes show only a modest dependence on solvent composition. Values of \bar{m} for these results are roughly -0.4 for $[\text{Cr}(\text{NH}_3)_5\text{Cl}]^{2+}$ and only -0.1 for $[\text{Cr}(\text{NH}_3)_4(\text{OH}_2)\text{Cl}]^{2+}$. These values may be compared with an \bar{m} -value of approximately -0.1 for mercury(II)-catalysed aquation of $[\text{Co}(\text{NH}_3)_5\text{Cl}]^{2+}$, and a much larger \bar{m} -value, 1.7, for mercury(II)-catalysed aquation of $[\text{ReCl}_6]^{2-}$. [The \bar{m} Y plots for these bimolecular reactions are not very good straight lines. The \bar{m} -values quoted are graphical estimates from the kinetic data for water rich mixtures.] The contrast between small values for the 2+ complexes and a large value for ReCl_6^{2-} may be understood in terms of an increase in charge on forming the transition state for the former complexes, but a cancellation of charge on reaction

of the $[\text{ReCl}_6]^{2+}$ anion with the Hg^{2+} cation, with consequent differences in the pattern of solvation changes. It may be noted here that activation volumes for mercury(II)-catalysed aquation of $[\text{Cr}(\text{NH}_3)_5\text{Cl}]^{2+}$, $[\text{Co}(\text{NH}_3)_5\text{Cl}]^{2+}$, $[\text{Rh}(\text{NH}_3)_5\text{Cl}]^{2+}$ and $[\text{Co}(\text{NH}_3)_5\text{Br}]^{2+}$ in aqueous solution (between -2 and $+1 \text{ cm}^3 \text{ mol}^{-1}$ ²⁷) are similar to the activation volume for lead(II)-catalysed aquation of $[\text{Co}(\text{NH}_3)_5\text{Br}]^{2+}$ in an aqueous polyelectrolyte medium ($+2.5 \text{ cm}^3 \text{ mol}^{-1}$ ²⁹). These small values suggest that release of electrostricted water from the metal(II) cation in transition state formation may make a significant positive contribution to ΔV^\ddagger , roughly offsetting the intrinsic negative ΔV^\ddagger for an associative process.

In the analysis of solvent effects on reactivity for these complexes, the opportunity will be taken to compare the results obtained using two different single ion assumptions for $\delta_{\text{m}\mu}^\ominus(\text{Cl}^-)$ and $\delta_{\text{m}\mu}^\ominus(\text{Ph}_4\text{B}^-)$ in methanol-water mixtures. Values reported by Wells will be used as a representative set of parameters obtained from a Born-type calculation. In contrast, values provided by Abraham are derived from the assumption that $\delta_{\text{m}\mu}^\ominus(\text{Ph}_4\text{P}^+) = \delta_{\text{m}\mu}^\ominus(\text{Ph}_4\text{B}^-)$ in methanol-water solvent mixtures. Additionally, the analysis is restricted to methanol-water because published values of $\delta_{\text{m}\mu}^\ominus(\text{Cl}^-)$ into aqueous ethanol³⁰ use a somewhat different single-ion splitting assumption [see Section (1.4.3)].

The analyses for kinetic data methanol-water mixtures are shown in Tables (4.8) and (4.9) and Figures (4.6) and (4.7). The major differences between the results obtained using the two differing single-ion assumptions are as follows:

- (i) for the analyses based on Wells' single ion transfer parameters, the chromium(III) cations are shown as being stabilised on transfer from water to water-methanol, in contrast to the analyses based on Abraham's values where these cations are shown as destabilised. The

TABLE (4.8)

Dissection of solvent effects on rates of mercury(II)-
catalysed aquation of chlorochromium(III) complexes into
initial state and transition state effects;
kJ mol⁻¹ (molar scale at 298.2 K)
Single ion assumption: Wells

	% methanol		
	23.3	34.5	46.6
$\delta_{m\mu}^{\ominus} \{ [\text{Cr}(\text{NH}_3)_5\text{Cl}]\text{Cl}_2 \}$	+5.7	+7.9	+11.1
$2 \delta_{m\mu}^{\ominus} (\text{Cl}^-)$ ^a	+6.2	+10.4	+16.2
$\therefore \delta_{m\mu}^{\ominus} \{ [\text{Cr}(\text{NH}_3)_5\text{Cl}]^{2+} \}$	-0.5	-2.5	-5.1
$\delta_{m\mu}^{\ominus} (\text{Hg}^{2+})$ ^b	+4.4	+6.9	+8.0
$\therefore \delta_{m\mu}^{\ominus} (\text{initial state})$	+3.9	+4.4	+2.9
$\delta_m \Delta G^\ddagger$	-0.2	-1.8	-2.5
$\therefore \delta_{m\mu}^\ddagger$	+3.7	+2.6	+0.4
$\delta_{m\mu}^{\ominus} \{ [\text{Cr}(\text{NH}_3)_4(\text{OH}_2)\text{Cl}]\text{Cl}_2 \}$	+2.4	+6.0	
$\therefore \delta_{m\mu}^{\ominus} \{ [\text{Cr}(\text{NH}_3)_4(\text{OH}_2)\text{Cl}]^{2+} \}$	-3.8	-4.4	
$\therefore \delta_{m\mu}^{\ominus} (\text{initial state})$	+0.6	+2.5	
$\delta_m \Delta G^\ddagger$	-0.8	-1.3	
$\therefore \delta_{m\mu}^\ddagger$	-0.2	+1.2	

^a Scale conversion and interpolation of values from
ref. 31.

^b Interpolated from values in ref. 3.

TABLE (4.9)

Dissection of solvent effects on rates of mercury(II)-
catalysed aquation of chlorochromium(III) complexes into
initial state and transition state effects;
kJ mol⁻¹ (molar scale at 298.2 K)
Single ion assumption: Abraham

	% methanol		
	23.3	34.5	46.6
$\delta_{m\mu}^{\ominus} \{ [\text{Cr}(\text{NH}_3)\text{Cl}]\text{Cl}_2 \}$	+5.7	+7.9	+11.1
$2 \delta_{m\mu}^{\ominus} (\text{Cl}^-)$ ^a	+2.0	+3.4	+5.4
$\therefore \delta_{m\mu}^{\ominus} \{ [\text{Cr}(\text{NH}_3)_5\text{Cl}]^{2+} \}$	+3.7	+4.5	+5.7
$\delta_{m\mu}^{\ominus} (\text{Hg}^{2+})$ ^b	+8.5	+13.1	~+19.5
$\therefore \delta_{m\mu}^{\ominus} (\text{initial state})$	+12.2	+17.6	+25.2
$\delta_m \Delta G^\ddagger$	-0.2	-1.8	-2.5
$\therefore \delta_{m\mu}^\ddagger$	+12.0	+15.8	+22.7
$\delta_{m\mu}^{\ominus} \{ [\text{Cr}(\text{NH}_3)_4(\text{OH}_2)\text{Cl}]\text{Cl}_2 \}$	+2.4	+6.0	
$\therefore \delta_{m\mu}^{\ominus} \{ [\text{Cr}(\text{NH}_3)_4(\text{OH})_2\text{Cl}]^{2+} \}$	+0.4	+2.6	
$\therefore \delta_{m\mu}^{\ominus} (\text{initial state})$	+8.9	+15.7	
$\delta_m \Delta G^\ddagger$	-0.8	-1.3	
$\therefore \delta_{m\mu}^\ddagger$	+8.1	+14.4	

^a Interpolation of values from ref. 32.

^b Using $\delta_{m\mu}^{\ominus} [\text{Hg}(\text{BPh}_4)_2]$ from ref. 3 and $\delta_{m\mu}^{\ominus} (\text{BPh}_4^-)$ from ref. 32.

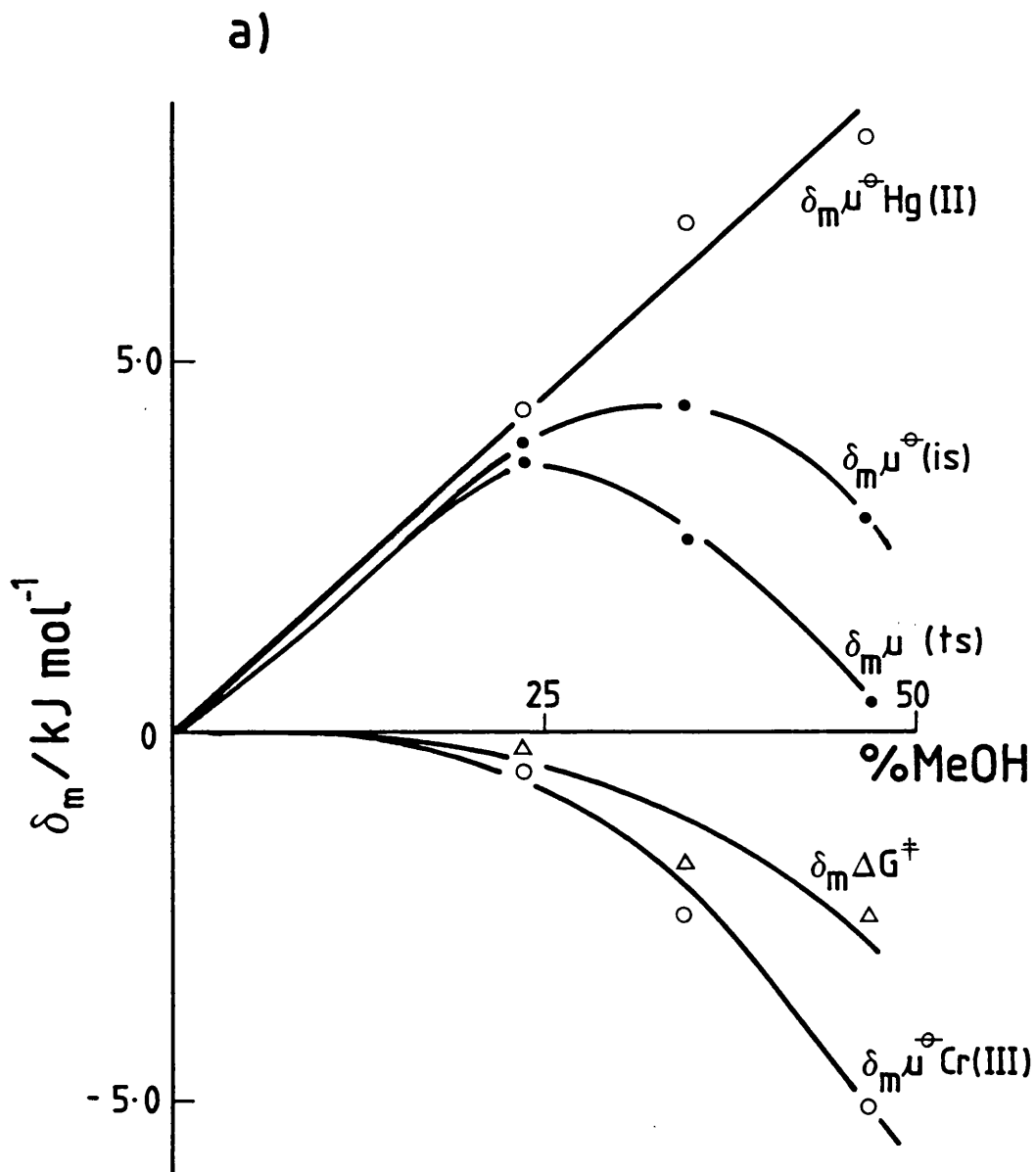
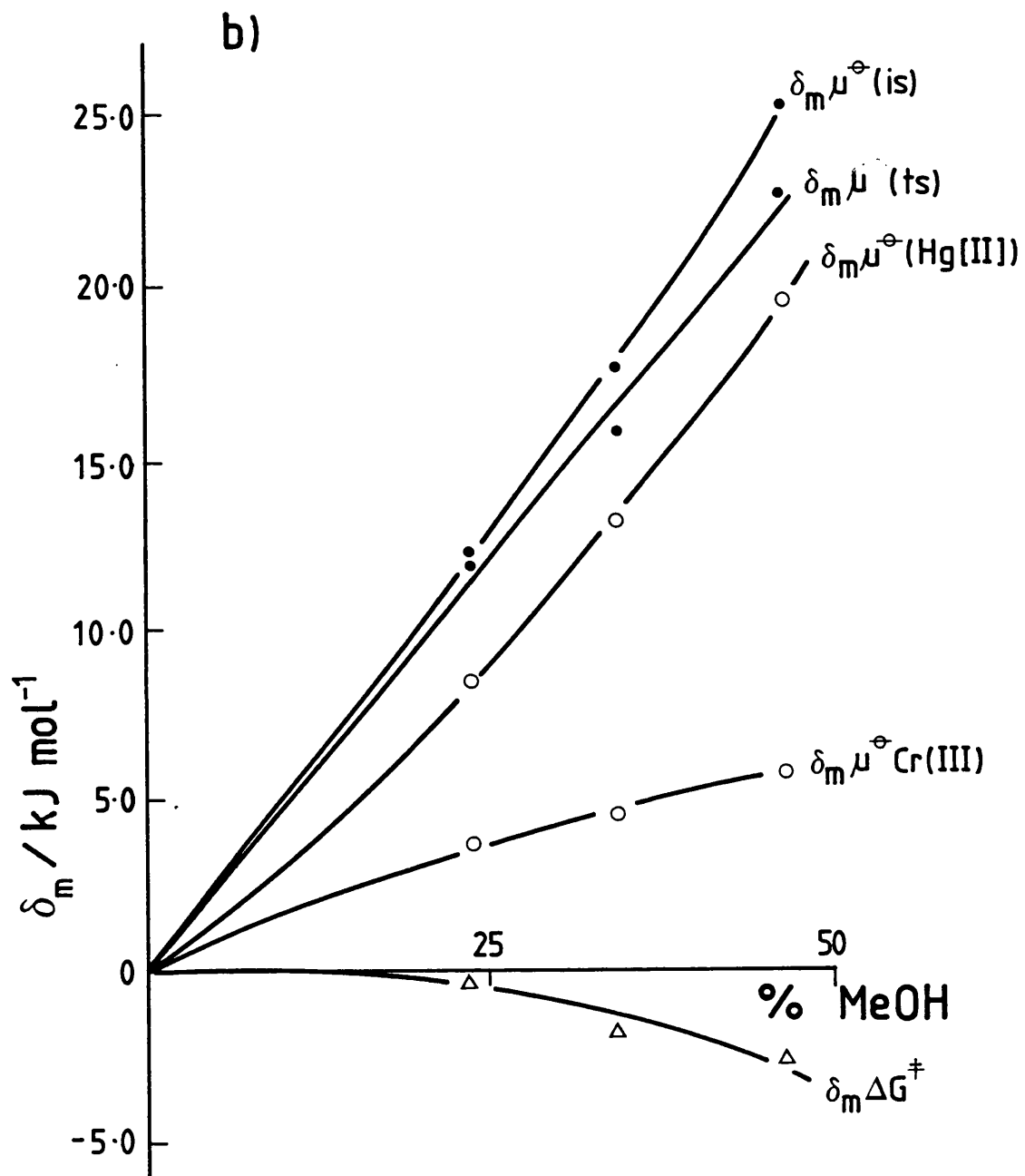


FIGURE (4.6)

Initial state - transition state analysis of solvent effects on reactivity for mercury(II)-catalysed aquation of the $[\text{Cr}(\text{NH}_3)_5\text{Cl}]^{2+}$ cation in aqueous methanol at 298.2 K.

Single ion assumptions: (a) Wells, (b) Abraham.



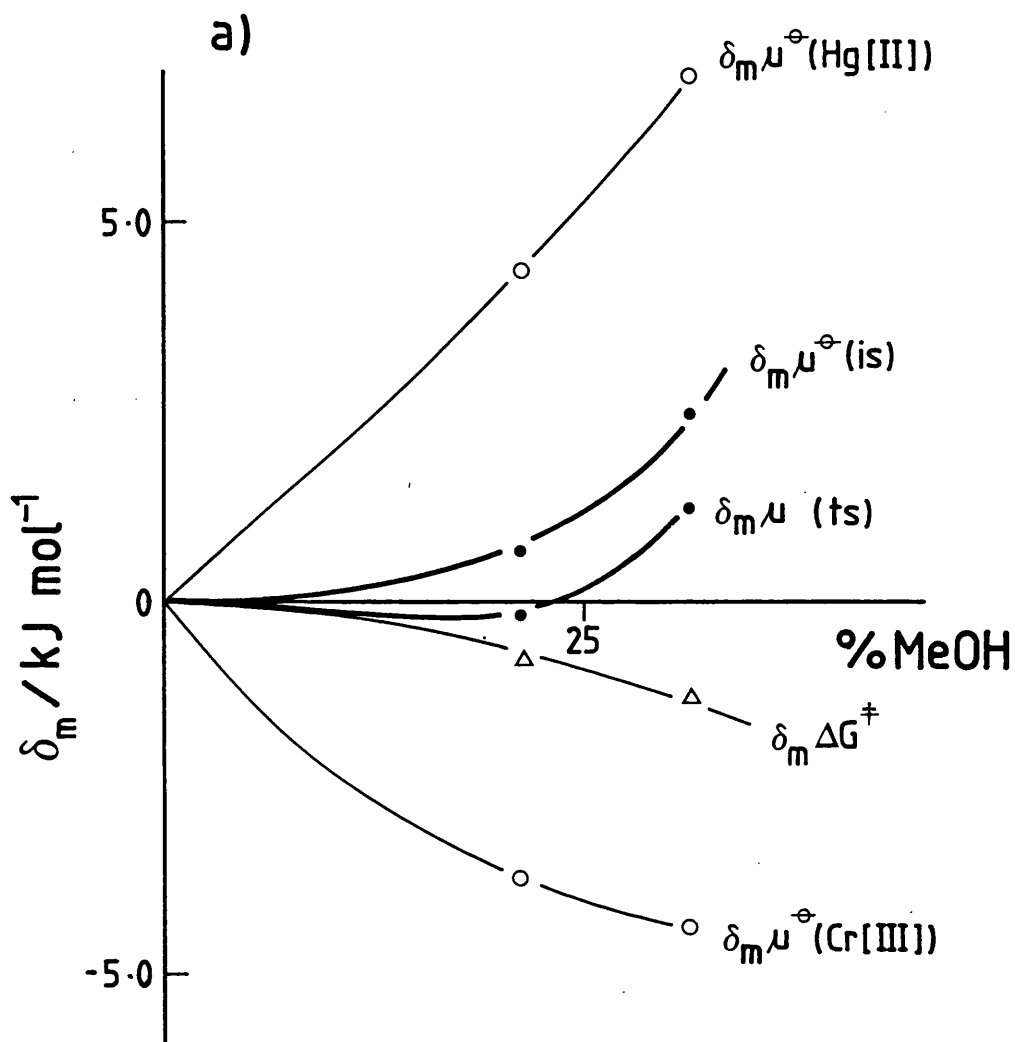
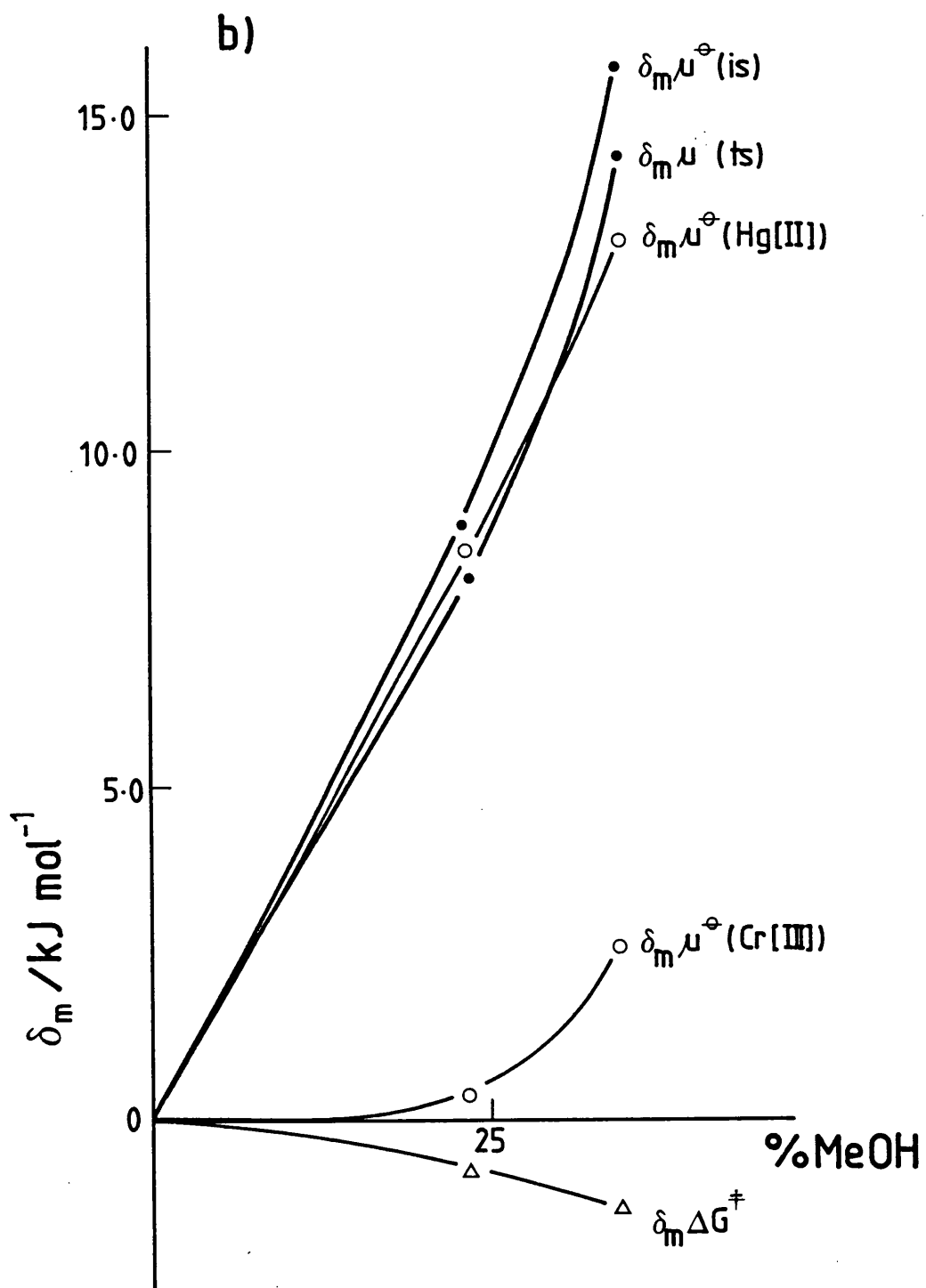


FIGURE (4.7)

Initial state and transition state analysis of solvent effects on reactivity for mercury(II)-catalysed aquation of the $[\text{Cr}(\text{NH}_3)_4(\text{OH}_2)\text{Cl}]^{2+}$ cation in aqueous methanol at 298.2 K.

Single ion assumptions: (a) Wells, (b) Abraham.



latter representation would seem more appropriate in view of the 2+ charge on these cations.

(ii) quantitatively, the values for $\delta_{m\mu}^{\ominus}(\text{Hg}^{2+})$ obtained using Wells' parameters are approximately one half those obtained using Abraham's parameters. Both are derived from the same values for $\delta_{m\mu}^{\ominus}[\text{Hg}(\text{BPh}_4)_2]$. Further, the values for $\delta_{m\mu}^{\ominus}(\text{Hg}^{2+})$ appear to be inordinately large when compared with values for other 2+ cations reported by the respective authors; in view of the instability of tetraphenylborates in acid solution³³ and subsequent difficulties caused in solubility measurements, poor experimental data for $\text{Hg}(\text{BPh}_4)_2$ may be the cause of the discrepancy.

Qualitatively, the alternative analyses both produce the same pattern for relative solvation changes in initial state and transition state. However, it may be noted that this is an inevitable result of the algebra used in the analyses.

Turning to the trends which do emerge, the reactivity patterns for these chlorochromium(III) complexes show the expected similarity to that established for the $[\text{Co}(\text{NH}_3)_5\text{Cl}]^{2+}$ cation,³ where single ion transfer parameters were provided by Wells or de Ligny [e.g. compare Figure (4.7b) with Figure (4b) of ref. 3]. With regard to initial state trends, smaller changes for $\text{cis-}[\text{Cr}(\text{NH}_3)_4(\text{OH}_2)\text{Cl}]^{2+}$ than for $[\text{Cr}(\text{NH}_3)_5\text{Cl}]^{2+}$ may be attributed to a slightly greater degree of hydrophilic character in the former, arising from the presence of the aquo-ligand. In this connection, it may be remarked that the solubility of $\text{cis-}[\text{Cr}(\text{NH}_3)_4(\text{OH}_2)\text{Cl}]\text{Cl}_2$ is about ten times that for $[\text{Cr}(\text{NH}_3)_5\text{Cl}]\text{Cl}_2$.³⁴ [This consideration ignores lattice energy contributions.] It is noteworthy that aquation of $[\text{Cr}(\text{NH}_3)_5\text{Cl}]^{2+}$ is considerably less sensitive to solvent variation than that of $[\text{Co}(\text{NH}_3)_5\text{Cl}]^{2+}$. It has been suggested that this may be attributed

to greater associative character in the former case,³⁵ but may be due to initial state or transition state solvation differences in a common dissociative mechanism. More extensive solubility and thermodynamic investigations will be needed to establish patterns and reasons for these relatively small chromium(III) - cobalt(III) differences.

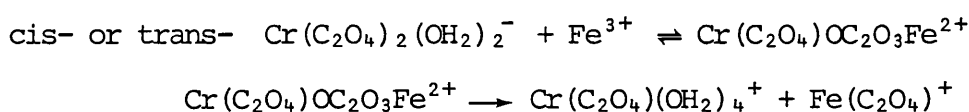
4.4 SUMMARY

In the systems described in this chapter, solvent effects on reactivity have been shown to be somewhat subtle when compared with, for example, the results reported in Chapter 3 for redox systems, or those for other substitution reactions represented in Table (1.1). Patterns for mercury(II)-catalysed aquation are ultimately dominated by the solvation characteristics of the mercury(II)-cation, whether as a reactant or in HgCl^+ as a leaving group in a transition state or intermediate.

4.5 METAL-ION CATALYSED AQUATION OF OXALATE COMPLEXES

An extension of the study of metal-ion catalysed aquation to cases where ligand and metal cation are 'hard' in character, in contrast to the systems described above which involve the 'soft' Hg^{2+} cation, has begun with an investigation of the possibility of catalysed aquation of oxalate complexes by metal ions such as Ca^{2+} , Mg^{2+} , La^{3+} and Cu^{2+} . One of the few examples of reactions of this type in the literature is the iron(III) catalysed aquation of the $\text{Cr}(\text{C}_2\text{O}_4)_2(\text{OH}_2)_2^-$ anion.³⁵ The bonds to the leaving oxalate are broken singly, forming a monodentate intermediate. The Fe^{3+} cation assists in the breaking of both these bonds:

ref 36



.... [4.6]

Initial qualitative experiments yielded two combinations of oxalate complex and metal ion suitable for kinetic study: $\text{Cr}(\text{C}_2\text{O}_4)_3^{3-}$ with Cu^{2+} and $\text{Co}(\text{C}_2\text{O}_4)_3^{3-}$ with La^{3+} .

Initial repeat scan spectra at 298.2 K for both reactions showed slow, single-stage processes which were first-order, though in the case of $\text{Cr}(\text{C}_2\text{O}_4)_3^{3-}$ not particularly 'smooth'.

Second-order rate constants for $\text{Cr}(\text{C}_2\text{O}_4)_3^{3-}$, obtained at 318.2 K by the isolation method, showed little variation when the solvent was changed from water to 40% methanol. The value was roughly $4 \times 10^{-3} \text{ dm}^3 \text{ mol}^{-1} \text{ s}^{-1}$ in each mixture. Satisfactory second-order plots could not be obtained in DMSO-water and acetonitrile mixtures.

For $\text{Co}(\text{C}_2\text{O}_4)_3^{3-}$ with La^{3+} , with the lanthanum concentration constant and in large excess, observed first-order rate constants at 308.2 K increased with increasing proportion of methanol cosolvent, and showed little variation with increasing proportion of DMSO cosolvent.

Full analyses of these preliminary results are not possible due to unavailability of much of the required ancillary data. However, it may be noted that the striking feature of the results is the insensitivity of the systems to solvent variation, especially in view of the high charges of the species involved. The fact that these charges are partially or fully cancelled on formation of the transition state means that the transition state and initial state have markedly different charge characteristics. Thus these systems might reasonably be expected to show the same reactivity pattern as in the mercury(II)-catalysed aquation of ReCl_6^{2-} , where rate constants increase with increasing proportion of organic cosolvent. However, the kinetic results for the oxalate complexes show that this trend in rate constant changes is not the case in these systems.

These systems are likely candidates for a fuller kinetic study and

characterisation of initial state properties in mixed aqueous media.

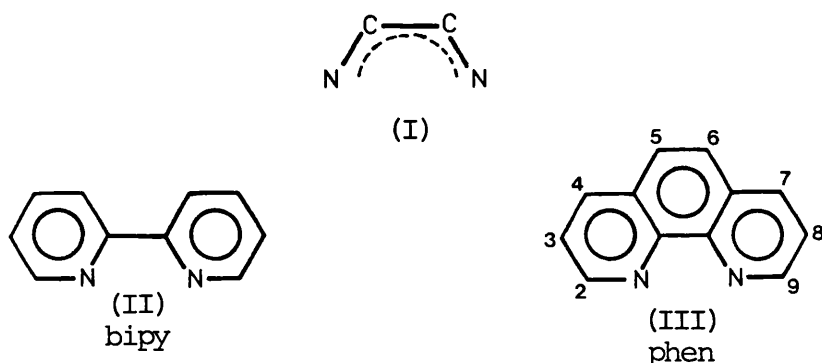
Investigation of the complexes $\text{Cr}(\text{C}_2\text{O}_4)_3^{3-}$, $\text{Cr}(\text{C}_2\text{O}_4)_2(\text{OH}_2)_2^-$ and $\text{Cr}(\text{C}_2\text{O}_4)(\text{OH}_2)_4^+$ would provide a link with their possible use in obtaining single-ion transfer parameters as suggested in Section (1.4.3).

CHAPTER 5

REACTIONS OF ANIONIC IRON(II) TRIS-DIIMINE COMPLEXES
AND DIIMINE LIGANDS WITH HYDROXIDE AND CYANIDE IN
AQUEOUS MEDIA; KINETICS AND EQUILIBRIA

5.1 INTRODUCTION

Most iron(II) complexes are high spin, $t_{2g}^4 e_g^2$, in configuration and kinetically labile. A few ligands interact sufficiently strongly with this metal centre to force spin pairing and produce the kinetically inert t_{2g}^6 configuration. Such ligands include cyanide ion and a series of aromatic nitrogen bases containing the chelating unit (I) shown below. Several complexes containing ligands such as 2,2'-bipyridine (II) and 1,10-phenanthroline (III) have been extensively studied, with kinetic results reported for a variety of reactions including aquation and reaction with hydroxide or cyanide ions.¹

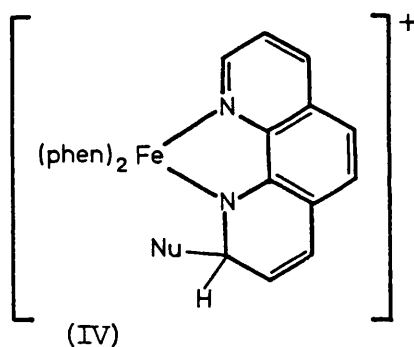


There have in recent years been many suggestions that ligand substituted derivatives may be intermediates in the reactions of these low-spin iron(II) complexes with nucleophiles such as hydroxide, cyanide or methoxide.

In the rate expression for base hydrolysis of $Fe(LL)_3^{2+}$, where LL is a diimine ligand, the dominant term is in $[Fe(LL)_3^{2+}][OH^-]$. Similarly, the rate expression for substitution of the ligand by cyanide ions contains a dominant term in $[Fe(LL)_3^{2+}][CN^-]$. The possibility that there is a pre-equilibrium involving the conjugate base of a coordinated ligand

may be discounted as there are no ionizable protons below pH 12, though such a mechanism was initially put forward to explain the kinetics of reaction between $[\text{Fe}(\text{5NO}_2\text{-phen})_3]^{2+}$ and hydroxide ion.² This mechanistic path was considered implausible because further examination³ revealed that no hydrogen exchange occurred at the free ligand in alkaline deuterium oxide. Thus the dominant second order term in the rate law indicates a bimolecular mechanism.

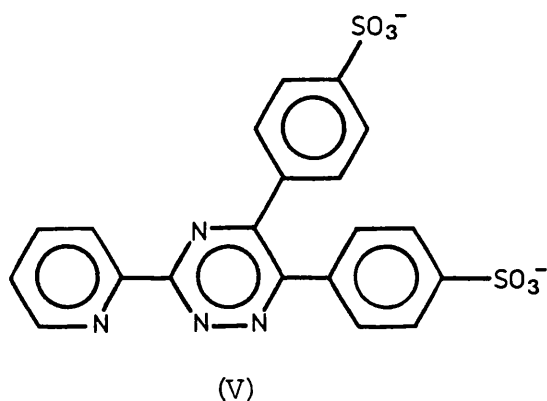
The argument is not fully settled as to whether nucleophilic attack takes place at the central metal atom^{2,4,5} or at some position of the coordinated ligand.^{3,6,7} Persuasive, but not incontrovertible, evidence has been presented in favour of a mechanism in which initial attack at the ligand occurs to give a transient intermediate such as (IV).⁶



The clearest and most convincing evidence for the intermediacy of such species comes from experiments involving the ligand 5-nitro-1,10-phenanthroline.⁸ This complex shows an initially reversible shift of its visible spectrum with changes in pH, the neutral solution having $\lambda_{\text{max}} = 510 \text{ nm}$ and the alkaline solution, initially, $\lambda_{\text{max}} = 528 \text{ nm}$. The electron withdrawing properties of the nitro-group apparently favour the formation of such intermediates. Spectroscopic and kinetic characteristics of intermediates of type (IV) are easier to obtain for ruthenium(II)^{8,9} than for iron(II) complexes, in view of the more rapid substitution (especially in the presence of a nitro substituent) at the latter centre. Neverthe-

less, a solid product has recently been obtained^{10,11} from the reaction of $[\text{Fe}(\text{5NO}_2\text{-phen})_3]^{2+}$ with cyanide, which may well be of type (IV) above.

The sulphonato group has similar electron withdrawing properties to the nitro-group, which suggests that complexes containing sulphonated diimine ligands such as the 3- or 5- sulphonato derivatives of 1,10-phenanthroline,¹² or 3-(2-pyridyl)5,6-bis-(4-sulphophenyl)-1,2,4-triazine¹³ (the so-called ferrozine or ppsa ligand), structure (V) below, may also yield evidence for nucleophilic attack via intermediates of the type discussed.



Substitution at $[\text{Fe}(\text{ppsas})_3]^{4-}$ is considerably slower¹⁴ than at $[\text{Fe}(\text{5NO}_2\text{-phen})_3]^{2+}$, facilitating spectroscopic detection of intermediates. The ferrozine complex has the advantage that, in view of its large negative charge, it is extremely unlikely to form ion-pairs or outer-sphere associated species with negatively charged nucleophiles such as OH^- , RO^- , and CN^- .

A kinetic and spectroscopic study of the reaction of the $[\text{Fe}(\text{ppsas})_3]^{4-}$ anion with hydroxide ion in aqueous methanol¹⁵ provided strong support for a mechanism in which a relatively rapid pre-equilibrium involving attack by hydroxide at the coordinated ferrozine is followed by rate-determining transfer of the hydroxyl group to the iron atom and subsequent rapid dissociation of the complex. The spectroscopic evidence was more

proton transfer in the opposite direction involving an adjacent water molecule.] The k_2 term could be ascribed to attack of another hydroxide anion at a second ligand, or directly at the iron atom now that the stability of the original complex has been reduced on formation of (VI).

The behaviour for hydroxide attack in aqueous dimethyl sulphoxide¹⁸ is very similar to that in aqueous methanol. The reaction of $[\text{Fe}(\text{ppsa})_3]^{4-}$ with cyanide follows a simple kinetic pattern in water,¹⁴ but in aqueous dimethyl sulphoxide¹⁸ a complicated pattern of changes in visible spectra is observed, though this pattern does point to the presence of intermediates with one or two cyanide ions bonded to the ligands.

This chapter reports an extension of the kinetic study of the reaction of $[\text{Fe}(\text{ppsa})_3]^{4-}$ with hydroxide and cyanide ions. The possibility that the presence of an intermediate might be revealed by the dependence of rate constant on temperature was examined. The consequences of ion-pairing equilibria at high ionic strengths were investigated to complement previous work involving cationic iron(II) complexes with other diimine ligands.

This chapter also reports an initial study of an anionic iron(II) complex containing a diimine ligand related to ferrozine, in an attempt to find another system where the presence of intermediates can be demonstrated.

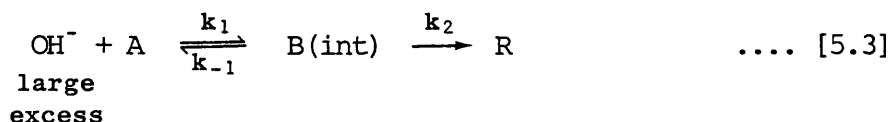
The final section of the chapter discusses equilibria between free diimine ligands and nucleophiles. This subject is essentially the basis for the whole of the above discussion concerning complexes. An original computer program for the evaluation of these equilibrium constants from spectrophotometric data is presented.

5.2 VARIABLE TEMPERATURE KINETICS OF THE REACTIONS OF TRIS-FERROZINE IRON(II) WITH ACID AND HYDROXIDE

5.2.1 Outline

In the spectroscopic study¹⁵ of the reaction between $[\text{Fe}(\text{ppsa})_3]^{4-}$ and hydroxide ions summarised above, evidence was presented for the existence of an intermediate in water. To extend the investigation of the kinetic consequences of the presence of this intermediate, the variation of the observed rate constant with temperature was measured. Depending on the kinetic characteristics of the proposed underlying reaction mechanism, the possibility arises that the Arrhenius plot of $\ln(k_{\text{obs}})$ against $1/T$ is curved. This consideration is discussed more fully in the analysis of the temperature dependence of the rate constant for solvolysis of t-butyl chloride in Chapter 7. However, the important points will be noted here.

Consider the mechanism



Applying the steady state approximation to B, then

$$k_{\text{obs}} = \frac{k_1}{(1+\alpha)} [\text{OH}^-] \quad \dots [5.4]$$

where $\alpha = k_{-1}/k_2$.

If it is assumed that for each rate constant in the scheme, $\ln(k_i)$ is a linear function of $1/T$ (i.e. $\Delta C_{p_i}^\ddagger = 0$), the result is that $\ln(k_{\text{obs}})$ is not a linear function of $1/T$. Curvature of the observed Arrhenius plot is therefore a result of the presence of an intermediate under steady-state conditions, i.e. $\frac{d}{dt} [\text{B}] = 0$, $[\text{B}]$ is small. ΔH^\ddagger (apparent) is a function of the values of ΔH^\ddagger for each k_i , and possible $\Delta C_{p_i}^\ddagger$ parameters. But even if each $\Delta C_{p_i}^\ddagger$ is zero, as is assumed, ΔH^\ddagger (apparent) still depends

on temperature.

Now consider the mechanism



where K represents a true equilibrium between A and B which is established much more quickly than reaction of B via the k_2 pathway. Then

$$k_{\text{obs}} = K k_2 [\text{OH}^-] \quad \dots [5.6]$$

This has the result that $\ln(k_{\text{obs}})$ is a linear function of $1/T$, again assuming each $\Delta C_{p_i}^\ddagger$ is zero, and so ΔH^\ddagger (apparent) = $(\Delta H_K^\ddagger + \Delta H_2^\ddagger)$.

To obtain an Arrhenius plot suitable for this level of examination, good kinetic data are needed over a wide temperature range. The rate constants for reaction of $[\text{Fe}(\text{ppsa})_3]^{4-}$ with H^+ (acid aquation) and OH^- ions were measured over as wide a temperature range as possible with the existing apparatus. The aquation reaction was studied to determine the extent of its contribution to the overall kinetics. A large contribution would effectively prevent an analysis in terms of the two schemes described above.

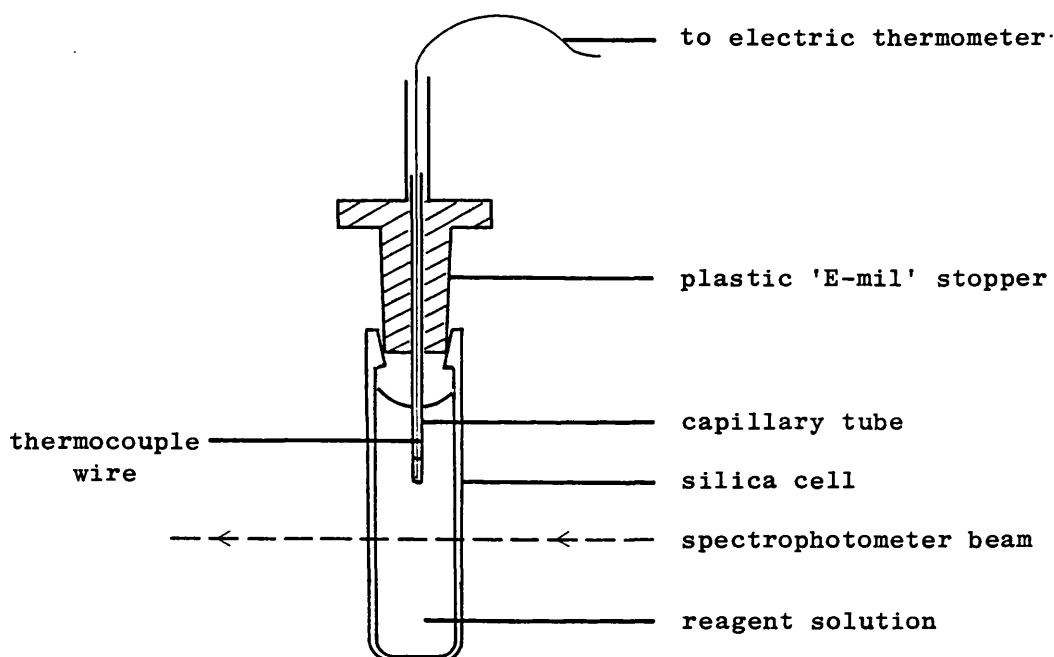
5.2.2 Experimental

The complex $[\text{Fe}(\text{ppsa})_3]^{4-}$ was prepared in concentrated solution by the reaction of ammonium iron(II) sulphate (AnalaR) with very slightly more than the stoichiometric quantity of ligand (Hach Chemical Co., Ames, Iowa). The visible spectrum of a diluted sample of the solution was checked against published data.¹³

Stock solutions of 0.1 mol dm^{-3} sodium hydroxide and 0.1 mol dm^{-3} hydrochloric acid were prepared using C.V.S. ampoules (B.D.H.) and kept firmly stoppered when not in use.

Rate constants were obtained from absorbance data paper-tape logged over at least $2\frac{1}{2}$ half-lives. Both reactions were monitored at 562 nm ($\epsilon = 27,900^{13}$). The initial concentration of complex was ca. 4×10^{-5} mol dm^{-3} .

To monitor the temperature in the reaction cell accurately a thermocouple was used, introduced into the cell via a glass capillary tube through a suitable plastic stopper, as shown diagrammatically below.



In this way the temperature in the cell was measured to ± 0.1 K. [The digital thermometer was calibrated against the quartz thermometer probe usually used to monitor the temperature of the cell block.]

For all kinetic runs, the reaction was initiated by introducing one drop of concentrated complex solution into a previously thermostatted cell containing about 3 cm^3 of 0.1M acid or alkali; thus the dilution effect was negligible. For the fastest reactions with alkali at the highest temperatures, the complex was introduced without removing the cell from

the cell block to prevent excessive cooling. [Experiments away from the spectrophotometer showed that the force of introduction of the complex from a syringe produced sufficient mixing.] At the higher temperatures, the syringe used to introduce the complex was preheated in an electrically thermostatted copper block.

The temperature in the reaction cell was monitored at all stages before and during a kinetic run. In the faster runs, the time taken for replacement of the thermocouple into the cell after introduction of the complex meant that the largest absorbance changes were not logged, but this meant accurate temperature measurement could still be carried out.

Rate constants obtained were selected for final analysis on the basis of two criteria:

- (i) the difference in temperatures at the start and the finish of the high-temperature runs did not exceed 0.5 K at the worst;
- (ii) the standard error on the rate constant as calculated by the computer program did not exceed 1%.

On the basis of these criteria, the results of approximately half the total number of kinetic runs were discarded. Given the limitations of the apparatus used for this type of experiment, the procedure described in this section emerged as the best compromise accommodating the major contributing factors.

5.2.3 Results

The reactions of $[\text{Fe}(\text{ppsa})_3]^{4-}$ with 0.1 mol dm^{-3} hydroxide and with 0.1 mol dm^{-3} hydrochloric acid followed first-order kinetics over at least $2\frac{1}{2}$ half-lives at all the temperatures studied. With hydroxide at the very lowest temperature, the absorbance at infinite time suggested incompleteness of reaction, so the reaction was not studied at lower temperatures. Observed first-order rate constants are reported in Tables (5.1) and

TABLE (5.1)

Temperature dependence of observed first-order rate constant for the acid aquation of tris-ferrozine iron(II), with derived activation parameters.

T/K	$k_{\text{obs}}/\text{s}^{-1}$
0.1 mol dm ⁻³ HCl	
298.2	4.189×10^{-5}
298.2	4.279×10^{-5}
303.2	9.169×10^{-5}
303.2	9.015×10^{-5}
308.2	2.077×10^{-4}
308.2	2.091×10^{-4}
308.2	2.044×10^{-4}
308.2	1.885×10^{-4}
313.0	3.907×10^{-4}
312.8	3.915×10^{-4}
312.9	3.973×10^{-4}
327.2	3.440×10^{-3}
327.3	3.556×10^{-3}
327.0	3.374×10^{-3}
327.5	3.511×10^{-3}
327.6	3.548×10^{-3}
0.075 mol dm ⁻³ HCl ^a	
313.2	3.957×10^{-4}
313.2	4.381×10^{-4}
0.050 mol dm ⁻³ HCl ^a	
313.2	4.450×10^{-4}
313.2	4.227×10^{-4}

^a ionic strength maintained with KCl

Activation energy = $123.8 \pm 0.9 \text{ kJ mol}^{-1}$

$\Delta H_{298}^{\ddagger} = E_a - RT = 121.3 \text{ kJ mol}^{-1}$

TABLE (5.2)

Temperature dependence of observed first-order rate constant for the reaction of tris-ferrozine iron(II) with hydroxide ions, with activation parameters.

T/K	$k_{\text{obs}}/\text{s}^{-1}$
0.1 mol dm ⁻³ NaOH	
289.5	3.051×10^{-4}
289.7	2.914×10^{-4}
289.6	2.846×10^{-4}
294.2	5.141×10^{-4}
294.2	5.089×10^{-4}
294.1	4.949×10^{-4}
298.2	8.925×10^{-4}
298.2	9.380×10^{-4}
303.2	1.769×10^{-3}
303.2	1.769×10^{-3}
303.3	1.802×10^{-3}
303.2	1.759×10^{-3}
302.8	1.671×10^{-3}
312.9	5.099×10^{-3}
312.7	5.125×10^{-3}
312.9	4.899×10^{-3}
312.8	4.903×10^{-3}
313.0	5.211×10^{-3}
313.0	5.167×10^{-3}
326.9	3.086×10^{-2}
326.9	3.029×10^{-2}
326.9	2.810×10^{-2}
327.0	3.163×10^{-2}
327.2	3.266×10^{-2}
326.2	2.768×10^{-2}
328.6	3.768×10^{-2}
328.4	3.614×10^{-2}
329.0	4.201×10^{-2}
328.9	4.014×10^{-2}
329.0	4.003×10^{-2}

Activation energy = $99.03 \pm 0.8 \text{ kJ mol}^{-1}$

$\Delta H_{298}^{\ddagger} = E_a - RT = 96.55 \text{ kJ mol}^{-1}$

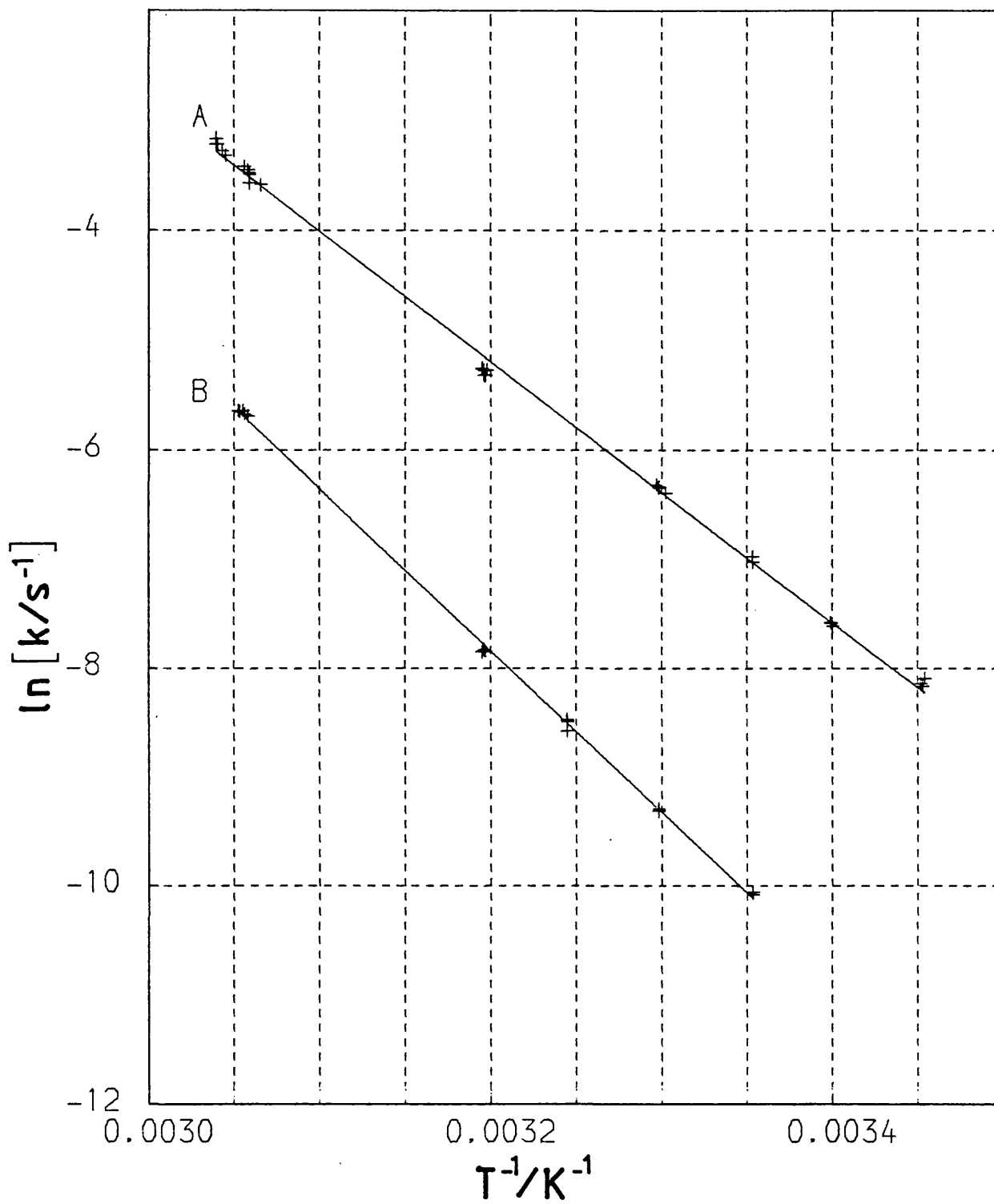


FIGURE (5.1)

Temperature dependence of the observed first-order rate constant for reaction of the $[Fe(ppsa)_3]^{4-}$ anion, (A) - with hydroxide; (B) - acid-catalysed aqutation.

(5.2). The rate constants in Table (5.1) for varying acid concentration were measured in order to check that the ligands were in a constant condition of deprotonation in the main experiment. The derived quantities in Tables (5.1) and (5.2) are shown diagrammatically in Figure (5.1).

The plots of $\ln(k_{obs})$ against $1/T$ for both reaction with hydrochloric acid and with sodium hydroxide are linear. It must be noted that any curvature arising from the operation of the mechanism in scheme [5.3] will not be marked. Indeed, the results reported in this section are probably still not accurate enough for use in this type of analytical approach. Moreover, the contribution of the aquation reaction is certainly significant over much of the temperature range studied, which essentially precludes the possibility of analysis in terms of the original hypothesis.

However, the kinetic results yield positive information in that the activation parameters for these reactions of the tris-ferrozine iron(II) complex have been accurately determined. These update those originally reported.¹⁴ It would be informative to measure the activation parameters for the complex containing the corresponding non-sulphonated ligand, which is available, in the reaction with acid and hydroxide, to obtain an indication of the effect of the presence of the sulphonate groups.

In spite of the above remarks, the results probably do indicate that any intermediate present is formed by a fast equilibrium prior to its subsequent slow reaction, as shown in scheme [5.6].

5.3 TRAPPING OF THE TRIS-FERROZINE IRON(II) ANION

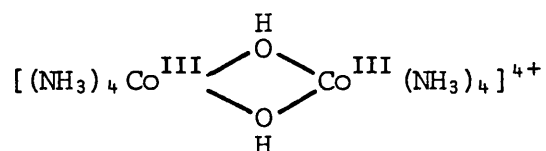
5.3.1 Discussion

In this chapter and in the literature, the tris-ferrozine iron(II) anion is written with a 4- charge. It is assumed that the two sulphonate groups on each of the three ligands are all ionized in solution. In view

of the large charge produced if this is the case, this state of complete ionization might not necessarily be expected. An important piece of background information to all the work on this anion is therefore a knowledge of its charge.

One approach to this problem was to expect that a large 4- anion would be precipitated by a large 4+ cation. As the tris-ferrozine iron(II) anion is intense purple in colour, its removal from solution could be easily observed.

One suitable, relatively easily prepared, cation with a 4+ charge is the following dinuclear cobalt(III) species:



Approximately 0.1g of the dithionate salt of this cation was dissolved in as small a quantity of distilled water as possible. To the resulting solution were added a few drops of concentrated solution containing the tris-ferrozine iron(II) anion.

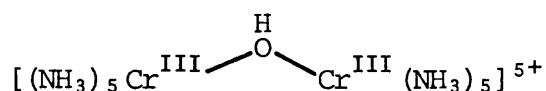
On standing, the purple colour was completely removed from the solution. A clear, colourless solution remained with a purple precipitate.

This observation does not necessarily prove that the complex is all present as the 4- anion. There are probably equilibria between the 4- anion and anions of lower charge. However, the complete precipitation shows that the 4- anion is a real, stable species.

It would be useful to find a salt of the anion with sufficient solubility to enable its measurement and subsequent calculation of $\delta_{\text{ml}}^{\ominus} \{ [\text{Fe}(\text{ppsa})_3]^{4-} \}$ for mixed aqueous media, for analysis of some of the existing kinetic data described in the introduction.

It may be possible to attempt to trap the postulated intermediate in

the reaction with hydroxide, which has a 5- charge, in the same manner. A suitable cation with a 5+ charge for which a straightforward preparation has been given¹⁹ is the following dinuclear chromium(III) species



However, this cation may not be stable in the alkaline media which are needed to generate the intermediate.

5.3.2 Experimental

$[(\text{NH}_3)_4 \text{Co}(\text{OH})_2 \text{Co}(\text{NH}_3)_4][\text{S}_2\text{O}_6]_2$ was prepared from $[\text{Co}(\text{NH}_3)_4 \text{CO}_3]_2 \text{SO}_4$ via the aquo hydroxo complex.²⁰

5.4 ION-PAIRING IN THE REACTION OF THE TRIS-PPSA IRON(II) ANION WITH CYANIDE IN AQUEOUS MEDIA AT HIGH IONIC STRENGTHS

5.4.1 Background

The general rate law for the reaction of low spin tris-diimine iron(II) complexes with nucleophiles (Nu) such as hydroxide or cyanide over a wide range of nucleophile concentrations at constant, and necessarily high, ionic strength is:⁴

$$-\frac{d}{dt} [\text{complex}] = \{k_1 + k_2 [\text{Nu}] + k_3 [\text{Nu}]^2 + k_4 [\text{Nu}]^3\} [\text{complex}] \quad \dots [5.7]$$

It was remarked in section (5.1) that the k_2 term is dominant. This is the case at low ionic strengths and thus at low nucleophile concentrations, where the simpler rate law holds:⁵

$$-\frac{d}{dt} [\text{complex}] = \{k_1 + k_2 [\text{Nu}]\} [\text{complex}] \quad \dots [5.8]$$

Under conditions of intermediate nucleophile concentration, or in

alcohol-water mixtures, an intermediate rate law containing the term in $[\text{Nu}]^2$ but not in $[\text{Nu}]^3$ provides a satisfactory fit of the experimental results. The k_1 term of each rate law corresponds to rate-determining iron-nitrogen bond cleavage. The k_2 term corresponds to a simple bimolecular reaction, the possible nature of which was discussed in section (5.1). The $k_3[\text{Nu}]^2$ and $k_4[\text{Nu}]^3$ terms of equation [5.7] may represent pathways involving participation of two or three hydroxide or cyanide ions previous to and in transition state formation, or they may be artefacts reflecting various ion-pairing equilibria in the concentrated solutions concerned. Such ion-pairing effects can indeed be important in determining the reactivity patterns in reactions of this type in aqueous media at high ionic strengths.

Ion-pairing in the reaction of the $[\text{Fe}(\text{phen})_3]^{2+}$ cation with cyanide has been studied.²¹ A brief summary of the results obtained provides the necessary background for the results reported here for the $[\text{Fe}(\text{ppsa})_3]^{4-}$ anion.

Observed first-order rate constants at 283.2 K, with cyanide in large excess, for the reaction of $[\text{Fe}(\text{phen})_3]^{2+}$ are shown graphically in Figure (5.2). Their dependence on cyanide concentration over the range 0 to 3.73 mol dm^{-3} when potassium nitrate is used to maintain the ionic strength can be represented by the simple linear expression of equation [5.8]. When potassium iodide or thiocyanate are used, this is not the case. There are specific anion effects operating, and the simplest and most plausible explanation of the observations is that ion-pairing is playing an important rôle at these high ionic strengths.

Competitive ion-pairing between $[\text{Fe}(\text{phen})_3]^{2+}$ and CN^- or X^- can provide a satisfactory explanation²¹ for the patterns in rate constant trends in terms of the following scheme, where $\text{X}^- = \text{I}^-$ or NCS^- ;

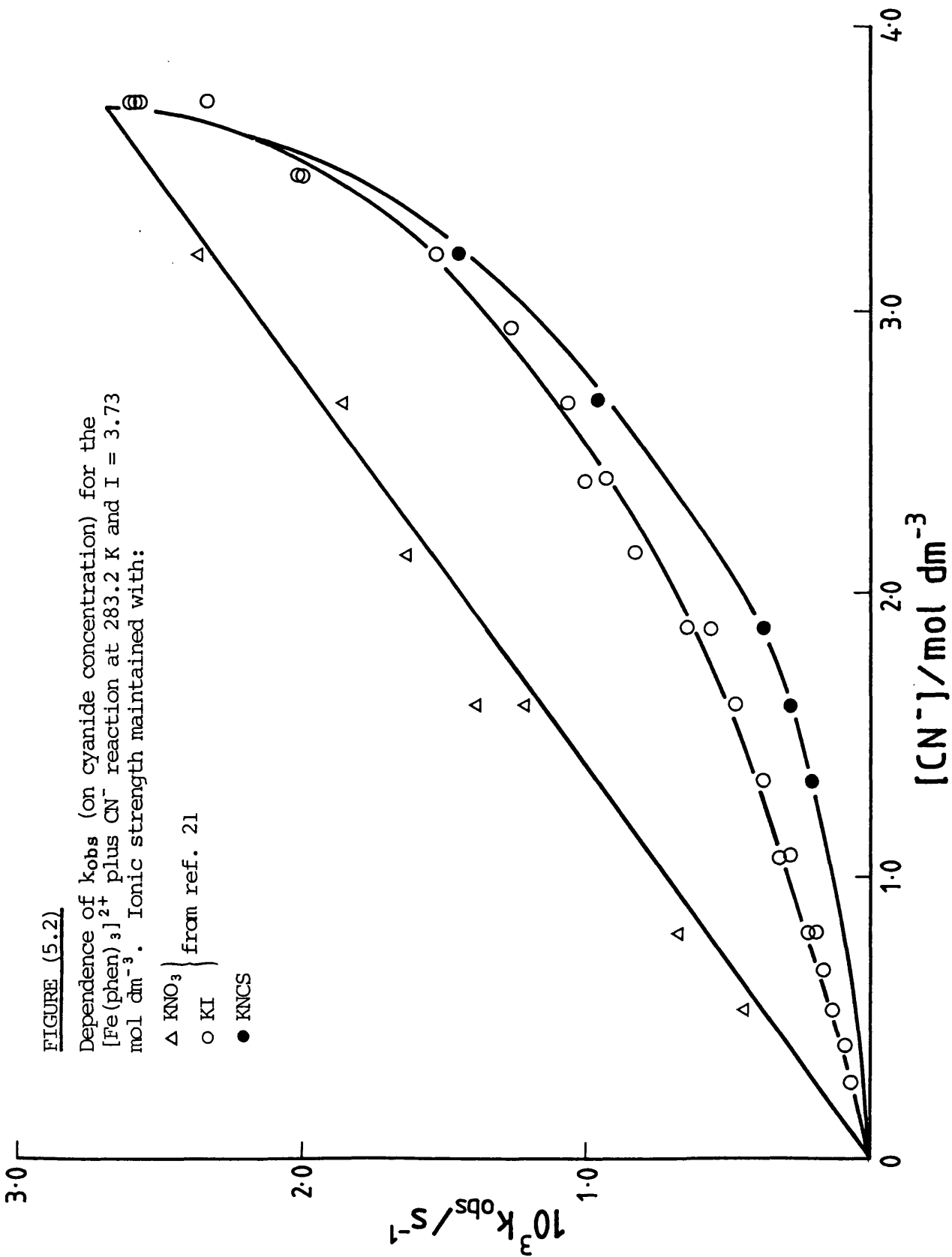
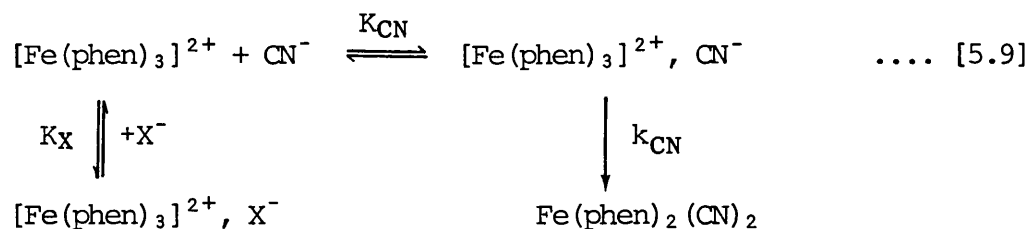


FIGURE (5.2)

Dependence of k_{obs} (on cyanide concentration) for the $[\text{Fe}(\text{phen})_3]^{2+}$ plus CN^- reaction at 283.2 K and $I = 3.73 \text{ mol dm}^{-3}$. Ionic strength maintained with:

- Δ KNO_3 } from ref. 21
- \circ KI
- \bullet KNCS



According to this scheme, the shapes of the k_{obs} versus cyanide concentration plots will depend on the ratio of the ion-pairing constants K_X/K_{CN} . Only when K_X is approximately equal to K_{CN} will the plot be linear: when K_X is greater than K_{CN} , then curvature of the type shown in Figure (5.2) will be obtained.

A plot of $1/k_{\text{obs}}$ against $1/[\text{CN}^-]$ is linear²¹ and the ratio K_X/K_{CN} can be evaluated from this plot. These ratios reveal that the relative ion-pairing tendencies are $\text{I}^- \sim \text{NCS}^- > \text{CN}^- \sim \text{NO}_3^-$.

This investigation was extended to cover the complementary situation of cyanide attack at the $[\text{Fe}(\text{ppsa})_3]^{4-}$ anion, where cation nature and concentration may determine reactivity.

5.4.2 Experimental

A concentrated solution containing the $[\text{Fe}(\text{ppsa})_3]^{4-}$ anion was prepared as described in section (5.2.2). Potassium cyanide (AnalaR), potassium chloride (AnalaR), potassium iodide (AnalaR), lithium chloride (B.D.H.), tetramethylammonium chloride (B.D.H.), potassium thiocyanate (May & Baker) and tetraethylammonium cyanide (Fluka) were used as supplied.

Rate constants were obtained using the minicomputer controlled apparatus. The required rapidity of the absorbance readings, and the small overall absorbance changes were near the operational limit of the apparatus.

The reaction was monitored at 562 nm. The reaction was initiated by introducing a few drops of concentrated solution containing the complex

into a cell containing 3.0 cm³ of reagents. The initial concentration of complex was ca. 2.5×10^{-5} mol dm⁻³.

5.4.3 Results and discussion

On addition of the red-purple complex to cyanide media where the ionic strength was maintained with chloride salts, a blue-purple solution was produced. The experimentally measured rate constants described the absorbance change at λ_{\max} for the original complex.

Observed first-order rate constants at 298.2 K are reported in Table (5.3) and shown graphically in Figure (5.3). The dependence of k_{obs} on cyanide concentration is not linear for any reaction medium. Some anomalous results were obtained as described below.

The straightforward results are those where the ionic strength is maintained with MCl, M = K⁺, Li⁺ or Me₄N⁺. The cause of the curvature of the plots in Figure (5.3) can be attributed to ion-pairing between the cations and the [Fe(ppsa)₃]⁴⁻ anion. The similarity of the effect of the alkali metals lithium and potassium is in marked contrast to the effect of the tetramethylammonium cation. To explain this difference, the concepts of solvent-structure effects of cations need to be employed. These concepts are discussed at the beginning of Chapter 6, but the important points will be briefly considered here.

The rate constants for 2.0 and 3.0 mol dm⁻³ potassium cyanide in the presence of the tetramethylammonium cation are higher in value than that for 4.0 mol dm⁻³ potassium cyanide. In real salt solutions, the solvent cospheres around the ions present overlap and interact. For overlap between a cation and the hydrophilic cyanide ion, the interaction for the tetramethylammonium cation is different from that for the potassium cation. For the former, hydration characteristics for the cation and anion are incompatible, and this results in destabilization which raises

TABLE (5.3)

Observed first-order rate constants for the reaction of $[\text{Fe}(\text{ppsa})_3]^{4-}$ with cyanide ion at 298.2 K at constant ionic strength (4.0 mol dm^{-3}) for various co-electrolytes

Added salt	[KCN]/mol dm^{-3}	$10^2 k_{\text{obs}}/\text{s}^{-1}$
KCl	{ 4.0	2.67
	{ 3.0	2.47
	{ 2.0	2.06
	{ 1.0	1.33
	{ 0.533	0.741
LiCl	{ 3.0	2.38
	{ 2.0	1.91
	{ 1.0	1.13
	{ 0.533	0.636
Me_4NCl	{ 3.0	3.27
	{ 2.0	2.88
	{ 1.0	2.30
	{ 0.533	1.92
	4.0 (Et_4NCN)	3.15 (average)
KI ^a	{ 3.0	2.32
	{ 2.0	1.92
KNCS ^a	{ 3.0	2.31

^a Absorbance changes are significantly smaller in the presence of these salts. See text.

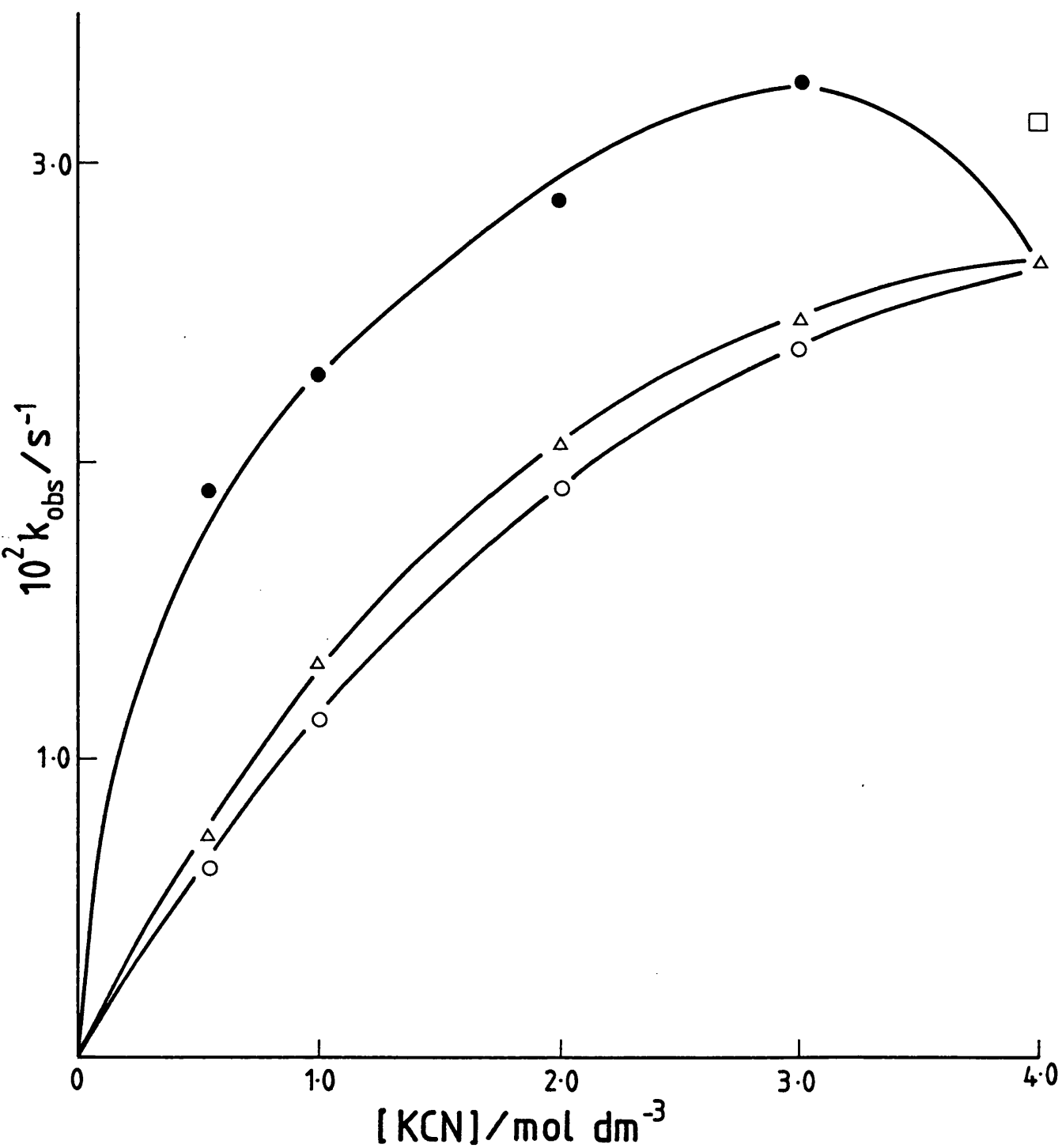


FIGURE (5.3)

Observed first-order rate constants for the reaction of $[\text{Fe}(\text{ppsa})_3]^{4-}$ with cyanide ion at 298.2 K at constant ionic strength, maintained with; \triangle KCl , \circ LiCl , \bullet Me_4NCl , \square Et_4NCN .

the chemical potential of the cyanide anion. The resulting enhanced reactivity means a faster rate constant is measured.

This concept also explains why the rate constant for 4.0 mol dm^{-3} tetraethylammonium cyanide is higher than that for 4.0 mol dm^{-3} potassium cyanide.

For the study of ion-pairing in this context, the tetramethylammonium cation is not altogether suitable because of these solvent-structure effects. A simple 'soft' cation would be a better choice, e.g. Tl^+ , or Cd^{2+} (for comparison with Mg^{2+}). However, these soft cations have a strong affinity for cyanide ions which precludes their use in these experiments.

On addition of the red-purple complex to cyanide media where the ionic strength was maintained with iodide or thiocyanate, the immediate production of the blue-purple colour was not observed. The rate constants reported in Table (5.3) were obtained from small absorbance changes, presumably arising from a different process from that occurring in the presence of potassium chloride. At lower concentrations of potassium cyanide than those reported in the Table, no absorbance change occurs at all, at least over the time-scale of the experiments using chloride salts. The iodide and thiocyanate anions may be preventing reaction of the complex with cyanide ions in some way, or at least slowing this reaction markedly.

Prevention of reaction might be occurring by addition to the ligands where cyanide ion would normally attack. Spectroscopic studies of the addition of iodide or thiocyanate ion to $[\text{Fe}(\text{ppsa})_3]^{4-}$ in the absence of cyanide with cosolvents such as t-butanol yielded no useful information which could assist in understanding the observations reported. [There is evidence that iodide and thiocyanate ions will attack coordinated aromatic

ligands in other, related systems.]

Further investigation of these phenomena is needed, preferably with extension to another suitable anionic tris-diimine iron(II) complex.

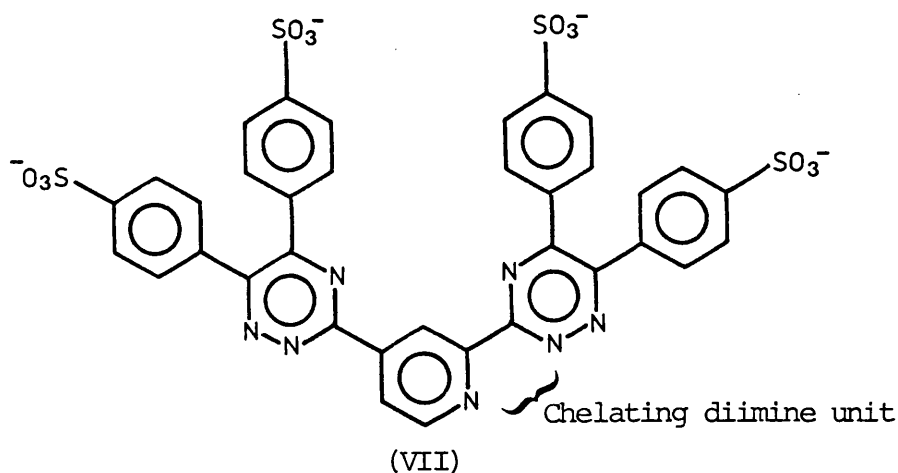
In view of the anomalous results obtained, a mechanistic scheme corresponding to scheme [5.9] cannot be adequately described at this stage, preventing a quantitative analysis of the kinetic results.

5.5 A KINETIC AND SPECTROSCOPIC STUDY OF THE REACTION OF THE TRIS-(2,4 BDTPS) IRON(II) ANION WITH HYDROXIDE IN WATER AND IN MIXED AQUEOUS MEDIA

5.5.1 Outline

In section (5.1), the kinetic and spectroscopic evidence for intermediates in the reaction of the $[\text{Fe}(\text{ppsa})_3]^{4-}$ anion with nucleophiles was discussed. A logical extension of this work is to study another anionic complex formed by a different ligand, with the possibility that this ligand has properties which might facilitate formation of, and stabilize, any intermediate formed.

A ligand suitable for this study is one related to ferrozine; 2,4-bis(5,6 diphenyl-1,2,4-triazin-3-yl) pyridine tetrasulphonic acid,²² the anion of which is structure (VII) below. Hereafter this ligand is referred to as bdtps.



An iron(II) complex containing three fully ionized bdtps ligands would have a formal charge of -10 . It is by no means certain that this is the case, so the iron(II) complex will be written as $[\text{Fe}(\text{bdtps})_3]^{n-}$.

The reaction of this complex with hydroxide ion in water and in mixed aqueous media was studied kinetically and spectroscopically. [The work was carried out under supervision as a third-year undergraduate project by Jane A. Franks and J. David Cowell.]

5.5.2 Experimental

A concentrated aqueous solution containing $[\text{Fe}(\text{bdtps})_3]^{n-}$ was prepared by the reaction of ammonium iron(II) sulphate (AnalaR) with very slightly more than the stoichiometric quantity of ligand (G. F. Smith Chemical Co.). A few drops of methanol assisted dissolution of the ligand.

Repeat scan spectra were recorded on the SP800 spectrophotometer. The reaction was initiated by the addition of a few drops of the concentrated complex solution to the appropriate reaction medium.

Accurate rate constants were measured using the minicomputer-controlled SP1800 spectrophotometer. The reaction was monitored routinely at 568 nm. This choice of wavelength was made after examination of the repeat scan spectra (for $[\text{Fe}(\text{bdtps})_3]^{n-}$ in water, $\lambda_{\text{max}} = 565 \text{ nm}$, $\epsilon = 32,200$).²² For these accurate measurements, a known volume of stock complex solution was used to ensure that its initial concentration was constant. Sodium hydroxide solutions were made up by direct weighing of AnalaR material and standardised by titration against standard hydrochloric acid (B.D.H., C.V.S. ampoule). Ionic strength was kept constant using sodium chloride (AnalaR).

Equilibrium constants were calculated from repeated continuous scan spectra generated by successive addition of micro litre volumes of concentrated sodium hydroxide solution (8 mol dm^{-3}) to a solution of the

complex in the appropriate solvent. The method of calculation is given in the discussion section.

Organic cosolvents were purified by established procedures.

5.5.3 Results and discussion

(i) Repeat-scan spectra

Spectra were obtained at 298.2 K for the reaction of the complex with hydroxide ion (0.1, 1.0 and 4.0 mol dm⁻³) in water and various methanol-water and DMSO-water mixtures. The spectrum of the complex in water is shown in Figure (5.4a). For reaction with 0.1 mol dm⁻³ hydroxide, the repeat-scan spectrum showed simple first-order disappearance of the peak at 565 nm.

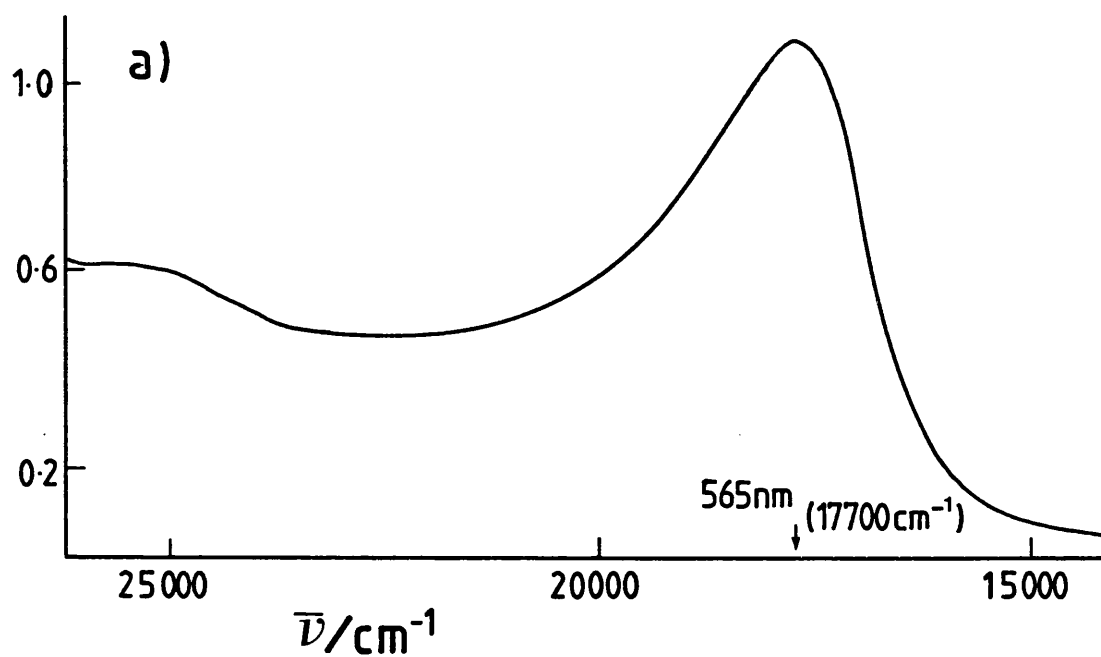
All other repeat-scan spectra for hydroxide attack consisted of two major bands at 565 nm and 645 nm. The spectrum for reaction with 1.0 mol dm⁻³ sodium hydroxide in 75% methanol is shown in Figure (5.4b). Comparison of these repeat-scan spectra with the spectrum of the complex alone shows that the peak at 565 nm corresponds to unchanged complex whilst the peak at 645 nm indicates that some other species is present. This second species must have been formed very quickly relative to the rate of subsequent reaction.

The ratio of the intensity of the peak at 565 nm to that of the peak at 645 nm was much greater in water than in aqueous methanol or aqueous DMSO mixtures. This would be expected because the chemical potential of OH⁻ in these mixtures is greater than in water. This enhanced reactivity would cause the equilibrium to shift in favour of the intermediate.

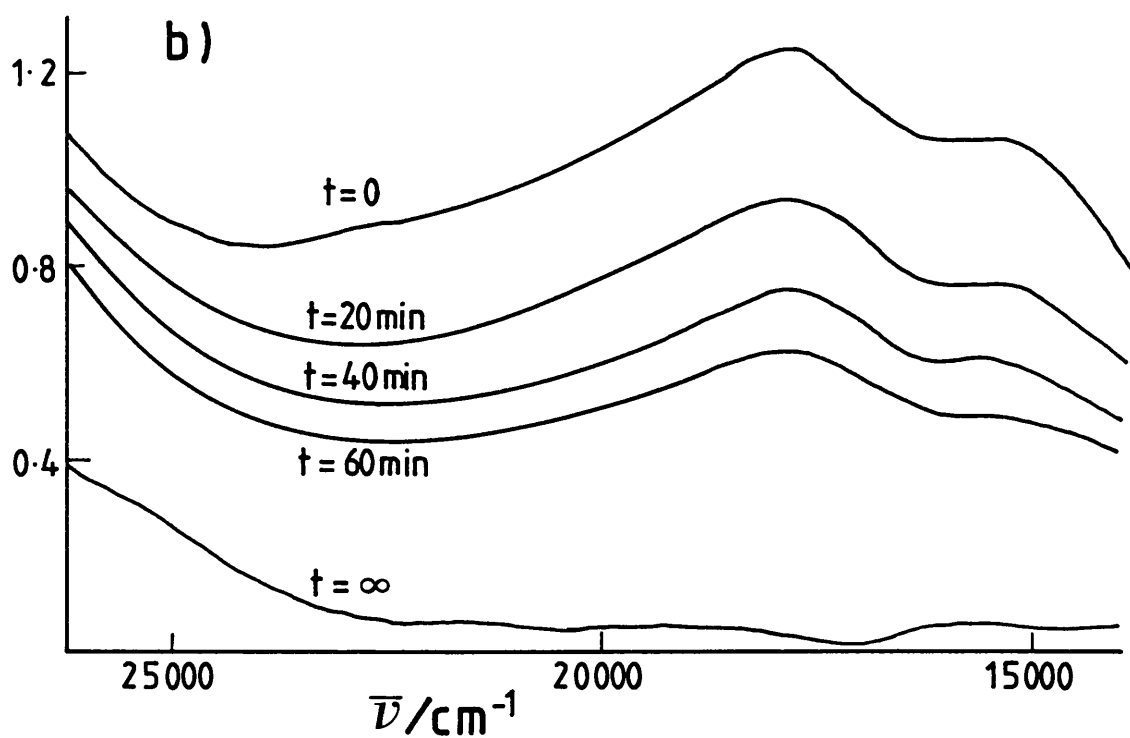
Repeat-scan spectra for reaction with 2.0 mol dm⁻³ potassium cyanide in 50% DMSO and 50% methanol showed a more complex dependence on time. As the two peaks at 565 nm and 645 nm disappeared, a new peak rose at 617 nm. The spectrum at infinite time in 50% DMSO had peaks at 602 nm

FIGURE (5.4)

(a) UV/visible spectrum of $[\text{Fe}(\text{bdtps})_3]^{n-}$ in water at 298.2 K.



(b) Repeat scan spectra for reaction in 75% methanol with 1.0 mol dm^{-3} NaOH at 298.2 K.



and 470 nm. This system was not studied further.

(ii) Kinetics

Before accurate rate constants for reaction with hydroxide were measured routinely, it was confirmed that the rate constants describing the absorbance changes at 565 nm and 645 nm were equal within the limits of experimental uncertainty. Hence the equilibrium between the two species is established rapidly relative to the process monitored spectroscopically in the kinetic runs.

Observed first-order rate constants and derived second-order rate constants in various solvent mixtures are shown in Table (5.4). Plots of k_{obs} against $[OH^-]$ were linear through the origin.

(iii) Equilibria

A typical set of spectra obtained when small, known volumes of concentrated sodium hydroxide are successively added to a solution of $[Fe(bdtps)_3]^{n-}$ is shown in Figure (5.5). This shows the peak at 565 nm falling as more OH^- is added, whilst a peak at 645 nm rises. Isosbestic points are observed at 600 nm, 489 nm and 417 nm, indicating that two species are in equilibrium and are reacting further only slowly compared with the interval between scans. In some cases, where proportions of DMSO or methanol cosolvent were large, isosbestic were not observed because the chemical reaction occurred fast compared with the scan-time of the spectrophotometer.

Assuming that these spectral changes are due to the formation of an intermediate species by addition of a hydroxide ion to the complex, the equilibrium constant may be calculated. For the equilibrium



the equilibrium constant, K_c , is given by

TABLE (5.4)

Observed first-order rate constants, k_{obs} , and derived second-order rate constants, k_2 , for the reaction of $[\text{Fe}(\text{bdtps})_3]^{n-}$ with hydroxide in aqueous media at 298.2 K at constant ionic strength (KCl)

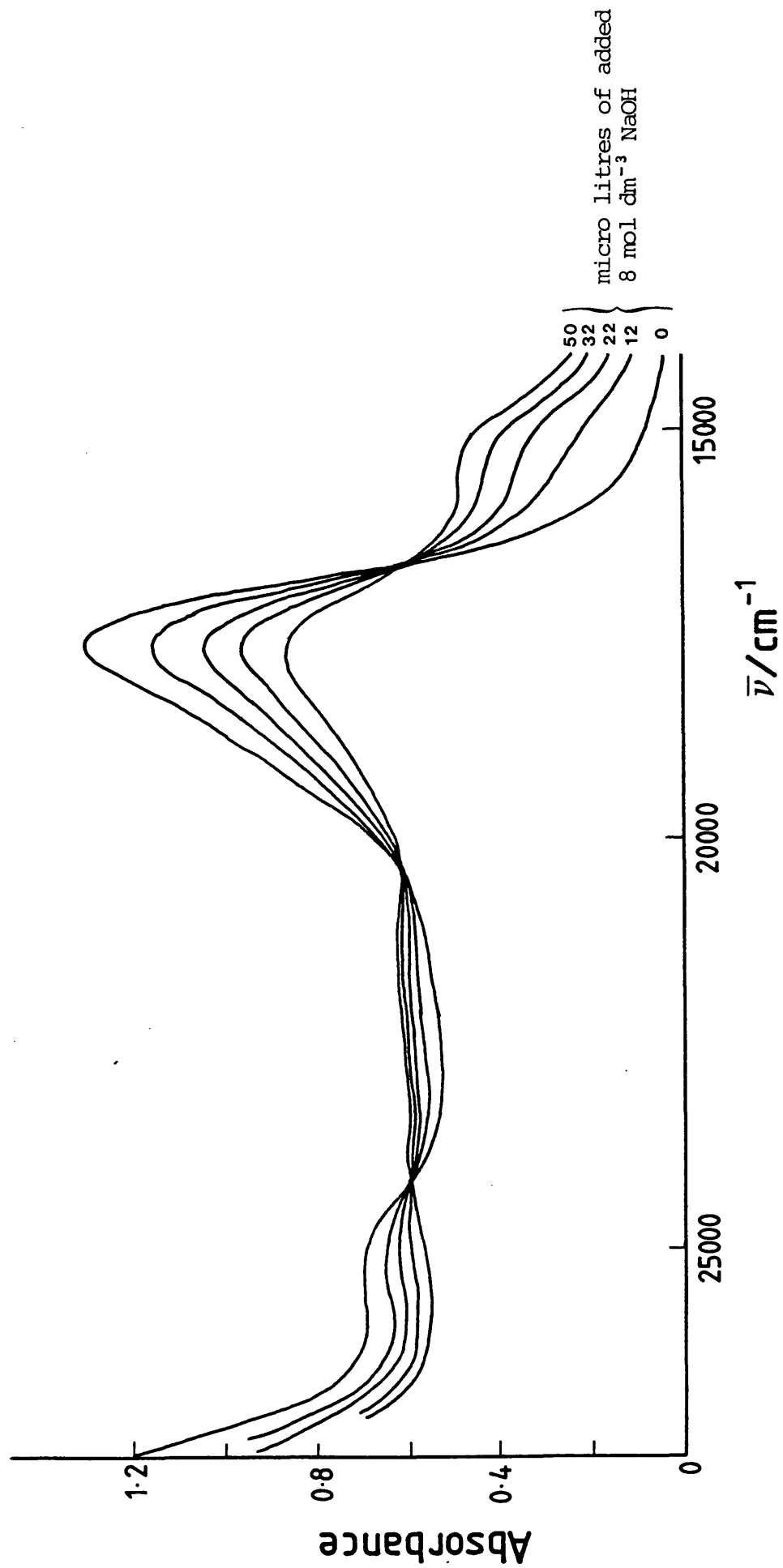
Solvent ^a	$[\text{OH}^-]/\text{mol dm}^{-3}$	$10^4 k_{\text{obs}}/\text{s}^{-1}$	$10^4 k_2 \pm \sigma^b / \text{dm}^3 \text{ mol}^{-1} \text{ s}^{-1}$
20% DMSO	0.981	6.92	6.91 ± 0.33
	0.785	5.35	
	0.589	4.10	
	0.491	3.27	
	0.393	2.47	
	0.196	1.61	
50% DMSO	1.000	11.72	11.1 ± 1.2
	0.785	9.03	
	0.589	6.72	
	0.491	4.58	
	0.393	3.32	
	0.196	1.94	
60% MeOH	0.951	7.28	7.40 ± 0.49
	0.781	5.69	
	0.571	3.75	
	0.476	3.51	
	0.380	2.72	
	0.190	1.67	

^a solvent compositions in volume % before mixing

^b standard errors

FIGURE (5.5)

Spectrophotometric titration of the $[\text{Fe}(\text{bdtps})_3]^{n-}$ anion with hydroxide in 20% DMSO at 298.2 K.



$$K_c = \frac{[(C-OH)^-]}{[C][OH^-]} \quad \dots [5.11]$$

Values for K_c were obtained from the spectrophotometric data by the use of the analysis and computer program discussed fully in section (5.6). The results are reported in Table (5.5). Some random error is present, but it is clear that these values are similar to those measured for $[Fe(ppsa)_3]^{4-}$ with hydroxide [see Table (5.7)]. In the media where there is a large proportion of organic cosolvent, the subsequent reaction of the intermediate is significant and this affects the repeat-scan spectra. This is reflected in the quoted uncertainties on the values for K_c . The trends in the variation of K_c with increasing proportion of organic cosolvent are compatible with the increased chemical potential of the hydroxide ion in these aqueous mixtures.

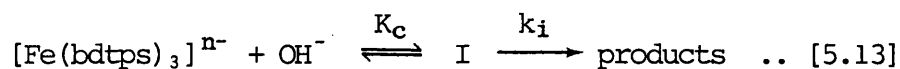
The estimated extinction coefficient for the intermediate at 645 nm is $20\,000 \text{ dm}^3 \text{ mol}^{-1} \text{ cm}^{-1}$.

(iv) Final discussion

The kinetic results and equilibria may be discussed in terms of a scheme analogous to scheme [5.1] for $[Fe(ppsa)_3]^{4-}$. From the dependence of the observed first-order rate constant on $[OH^-]$ we have:

$$k_{obs} = k_2 [OH^-] \quad \dots [5.12]$$

Consider the reaction scheme:



The equilibrium is rapidly established, so:

$$-\frac{d}{dt} [\text{complex}] = -\frac{d}{dt} [I] = k_i [I] \quad \dots [5.14]$$

But $K_c = [I]/[\text{complex}][OH^-] \quad \dots [5.15]$

So $[I] = K_c [OH^-] [\text{complex}]$

TABLE (5.5)

Spectrophotometrically determined equilibrium constants for the reaction between $[\text{Fe}(\text{bdtps})_3]^{n-}$ and hydroxide in aqueous media at 298.2 K

% cosolvent ^a	$K_C/\text{dm}^3 \text{ mol}^{-1}$		
	water	MeOH	DMSO
0	5 ± 2		
20		14 ± 1.4	8 ± 0.8
30		12 ± 3	24 ± 6
40			76 ± 7
50		44 ± 3	77 ± 10
60		16 ± 3	
80		37 ± 14	

^a % by volume before mixing

TABLE (5.6)

Calculated values for k_1 in scheme [5.13] for the reaction between $[\text{Fe}(\text{bdtps})_3]^{n-}$ and hydroxide in aqueous media at 298.2 K

	Solvent ^a		
	20% DMSO	50% DMSO	60% MeOH
$10^4 k_2/\text{dm}^3 \text{ mol}^{-1} \text{ s}^{-1}$	6.85	11.1	7.40
$K_C/\text{dm}^3 \text{ mol}^{-1}$	8	77	16
$\therefore 10^5 k_1/\text{s}^{-1}$	8.56	1.44	4.62

^a % by volume before mixing

Therefore
$$-\frac{d}{dt}[\text{complex}] = k_i K_c [\text{OH}^-][\text{complex}] \quad \dots [5.16]$$

Comparison of [5.12] and [5.16] gives

$$k_2 = k_i K_c \quad \dots [5.17]$$

Using values for k_2 and K_c in the same solvent medium, k_i for this medium may be calculated. The results of this calculation are reported in Table (5.6). The variation in the values reported may not be significant bearing in mind the overall uncertainties in the values for K_c . The values for k_i would be expected to be constant for the simple intramolecular migration of the hydroxyl group from the ligand to the iron atom.

The results reported in this section provide a clear confirmation of those obtained for $[\text{Fe}(\text{ppsa})_3]^{4-}$, the intermediate being readily detectable in all the aqueous media studied. It may be possible to study the temperature variation of K_c for the reaction between $[\text{Fe}(\text{bdtps})_3]^{n-}$ and hydroxide, to obtain enthalpy quantities for the equilibrium in aqueous media.

The sulphonated diimine ligand 4,7-diphenyl-1,10-phenanthroline disulphonate forms an anionic complex with iron(II). No spectroscopic evidence could be obtained for intermediates in the reaction of this complex with hydroxide ions for concentrations of sodium hydroxide up to 2.0 mol dm^{-3} , and in mixed solvents up to 40% by volume of methanol or DMSO. This complex may be suitable for further ion-pairing studies in the reaction with cyanide as described in the previous section. The $[\text{Fe}(\text{bdtps})_3]^{n-}$ anion is not suitable for this work because of the observed complexity of the reaction with cyanide ions.

5.6 EQUILIBRIA BETWEEN DIIMINE LIGANDS AND HYDROXIDE IONS IN AQUEOUS MEDIA

5.6.1 Background

In the previous section, an example was given where the equilibrium constant describing a chemical system was calculated from absorbance data produced in a spectrophotometric titration experiment. The analysis of this type of data to obtain equilibrium constants was originally given by Benesi and Hildebrand,²³ who employed certain approximations to enable a straight-line graphical analysis.

The interaction of diimine ligands such as 5-nitro-1,10-phenanthroline with nucleophiles such as hydroxide and cyanide can be conveniently followed spectroscopically, using the titration method of the previous section. A general, and rigorous, treatment of the absorbance data to yield the equilibrium constant seemed desirable, and appropriate in cases where the species produced does not undergo subsequent decomposition.

A suitable treatment has been given by Rose and Drago²⁴ (who also discuss the inadequacies of the Benesi-Hildebrand and related methods). This treatment is used as the basis for an original computer program which calculates the equilibrium constant by applying the method of least squares to all the available data points. The principles behind this analysis are given here, and the program is listed and documented in Appendix 3.

Consider the equilibrium



where L is a diimine ligand, Nu is a nucleophile such as hydroxide and NuL is the addition product formed by the equilibrium. If the initial concentrations of ligand and nucleophile are c_0 and $y \text{ mol dm}^{-3}$, and at equilibrium the concentration of NuL is $c \text{ mol dm}^{-3}$, then the equilibrium

constant in terms of concentrations, K_c , may be written as follows:

$$K_c = \frac{[\text{NuL}]}{[\text{L}][\text{NuL}]} = \frac{c}{(c_0 - c)(y - c)} \quad \dots [5.19]$$

If the extinction coefficients of L and NuL at a given wavelength, λ , are ϵ_L and ϵ_{NuL} respectively, the absorbance A at wavelength λ is given by

$$A = \epsilon_L (c_0 - c) + \epsilon_{\text{NuL}} c \quad \dots [5.20]$$

Substitution for c from [5.20] into [5.19] and rearrangement gives

$$K_c^{-1} = \frac{A - c_0 \epsilon_L}{(\epsilon_{\text{NuL}} - \epsilon_L)} - c_0 - y + y c_0 \frac{(\epsilon_{\text{NuL}} - \epsilon_L)}{(A - c_0 \epsilon_L)} \quad \dots [5.21]$$

If A_0 is the absorbance at wavelength λ of the ligand before any nucleophile is added, then from Beer's Law

$$A_0 = \epsilon_L c_0 \ell \quad \dots [5.22]$$

where ℓ is the path length, 1 cm. When the concentration of nucleophile is very large, effectively all L has been converted to NuL, so if A_∞ is the absorbance at very high [Nu], then

$$A_\infty = \epsilon_{\text{NuL}} c_0 \ell \quad \dots [5.23]$$

Substituting for ϵ_L (but not for ϵ_{NuL} for reasons explained below) in [5.21] gives

$$K_c^{-1} = \frac{(A - A_0) c_0 - c_0 - y + y \frac{(c_0 \epsilon_{\text{NuL}} - A_0)}{(A - A_0)}}{(c_0 \epsilon_{\text{NuL}} - A_0)} \quad \dots [5.24]$$

Rearrangement gives a quadratic equation in $(A - A_0)$:

$$0 = (A - A_0)^2 \frac{c_0}{(c_0 \epsilon_{\text{NuL}} - A_0)} - (K_c^{-1} + c_0 + y)(A - A_0) + y(c_0 \epsilon_{\text{NuL}} - A_0) \quad \dots [5.25]$$

which has the solution

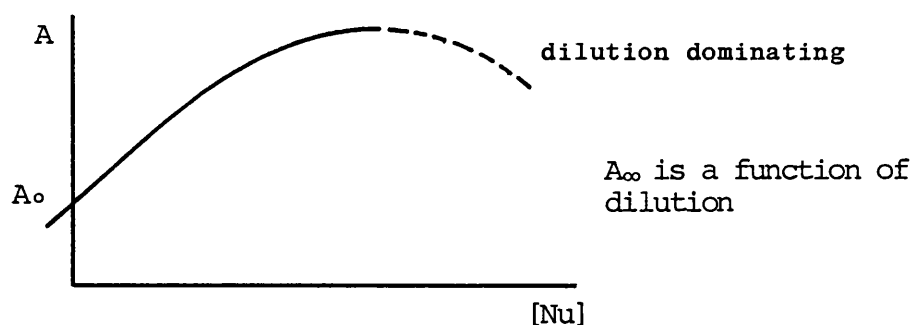
$$(A - A_0) = \left[(K_c^{-1} + c_0 + y) - \left\{ (K_c^{-1} + c_0 + y)^2 - 4 c_0 y \right\}^{1/2} \right] \frac{(c_0 \epsilon_{\text{NuL}} - A_0)}{2 c_0} \quad \dots [5.26]$$

(Inspection shows that the negative root is taken). This is an equation for the change in absorbance at a given wavelength as a function of the variable y and the constants K_c , ϵ_{NuL} , A_0 and c_0 . Effectively this is what is required. However, if the nucleophile is added as a (small) volume of concentrated solution, a dilution effect is also in operation which will become increasingly important as more nucleophile is added. A compensation for this effect is built into the equation to produce the final form used. If the initial volume of solution is $\text{cellvol}_0 \text{ cm}^3$, and at a given stage of nucleophile addition it is $\text{cellvol} = (\text{cellvol}_0 + \text{total vol. Nu added}) \text{ cm}^3$, then at this stage the corrected values of c_0 and y are given by

$$c'_0 = c_0 \cdot r, \quad y' = y \cdot r \quad \dots [5.27]$$

where $r = (\text{cellvol}_0)/(\text{cellvol})$.

Thus equation [5.26] in conjunction with [5.27] gives the observed absorbance change as a function of chemical effects and dilution effects. This change has the general form shown below:



Finer details of the program are given in Appendix 3. Equation [5.26] is fitted to a data set of absorbance against micro-litre volume of nucleophile added, by the Newton-Raphson non-linear least squares technique.

The program was tested on some fifty sets of results for spectrophotometric titrations of free and coordinated diimine ligands. In a few

TABLE (5.7)

Equilibrium constants ($\text{dm}^3 \text{mol}^{-1}$; 298 K) for interaction of hydroxide with diimines and their metal complexes

	water	aqueous					
		DMSO	MeOH	EtOH	i-PrOH	t-BuOH	
5NO ₂ phen	1 ^a	20%	1.1	1.0	2.1		
		40%	2.1	0.8	2.3	(2)	(4)
		60%		0.3	3.1		
		80%	large			(8)	(11)
Fe(5NO ₂ phen) ₃ ²⁺	143						
Ru(5NO ₂ phen) ₃ ²⁺	33						
Fe(5NO ₂ phen) ₂ (CN) ₂		27		(15)			
		82					
		690					
		2040		(50)			
Fe(bipy) ₂ (CN) ₂		9					
Mo(5NO ₂ phen)(CO) ₄				5			
				6			
Fe(fz) ₃ ⁴⁻	3						
		228	16				
		8	14				
Fe(bdtps) ₃ ⁿ⁻	5	76					
			16				
			50				

^a Data (293 K) from Ref. 25, using the modified program (see Appendix 3)

cases, some effort was required at a computer terminal to find the least squares minimum, especially if the data were poor. However, all data tested were eventually fitted successfully. The uncertainty on the derived parameters depended ultimately on the quality of the data.

5.6.2 Results

Table (5.7) shows some estimated equilibrium constants for diimine ligands with hydroxide. The accumulation of data is at an incomplete stage and there are surprising random errors in some of the trends obtained. Hence it is not possible to give a full discussion of the results at this stage. However, the values reported in the Table are compatible with changes in the chemical potential of the hydroxide ion in these solvent mixtures, and with the relative activation of the coordinated ligands towards nucleophiles by the metal centres Mo^0 and Fe^{2+} .

The value for 5- NO_2 -phen with hydroxide in water was calculated using a modified version of the program applicable to concentration data, using some literature results.²⁵ The value obtained agrees satisfactorily with that derived graphically in the reference.

CHAPTER 6

INITIAL STATE AND TRANSITION STATE
CONTRIBUTIONS TO SALT EFFECTS ON KINETICS
IN INORGANIC SYSTEMS

6.1 BACKGROUND

6.1.1 Introduction

Considerable progress has been made in analysing solvent effects on reactivity into initial state and transition state contributions for organic and inorganic reactions [see Section 1.5]. Such analyses have been carried out both for series of single solvents and for a variety of binary aqueous mixtures. In contrast, there have been very few successful attempts regarding similar analyses of medium effects on reactivity for aqueous salt solutions, despite the fact that the concentration and nature of an added salt can have a marked effect on reaction rates.¹

This chapter reports three initial state - transition state studies of salt effects on kinetics in inorganic systems. These systems comprise the reactions of two square-planar d^8 transition metal complexes and the hydrolysis of trimethylamine sulphur trioxide. The discussion contrasts the difficulty involved in the analysis when the reactants are charged with the more straightforward analysis when the reactants are neutral. A brief description of the structure of salt solutions provides the necessary background for this discussion.

6.1.2 Salt solutions

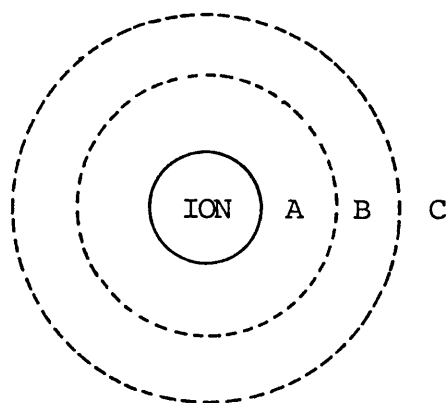
(i) Ionic hydration

The environment of an ion in aqueous solution can be discussed in terms of a cosphere of solvent around an ion where the structure differs from that in the bulk. In one treatment² the cosphere is divided into two regions, as shown in Figure (6.1). Zones A and B comprise the cosphere of the ion.

Zone A is the primary solvation shell of the ion. Water molecules hydrate the ion in an electrostricted layer of solvent molecules.

Zone C contains water whose structure is essentially unperturbed from

FIGURE (6.1)



bulk water itself at the same temperature and pressure, except that it is subjected to the electric field of the ion.

Zone B is a fault zone in which the water structure is broken down. This disorder arises because the ordering in Zone A is different from that in Zone C.

Zone B increases with increase in the size of the ions. The larger the ion, the more water structure is broken. Ions such as Cl^- , Br^- and I^- are therefore called 'electrostrictive structure breakers'. For small ions, e.g. Li^+ and F^- , Zone B is absent, the hydrated ion matching into and enhancing water-water interaction. These ions are called 'electrostrictive structure formers'.

This formalised model only applies to dilute solutions, where the mole ratio water: ions is large enough to provide sufficient water molecules so as to surround each ion to the extent indicated. The average separations of ions in a 1:1 electrolyte solution of 10, 1 or 0.1 mol dm^{-3} are 4.4, 9.4 and 20 \AA respectively.² Hence the model of Figure (6.1) can only be employed legitimately at a salt concentration of lower than about 0.1 mol dm^{-3} for a 1:1 electrolyte.

This model is also unsatisfactory for alkylammonium ions, R_4N^+ . The hydration of these ions is controlled by the apolar alkyl groups. As such, these ions are hydrophobic structure formers, the extent of

structure forming increasing with increase in the size of the alkyl group. More specifically, this is true when R is larger than ethyl; the Me₄N⁺ ion is usually classed as a structure breaker, and the Et₄N⁺ ion appears to have no marked effects on water structure.

(ii) Real salt solutions

It would be expected that the characteristics of ionic hydration would be reflected in the non-ideality of a given salt solution. The presence of some underlying pattern to mean ionic activity coefficients, γ_{\pm} , not readily accounted for by the Debye-Hückel treatment of ion-ion interactions, has been known for many years. Such patterns are apparent when values of γ_{\pm} for salt solutions at fixed molality and temperature are examined as a function of the anion. For example, $\gamma_{\pm}(\text{Pr}_4\text{N}^+\text{F}^-)$ is larger than $\gamma_{\pm}(\text{Cs}^+\text{F}^-)$ but $\gamma_{\pm}(\text{Cs}^+\text{I}^-)$ is larger than $\gamma_{\pm}(\text{Pr}_4\text{N}^+\text{I}^-)$.

For a 1:1 salt in solution, the chemical potential of the salt can be related to the composition of the salt solution by

$$\begin{aligned} \mu_2 &= \mu_2^{\ominus} + 2RT \ln m_2 \gamma_{\pm} \\ \text{or} \quad \mu_2 &= \underbrace{\mu_2^{\ominus} + 2RT \ln m_2}_{\text{ideal}} + \underbrace{2RT \ln \gamma_{\pm}}_{\text{non-ideal}} \quad \dots [6.1] \end{aligned}$$

where $\gamma_{\pm} \rightarrow 1$ as $m_2 \rightarrow 0$.

The Debye-Hückel limiting law (DHLL) treats γ_{\pm} in terms of charge-charge interactions. The limiting law is:

$$\ln(\gamma_{\pm i}) = -S_{\gamma} z_i^2 (I)^{\frac{1}{2}} \quad \dots [6.2]$$

where I = ionic strength/mol dm⁻³

S_{γ} = a function of the solvent properties at the given temperature and pressure

z_i = valency of the ion.

The trends not accounted for by the DHLL can be understood in terms of

the effect on γ_{\pm} of overlapping cospheres: this concept has been developed particularly by Desnoyers. Thus for two ions in solution, a general expression for γ_{\pm} is as follows:

$$\ln \gamma_{\pm} = \text{DHLL} + f(\text{cospheres}) \quad \dots [6.3]$$

$$\therefore \ln \gamma_{\pm} - \text{DHLL} = f(\text{cospheres})$$

where $f(\text{cospheres})$ describes the effect on γ_{\pm} of cosphere overlap interaction. If $f(\text{cospheres})$ is less than zero, the cosphere interaction leads to a lowering of μ_2 and therefore stabilization. If $f(\text{cospheres})$ is greater than zero, there is destabilization.

As a general rule, two ions in aqueous solution will attract each other if their structural influences or tendencies to orient water molecules are compatible, but they will repel each other if their influences are incompatible. Attraction will lower, and repulsion will raise, the activity coefficients and hence the chemical potentials. For example, overlap between cospheres of Bu_4N^+ ions in aqueous solution (hydrophobic hydration) is attractive and this is the dominant influence in $\text{Bu}_4\text{N}^+\text{I}^-$ solutions, cation-cation interactions leading to a low value of γ_{\pm} . In contrast, overlap between Bu_4N^+ cospheres (hydrophobic hydration) and F^- cospheres (hydrophilic hydration) leads to repulsion, the cation-cation interaction raising γ_{\pm} . As a general rule, interactions between solvent cospheres of alkylammonium ions in their salt solutions are the dominant influence on the properties of these solutions.

The success of the DHLL is often limited to the analysis of chemical potentials and related quantities, e.g. the effect of ionic strength on solubility products. The failure of the DHLL to account for the dependence of enthalpy, entropy and volume properties on salt concentration is often striking, compensation between H- and S- quantities minimising the changes in Gibbs functions.

6.1.3 Salt effects on reaction rates

In aqueous solution, the rate of a reaction involving charged or neutral reactants is sensitive to the concentration and nature of added salts. The classical Brønsted-Bjerrum treatment of salt effects, incorporating the DHLL or a related expression, has been particularly successful where the reactants are ionic and there is either a cancellation or generation of charge. The final equation yields the dependence of rate constant on ionic strength. The ionic strength principle appears to be satisfactory when the reaction involves ions of opposite charge, but less so when ions of the same charge are involved.³

With reference to salt effects on reactivity of neutral organic molecules, the first-order rate constant for the base-catalysed decomposition of diacetyl alcohol increases rapidly when $\text{Pr}_4\text{N}^+\text{OH}^-$ is added, less rapidly when $\text{Me}_4\text{N}^+\text{OH}^-$ is added, and decreases on addition of KOH. The conclusion that the variation in the rate constant stems from the effect of the added cation is verified by the observation that, at a fixed concentration of KOH, the addition of $\text{Et}_4\text{N}^+\text{I}^-$ increases and KI decreases the rate.⁴

For the aquation of the iron(II)-diimine complex $[\text{Fe}(\text{5NO}_2\text{-phen})_3]^{2+}$, addition of potassium bromide leads to a decrease but addition of tetra-*n*-butylammonium bromide leads to an increase in the rate constant.⁵ Following the analysis of these effects it was concluded that the changes in rate are a result of cation-cation interactions in water which, in turn, depend on the hydration characteristics of these ions: Bu_4N^+ is a hydrophobic structure-forming ion in water, K^+ is an electrostrictive structure-breaking ion. These and related salt effects for various reaction types and solvent systems were examined.^{6,7} More recently a statistical thermodynamic analysis was used to probe the rôles of solute and ionic hydration, and of ion-size effects.⁸

However, for the most part, only trends in rate constants were examined. It was not possible to identify in the case of, for example, an increase in rate constant produced by added salt whether this trend arose from a predominant destabilization of the initial state or stabilization of the transition state.

Non-kinetic information is required before the analysis can be taken further, and this chapter describes such analyses for charged and uncharged reactants. The results are compared and contrasted in the final section of the chapter.

6.2 SALT EFFECTS ON THE RATE OF BROMIDE SUBSTITUTION AT THE [Pd(Et₄dien)Cl]⁺ CATION

6.2.1 Outline

Substitution at the [Pd(Et₄dien)Cl]⁺ cation usually follows a simple first-order rate law:⁹

$$-\frac{d}{dt} [\text{Pd}(\text{Et}_4\text{dien})\text{Cl}^+] = k_1 [\text{Pd}(\text{Et}_4\text{dien})\text{Cl}^+] \quad \dots [6.4]$$

The bulky ligand substituents prevent significant associative attack by all but the most powerful nucleophiles at relatively high concentrations. Bromide substitution follows the rate law given by equation [6.4].¹⁰

First-order rate constants were determined for dissociative substitution in aqueous solutions containing various concentrations of added bromide salts, e.g. KBr, Et₄NBr and Bu₄NBr.

The solubility of the complex salt in a range of salt solutions was measured. These salts had to be chlorides, to prevent aquation of the palladium complex (equations [1.32]).

6.2.2 Experimental

The complex [Pd(Et₄dien)Cl]Cl was prepared by reaction between

palladium(II) chloride (Johnson Matthey) and the ligand (Merck).¹¹

Solutions of the alkali-metal and tetra-alkylammonium bromides and chlorides were prepared using materials of the best quality grade available (AnalaR; Aldrich; Eastman-Kodak; Fluka).

Rate constants were calculated from paper-tape logged absorbance data for the decrease at 345 nm (disappearance of complex) over at least 2½ half-lives. The initial concentration of complex was $1.72 \times 10^{-3} \text{ mol dm}^{-3}$.

Solubilities of the complex were measured in a series of solutions containing 1.0 mol dm^{-3} KCl, Et_4NCl or Bu_4NCl . The saturated solutions were maintained at 298 K for a period of several days and diluted aliquots were analysed using the Unicam SP1800 spectrophotometer and a Perkin-Elmer 360 atomic absorption spectrometer operating with a single-element palladium lamp.

6.2.3 Results

The first-order rate constants for the substitution reaction between $[\text{Pd}(\text{Et}_4\text{dien})\text{Cl}]^+$ cations and bromide ions are summarized in Table (6.1). In all solutions, the change of absorbance with time followed first-order kinetics over at least 2½ half-lives. Repeat scans of the absorption spectra showed a gradual change with time and two well-defined isosbestic points at 361 and 265 nm. There was no observable solvolysis of reactants or products.

The kinetic data, summarized in Figure (6.2), show that with increase in concentration of added bromide salt the rate constant decreases, the effect being more marked through the series of salts where the order of cation is $\text{Bu}_4\text{N}^+ > \text{Pr}_4\text{N}^+ > \text{Et}_4\text{N}^+ > \text{Me}_4\text{N}^+ > \text{K}^+ \approx \text{Na}^+$.

The solubility data obtained from atomic absorption measurements, summarized in Table (6.2), show that in a salt solution, concentration

TABLE (6.1)

Rate constants at 298 K for reaction between $[\text{Pd}(\text{Et}_4\text{dien})\text{Cl}]^+$ cations and bromide ions in aqueous solutions containing added salts

Salt	concentration of added salt/mol dm^{-3}	$10^3 k_{\text{obs}}/\text{s}^{-1}$
None	0	2.43
KBr	0.5	2.39
KBr	1.0	2.31
NaBr	0.5	2.41
NaBr	1.0	2.16
Me_4NBr	0.5	2.06
Me_4NBr	1.0	1.80
Et_4NBr	0.5	1.71
Et_4NBr	1.0	1.38
Pr_4NBr	0.25	1.75
Pr_4NBr	0.5	1.50
Pr_4NBr	1.0	1.03
Bu_4NBr	0.2	1.71
Bu_4NBr	0.5	0.896
Bu_4NBr	1.0	0.712
KI	0.5	2.00
KI	1.0	2.02

TABLE (6.2)

Solubility of $[\text{Pd}(\text{Et}_4\text{dien})\text{Cl}]\text{Cl}$ in salt solutions, 1.0 mol dm^{-3} , at 298 K

Salt	KCl	Et_4NCl	Bu_4NCl
Solubility/mol dm^{-3}	1.04	1.08	1.35

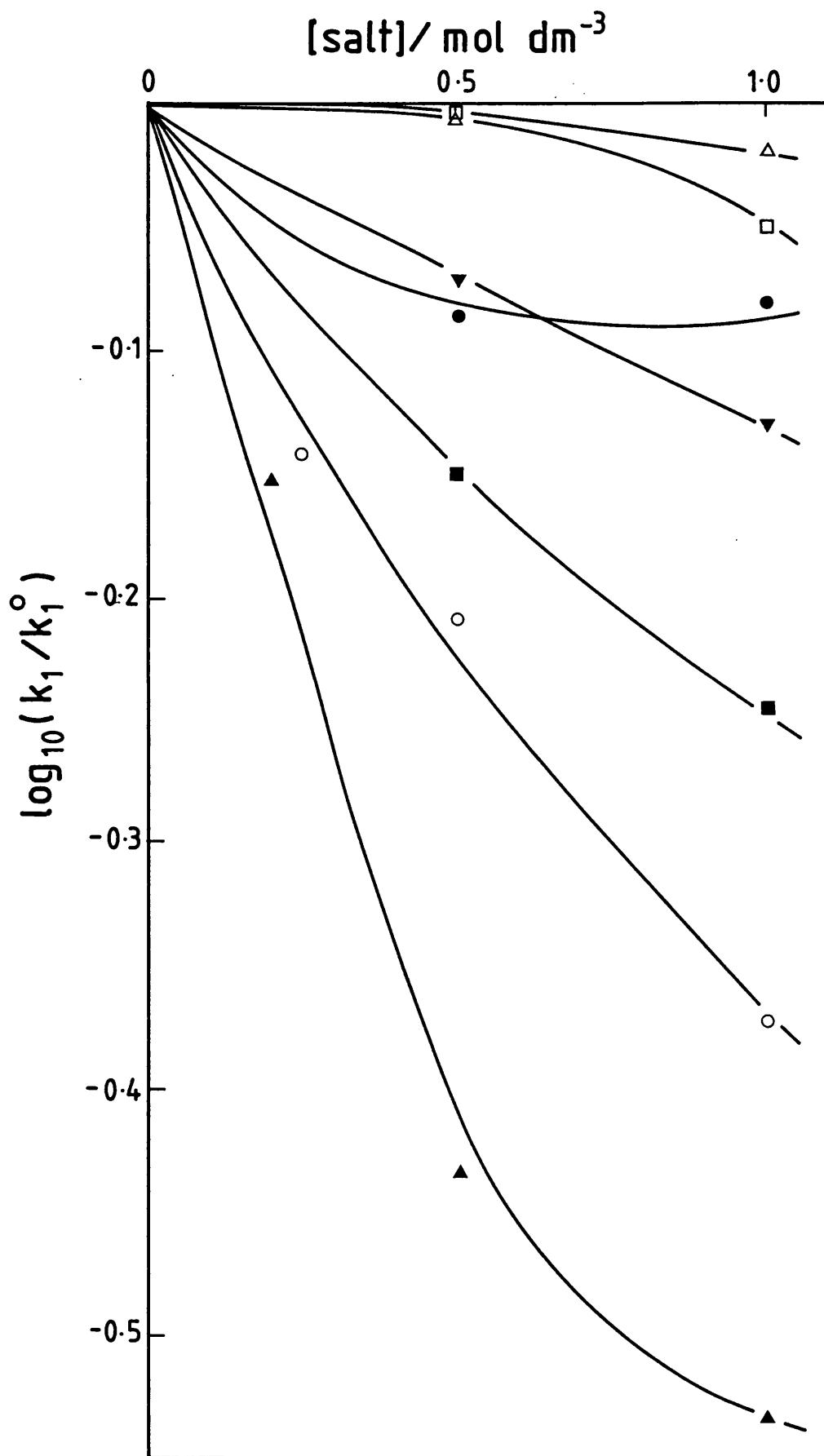


FIGURE (6.2)

Effect of added bromide salts on the rate constant for reaction of the $[\text{Pd}(\text{Et}_4\text{dien})\text{Cl}]^+$ cation with bromide ion at 298.2 K in aqueous solution. Cations are: Δ Na^+ , \square Me_4N^+ , \bullet Et_4N^+ , \blacktriangledown Pr_4N^+ , and \blacktriangle Bu_4N^+ . [\circ — data for potassium iodide]

1.0 mol dm⁻³, the effect of added salt on solubility of the complex is in the order Bu₄NCl > Et₄NCl > KCl. This trend was confirmed by the absorption spectra of the saturated solutions in the visible region.

6.2.4 Analysis and discussion

A full quantitative analysis of the kinetic and solubility data has been described elsewhere.¹² The nature and number of extra-thermodynamic assumptions needed renders the conclusions somewhat equivocal. However, the results of this analysis are reproduced here to complement the subsequent qualitative discussion.

The use of medium operators in the manner described in Chapter 1 involves a slight modification in this context. The reference solution is a salt solution containing 1.0 mol dm⁻³ KBr. Thus

$$\begin{aligned} \delta_m \Delta G^\ddagger &= \Delta G^\ddagger(1.0 \text{ mol dm}^{-3} \text{ Bu}_4\text{NBr}) - \Delta G^\ddagger(1.0 \text{ mol dm}^{-3} \text{ KBr}) \\ &= \delta_m \mu^\ddagger - \delta_m \mu^\ominus(M^+; \text{initial state}) \end{aligned} \quad \dots [6.5]$$

where $M^+ \equiv [\text{Pd}(\text{Et}_4\text{dien})\text{Cl}]^+$.

To relate equation [6.5] to experimentally measured quantities, two assumptions are needed. Firstly, since the kinetic data refer to the dependence of rate constant on salt effects where the anion, bromide, is held constant and also in view of the small change in k_{obs} when KBr is replaced by KI, it is assumed that the added cation has the dominant effect on the rate constant. Thus the ratio of the single-ion activity coefficients for the chloride counter-ion of the palladium cation is set equal to unity and the ratio of the single-ion activity coefficients for $[\text{Pd}(\text{Et}_4\text{dien})\text{Cl}]^+$ in the chloride salt solutions is set equal to the same ratio for this cation in bromide salt solutions. The final expression relating rate constants and solubility data with the ratio of the single-ion activity coefficients for the transition state $(M^+)^\ddagger$, in the two salt

solutions is:

$$\begin{aligned}
 & RT \ln \left\{ \frac{k (1.0 \text{ mol dm}^{-3} \text{ Bu}_4\text{NBr})}{k (1.0 \text{ mol dm}^{-3} \text{ KBr})} \right\} \\
 &= -2 RT \ln \left\{ \frac{s (\text{MCl} : 1.0 \text{ mol dm}^{-3} \text{ Bu}_4\text{NCl})}{s (\text{MCl} : 1.0 \text{ mol dm}^{-3} \text{ KCl})} \right\} \quad \dots [6.6] \\
 &+ RT \ln \left\{ \frac{y ([\text{M}^+]^\ddagger : 1.0 \text{ mol dm}^{-3} \text{ KBr})}{y ([\text{M}^+]^\ddagger : 1.0 \text{ mol dm}^{-3} \text{ Bu}_4\text{NBr})} \right\}
 \end{aligned}$$

k = observed first-order rate constant

s = solubility/mol dm^{-3}

y = single-ion activity coefficient.

The experimental data were substituted into equation [6.6]. The results of this analysis are given in Figure (6.3). From this figure it is apparent that on changing from a solution in KBr to solutions of the bromide salts of Et_4N^+ and Bu_4N^+ the initial state is stabilised, more markedly for tetrabutylammonium salt solutions than for tetraethylammonium salt solutions. The transition state is destabilised in the order

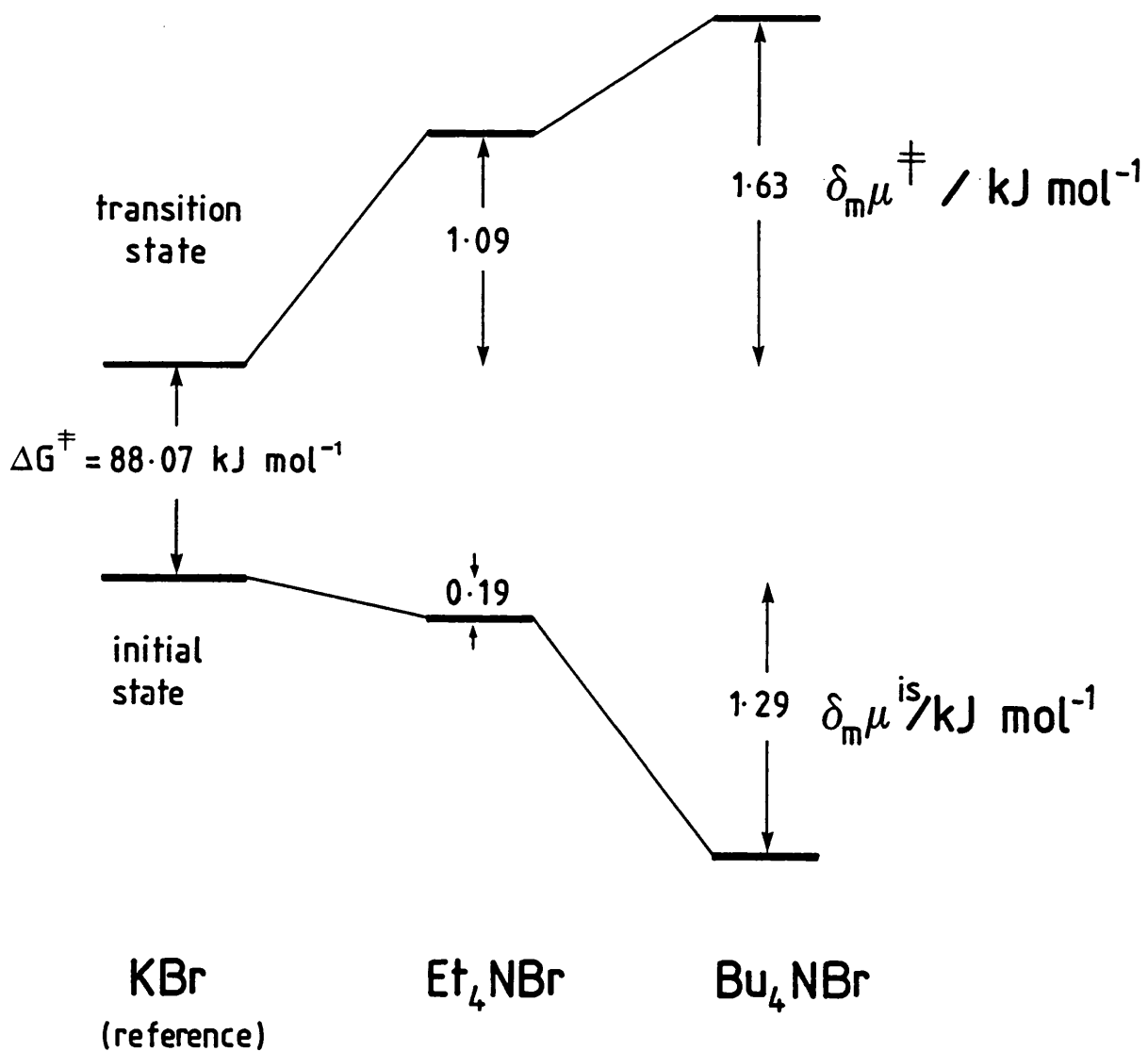


The effect here is more dramatic than for the initial state. The decrease in rate constant on transfer from salt solutions containing KBr to those containing Et_4NBr and Bu_4NBr is thus not solely due to stabilization of the initial state nor destabilization of the transition state, but rather a combination of both with the transition state destabilization being dominant.

The striking observation is the sensitivity of the rate constant to the concentration of added salt and the nature of the added cation [Figure (6.2)]. The inadequacy of a Brønsted-Bjerrum analysis, incorpora-

FIGURE (6.3)

Comparison of the effects of 1.0 mol dm^{-3} Et_4NBr and Bu_4NBr on the chemical potentials of initial and transition states for the reaction of $[\text{Pd}(\text{Et}_4\text{dien})\text{Cl}]^+$ relative to these potentials in 1.0 mol dm^{-3} KBr in aqueous solution at 298 K.



ting the DHLL, is revealed by the fact that this analysis would predict no change in rate constant for the unimolecular dissociation of the cation when a salt is added. A similar point was made in the analysis of the effects of added salts on the rate constant for the aquation of the $[\text{Fe}(\text{5NO}_2\text{-phen})_3]^{2+}$ cation.⁵ Extension of the analysis to include the full Debye-Hückel equation, which takes account of ion-size parameters, gave poor agreement between theory and experiment. An assessment of the effect of added salt on the initial state was necessary.

In the comparison of initial and transition states, it is reasonable to assume that the transition state is larger than the initial state in view of the known reaction mechanism. On activation there is considerable stretching of the Pd-Cl bond and contemporary charge development on the chlorine, with associated enhancement of Cl-solvent interaction. In the transition state a balance is struck between neighbouring solvent-solvent interaction and Cl-solvent interaction. After some initial stage of charge development, exothermic solvation of the developing anion increases until the full charge is produced on the chloride ion on the product side of the energy profile for the reaction. Strong solvent-Cl interaction in the transition state means that the transition state is more hydrophilic than the initial state. In view of the character of the Et_4dien ligand, the hydration of the initial state resembles that of an alkylammonium ion.

In Figure (6.2) the curves follow the order expected if the size of the cation is the determining factor.^{7,8} A statistical mechanical analysis of salt effects⁸ showed that repulsive effects play a significant rôle which implies that the size of the cation is important. However, the solubility data show that for the initial state, the trend of increasing stabilization is opposite to that predicted by this line of argument. This must be due to a second effect, namely the hydration characteristics

of the ions involved. In a solution of a salt or a mixture of salts where the concentration is as high as 1.0 mol dm^{-3} , the rôle of hydration effects can be understood in terms of overlapping cospheres as described at the beginning of this chapter.

In the present context it follows that in the KBr solutions, overlap of the K^+ cosphere with the positively charged, hydrophobic initial state is a destabilizing influence, but with the hydrophilic transition state a stabilizing influence. Replacement of K^+ by Et_4N^+ , and more significantly, by Bu_4N^+ leads to a relative stabilization of the initial state and a destabilization of the transition state.

If the two effects of ion size and hydration are considered together, they result in different effects on the initial state. Repulsive effects increase the chemical potential of the palladium cation in the order K^+ , Et_4N^+ , Bu_4N^+ while hydration effects lower the chemical potential across the same series. The solubility results show that the hydration effect is more important. Both effects operate in the same direction on the transition state, producing a marked destabilization. In these terms the fall in rate constant as salt is added [Figure (6.2)] appears to be dominated by the effect of added salt on the transition state.

6.3 SALT EFFECTS ON THE KINETICS OF REACTION OF CIS-BIS(4-CYANOPYRIDINE) DICHLOROPLATINUM(II) WITH THIOUREA

6.3.1 Outline

The main obstacle in the analysis of salt effects on reactivities into initial state and transition state components, at least in respect of the majority of inorganic systems, is the need for single-ion thermodynamic transfer parameters from water into aqueous salt solutions. These are needed in order to establish the transfer behaviour of the initial state when this involves a charged complex. For the transfer of ions into

binary aqueous solvent mixtures there is a profusion of data, as described in Chapter 1. For the transfer of ions into aqueous salt solutions, information is minimal and the extra-thermodynamic assumptions involved hardly considered as yet. In the analysis of reactivity trends for the $[\text{Pd}(\text{Et}_3\text{dien})\text{Cl}]^+$ cation described in the previous section, the quantitative analysis employed extra-thermodynamic assumptions in an attempt to circumvent this problem. This treatment was not altogether satisfactory.

These problems associated with transfer of ions can be avoided by dealing with systems involving non-electrolytes, though this inevitably restricts the possible applications to a small percentage of inorganic reactions, with the choice further narrowed by the very limited solubilities of most uncharged organometallic compounds in aqueous media.

In the field of substitution at square-planar d^8 complexes there are several examples of uncharged complexes and nucleophiles. The kinetics and products of the reaction of cis-bis(4-cyanopyridine)dichloroplatinum (II) with thiourea in aqueous media have been characterised.¹³

Second-order rate constants for this reaction in aqueous solution of potassium chloride, gadolinium trichloride and tetraethylammonium chloride were measured. From these kinetic data and solubility measurements on the reactants, the observed medium effect is dissected into contributions of medium effect on the chemical potentials of the initial state and transition state.

6.3.2 Experimental

Cis-bis(4-cyanopyridine)dichloroplatinum(II), $\text{Pt}(\text{4CN-py})_2\text{Cl}_2$, was prepared from platinum dichloride (Johnson Matthey) and 4-cyanopyridine (Koch-Light) using the method given¹⁴ for the preparation of cis-dichlorobis(pyridine)platinum(II). Thiourea (Fisons) was used as supplied, fresh stock solutions being made up at regular, short intervals.

The reaction was monitored at 317 nm (disappearance of complex) using the minicomputer-controlled apparatus. The small absorbance change (about 0.15 units) was near the operational limit of the SP1800 spectrophotometer. The initial concentration of the complex was ca. 3×10^{-4} mol dm^{-3} . Second-order rate constants were obtained by the isolation method described in Chapter 2, thiourea concentrations being in the range 0.02 to 0.06 mol dm^{-3} .

Solubilities of the platinum complex in the salt solutions were obtained from absorbance measurements of saturated solutions, measured at 317 nm. These absorbances were corrected for the absorbance of the salt solutions at this wavelength. The absorbances were converted to solubilities using the value given for water obtained by atomic absorption spectroscopy.¹³

Thiourea solubilities were obtained by evaporation to dryness of known volumes of the saturated solutions for each medium. The theoretical weight of anhydrous salt for the aliquot was subtracted from the residue. There was some uncertainty as to whether Et_4NCl and GdCl_3 remained as the monohydrates after evaporation. However, in view of the large molecular weights of these salts, the assumption that all water was absent did not greatly affect the numerical values of the solubilities.

6.3.3 Results and discussion

The dependence of observed first-order rate constants on thiourea concentration (thiourea in large excess) in each salt solution is reported in Table (6.3). For each salt solution, the rate law is second-order; thiourea is such a powerful nucleophile for Pt(II) centres that the parallel solvolysis path normally found for substitution at square planar centres (Chapter 1) is negligible here. Second-order rate constants are reported in Table (6.3) and their dependence on concentration of added

TABLE (6.3)

Mean^a observed first-order rate constants (k_{obs}) and derived second-order rate constants (k_2) for the reaction of cis-[Pt(4CN-py)₂Cl₂] with thiourea in aqueous salt solutions at 298.2 K

Medium	$10^3 k_{\text{obs}}/\text{s}^{-1}$					$k_2 \pm \sigma / \text{dm}^3 \text{ mol}^{-1} \text{ s}^{-1}$
	[thiourea]/mol dm ⁻³					
	0.020	0.030	0.040	0.050	0.060	
Water	4.0	6.3	8.4		13.3	0.22 ± 0.01
1.0M KCl	4.7	7.2	10.4		14.9	0.25 ± 0.01
2.0M KCl	5.6	8.1	10.6		16.0	0.26 ± 0.01
1.0M GdCl ₃ ^b		8.9	12.5	14.7		0.30 ± 0.03
0.5M Et ₄ NCl		4.0	5.6	7.1		0.14 ± 0.02
1.0M Et ₄ NCl	1.9	3.0	4.1	5.1		0.10 ± 0.003

^a Of between 2 and 4 independent determinations

^b Ionic strength = 6.0 mol dm⁻³

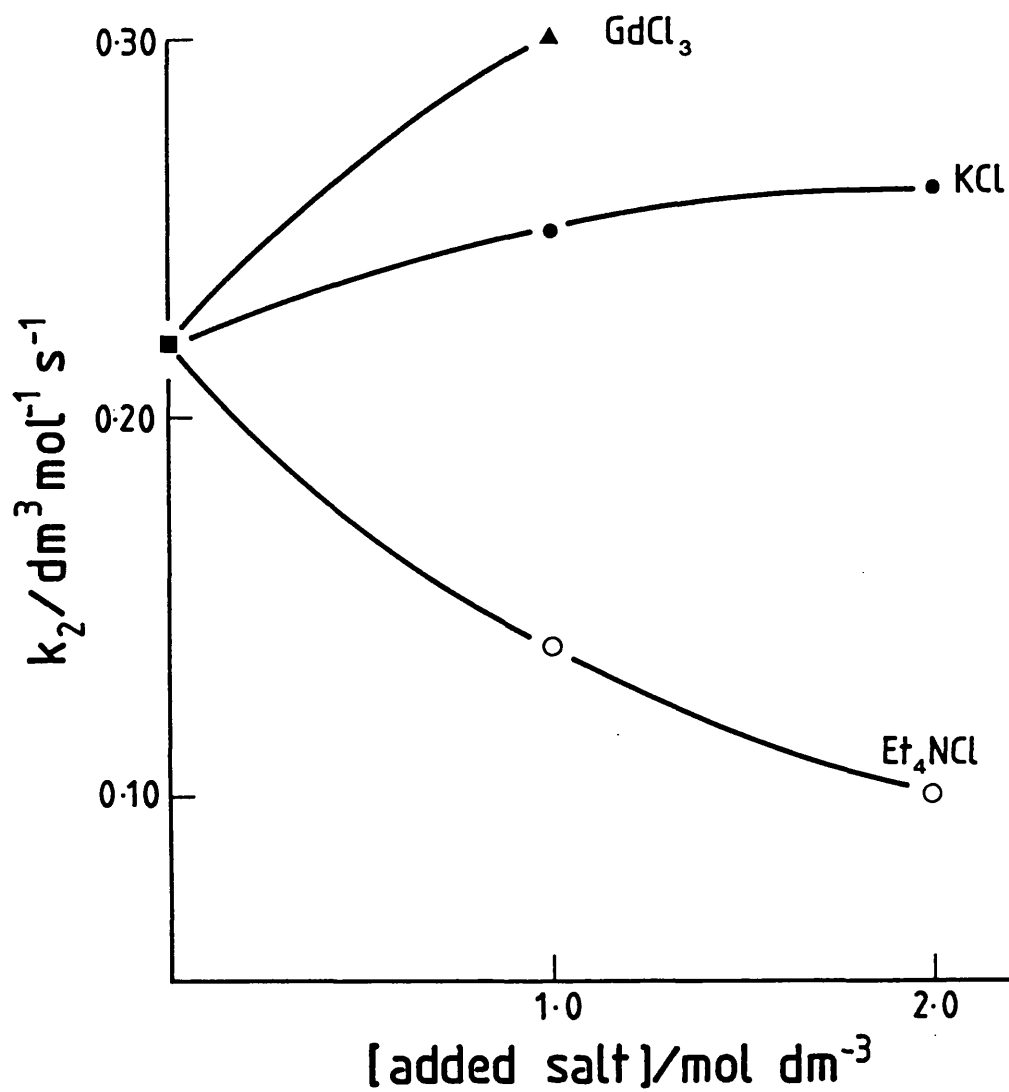


FIGURE (6.4)

Dependence of the second-order rate constant, k_2 , for the reaction between $\text{cis-}[\text{Pt}(\text{4CN-py})_2\text{Cl}_2]$ and thiourea on concentration of added salt at 298.2 K.

salt depicted in Figure (6.4). This figure shows the opposite effect of Et_4NCl to KCl and GdCl_3 .

The results of the solubility measurements are incorporated into Table (6.4), depicting the analysis of the medium effect in terms of initial state and transition state contributions [Table (6.4)]. Both the platinum complex and thiourea are salted in by Et_4NCl , but both are salted out by KCl and GdCl_3 .

Figure (6.4) shows that the effect of potassium chloride or gadolinium trichloride is opposite to that of tetraethylammonium chloride. Because both the platinum complex and thiourea are non-electrolytes, no extra-thermodynamic assumptions need be invoked in the initial state-transition state dissection, which is set out in Table (6.4) and shown diagrammatically in Figure (6.5).

Figure (6.5a) shows that the small increase in rate constant on adding potassium chloride represents the difference between a modest increase in the chemical potential of the initial state and a smaller increase in the chemical potential of the transition state. The increase in the chemical potential of the initial state is due to increases for both the platinum complex and the thiourea. Addition of gadolinium trichloride, Figure (6.5b), produces similar effects to potassium chloride, on the reactants and the transition state. Addition of tetraethylammonium chloride, Figure (6.5c), has the opposite effect on both the complex and thiourea, but it destabilizes the transition state to a similar extent to the metal salts. Therefore the difference in reactivity trends between the metal chlorides and tetramethylammonium chloride can be attributed almost entirely to the initial state.

In the earlier study of this reaction in binary aqueous solvent mixtures,¹³ both the initial state and the transition state were stabilized

TABLE (6.4)

Dissection of salt effects on reactivity into initial state and transition state components for reaction of $\text{cis-}[\text{Pt}(\text{4CNpy})_2\text{Cl}_2]$ with thiourea in aqueous salt solutions at 298.2 K. Transfer quantities are on the molar scale.

	water	KCl		GdCl ₃	Et ₄ NCl	
		1.0M	2.0M		0.5M	1.0M
$k_2/\text{dm}^3 \text{ mol}^{-1} \text{ s}^{-1}$	0.22	0.25	0.26	0.30	0.14	0.10
$\therefore \delta_m \Delta G^\ddagger / \text{kJ mol}^{-1}$		-0.32	-0.41	-0.77	+1.12	+1.95
$10^4 \text{ soly. Pt}(\text{4CNpy})_2\text{Cl}_2 / \text{mol dm}^{-3}$	$3.4^{\text{a}}, \text{b}$	3.1	3.0	1.5	4.4	5.0
$\therefore \delta_m \mu^\ominus [\text{Pt}(\text{4CNpy})_2\text{Cl}_2] / \text{kJ mol}^{-1}$		+0.25	+0.31	+2.1	-0.67	-0.96
$\text{soly. thiourea} / \text{mol dm}^{-3}$	1.92^{a}	1.61	1.52	0.88	2.01	2.40
$\therefore \delta_m \mu^\ominus (\text{tu}) / \text{kJ mol}^{-1}$		+0.44	+0.58	+1.9	-0.11	-0.55
$\therefore \delta_m \mu^\ominus (\text{is}) / \text{kJ mol}^{-1}$		+0.7	+0.9	+4.0	-0.8	-1.5
$\therefore \delta_m \mu^\ddagger / \text{kJ mol}^{-1}$		+0.4	+0.5	+3.2	+0.3	+0.45

^a from ref. 13

^b by atomic absorption spectroscopy

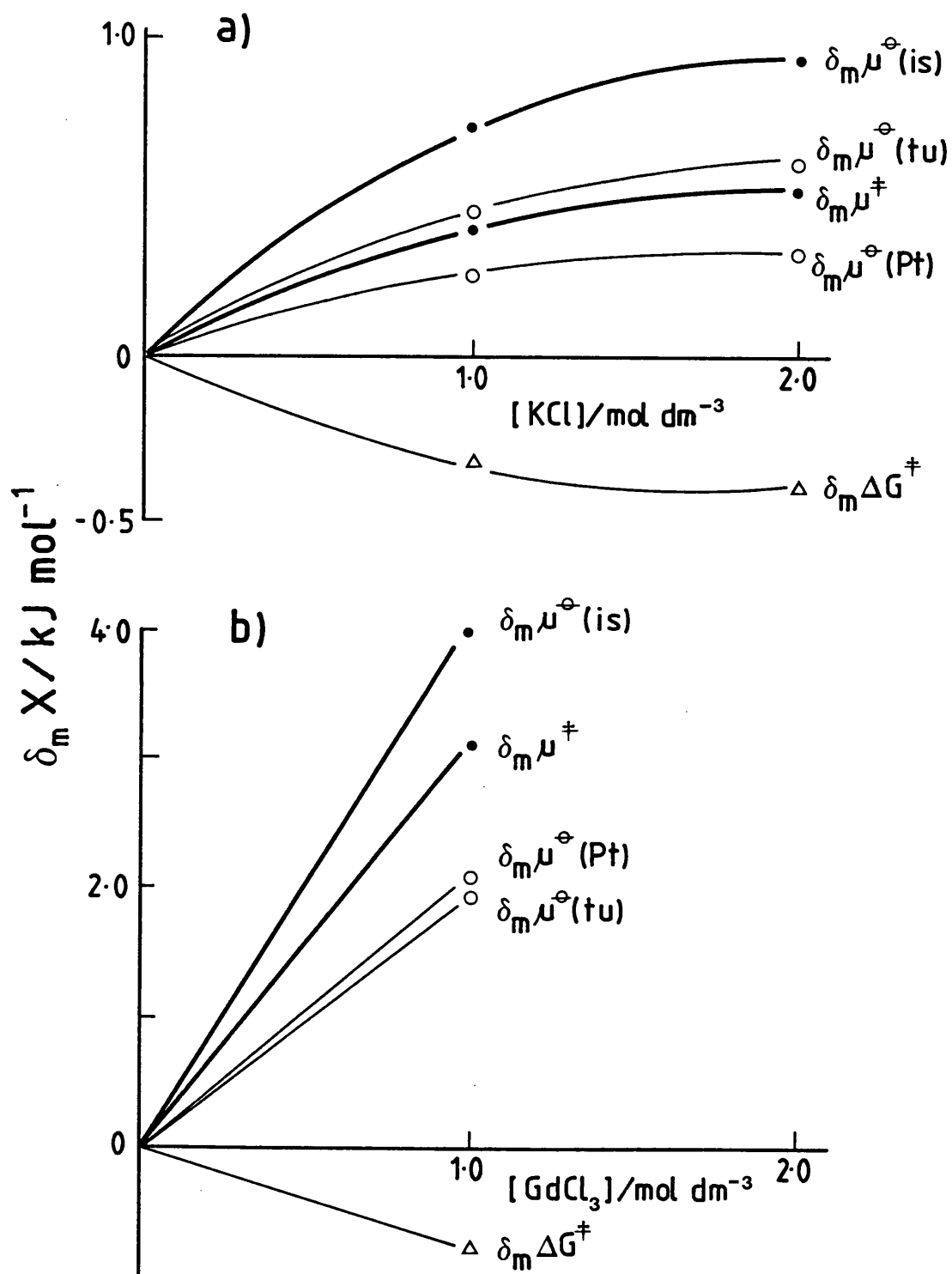
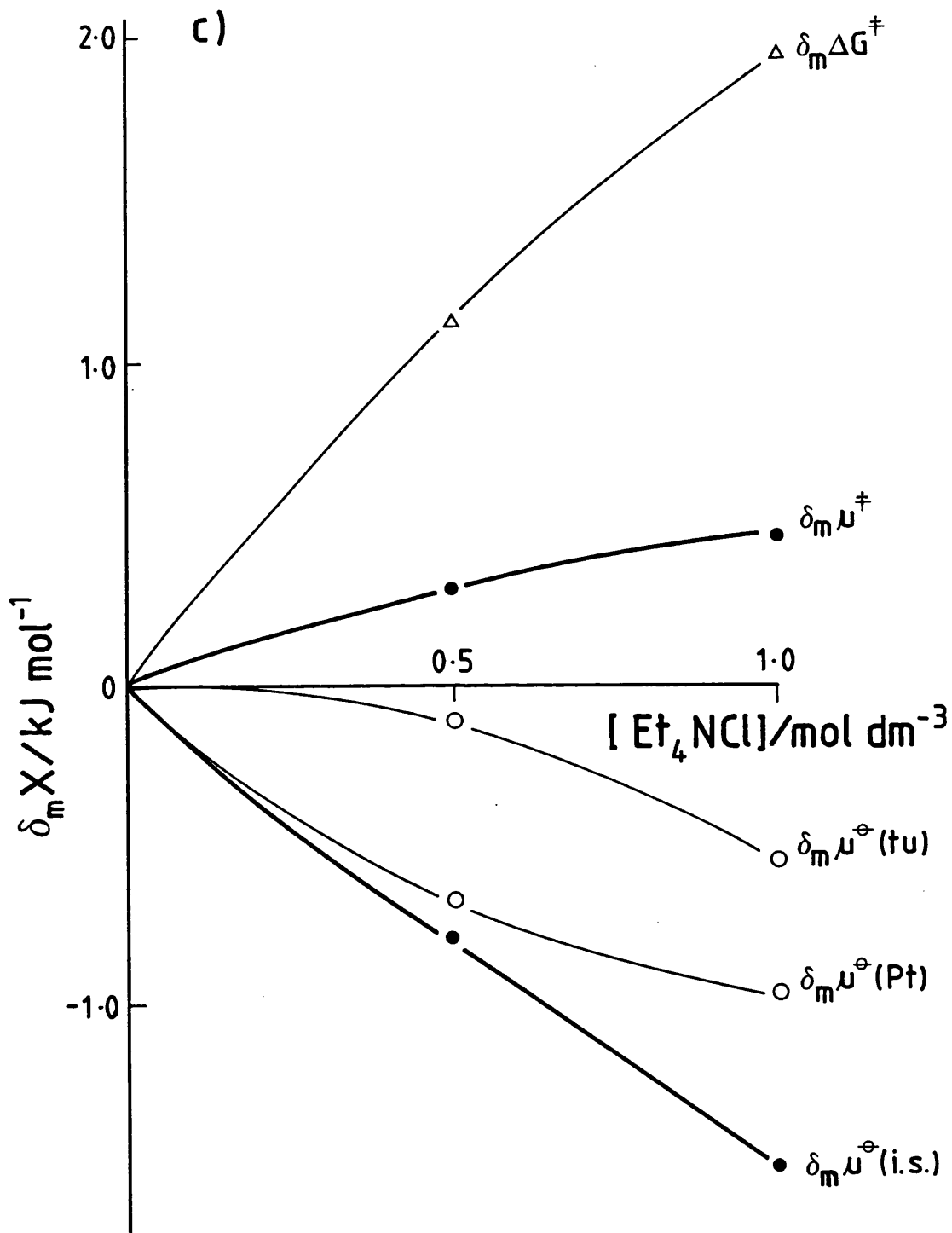


FIGURE (6.5)

Dissection of salt effects on reactivity into initial state and transition state components for reaction of $\text{cis-}[\text{Pt}(\text{4CN-py})_2\text{Cl}_2]$ with thiourea in aqueous salt solutions at 298.2 K.

(a) KCl , (b) GdCl_3 , (c) Et_4NCl .



on transfer from water into binary aqueous mixtures, regardless of whether these mixtures were TA, TNAP or TNAN (Chapter 1). This contrasts with the effects of potassium chloride and gadolinium trichloride, addition of either of which leads to destabilization of both the initial state and the transition state. Tetraethylammonium chloride provides a further variant, in that it stabilizes the initial state but destabilizes the transition state. The one common factor in all these medium effects is that initial state chemical potential changes are, in all cases, larger than transition state changes.

By displaying the results in a slightly different manner, the relative effect of the added salts becomes clearer. The pattern which emerges is compatible with results obtained for other systems, as will be discussed in the closing section of the chapter.

Although the prime concern of the analysis is medium effects on reactivity, it is interesting to consider the effect of added salts on solubilities of non-electrolytes in terms of Setchenow coefficients, K_s , which are the slopes of plots (usually linear) of $\log_{10}(S_0/S)$ against concentration of added salt.¹⁵ Here S_0 is the solubility in water, S the solubility in the salt solution. Hence the salting-in and salting-out of $\text{cis-}[\text{Pt}(\text{4CN-py})_2\text{Cl}_2]$ and thiourea can be placed in the context of other inorganic and organic solutes. Setchenow plots for both the platinum complex and thiourea are shown in Figure (6.6a). Setchenow coefficients estimated for low concentrations of added salts are reported in Table (6.5), which shows that K_s values for potassium chloride and bromide are quite similar for the small number of inorganic non-electrolytes for which information is available, and that K_s values are fairly large and negative for Et_4NX . Perhaps coincidentally, K_s values for $\text{cis-}[\text{Pt}(\text{4CN-py})_2\text{Cl}_2]$ are very close to those for Me_3NSO_3 . For thiourea, the K_s value for added

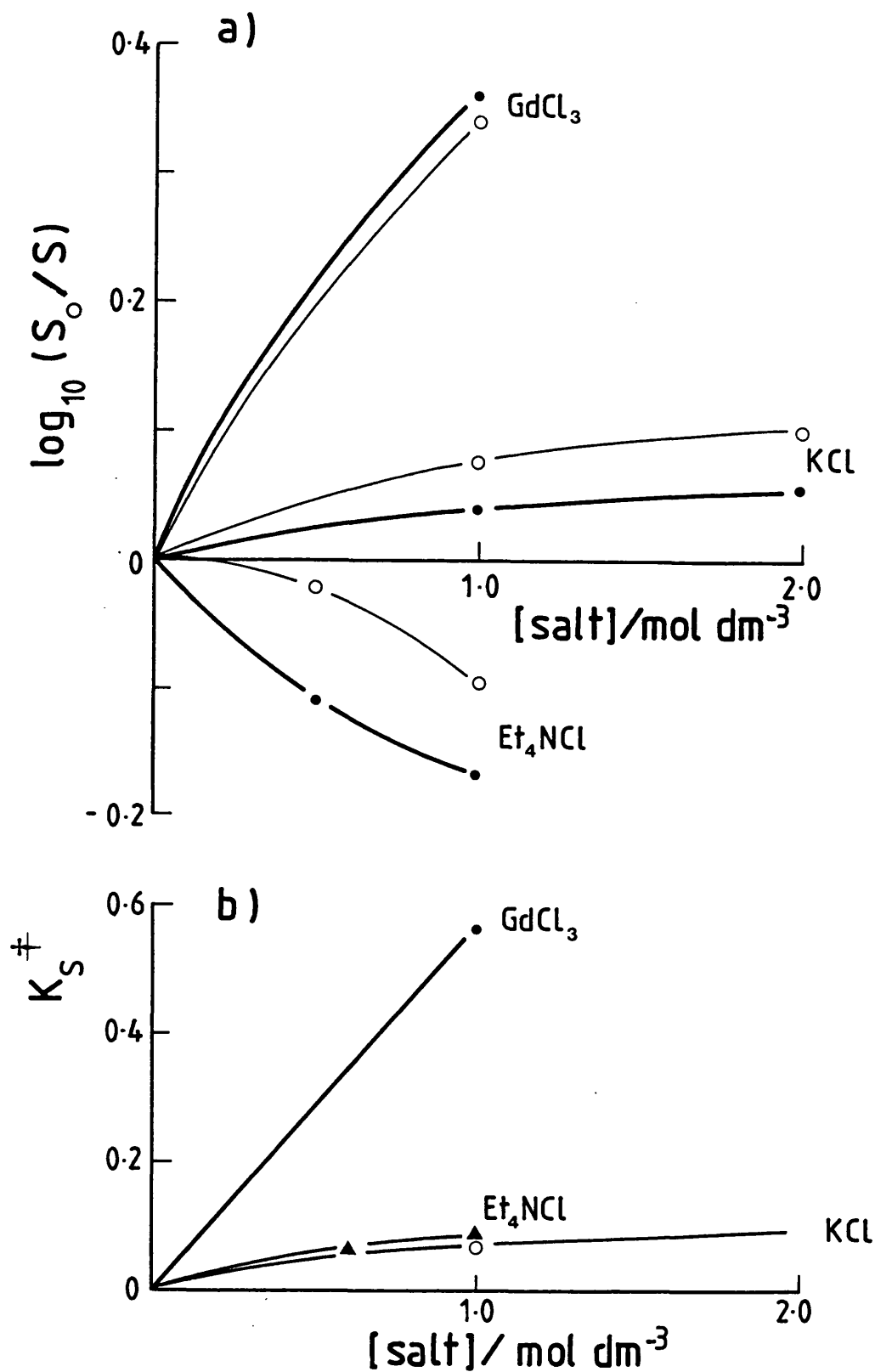


FIGURE (6.6)

Setchenow plots for the reaction between $\text{cis-}[\text{Pt}(\text{4CN-py})_2\text{Cl}_2]$ and thiourea in aqueous salt solutions at 298.2 K.

a) initial state: \circ = thiourea, \bullet = Pt complex.

b) transition state: $K_S^\ddagger = \delta_m \mu^\ddagger / 2.303 RT$.

TABLE (6.5)

Setchenow coefficients (K_s) for inorganic non-electrolytes
 [at 298.2 K unless otherwise indicated]

	cis-Pt(4CNpy) ₂ Cl ₂	Fe(bipy) ₂ (CN) ₂ ^a	Co(NH ₃) ₃ (NO ₂) ₃ ^a	Me ₃ NSO ₃ ^b
KCl KBr	+0.06	-0.12	-0.24	+0.03
Et ₄ NCl Et ₄ NBr	-0.3	-0.8		
Bu ₄ NBr				-0.35

^a from ref. 16

^b from section (6.4); 336.2 K

KCl (ca. +0.15) lies between those for nitrobenzene and phenol, i.e. in the range of values corresponding to hydrophobic organic compounds containing a small hydrophilic centre. There is no direct comparison for the K_s value for thiourea in Et_4NCl solutions ($K_s = \text{ca. } -0.1$).

Setchenow coefficients for the transition state (K_s^\ddagger) of the cis- $[\text{Pt}(\text{4CNpy})_2\text{Cl}_2]$ plus urea reaction are +0.05 and +0.1 for added KCl and Et_4NCl [see Figure (6.6b)]. The value for KCl lies between the values for the two reactants, themselves almost equal. It seems odd that K_s^\ddagger values in KCl and in Et_4NCl are almost the same. However, for t-butyl chloride solvolysis, one of the few reactions for which K_s^\ddagger values have been estimated,²⁰ the range of K_s^\ddagger values is much smaller than that for K_s (initial state).

6.4 SALT EFFECTS ON REACTIVITY FOR THE HYDROLYSIS OF TRIMETHYLAMINE SULPHUR TRIOXIDE

6.4.1 Outline

As described at the beginning of the previous section, the use of uncharged reactants allows analysis of salt effects on reactivity without recourse to the extrathermodynamic assumptions inescapably involved with ionic substrates. The availability of kinetic data for hydrolysis of the Lewis acid-base adduct trimethylamine sulphur trioxide, Me_3NSO_3 , in neutral aqueous solutions of potassium bromide and tetra-n-butylammonium bromide⁶ suggested this reaction as suitable for an initial state-transition state analysis of reactivity trends.

The solubilities and enthalpies of solution of Me_3NSO_3 in appropriate aqueous salt solutions were measured. These results permit the calculation of Gibbs free energies, enthalpies, and entropies of transfer of Me_3NSO_3 from water into aqueous salt solutions, and enable dissection of the overall salt effect on reactivity into initial state and transition

state contributions.

6.4.2 Experimental

Me_3NSO_3 (Aldrich) was used as supplied for solubility measurements and was dried in a desiccator over phosphorus pentoxide before use in calorimetric experiments.

Solubilities were determined by equilibrating an excess of the compound with the respective salt solution, at the appropriate temperature (336 K) with frequent agitation, for periods of time as long as possible consistent with negligible hydrolysis. Aliquots of the saturated solutions were withdrawn and treated with dilute sodium hydroxide to hydrolyse the adduct. Sulphate contents of the hydrolysates were estimated by precipitation of barium sulphate from the acidified (HCl) solutions; agar-agar was used to improve the filtration properties of the precipitate.¹⁷

Enthalpies of solution at 298.2 K were measured using a calorimetric apparatus, based on an LKB 8700 calorimeter and a Kipp-Zonen BDS recorder, described elsewhere.¹⁸ Samples of ca. 0.03g Me_3NSO_3 , dissolving in ca. 35 cm³ of water or salt solutions, were used. The performance of the calorimeter was checked periodically against the enthalpy of solution of potassium chloride.¹⁹

Potassium bromide (AnalaR) and tetra-n-butylammonium (Aldrich) were used as supplied.

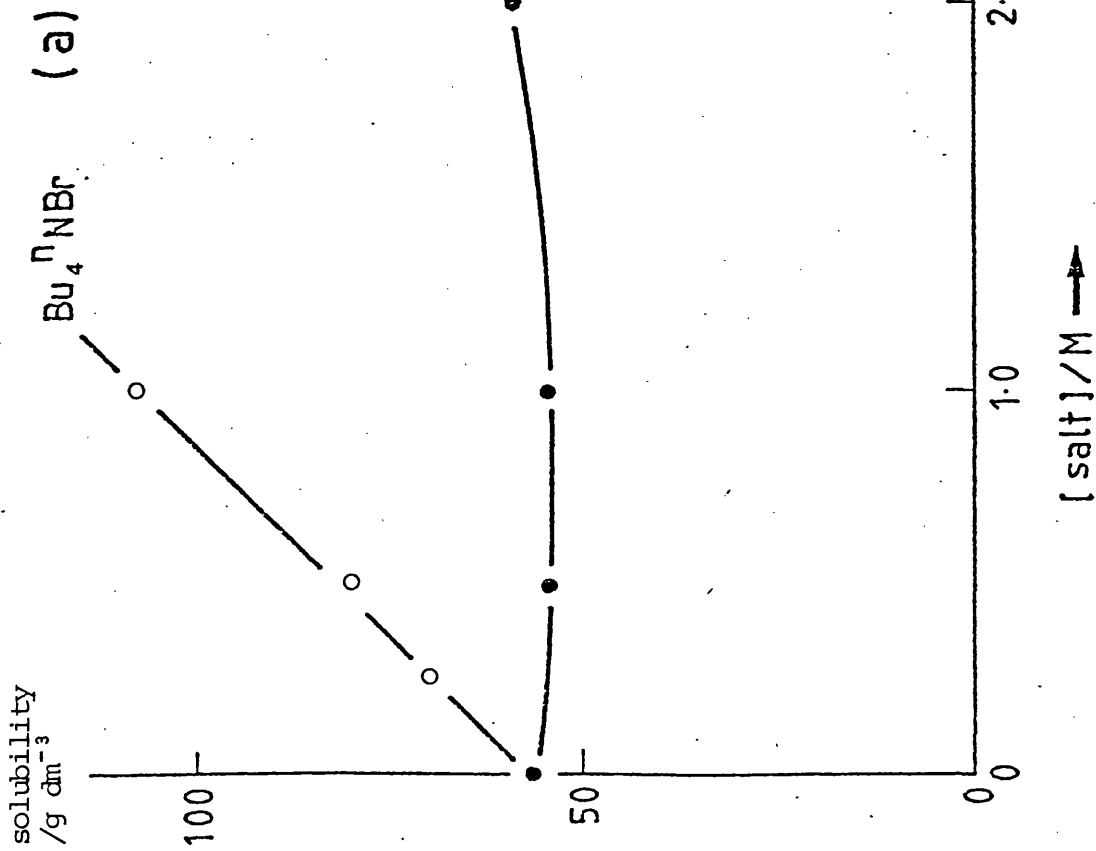
6.4.3 Results

Solubilities of Me_3NSO_3 at 336.2 K are reported in Table (6.6). Each result represents the mean of between two and four consistent determinations (duplicate sulphate analyses in several cases). The solubility pattern is shown in Figure (6.7a). The uncertainties in the values are

TABLE (6.6)

Initial state and transition state contributions to reactivity trends for hydrolysis of Me_3NSO_3 in aqueous salt solutions, at 336.2 K.
 [Transfer quantities are on the molar scale]

	water	$[\text{KBr}]/\text{mol dm}^{-3}$			$[\text{Bu}_4\text{NBr}]/\text{mol dm}^{-3}$		
		0.5	1.0	2.0	0.25	0.5	1.0
solubility/g dm^{-3}	56.4	54.6	54.7	59.2	70	81	108
$\therefore \delta_{\text{m}}^{\ddagger}(\text{Me}_3\text{NSO}_3)/\text{kJ mol}^{-1}$		+0.09	+0.08	-0.13	-0.59	-0.99	-1.78
10^6 k/s^{-1}	5.86	4.38	3.47	2.49		6.0	8.4
$\therefore \delta_{\text{m}}\Delta G^{\ddagger}/\text{kJ mol}^{-1}$		+0.81	+1.46	+2.39		-0.07	-1.01
$\therefore \delta_{\text{m}}^{\ddagger}/\text{kJ mol}^{-1}$		+0.9	+1.5	+2.3		-1.1	-2.8



(b)

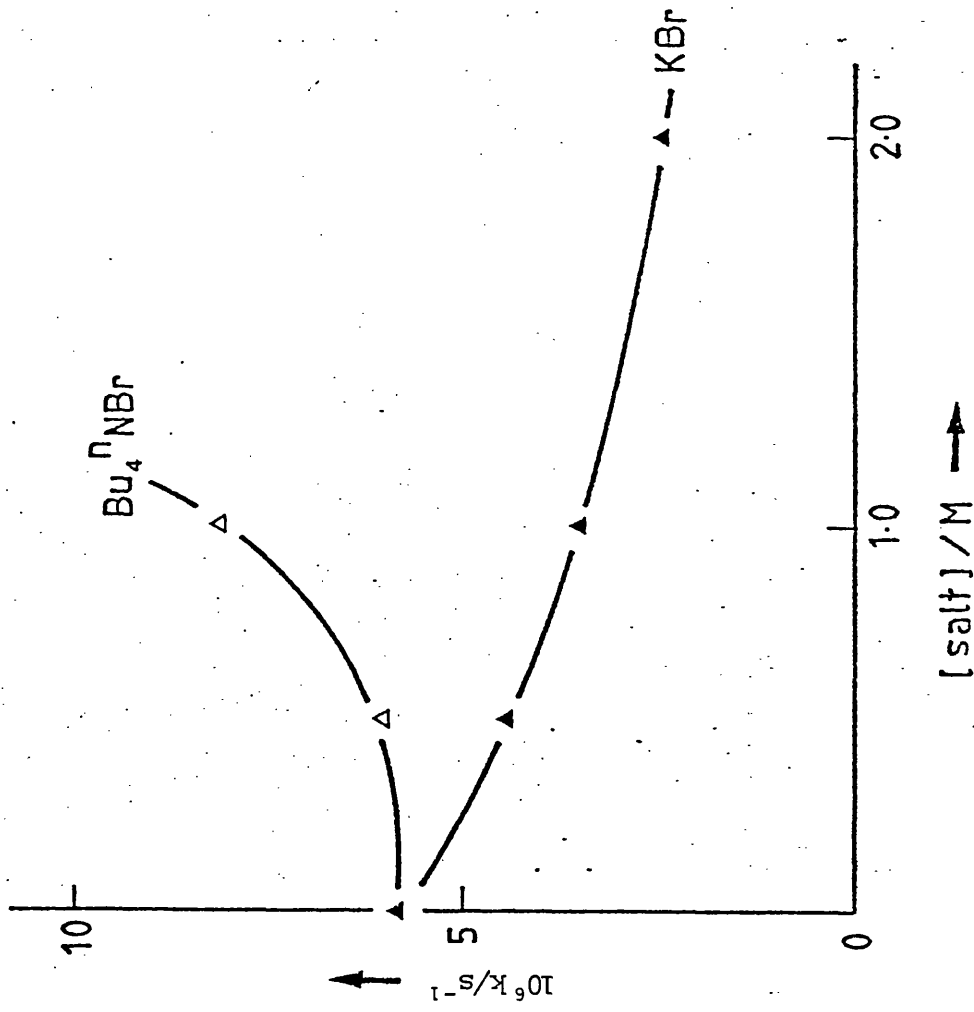


FIGURE (6.7)

Solubilities (a) and rate constants for hydrolysis (b) of Me₃NSO₃ in aqueous salt solutions at 336.2 K.

TABLE (6.7)

Transfer quantities for Me₃NSO₃ from water
into aqueous salt solutions

	KBr (2.0 mol dm ⁻³)	Bu ₄ Br (1.0 mol dm ⁻³)
$\Delta H_{tr}/\text{kJ mol}^{-1}\text{a}$	-4.5	+3.0
$\Delta G_{tr}/\text{kJ mol}^{-1}\text{b}$	-0.14	-1.8
$\Delta S_{tr}/\text{J K}^{-1} \text{mol}^{-1}\text{c}$	-13.0	+14.3

^a 298.2 K; ^b 336.2 K, molar scale;

^c 336.2 K, assuming $\Delta H_{tr}(336.2 \text{ K}) = \Delta H_{tr}(298.2 \text{ K})$

of the order of 5%, arising from the difficulties of working at a temperature well above ambient with a compound whose temperature coefficient of solubility is large.

The solubility of Me₃NSO₃ in water was also measured at 298.2 K, as 23.1 g dm⁻³. Hence a van't Hoff estimate for the enthalpy of solution of the adduct is +19.6 kJ mol⁻¹ (for the temperature range 298–336 K). Direct determination of the enthalpy of solution in water at 298.2 K gave a value of +23.0 kJ mol⁻¹. Direct calorimetric determinations of the enthalpy of solution of Me₃NSO₃ in aqueous salt solutions gave values of +18.5 kJ mol⁻¹ for 2.0 mol dm⁻³ potassium bromide and +26.0 kJ mol⁻¹ for 1.0 mol dm⁻³ tetra-n-butylammonium bromide, in both cases at 298.2 K.

6.4.4 Discussion

The analysis of the variation of rate constants for Me₃NSO₃ hydrolysis [Figure (6.7b)] with medium composition is set out in Table (6.6), with the results of the initial state-transition state dissection summarized

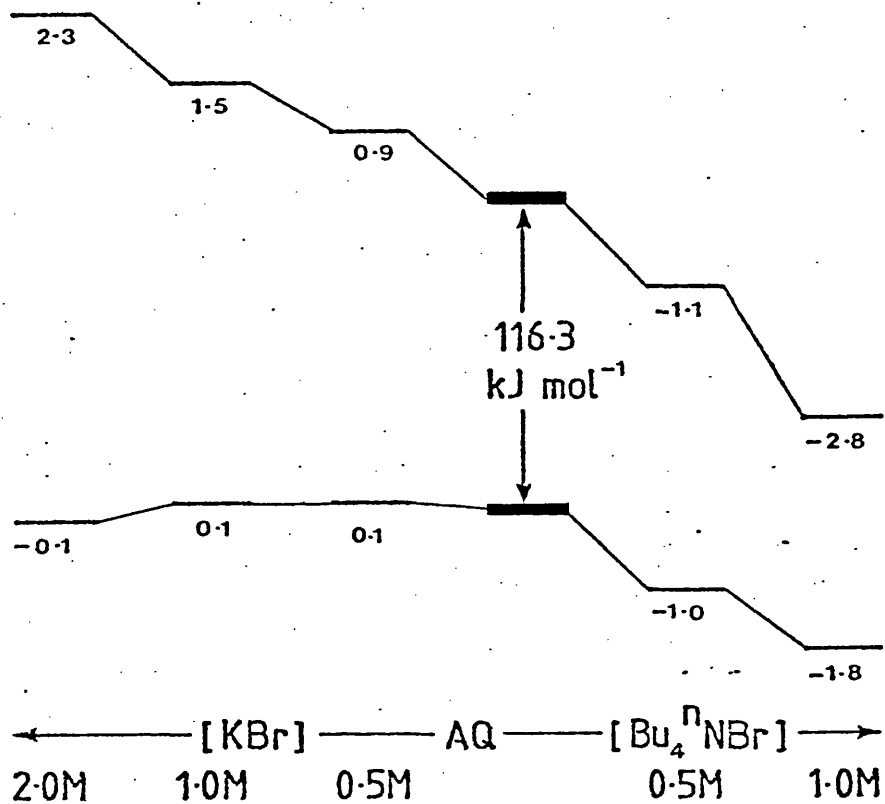


FIGURE (6.8)

Effect of added salts on initial and transition state for hydrolysis of Me_3NSO_3 .

in Figure (6.8). This analysis assumes a dissociative mechanism for hydrolysis in neutral solution.⁶ Both the initial states and transition states are destabilized on adding successive amounts of potassium bromide to water (except for the initial state in 2.0 mol dm^{-3} KBr); the reverse is true for tetra-n-butylammonium bromide. The observed reactivity trends thus represent the relatively small resultants of initial state and transition state effects operating in the same sense, with transition state effects somewhat more marked than initial state effects.

The dissociative solvolysis of Me_3NSO_3 involves simply the lengthening of the nitrogen-sulphur bond, with no separation of charge. It is therefore not surprising that the transition state behaves similarly to the initial state.

Gibbs free energies, enthalpies and entropies of transfer of Me_3NSO_3 from water into aqueous salt solutions are reported in Table (6.7). No simple pattern is apparent. For transfer into potassium bromide solution the small Gibbs free energy term represents the difference between opposite enthalpy and entropy terms, but the Gibbs free energy of transfer into tetra-n-butylammonium bromide solution is not much smaller in magnitude than the enthalpy of transfer.

As in the previous section, the effect of added salts on the solubility of Me_3NSO_3 can be discussed in terms of Setchenow plots, which are shown in Figure (6.9). Both plots are somewhat curved, but it is possible to estimate that Setchenow coefficients are approximately +0.03 for KBr and -0.35 for Bu_4Br for the low concentration region. The Figure (6.9) pattern and these derived values are reminiscent of the behaviour¹⁶ of nitrobenzene or of 5-nitro-1,10 phenanthroline, compounds having similar hydrophobic-hydrophilic peripheries to Me_3NSO_3 .

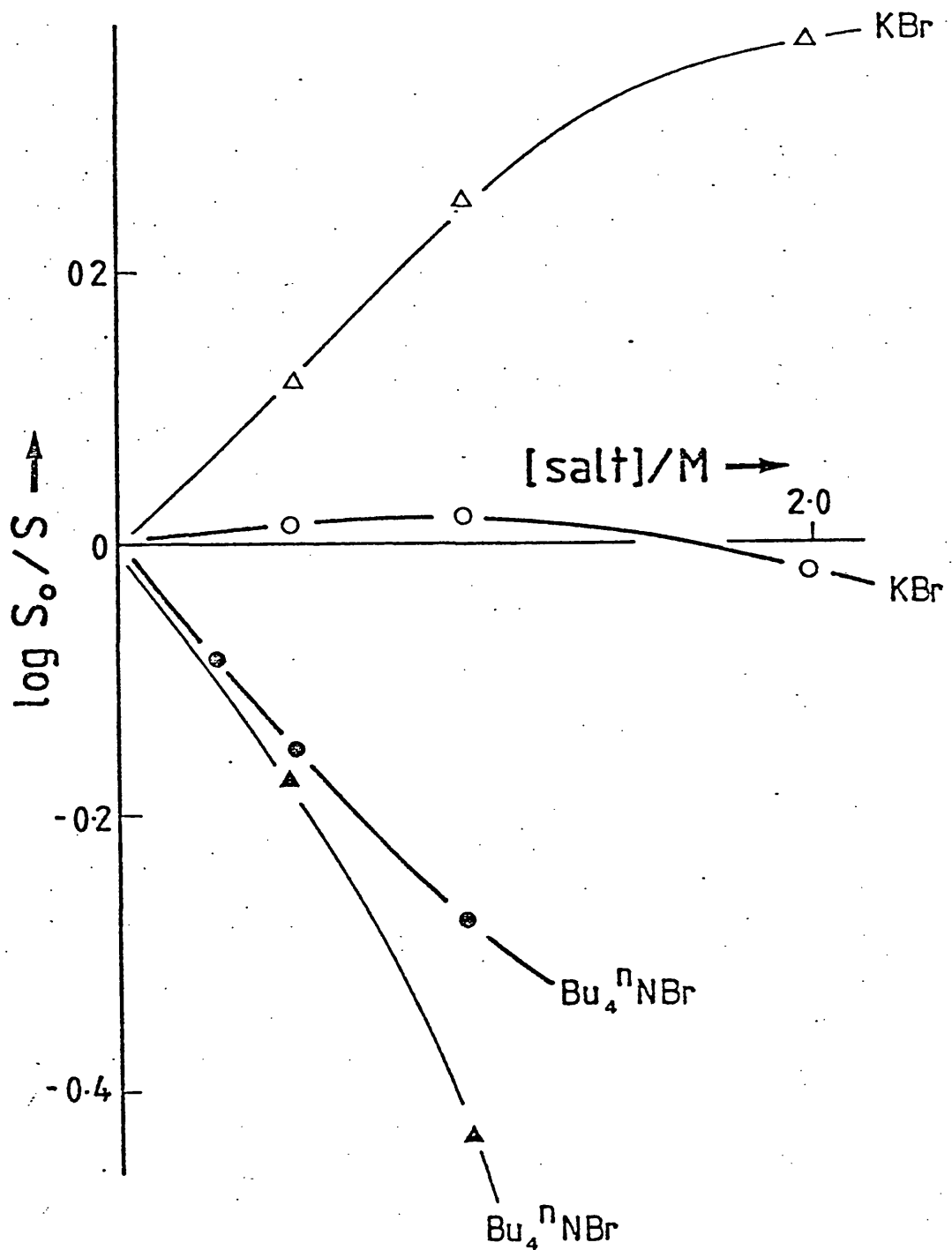


FIGURE (6.9)

Sethchenow plots for Me_3NSO_3 (thick lines, circles) and for its hydrolysis transition state (thin lines, triangles); open symbols KBr, filled symbols $\text{Bu}_4^{\text{n}}\text{NBr}$ (all at 336.2 K).

Setchenow coefficients for the transition state for the hydrolysis of Me_3NSO_3 are calculable directly from $\delta_{\text{m}\mu}^\ddagger$. These are shown in Figure (6.9) and are again curved, but they do indicate that values of K_s are similar for the initial and transition states for the tetra-n-butyl-ammonium salt, but that K_s for the transition state is, unlike K_s for the initial state, markedly positive for potassium bromide. This may be contrasted with t-butyl chloride hydrolysis where, as remarked at the end of Section (6.3), Setchenow coefficients²⁰ for a variety of electrolytes cover a smaller range in the transition state than in the initial state.

6.5 GENERAL CONCLUSION

Figure (6.10) shows the results of the three analyses described in this chapter in a form which enables their direct comparison. It is not possible to make comparisons of transfer from salt-free water, because the palladium(II) cation is too susceptible to hydrolysis. The Figure also shows data for the solvolysis of t-butyl chloride, calculated from the Setchenow coefficients²⁰ for the only suitable alkali-metal/tetra-alkylammonium cation pair, assuming the reaction is completely $\text{S}_{\text{N}}1$ in these strongly basic media.

Although the quantitative results for the palladium(II) cation are somewhat dependent on the extra-thermodynamic assumptions used, the qualitative pattern which emerges is probably correct.

Taken as a whole, the results for the four systems may be rationalized in terms of a discussion which is essentially that given for solvolysis of the palladium cation. A consideration of the hydrophilic or hydrophobic nature of the initial and transition states determines the hydration characteristics of these species. Overlap of these solvent cospheres with those of the added salt cations produces a relative stabilization or

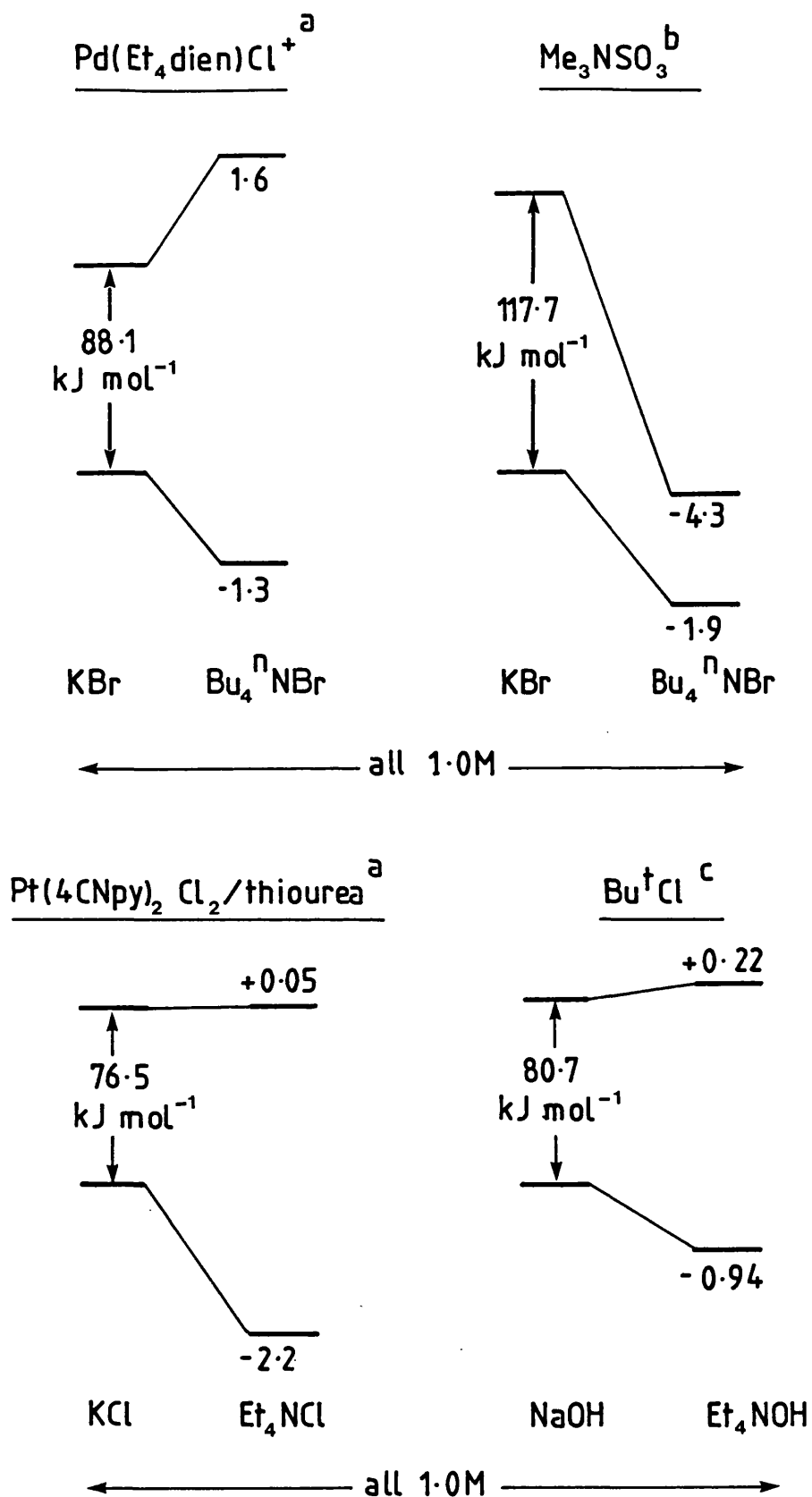


FIGURE (6.10)

Comparison of the effect of added salts on initial and transition states for kinetics of substitution and hydrolysis in inorganic and organic systems.

(a) 298.2 K, (b) 336.2 K, (c) 289 K.

destabilization as the cation is changed from alkali metal to tetra-alkylammonium.

Thus for the $[\text{Pd}(\text{Et}_4\text{dien})\text{Cl}]^+$ cation and t-butyl chloride, the hydration characteristics of the initial states are dominated by the hydrophobic organic parts of the peripheries, which leads to stabilization on transfer from KBr to Bu_4NBr solutions. For the palladium cation this is borne out by the fact that the chloride salt is more soluble in methanol and methanol-water mixtures than in water.²¹ In the formation of the transition states for solvolysis, the metal-chlorine and carbon-chlorine bonds are lengthened, causing development of negative charge on the chlorine and some hydrophilic character with hydration compatible with that of K^+ . Replacement of K^+ by Bu_4N^+ will therefore destabilize the transition state. The small change calculated is the resultant of this effect and the stabilizing influence of the organic hydrophobic periphery, which still makes an important contribution in the transition state because it accounts for a large portion of the periphery of these molecules.

With regard to transition state effects, the results for solvolysis of these chloro-compounds contrast with those for solvolysis of Me_3NSO_3 . For the latter, solvolysis does not involve the production of charge, and so the transition state behaves in the same fashion to the initial state, whose hydrophobic-hydrophilic periphery shows similar behaviour to that of the chloro-compounds.

The results for thiourea substitution at $\text{Pt}(\text{4CN-py})_2\text{Cl}_2$ are compatible with this discussion if it is assumed that Cl^- is the displaced species. Hydrophilic hydration of the lengthened Pt-Cl bond in the transition state is offset by the contribution of the coordinated hydrophobic thiourea molecule, resulting in a similar pattern to that for t-butyl chloride.

In order to lend weight to this discussion, it would be desirable to study the effect of added salts on the rate of solvolysis of a neutral transition-metal chloro-complex. $\text{Co}(\text{NH}_3)_3\text{Cl}_3$ is not particularly suitable because it aquates very quickly and there may be complexity in the kinetics arising from consecutive removal of the chlorides. A mono-chloro complex would be preferable. Species such as $\text{Co}(\text{NH}_3)_3(\text{NO}_2)_2\text{Cl}$ or $\text{Co}(\text{NH}_3)_3(\text{C}_2\text{O}_4)\text{Cl}$ might be suitable and have been vaguely alluded to,²² though their preparations of these complexes are far from clear. Complexes such as $\text{Co}(\text{dmgH})\text{pyCl}$ are well-known, though this particular example has a very low solubility in water, and the change in its UV/visible absorption spectrum on hydrolysis is unsuitable for kinetic studies.

It would also be useful to study the solvolysis of a complex where the leaving group is a neutral species. For example, the complex $\text{Fe}(\text{sb})_2\text{CN}_2$ was prepared, where sb is the Schiff base formed between pyridine-2-aldehyde and p-toluidene. However, solvolysis of this complex (in the presence of 2,2'-bipyridyl as scavenger) did not appear to proceed to completion and the kinetics were generally unsatisfactory from the quantitative standpoint. The use of 1,10-phenanthroline as scavenger, which should have driven the reaction to completion, was ruled out by its much lower solubility in water.

To summarize, the results of the analysis of salt effects on reaction kinetics for the systems described in this chapter are consistent and may be rationalized in terms of solvent cosphere overlap. The inclusion of data for t-butyl chloride provides a convenient link with the following chapter, where the rate of solvolysis of this compound in mixed solvents is analysed using a somewhat different approach to that described in previous chapters.

CHAPTER 7

A RE-EXAMINATION OF THE SOLVENT EFFECT
ON THE ACTIVATION PARAMETERS FOR SOLVOLYSIS OF
t-BUTYL CHLORIDE IN AQUEOUS SOLUTION

7.1 GENERAL INTRODUCTION

There are a number of areas where considerations of kinetics and thermodynamics merge, most notably in the analysis of a rate constant in terms of the energetics of the activation process. In most of the work in this thesis, this analysis is in terms of Gibbs free energy quantities.

Another aspect of this type of analysis is the temperature dependence of the rate constant. A common formulation of this dependence is the empirical Arrhenius relation, equation [7.1].

$$k_r = A \exp (-E_a/RT) \quad \dots [7.1]$$

The parameter A is the pre-exponential factor and is taken as independent of temperature. The parameter E_a is the activation energy.

Transition state theory yields an equation which also employs two parameters. These are the activation enthalpy, ΔH^\ddagger and activation entropy, ΔS^\ddagger . From equation [1.34] it may be shown that

$$k_r = \frac{kT}{h} \exp (\Delta S^\ddagger / R) \cdot \exp (-\Delta H^\ddagger / RT) (C^\ominus)^{(1-m)} \quad \dots [7.2]$$

The numerical values of the activation parameters based on these two different equations are related to each other. The defining relations from equations [7.1] and [7.2] are

$$E_a = -R \frac{d \ln k}{d (1/T)} \quad \dots [7.3]$$

$$\begin{aligned} \text{and } \Delta H^\ddagger &= -R \frac{d \ln(k/T)}{d (1/T)} \\ &= -R \frac{d \ln k}{d (1/T)} - R \frac{d \ln(1/T)}{d (1/T)} \quad \dots [7.4] \end{aligned}$$

From equations [7.3] and [7.4]

$$\Delta H^\ddagger = E_a - RT \quad \dots [7.5]$$

Equations [7.1] and [7.2] describe a linear dependence of $\ln(k_r)$ or

$\ln(k_r/T)$ on the reciprocal of temperature. The validity of these equations has been excellently confirmed in this way for a large number of experimental rate constants. It must be noted that these expressions are properly applied only to an authentic rate constant. Values of rate constants which contain unaccounted for concentration dependences cannot correctly be used.

It is observed that, for solvolysis of many alkyl halides in water, a plot of $\ln[k_{obs}]$ against $1/T$ is not a straight line. With increase in temperature, the rate constant falls below that required by a linear dependence based on values of k_{obs} at low temperatures. This trend may be accounted for in three possible ways.

First, it can be assumed that the chemical reaction is elementary, only one important activation barrier being involved. Therefore, the curvature is attributed to the complexity in the dependence of, for example, the related enthalpy of activation on temperature. This dependence is quantified as the heat capacity of activation by analogy with equilibrium thermodynamics:

$$\Delta C_p^\ddagger = \frac{d}{dT} \Delta H^\ddagger \quad \dots [7.6]$$

Secondly, it may be assumed that the reaction scheme is complicated, the observed rate constant being a function of two or more rate constants, k_i , describing individual steps. The latter assumption is combined with the assumption that in each case $\ln(k_i)$ is a linear function of $1/T$ with the result that $\ln[k_{obs}]$ is not a linear function of $1/T$.

The third approach combines complexity in the reaction mechanism with complexity in the dependence of individual rate constants on temperature.

Highly precise kinetic data giving accurate values of rate constants and temperatures are needed to obtain values of ΔH^\ddagger which are sufficiently

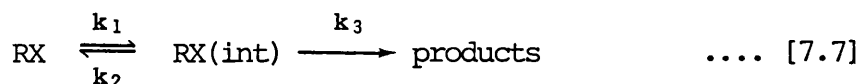
precise to warrant treatment along the above lines. The extent of curvature is slight and is best revealed by calculating values of ΔH_i^\ddagger from successive pairs of values of (k', T') and (k'', T'') ;

$$\Delta H_i^\ddagger = \frac{R \ln (k''/k')}{1/T' - 1/T''} \quad \dots [7.6]$$

Values of ΔH_i^\ddagger decrease smoothly with increasing temperature and so the curvature is considered a real effect.

7.2 SOLVOLYSIS OF T-BUTYL CHLORIDE

Two explanations have been offered for the large negative heat capacity of activation, ΔC_p^\ddagger , for solvolysis of t-butyl chloride in water. Robertson and co-workers^{1,2} have used the first approach described above (model 1) to calculate ΔC_p^\ddagger by fitting the dependence of rate constant on temperature to the Valentiner equation.^{1,3} Thus ΔC_p^\ddagger is linked to the breakdown of enhanced water-water interactions around the hydrophobic initial state.⁴ Albery and Robinson⁵ argued that the solvolytic reaction is a two-stage process described by the following mechanistic scheme (model 2);



$$k(\text{obs}) = k_1/(1 + \alpha) \quad \dots [7.8]$$

$$\text{where} \quad \alpha = k_2/k_3 \quad \dots [7.9]$$

In equation [7.7], RX(int) represents an intermediate; Albery and Robinson⁵ indicate one possibility is an ion-pair, e.g. $(\text{CH}_3)_3\text{C}^+\text{Cl}^-$. The curvature in the plot of $\ln[k(\text{obs})]$ against $1/T$ is a consequence of the different enthalpy of activation terms associated with k_1 and α .

Robertson and Scott⁶ were not persuaded to abandon model 1, which

assumes that ΔC_p^\ddagger is independent of temperature, in favour of model 2. Part of the case offered in favour of model 1 was the self-consistency of the explanations offered for the dependence of calculated activation parameters on mole fraction of added cosolvent.⁷⁻¹⁰ In all cases, the observed rate constant for solvolysis of t-butyl chloride in water decreases when an organic cosolvent is added. The derived enthalpy of activation ΔH^\ddagger (model 1) decreases, passes through a minimum and then increases with increase in mole fraction x_2 of cosolvent. More striking is the dependence of the calculated heat capacity of activation ΔC_p^\ddagger on x_2 . When ethanol,⁷⁻¹⁰ iso-propanol,⁸ t-butanol⁸ or THF⁹ are added, ΔC_p^\ddagger becomes more negative and then increases with increase in x_2 . However, when acetonitrile⁹ is added, ΔC_p^\ddagger gradually increases. These trends were discussed in terms of the effect of cosolvent on the water-water interactions and hence on the solvation characteristics of the initial state.^{4,7-10}

The disagreement between the two mechanistic interpretations,^{1,5} models 1 and 2, is one of analysis, there being no disagreement over the kinetic data. More recently it has become apparent that the Valentiner equation³ has various statistical shortcomings¹¹ and that the kinetic data may be consistent with a more complex dependence of ΔC_p^\ddagger on temperature¹² than was originally appreciated. If this is correct, the whole question of the interpretation of solvent effects on the derived activation parameters must be re-opened. Further, it is necessary to reconsider the analysis given by Arnett and co-workers¹³ of the effect of added ethanol on the partial molar enthalpies of initial and transition states for the solvolysis of t-butyl chloride (using model 1).

This re-examination is the subject of this chapter. The basis used is the Albery-Robinson mechanism, equation [7.7], model 2. The various

problems which emerge from either this model or model 1 make it clear that adoption of the third approach described at the beginning of the chapter is not justified at this stage.

7.3 ANALYSIS

The measured first-order rate constant is designated $k(\text{obs})$. For the solvolysis of t-butyl chloride in water averaged rate constants were used.¹ For solvolysis in the aqueous mixtures⁷⁻⁹ individual rate constants from the original laboratory notebooks were used (the only exception concerns the data¹⁰ for an aqueous ethanol mixture where the mole fraction of ethanol is 0.2).

The activation parameters calculated^{1,7-10} using model 1 in conjunction with the Valentiner equation are labelled with the symbol V ; thus the heat capacity of activation calculated from the dependence of $\ln k(\text{obs})$ on $1/T$ is called $\Delta C_p^\ddagger(V)$.

The following analysis generates another set of activation parameters by differentiation of equation [7.8] with respect to temperature. This leads to an expression for $\Delta H^\ddagger(1)$ in terms of the activation enthalpies for the processes described by k_1 - k_3 :

$$\Delta H^\ddagger(1) = \Delta H_1^\ddagger + \Delta \Delta H^\ddagger \cdot \alpha / (1 + \alpha) \quad \dots [7.10]$$

$\Delta H^\ddagger(1)$ is the overall activation enthalpy obtained by fitting the dependence of $\ln [k(\text{obs})]$ on temperature according to the requirements of model 2. It is the activation enthalpy which model 2 predicts would have been obtained had the data been described by model 1. The quantity $\Delta \Delta H^\ddagger$ is defined as follows:

$$\Delta \Delta H^\ddagger = \Delta H_3^\ddagger - \Delta H_2^\ddagger \quad \dots [7.11]$$

A further differentiation of equation [7.10] with respect to temperature

leads to an expression for $\Delta C_p^\ddagger(1)$;

$$\Delta C_p^\ddagger(1) = \Delta C_{p1}^\ddagger + \frac{\Delta \Delta C_p^\ddagger \alpha}{(1+\alpha)} - \frac{\alpha}{(1+\alpha)^2} \frac{(\Delta \Delta H^\ddagger)^2}{RT^2} \quad \dots [7.12]$$

where

$$\Delta \Delta C_p^\ddagger = \Delta C_{p3}^\ddagger - \Delta C_{p2}^\ddagger \quad \dots [7.13]$$

The quantity α is temperature dependent and this accounts for the complexity in a comparison of models 1 and 2, and in the analysis of $k(\text{obs})$ in terms of model 2. The dependences of $\ln k_1$ and $\ln \alpha$ on $1/T$ are probably non-linear. Thus ΔC_{p1}^\ddagger and $\Delta \Delta C_p^\ddagger$ would be real quantities, possibly with temperature derivatives. However, if these factors are recognised, equation [7.13] becomes hopelessly complicated. At this stage in the analysis it was decided to examine a simplified version of model 2 which sets ΔC_{p1}^\ddagger and $\Delta \Delta C_p^\ddagger$ to zero. This implies the assumption that $\ln k_1$ and $\ln \alpha$ are linear functions of $1/T$. In that case, these dependences can be written as follows:

$$k_1 = a_1 \exp(a_2/T) \quad \dots [7.14]$$

$$\alpha = a_3 \exp(a_4/T) \quad \dots [7.15]$$

Hence

$$k(\text{obs}) = \frac{a_1 \exp(a_2/T)}{[1.0 + a_3 \exp(a_4/T)]} \quad \dots [7.16]$$

and

$$\Delta H_1^\ddagger = -R(a_2 + T) \quad \dots [7.17]$$

$$\Delta \Delta H^\ddagger = a_4 k \quad \dots [7.18]$$

where R is the gas constant.

Consistent with the above assumption is the following equation for $\Delta C_p^\ddagger(1)$ (cf. equation [7.12]);

$$\Delta C_p^\ddagger(1) = - \frac{\alpha}{(1+\alpha)^2} \frac{(\Delta \Delta H^\ddagger)^2}{RT^2} \quad \dots [7.19]$$

Even with this simplified version of model 2, equation [7.16] expresses the dependence of $k(\text{obs})$ on temperature in a form which cannot be analysed

using a conventional linear least-squares technique. Consequently, a program (FORTRAN for the CDC Cyber 73) was written which incorporated a procedure for fitting the data using a Gauss-Newton technique in conjunction with subroutines which calculated the associated Jacobian and Hessian matrices.¹⁴ The program is listed in Appendix 4.

The calculations started with seed values and hunted estimates of a_1 , a_2 , a_3 and a_4 which minimised $\sum [k(\text{obs}) - k(\text{calc})]^2$ over n data points. It was found advantageous to rewrite equation [7.16] incorporating various powers of 10 as multiplying factors of each a -parameter so that the final estimates of these parameters were of similar order of magnitude. Considerable trial and error was necessary before satisfactory minima were obtained, as judged by the ability to reproduce $k(\text{obs})$ within the estimated experimental accuracy, e.g. within $\pm 1\%$.

The source of this difficulty arises from the form of equation [7.16]. If this is rewritten in terms of $[k(\text{obs})]^{-1}$ this quantity is expressed as the sum of two exponential terms. These equations often have more than one solution and Moore comments on this problem¹⁵ in the context of calculating from kinetic data the rate constants for consecutive reactions. With regard to equation [7.16] there is not therefore one global minimum characterised by a unique set of a -parameters. The criteria employed for an acceptable set were that a_1 and a_3 were both positive, a_2 was negative and that the magnitude of a_2 was larger than that for a_4 . In addition, it was required that the plot of residuals $\Delta [= k(\text{obs}) - k(\text{calc})]$ showed random scatter about zero.

The least-squares parameters were used to calculate the activation parameters discussed above together with values of k_1 and α over and beyond the experimental temperature range. The calculation was extended in this way in order to find the temperature at which $\alpha = 1$ and to

examine the dependence of $\Delta C_p^\ddagger(1)$ on temperature as predicted by equation [7.19].

7.4 RESULTS

The results of the analysis of 20 sets of kinetic data are summarized in Table (7.1). The latter shows the number of data points for each system together with the range of temperatures over which $k(\text{obs})$ was measured. This range, T_R , plays an important part in the discussion. For t-butyl chloride in water (and water-rich solvent mixtures) T_R is determined by the freezing point of the solvent and the short half-life at high temperatures. As cosolvent is added the lower limit of T_R was determined by the problem of holding the thermostats to within ± 0.002 K over extended periods. Thus as the mole fraction x_2 increases the mean temperature of the measured range T_R increases [Table (7.1)]. As an indication a value T_m is reported in the Table, which is the experimental temperature closest to the arithmetic mean temperature.

The kinetic data for all systems were fitted satisfactorily to equation [7.16]. A typical plot of the residuals Δ is shown in Figure (7.1) for the solvolysis of t-butyl chloride in water. The values of k_1 and α at temperatures T_m are given in Table (7.1) together with calculated values of ΔH_1^\ddagger and $\Delta \Delta H^\ddagger$. The calculated temperature T_α at which $\alpha = 1$, together with the value of $\Delta C_p^\ddagger(1)$ at its minimum and the temperature corresponding to this minimum, are also reported together with the values of $\Delta C_p^\ddagger(1)$ at T and a common temperature 290 K. The minimum value of $\Delta C_p^\ddagger(1)$ occurs at the temperature where a plot of $\Delta H^\ddagger(1)$ against temperature has a point of inflection.⁵ Table (7.1) also includes the value of $\Delta H^\ddagger(1)$, calculated from equation [7.11], at T_m . The dependence of $\Delta C_p^\ddagger(1)$ on temperature for a number of systems is shown in Figure (7.2).

TABLE (7.1)

KINETIC PARAMETERS FOR SOLVOLYSIS OF t-BUTYL CHLORIDE DERIVED USING THE ALBERY-ROBINSON MECHANISM

mole fraction of co-solvent x_2	no. of data points n	temp. range T_R/K	T_m/K	$10^4 k(\text{obs})/s^{-1}$	$\alpha(T_m)$	$10^3 k_1(T_m)/s^{-1}$	$\Delta H_1^*(298 K)/kJ mol^{-1}$	$\Delta H^*/kJ mol^{-1}$	$T(\alpha=1)/K$	$\Delta C_p^*(1)_{max}/J mol^{-1} K^{-1}$ at T/K	$\Delta C_p^*(1)_{at 290 K}/J mol^{-1} K^{-1}$	$\Delta C_p^*(1; T_m)/J mol^{-1} K^{-1}$	$\Delta H^*(1; T_m)/kJ mol^{-1}$
0	20	274-293	284	41.45	0.13	4.68	104.6	-47.2	316.7	-672	-431	-348	99.2
ethyl alcohol													
0.075	37	273-293	283	14.37	1.19	3.14	111.6	-36.3	280.0	-514	-439	-479	91.9
0.11	36	266-293	281	7.113	0.96	1.40	114.1	-45.6	281.2	-796	-682	-796	91.7
0.15	36	275-300	288	6.579	8.34	6.16	117.0	-38.4	254.5	-692	-186	-186	82.7
0.25	6	279-303	293	2.153	4.44	0.17	109.7	-25.7	256.8	-309	-152	-152	88.7
Pr ^t OH													
0.02	46	273-295	283	25.45	0.198	3.05	105.5	-49.1	306.8	-777	-641	-500	97.4
0.05	59	273-297	285	23.56	0.235	2.91	100.1	-48.3	307.0	-752	-623	-529	90.9
0.075	42	273-297	285	13.01	4.06	6.57	114.0	-41.6	264.3	-770	-332	-416	80.6
0.10	60	277-297	289	8.353	0.571	1.35	92.8	-46.2	297.9	-732	-717	-711	76.0
0.20	56	289-320	306	4.649	6.86	3.66	114.1	-32.8	266.0	-465	-270	-154	85.5
Bu ^t OH													
0.02	39	273-295	285	34.85	0.172	4.08	103.6	-51.2	310.0	-821	-596	-486	96.1
0.05	41	275-295	285	18.72	1.18	4.07	104.8	-47.4	282.8	-854	-756	-826	79.1
0.10	56	288-318	303	12.64	9.74	13.56	107.7	-26.2	248.7	-341	-119	-75.9	83.9
0.20	48	298-326	313	5.100	4.83	2.98	114.1	-28.8	274.1	-338	-263	-144	90.2
THF													
0.05	52	277-297	287	16.37	2.83	6.27	113.4	-38.9	269.9	-631	-385	-425	84.7
0.10	42	283-313	297	6.977	64.3	44.9	109.0	-30.0	221.3	-558	-25.9	-18.5	79.5
0.20	39	298-323	310	2.257	8.36	2.10	114.5	-29.8	262.3	-395	-213	-105	87.9
acetonitrile													
0.05	40	273-293	283	19.98	2.27	6.55	109.4	-28.9	265.4	-364	-222	-265	89.3
0.10	44	275-297	287	12.96	0.10	1.43	89.1	-37.9	336.0	-391	-192	-173	85.7
0.20	50	286-313	300	9.542	8.33	8.90	117.1	-34.4	260.5	-531	-234	-150	86.4

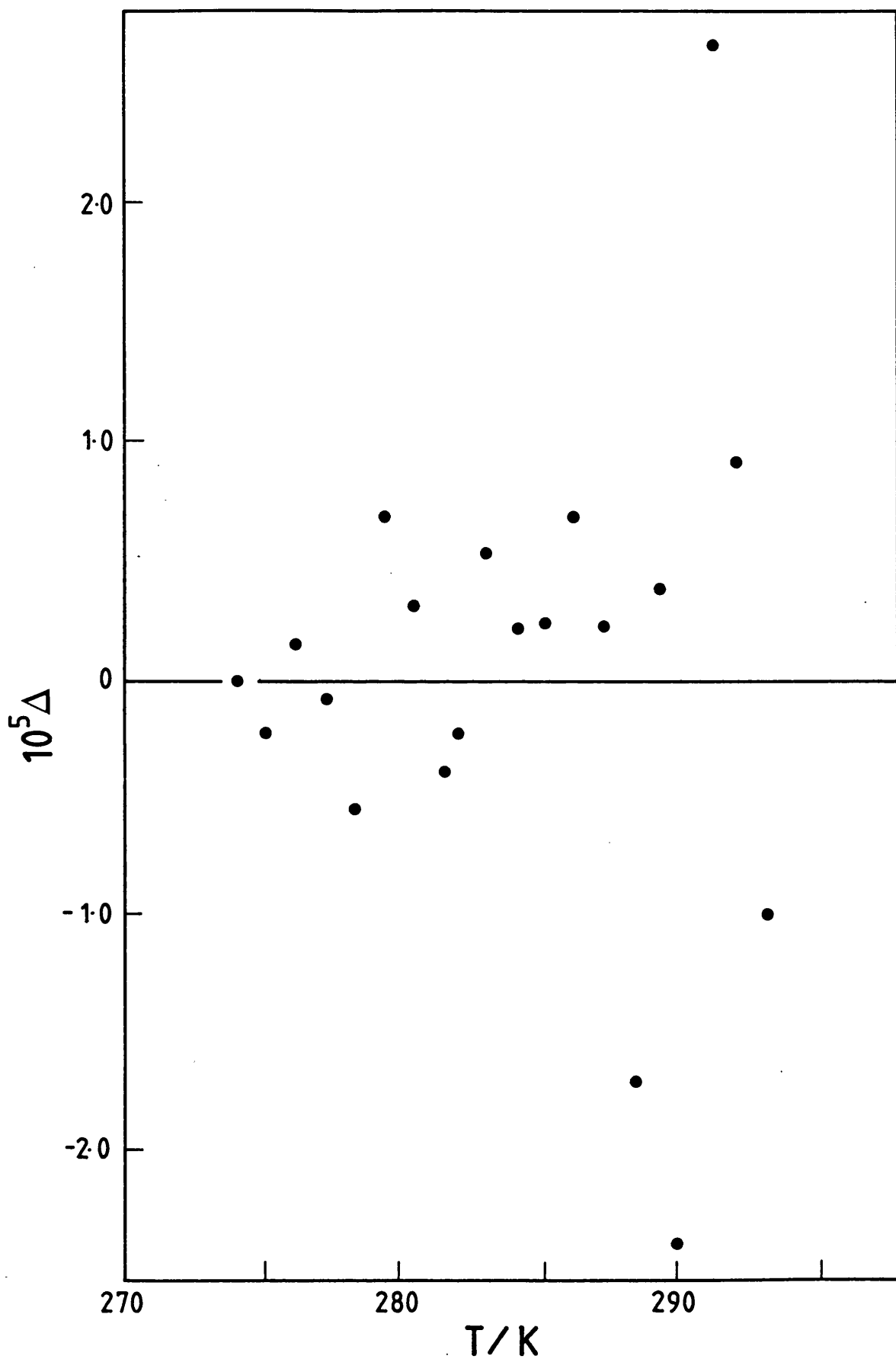


FIGURE (7.1)

Plot of residuals, Δ , against temperature for t-butyl chloride in water.

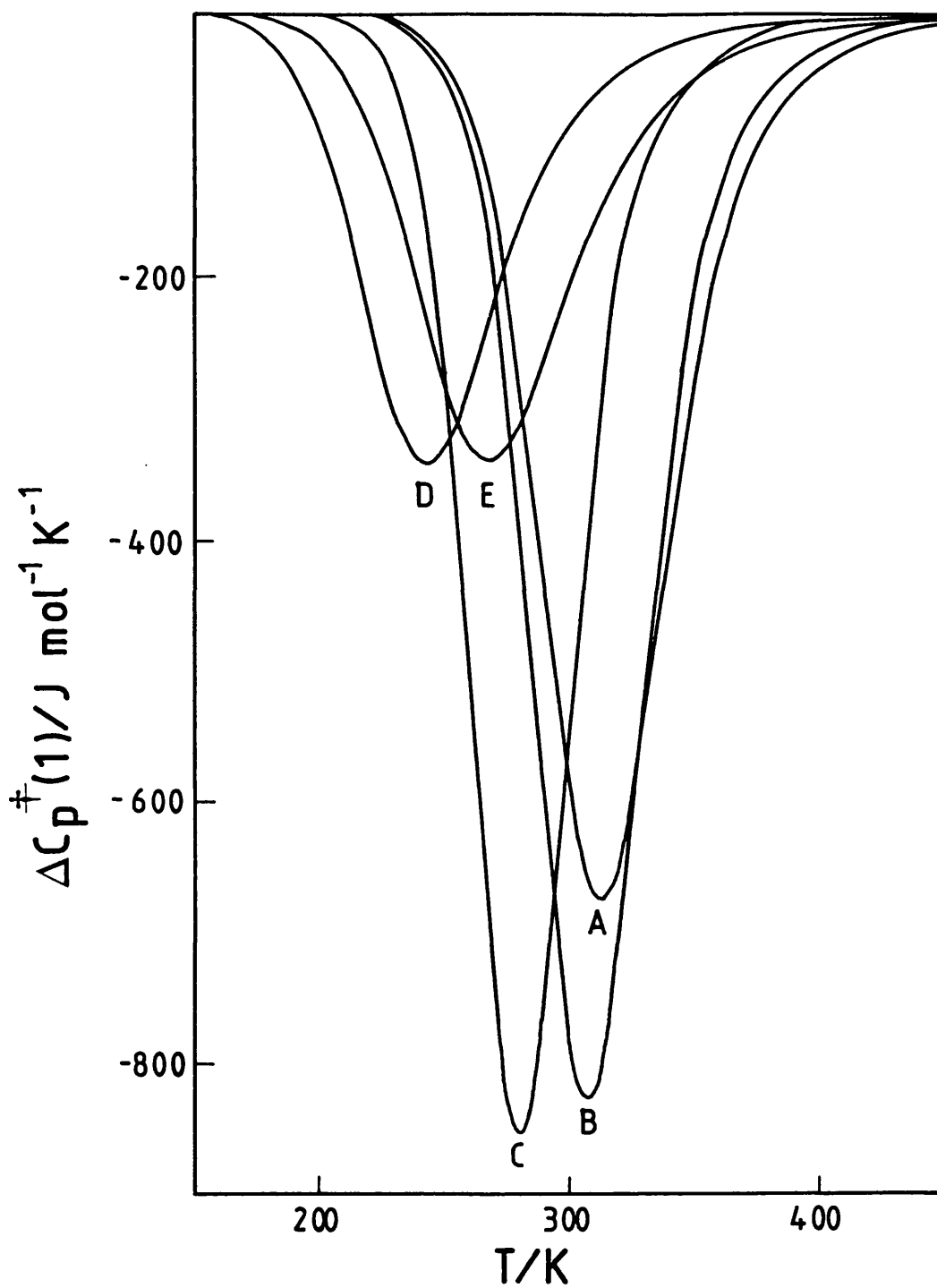


FIGURE (7.2)

Dependence of $\Delta C_p^\ddagger(1)$ on temperature for solvolysis of t-butyl chloride in water (A), and in t-butyl alcohol+water mixtures where mole fraction of organic co-solvent $x_2 = 0.02$ (B), 0.05 (C), 0.10 (D) and 0.20 (E).

7.5 DISCUSSION

This section falls into three main divisions. Firstly, consideration is given to how the parameters derived using the Albery-Robinson mechanism, model 2, account for the patterns shown by the activation parameters calculated using model 1 and the Valentiner equation. Secondly, the initial state - transition state dissection on reactivity for solvolysis in aqueous ethanol is repeated using some of the new quantities and the results are compared with the previous analysis given.¹³ Finally, the significance of some of the parameters describing model 2 are considered in their own right.

The ability of equation [7.16] to fit the data is confirmed by, for example, the small residual sum of squares, 3.796×10^{-10} , for solvolysis in water. According to model 2, both k_1 and α increase with increase in temperature over the measured temperature range. The ratio α equals 1.0 at 316.7 K, a temperature only slightly above that previously predicted, but, more importantly, above the highest temperature of the measured range. Similarly the extremum in $\Delta C_p^\ddagger(1)$, while not at this temperature T_α , is also just above the highest temperature in T_R . Across T_R , $\Delta C_p^\ddagger(1)$ is decreasing rapidly. Thus $\Delta C_p^\ddagger(V)$, calculated using the Valentiner equation, is some averaged value across T_R . Indeed, the previously reported value for $\Delta C_p^\ddagger(V)$ is close to that for $\Delta C_p^\ddagger(1)$ at the mean temperature, T_m , i.e. $347 \text{ J mol}^{-1} \text{ K}^{-1}$ and $348 \text{ J mol}^{-1} \text{ K}^{-1}$ respectively.

When ethanol is added, $k(\text{obs})$ and k_1 decrease while ΔH_1^\ddagger increases [Table (7.1)]. The temperature at which $\alpha = 1$, T_α , decreases such that when $x_2 = 0.25$ T_α is below T_R and T_m has moved to 288 K. The same trend in T_α is observed for all added solvents although at the highest value of x_2 , T_α increases again but remains below T_R . At the mean temperature T_m

α changes from <1.0 to >1.0 with increase in x_2 .

The dependence of α on T and x_2 impinges directly on the dependence of $\Delta H^\ddagger(1)$ and $\Delta C_p^\ddagger(1)$. The other important feature is the dependence of $\Delta\Delta H^\ddagger$, which becomes less negative with increase in x_2 , the trend when either t-butanol or tetrahydrofuran are added being particularly marked. From the values of ΔH_1^\ddagger , $\Delta\Delta H^\ddagger$ and α at T_m , the dependence of $\Delta H^\ddagger(1)$ at T_m on x_2 can be calculated. In all cases, $\Delta H^\ddagger(1)$ decreases and then increases with increase in x_2 as shown in Figure (7.3). The plots in this figure track closely to those in Figure 1 of ref. (8) and Figure 1 of ref. (9). If, on the other hand, $\Delta H^\ddagger(1)$ had been calculated at T_α , a different pattern would have been obtained. It was surprising⁹ that the change in enthalpy of activation with increase in x_2 does not distinguish between cosolvents. This feature has been noted before but the problem side-stepped in view of the quite striking differences in the dependence of heat capacities of activation on x_2 .⁹ However, this aspect may not be as clear-cut as originally suggested.⁹

The heat capacity parameters calculated on the basis of model 2 depend on three important features: (a) the temperature T_α , (b) the position of T_α with respect to T_R and T_m and (c) the value of $\Delta\Delta H^\ddagger$. The calculated maximum value of $\Delta C_p^\ddagger(1)$ shows a complex dependence on x_2 but tends to decrease and then increase with increase in x_2 . As for α , the maximum in $\Delta C_p^\ddagger(1)$ occurs at lower temperatures with increase in x_2 eventually crossing T_m and falling below the minimum value in T_R . As a result $\Delta C_p^\ddagger(1)$ calculated at T_m shows a marked dependence on x_2 . In the case of aqueous mixtures containing ethanol, iso-propanol, tetrahydrofuran and t-butanol, $\Delta C_p^\ddagger(1)$ at T_m decreases and then increases, the same pattern being shown as the previously reported dependence on $\Delta C_p^\ddagger(V)$ on x_2 [Figure 3 of ref. (8)]. The dependence of $\Delta C_p^\ddagger(1)$ at T_m on x_2 for

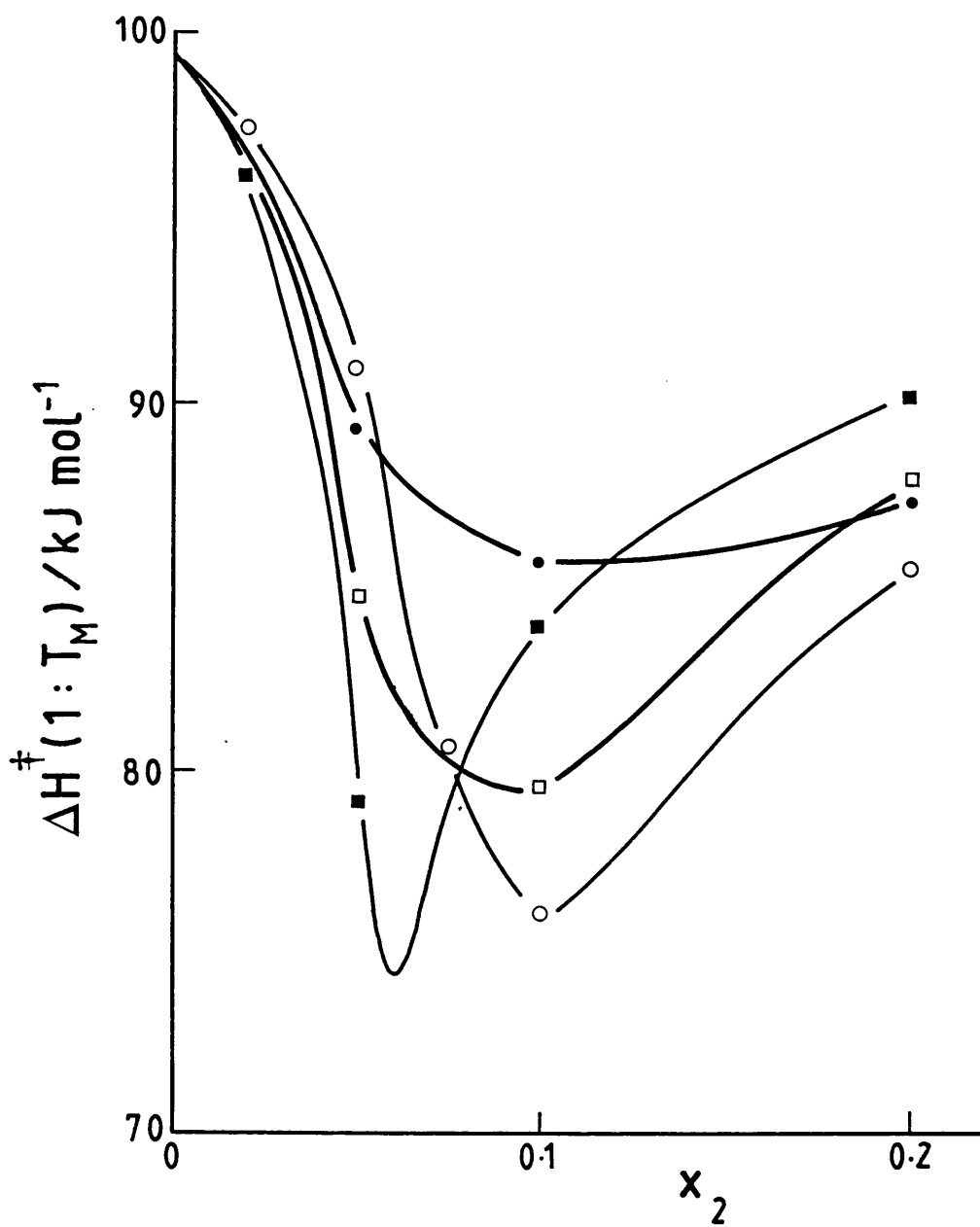


FIGURE (7.3)

Dependence of $\Delta H^\ddagger(1:T_m)$ for solvolysis of t-butyl chloride on mole fraction of added organic cosolvent.

■ t-BuOH, ○ i-ProH, □ THF, ● MeCN.

mixtures containing acetonitrile is consistent with the steady increase reported for ΔC_p^\ddagger (V) [Figure 2 of ref. (10)].

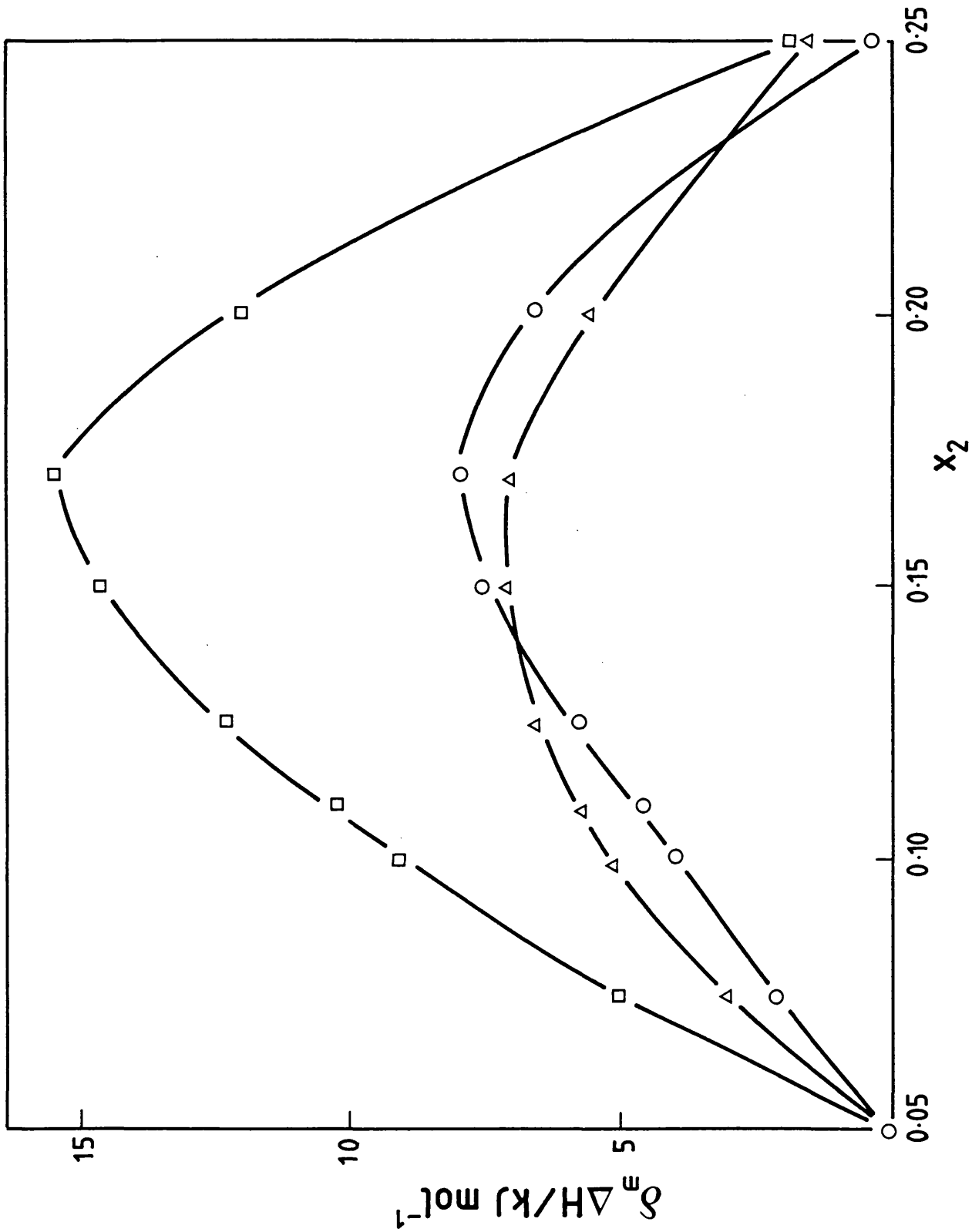
The above discussion, based on the data reported in Table (7.1), shows how the parameters calculated on the basis of model 2 permit another interpretation of the previously reported parameters based on model 1. If these data are combined with initial state data, more comparisons emerge. Here attention is concentrated on the analysis reported by Arnett et al.¹³ of the enthalpy data. Enthalpies of solution for t-butyl chloride in a series of ethanol-water mixtures were combined with enthalpies of activation for the solvolytic reaction¹⁶ to yield¹³ the dependence on x_2 of the partial molar enthalpy of the transition state, model 1. The dependence of the enthalpy of activation on x_2 could be accounted for almost completely in terms of the initial state enthalpy on x_2 . In other words, the partial molar enthalpy of the transition state is effectively independent of x_2 . This was a surprising discovery, because almost all solutes, including salts and neutral molecules, show an endothermic maximum.¹³ Arnett et al. were led to the conclusion that this was a 'fortuitous' consequence of the size and shape of the trimethyl-carbonium chloride transition state. In terms of model 2, this result is a natural consequence of the values of ΔH_1^\ddagger , $\Delta\Delta H^\ddagger$ and the value of α at T_m . It is possible to repeat the analysis but now combining the initial state data and ΔH_1^\ddagger (at 298.2 K) to obtain the dependence on x_2 of the partial molar enthalpy of the transition state associated with rate constant k_1 by the use of the following relation analogous to equation [1.37]

$$\delta_m \Delta H_1^\ddagger = \delta_m H^\ddagger - \delta_m H_{1S} \quad \dots [7.20]$$

δ_m - solvent operator

FIGURE (7.4)

Dependence on mole fraction of added ethyl alcohol for the partial molar enthalpies of (1) the initial state (Δ), (2) the transition state for k_1 (model 2) (\square) and (3) activation (O).



H^\ddagger - partial molar enthalpy of transition state

H_{is} - partial molar enthalpy of initial state.

The results of this analysis are shown in Figure (7.4) [some interpolation of enthalpies of solution and activation was needed to produce this figure]. The enthalpies of solution for both initial and transition states show endothermic maxima, consistent with the pattern for more conventional solutes,¹³ and can be accounted for in the manner outlined by Arnett et al.¹³ in terms of the relative effectiveness of solvent structure-making or -breaking of the solute and cosolvent.

The foregoing analysis shows that the arguments based on the effect of added cosolvent on water-water interactions in the context of model 1 can, with modification, be used to explore the solvent effects as described by model 2. In this regard, the data for the t-butanol + water mixtures [Table (7.1)] are informative because for a wide range of phenomena the properties of this mixture and solutes in it are markedly dependent on solvent composition.⁴ As discussed in Chapter 1, two features are often looked for in plots of such properties against x_2 . At low x_2 (i.e. <0.04) t-butanol enhances water-water interactions but when $x_2 > 0.04$ the addition of alcohol brings about a disruptive influence. Ultrasonic absorption properties indicate extensive fluctuations in composition, these effects maximizing around $x_2 = 0.1$. With these points in mind the trends in Table (7.1), shown in Figure (7.5), can be examined.

With increase in x_2 , ΔH_1^\ddagger remains unaltered until $x_2 > 0.05$. Thus the formation of the ion pair over this initial region is taking place within an essentially aqueous environment dominated by extensive and strong water-water interactions. Creation of the ion pair will require separation

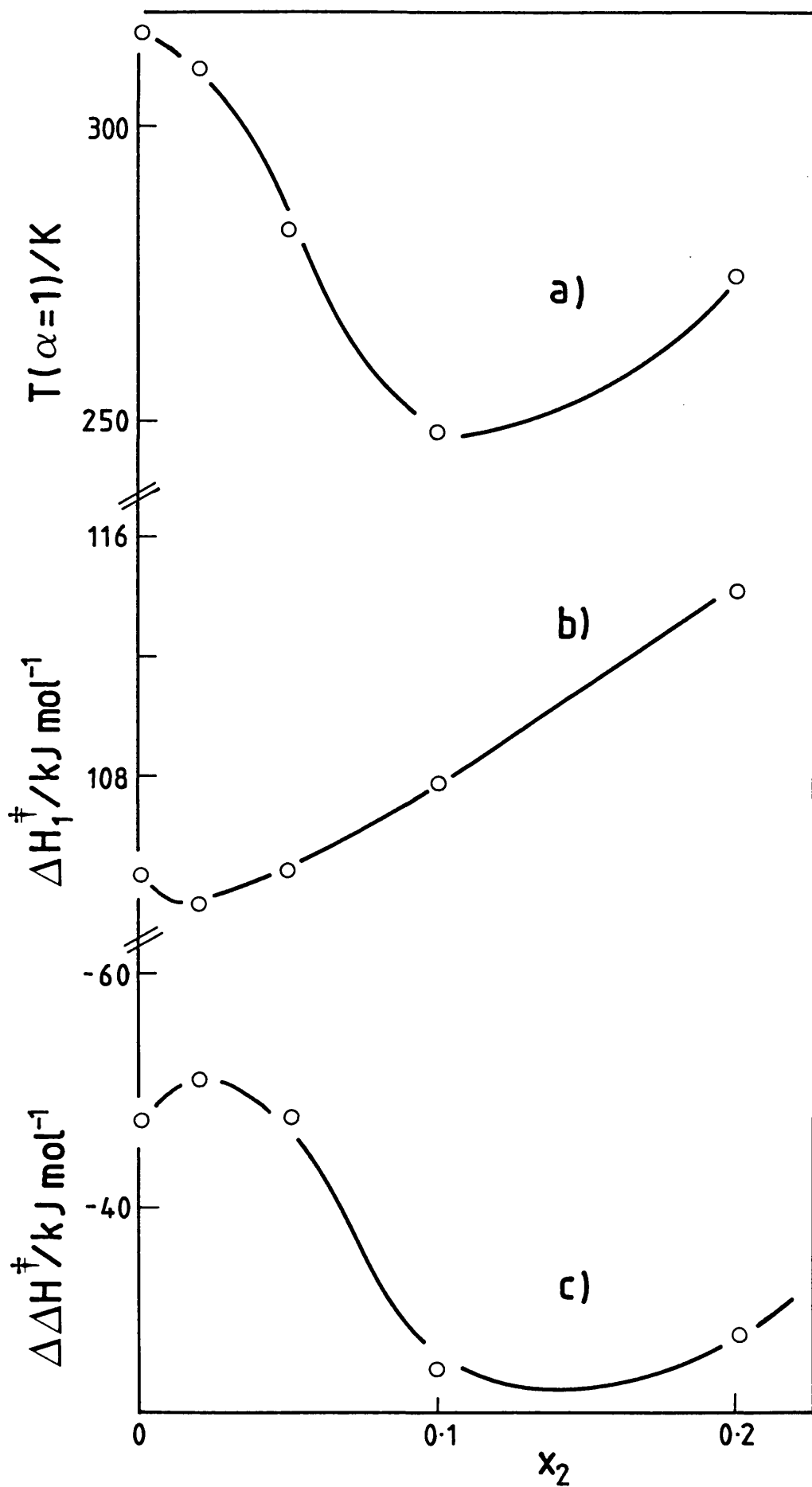


FIGURE (7.5)
 Dependence on mole fraction of added t-butyl alcohol for (a) the temperature at which $\alpha = 1$,
 (b) ΔH_1^\ddagger and (c) $\Delta\Delta H^\ddagger$.

of charge and disruption of this water structure into a configuration which can solvate the developing chloride ion. When $x_2 > 0.04$, ΔH_1^\ddagger increases because the solvating power of the local environment will be much less. The counterbalance between solvent structure/re-organisation and the solvating power of the medium plays an important rôle in determining α and its related activation parameters. In water over the measured range $\alpha < 0.1$ (i.e. $k_3 > k_2$), $\Delta\Delta H^\ddagger$ being negative. When $x_2 > 0.04$, the difference between ΔH_2^\ddagger and ΔH_3^\ddagger diminishes but is still negative. Nevertheless, α moves to values greater than unity over the measured range. Here the magnitude of α is clearly controlled by the entropy of activation. Indeed, a feature of aqueous systems⁴ is the importance of entropy terms.

Finally, one other feature of the analysis is noted. The variation of the following quantities on temperature for each solvent mixture was calculated:

$$[1] \quad \ln \left\{ \frac{k^m(\text{obs})}{k^o(\text{obs})} \right\} \quad [2] \quad \ln \left\{ \frac{k_1^m}{k_1^o} \right\} \quad [3] \quad \ln \left\{ \frac{\alpha^m}{\alpha^o} \right\}$$

k^o , k_1^o , α^o are the rate parameters for solvolysis in water and k^m , k_1^m and α^m are those for a given aqueous mixture. These quantities were plotted by computer as continuous functions using the appropriate a -parameters in each case over a temperature range which accommodated all those in Table (7.1).. The nineteen traces for each quantity were plotted on the same graph. It was found that for quantities [1] and [3] these traces crossed in a highly complex manner, but the traces for quantity [2], although curved, did not cross at all over the given temperature range. This might be expected because quantities [1] and [3] are complex functions of four rate constants, but quantity [2] a function of a ratio of only two. However, when the order of cosolvents corresponding to each

trace for quantity [2] was examined, it was found that these occurred in an effectively random order for increasing $\ln \left\{ \frac{k_1^m}{k_1} \right\}$ at a given temperature. Why this quantity combines such simplicity with such randomness is not clear.

7.6 SUMMARY

The preceding comments identify the more obvious features of the data given in Table (7.1). However, the overall problem of understanding solvent effects on the basis of model 2 is not straightforward. Nevertheless, this analysis has suggested that the explanation of the derived parameters based on the Albery-Robinson scheme (model 2) is more satisfactory than that based on model 1.

This approach answers some problems but not all. One major criticism is the fact that the partial molar heat capacities of solutes in water are not negligible.² The analysis described above assumed that the real heat capacity of activation, $\Delta C_{p_1}^\ddagger$ is zero. The assertion that both $\ln k_1$ and $\ln \alpha$ are linear functions of $1/T$ cannot be a complete description. Clearly these assumptions are too drastic. The next stage requires that the 'complex-complex' approach is adopted where there is both complexity in mechanism and complexity in the dependence of rate constants on temperature. This approach makes enormous demands on the kinetic data, which must be very precise and cover a wide temperature range. Progress along these lines is extremely limited at present.

It is felt that there is a great deal of information to be extracted from such derived parameters as have been discussed in this Chapter. Unfortunately, the patterns which emerge are in general not clear-cut, but the significance of these parameters is certainly emphasised.

CHAPTER 8

ANALYSIS OF THE TEMPERATURE DEPENDENCE
OF ACID DISSOCIATION CONSTANTS IN WATER

8.1 INTRODUCTION

8.1.1 Equilibria and kinetics

Probably all chemical reactions can take place in both directions, but in many cases the extent of the reverse reaction is so small as to be negligible. Such chemical reactions may thus be regarded as proceeding to completion in one direction.

When the conditions are such that forward and reverse reactions can both occur to a noticeable extent, the process is described as a reversible reaction. [Like other chemical reactions, a reversible reaction takes place spontaneously and so the actual process is thermodynamically irreversible.] The overall reaction does not go to completion in either direction. After the lapse of a sufficient interval of time, all reversible reactions in a closed system at constant temperature and pressure reach a state of chemical equilibrium, i.e. a state in which no further change in composition with time can be detected. Guldberg and Waage (1863) recognized that chemical equilibrium is a dynamic and not a static condition. It is characterized not by cessation of all interaction but by the fact that the rates of forward and reverse reactions have become the same. These rates were formulated in terms of the concentrations of the species involved using the law of mass action. The equilibrium law stated that the equilibrium constant was given by the ratio of the rate constants for the forward and reverse reactions, k_f/k_r .

Guldberg and Waage's work did not constitute a general proof of the equilibrium law, but was important because they recognized that the equilibrium is influenced by two factors, a concentration effect and an effect which depends on the chemical natures of the reacting species, their temperature and pressure. The correct derivation of the equilibrium law is from thermodynamic principles beginning with the condition that

$\Delta G = 0$ at equilibrium.

In previous chapters, the reaction kinetics for several systems were discussed in terms of mechanisms which included equilibria involving intermediate or precursor species. In this chapter, attention is focussed on systems which involve only equilibria.

8.1.2 Acid dissociation constants

For a weak acid dissolved in water, the dissociation equilibrium is usually written as follows:



If the total concentration of acid in the water is not too large, the activity of the water molecules is approximately equal to that in pure water, and this, by convention, is taken as unity. The equilibrium constant for the dissociation, K_a , is given by

$$K_a = \frac{a_{\text{H}_3\text{O}^+} \cdot a_{\text{A}^-}}{a_{\text{HA}}} \quad \dots [8.2]$$

where a_i is the activity of species i . Each activity term may be replaced by the product of the corresponding concentration and activity coefficient. The concentration quotient, K_c , is given by

$$K_c = \frac{c_{\text{H}_3\text{O}^+} \cdot c_{\text{A}^-}}{c_{\text{HA}}} = \frac{\alpha^2 c}{(1-\alpha)} \quad \dots [8.3]$$

where c_i = concentration of species i /mol dm⁻³

c = total concentration of HA/mol dm⁻³

α = degree of dissociation.

K_c becomes equal to K_a at infinite dilution, when the activity coefficients are all unity. Values for K_c can be derived from conductance or e.m.f. measurements.

The variation of K_a for weak monobasic carboxylic acids with temperature

passes through a maximum. This chapter reports two approaches to the analysis of this dependence, in attempts to account quantitatively for the observed behaviour in terms of various chemical phenomena. The final section of the chapter contains closing comments linking this chapter with previous chapters.

8.2 ANALYSIS USING THE GURNEY EQUATION

8.2.1 Background

Over many years, extensive efforts have been made to formulate equations which describe the dependence of acid dissociation constants on temperature.¹ For the most part, these equations express the dependence of $\ln K$ on temperature T , in an equation which contains several terms each being a different function of T . Moreover, these equations have often been written in such a way that the data can be fitted to the final equation using a linear least-squares technique. A rather different approach to the problem is to begin with a model which attempts to describe those factors which determine the value of K at temperature T . Gurney² suggested that $\ln K$ for a given acid is determined by two contributions;

$$\Delta G^\ominus = -RT \ln K \quad \dots [8.4]$$

$$\text{and } \Delta G^\ominus = \Delta G_{\text{non}}^\ominus + \Delta G_{\text{e1}}^\ominus \quad \dots [8.5]$$

The factors affecting the two contributions were taken to be quite separate and independent. $\Delta G_{\text{e1}}^\ominus$ is sensitive to the environment and, according to Gurney, is entirely electrostatic in origin. It is proportional to ϵ^{-1} , where ϵ is the dielectric constant for the solvent at that temperature, given by

$$\epsilon^{-1} = \epsilon_0^{-1} \exp (T/\theta) \quad \dots [8.6]$$

θ , in the Gurney temperature, is characteristic of the solvent. ϵ_0 is the dielectric constant at this temperature.

In contrast, $\Delta G_{\text{non}}^\ddagger$ is insensitive to both the environment and temperature. It represents quantum-mechanical forces arising from the internal motions of electrons. These motions are so rapid that the molecular dipoles cannot respond: the forces are therefore independent of environment.²

The resulting equation for $\ln K$, the Gurney equation, has the following form:

$$\ln K = -C[a + \exp(T/\theta)]/T \quad \dots [8.7]$$

This may be rewritten as follows;

$$\ln K = a_1 T^{-1} + a_2 T^{-1} \exp(T/\theta) \quad \dots [8.8]$$

The Gurney equation is often mentioned in the literature, but as far as is known, no attempt has been made to fit the data to it in any quantitative fashion apart from various comments on the general dependence of the two terms in equation [8.8] on temperature. This omission probably arises from the fact that the analysis cannot be based on a conventional least-squares technique to yield estimates of a_1 , a_2 and θ . This section reports the results of an attempt to fit the data for several acids to equation [8.8].

8.2.2 Analysis

The basis of the analysis described here is the Gauss-Newton method³ which, starting with estimates for a_1 , a_2 and θ , obtains values for these parameters which minimise the residual sum of squares $[\ln K(\text{obs}) - \ln K(\text{calc})]^2$. A computer program (FORTRAN for the CDC Cyber 73) to perform this analysis, listed in Appendix 5, contained subroutines which calculated the Jacobian and Hessian matrices. The assumption was made that the local minimum obtained from a range of initial estimates is also the global minimum.³

From the best-fitted parameters the dependences on temperature of $a_1 T^{-1}$ and $a_2 T^{-1} \exp(T/\theta)$ were calculated.

8.2.3 Results

The results of the analysis are summarized in Table (8.1) for fifteen carboxylic acids in water. Also included for comparison are the parameters calculated for the self-dissociation of water and deuterium oxide, which will not be discussed further because the chemical process is quite different. The fit, as measured by the residual sum of squares, is satisfactory.

The dependences on temperature of both $a_1 T^{-1}$ and $a_2 T^{-1} \exp(T/\theta)$ for cyanoacetic and acetic acids in water are shown in Figure (8.1) together with the sum of the two curves over an extended temperature range to include θ where $a_2 T^{-1} \exp(T/\theta)$ is a maximum. Thus for acetic acid, the non-electrostatic term shifts the maximum from 184 K to around 298 K, bringing it within the experimental range. For cyanoacetic acid, θ is lower and hence the resulting curve [Figure (8.1b)] has its maximum near 270 K, just below the experimental range.

8.2.4 Discussion

The most striking feature is the ability of equations [8.7] and [8.8] to fit the data for a range of systems having quite marked differences in their dependence of $\ln K$ on T . Nonetheless, the residual sum of squares is, in all cases, larger than that obtained if the data are fitted using three parameters as with, for example, the Valentiner⁴ or the Clark-Glew⁵ equations. Thus for cyanoacetic acid, the residual sum of squares obtained from the latter two equations is 0.22×10^{-5} . In general the residual sum of squares is only slightly larger than that obtained from the Valentiner equation, an equation which is less constrained than

TABLE (8.1)

Derived parameters for the dependence on temperature of acid dissociation constants according to the Gurney equation (equation [8.7])

Acid ^{ref.}	10 ² C	<u>a</u>	θ/K	10 ⁵ Δ ^{<u>a</u>}
Acetic ⁶	4.066	3.000	184.6	3.190
Acetic-d ₃ ⁷	4.644	2.418	194.4	4.434
Formic ⁸	1.143	12.692	130.3	10.579
Propanoic ⁹	4.724	2.394	192.9	9.449
Isobutanoic ¹⁰	6.349	1.124	211.8	10.535
Cyanoacetic ¹¹	0.4923	18.74	108.3	1.052
Isopropylcyanoacetic ¹²	2.900	0.1426	174.3	35.466
Diisopropylcyanoacetic ¹³	7.481	-1.259	232.5	0.3859
Dimethylcyanoacetic ¹²	1.493	2.879	141.2	0.4407
Fluoroacetic ¹⁴	0.0818	134.36	71.0	23.247
Chloroacetic ¹⁴	0.5888	17.74	108.4	1.047
Bromoacetic ¹⁴	1.317	6.098	135.5	0.037
Iodoacetic ¹⁴	3.052	1.604	174.2	0.052
Water ¹⁵	0.8996	94.47	118.4	25.94
Acetic ^{16 <u>b</u>}	4.231	3.530	183.2	1.171
Acetic-d ₄ ^{16 <u>b</u>}	4.538	3.180	188.2	0.827
Deuterium oxide ^{17 <u>b</u>}	0.8163	116.6	112.6	6.501

^a Residual sum of squares on lnK

^b In deuterium oxide

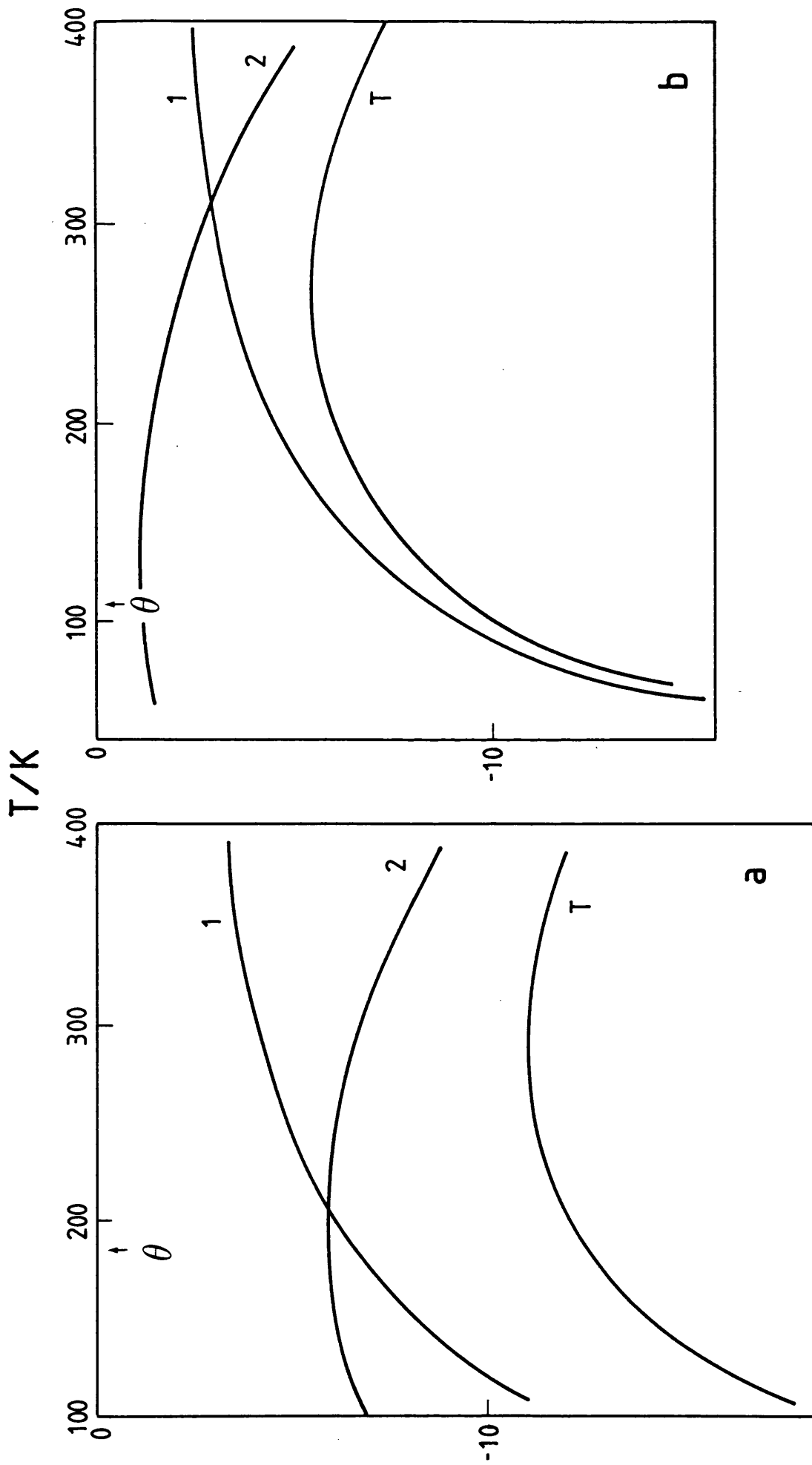


FIGURE (8.1)

Analysis of the dependence on temperature of $\ln K$ for (a) acetic and (b) cyanoacetic acids in water. Curve 1 shows the dependence on temperature of $a_1 T^{-1}$, curve 2 shows that for $a_2 T^{-1} \exp(T/\theta)$, and curve T indicates the dependence of their sum on temperature.

the Gurney equation. However, the derived parameters must be examined in the light of the comments made by Gurney.²

A plot of $-\exp(T/\theta)/T$ passes through a maximum at temperature θ . When this electrical contribution is combined with the non-electrical contribution, the actual maximum in $\ln K$ is shifted away from θ [Figure (8.1)]. For water, θ is 219 K but the maximum in $\ln K$ for acetic acid is found at 298 K. For cyanoacetic acid, the shift is less marked and the maximum is below 273 K. However, the theory² requires that for all acids in water θ should be constant at 219 K (218 K for D_2O). This turns out not to be the case, and in most systems the calculated value is less than the theoretical value. Nonetheless, the disagreement is certainly not marked with the possible exception of fluoroacetic acid. Thus of the 15 carboxylic acids, 9 have values of θ within 50 K of the required temperature.

Perhaps the most dramatic assumption in the Gurney treatment is the independence of temperature for the non-electrical contributions to ΔG^\ominus . Unfortunately, even with the increase in understanding of solute-solvent interactions it is still not clear how this equation should be modified. In this sense this criticism of the Gurney equation is not as harsh as that advanced by King,¹ whose comments were based on a qualitative examination of the data.

In the following section, a different model is taken as the basis for the analysis, which is taken somewhat further than that given in this section, with an examination of the second derivative of K with respect to temperature.

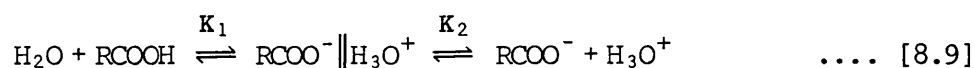
8.3 ANALYSIS USING THE EIGEN MECHANISM

8.3.1 Background

Nearly twenty years ago, Eigen¹⁸ noted that the association of carboxylate anion and hydroxonium ion in water is correctly written in a mathematical sense as a two-stage process, the first stage being the formation of an encounter complex. In an examination of the analysis of the dependence on temperature of acid dissociation constants, it was noted¹⁹ how the Eigen mechanism can lead to an equation relating K and T . The final equation cannot be fitted to the data using a conventional linear least-squares analysis. As in the previous section a non-linear curve-fitting technique must be used.^{3,19} Previously¹⁹ the concern was with the ability of the equation to fit the data. In this section, the analysis is examined in greater depth with particular reference to the interpretation of heat capacity quantities describing the dissociation of carboxylic acids in water. There is a close relationship between this analysis and that described in Chapter 7 in the examination of solvent effects on activation parameters for the solvolysis of *t*-butyl chloride in water.

8.3.2 Analysis

The dissociation of a carboxylic acid in water is represented by equation [8.9] leading to the definition of two equilibrium constants K_1 and K_2 :



Here $\text{RCOO}^- \parallel \text{H}_3\text{O}^+$ represents the encounter complex, whereas RCOO^- and H_3O^+ on the extreme right-hand side of equation [8.9] represent the free ions. It is now assumed that the measured (experimental) dissociation constant characterizes the proportion of solute present as free ions. Hence the

measured dissociation constant, K , is given by:

$$K = K_2/(K_1^{-1} + 1) \quad \dots [8.10]$$

The dependence of K on temperature is determined by the dependence of K_1 and K_2 on temperature. Application of the van't Hoff equation to equation [8.10] yields an expression for the enthalpy quantity ΔH^\ominus :

$$\Delta H^\ominus = \Delta H_2^\ominus + \Delta H_1^\ominus/(1 + K_1) \quad \dots [8.11]$$

Thus at a given temperature T , ΔH^\ominus is the enthalpy term characterizing the dependence of K and T as described by the van't Hoff equation.

Similarly, ΔH_1^\ominus and ΔH_2^\ominus characterize the dependence on T of K_1 and K_2 respectively. Because K_1 is dependent on temperature, ΔH^\ominus is dependent on temperature even if ΔH_1^\ominus and ΔH_2^\ominus are not. At the temperature where K is an extremum (e.g. maximum), ΔH^\ominus is zero. Therefore at this temperature, T_m , the following condition holds:

$$\Delta H_1^\ominus = -\Delta H_2^\ominus (1 + K_1) \quad \dots [8.12]$$

Because by definition K_1 is positive, ΔH_1^\ominus and ΔH_2^\ominus have opposite signs at T_m .

A further differentiation of equation [8.10] with respect to temperature yields an equation for the heat capacity term ΔC_p^\ominus in terms of $\Delta C_{p_1}^\ominus$ and $\Delta C_{p_2}^\ominus$:

$$\Delta C_p^\ominus = \Delta C_{p_2}^\ominus + \frac{\Delta C_{p_1}^\ominus}{(1+K_1)} - \frac{K_1}{(1+K_1)^2} \cdot \frac{(\Delta H_1^\ominus)^2}{RT^2} \quad \dots [8.13]$$

Therefore, at temperature T , the heat capacity characterizing the dependence of ΔH^\ominus on temperature is not simply the sum of $\Delta C_{p_1}^\ominus$ and $\Delta C_{p_2}^\ominus$. If $\Delta C_{p_2}^\ominus$ and $\Delta C_{p_1}^\ominus$ are either zero or small compared with the term on the far right-hand side of equation [8.13], it follows that ΔC_p^\ominus is negative irrespective of the sign of ΔH_1^\ominus . If $\Delta C_{p_1}^\ominus$ is zero, then ΔC_p^\ominus has an extreme value at a temperature T^* given by:

$$T^* = \frac{\Delta H_1^\ominus}{2R} \left[\frac{1-K_1}{1+K_1} \right] \quad \dots [8.14]$$

In order that T^* is a real temperature, if at T^* , $K_1 > 1$ then ΔH_1^\ominus is negative but if $K_1 < 1$ then ΔH_1^\ominus is positive. At temperature T^* , equation [8.13] shows that ΔC_p^\ominus is given by

$$\Delta C_p^\ominus (T^*) = -4RK_1/(1-K_1)^2 \quad \dots [8.15]$$

The assumption that both ΔC_{p1}^\ominus and ΔC_{p2}^\ominus are zero carries with it the requirement that $\ln(K_1)$ and $\ln(K_2)$ are linear functions of $1/T$. Hence the dependence of K on T can be expressed as

$$K = a_1 \exp(-a_2/T) / [1 + a_3 \exp(-a_4/T)] \quad \dots [8.16]$$

where $\Delta H_1^\ominus = -a_4/k \quad \dots [8.17]$

and $\Delta H_2^\ominus = -a_2/k \quad \dots [8.18]$

R is the gas constant. The temperature T_m is given by

$$T_m = a_4 \left\{ \ln \left[\frac{a_3(a_4 - a_2)}{a_2} \right] \right\}^{-1} \quad \dots [8.19]$$

As in Chapter 7, a Gauss-Newton method³ was used to fit the dependence of K on T to equation [8.16]. A program (FORTRAN) was written which incorporated subroutines to calculate the associated Hessian and Jacobian matrices. Various powers of 10 were incorporated into equation [8.16] such that the calculated a -parameters were of the same order of magnitude. The analysis sought those a -parameters which minimized $\sum [K(\text{obs}) - K(\text{calc})]^2$ over n data points.

As before, additional criteria are required in fitting the data to equation [8.16], there being no global minimum. Both a_1 and a_3 must be positive because K_1 and K_2 are positive. Additional criteria follow from examination of equation [8.9]. The process characterized by K_1 involves formation of two ions from a neutral molecule in solution whereas K_2 characterizes their separation, so it is anticipated that $|\Delta H_1^\ominus| > |\Delta H_2^\ominus|$.

The computer program was written to calculate the four a-parameters together with values of ΔH^\ominus and ΔC_p^\ominus according to equations [8.11] and [8.13] respectively. The program is not listed in Appendix 5 because it is essentially that given in Appendix 4, with simple modifications in the calculations subsequent to the generation of the a-parameters.

8.3.3 Results

The outcome of the analysis for four typical systems is summarized in Table (8.2) which includes the measured value of K and calculated values of K_1 and K_2 at 298.15 K together with the calculated values of ΔH^\ominus and ΔC_p^\ominus at this temperature. The temperature T_m at which K is a maximum was calculated using equation [8.19]. The residual sum of squares (r.s.s.) shows that equation [8.16] fits the data satisfactorily. Plots of residuals Δ expressed as a percentage of K against temperature showed satisfactory scatter. For acetic acid all points lie within the range $\Delta = \pm 0.24\%$, for formic acid within $\pm 0.26\%$, for propanoic acid $\pm 0.22\%$ and for cyanoacetic acid within $\pm 0.07\%$. It is emphasised that these residuals follow fitting the data to an equation for K. This contrasts with the methods of analysis based on the Valentiner,⁴ Clark-Glew⁵ or polynomial¹⁹ equations where the fitted quantity is $\ln K$. The importance of this distinction may be illustrated as follows. Suppose, for example, that the experimental value of K is 1.000×10^{-5} and the calculated value is 1.002×10^{-5} , a difference of 0.2%. The corresponding values for $\ln K$ are -11.5129 and -11.5109, a difference of 0.017%. Hence a comparison based on K rather than $\ln K$ provides a stringent test of the ability of an equation to fit the dependence of K on temperature.

As required by the analysis, both $\ln(K_1)$ and $\ln(K_2)$ are linear functions of $1/T$. The calculated dependences of ΔH^\ominus (equation [8.11]) and ΔC_p^\ominus (equation [8.13] with ΔC_{p1}^\ominus and ΔC_{p2}^\ominus equal to zero) on temperature

TABLE (8.2)

Derived parameters (Eigen mechanism) for equilibrium constants
describing acid dissociation constants in water

Acid	Temp. range/K	K (298.15 K)	r.s.s.	K ₁ (298 K)
Formic ⁸	273.15 – 333.15	1.772×10^{-4}	1.12×10^{-12}	1.565
Acetic ⁶	273.15 – 333.15	1.754×10^{-5}	3.22×10^{-12}	1.939
Propanoic ⁹	273.15 – 333.15	1.336×10^{-5}	2.66×10^{-15}	1.084
Cyanoacetic ¹¹	278.15 – 318.15	3.3876×10^{-3}	2.12×10^{-11}	1.043

acid (cont.)	K ₂ (298 K)	T _m /K	$-\Delta H^{\ominus}$ (298 K) /J mol ⁻¹	$-\Delta H_1^{\ominus}$ /kJ mol ⁻¹
Formic	2.902×10^{-4}	297.24	164.1	23.66
Acetic	2.660×10^{-5}	295.57	404.2	22.76
Propanoic	2.570×10^{-5}	292.93	855.2	21.89
Cyanoacetic	6.640×10^{-3}	276.18	3740	22.12

acid (cont.)	ΔH_2^{\ominus} /kJ mol ⁻¹	$-\Delta C_p^{\ominus}$ (298 K) /J mol ⁻¹ K ⁻¹	$-\Delta C_p^{\ominus}$ (max) /J mol ⁻¹ K ⁻¹	at T*	/K
Formic	9.062	180.2	180.2	298.15	
Acetic	7.339	154.0	159	305	
Propanoic	9.645	161.8	167	285	
Cyanoacetic	7.086	165.4	172	285	

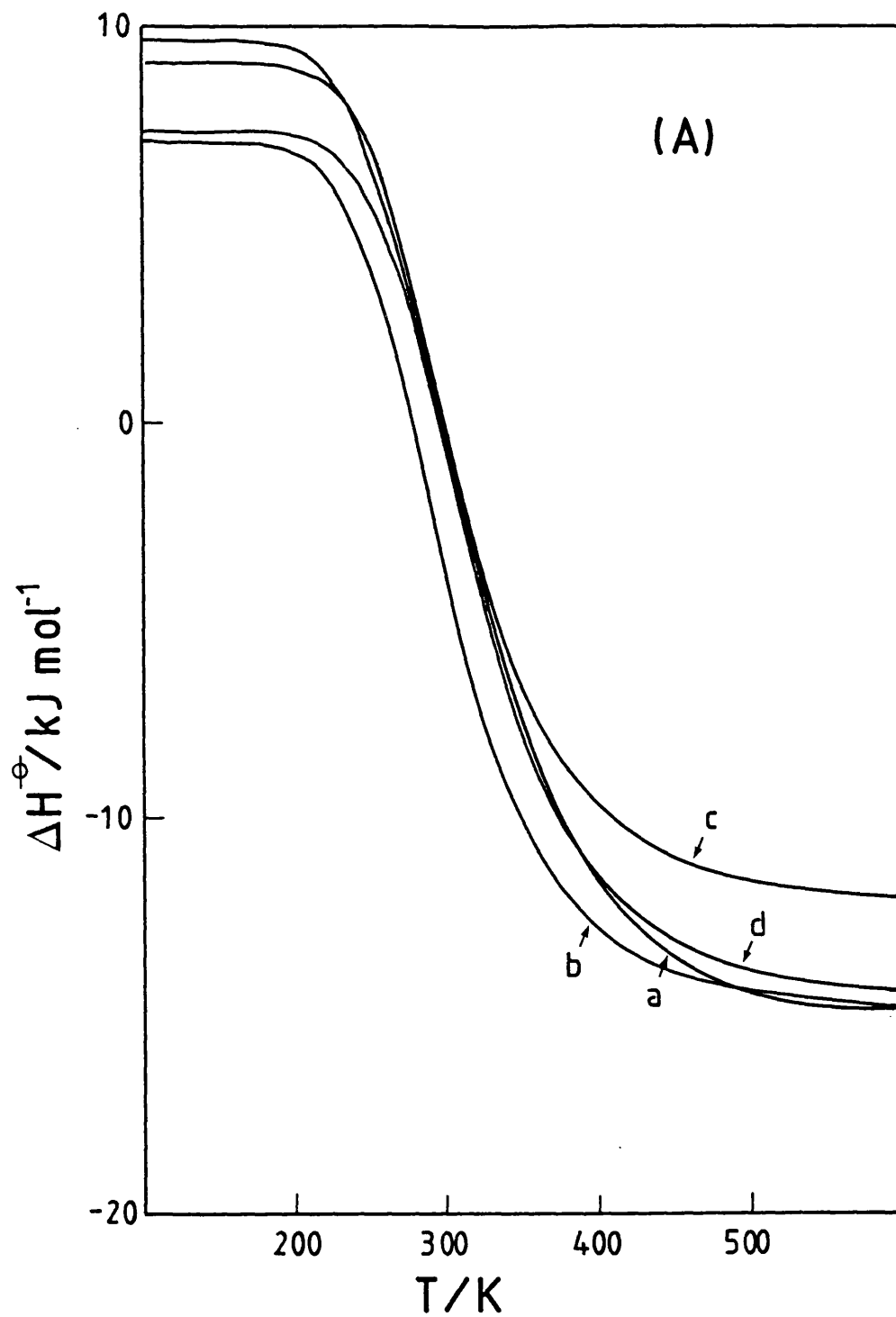
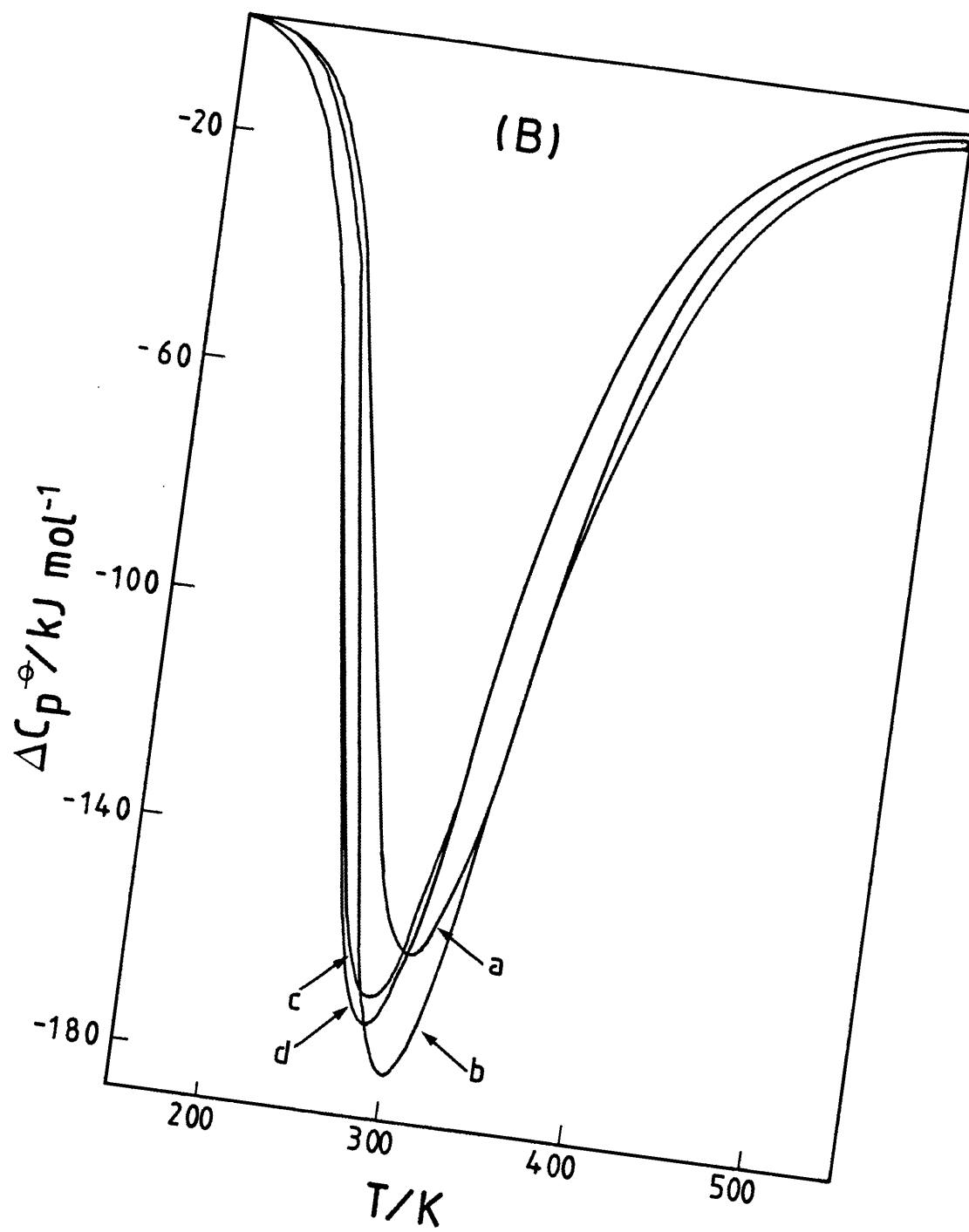


FIGURE (8.2)

Dependence on temperature of the overall enthalpy (A) and heat capacity (B) of dissociation for (a) acetic, (b) formic, (c) propanoic and (d) cyanoacetic acids.



are shown in Figure (8.2). In order to indicate the overall pattern required by the analysis, these values have been calculated over an extended temperature range.

8.3.4 Discussion

For the most part, analysis of the dependence on temperature of acid dissociation constants begins with the assumption that the equilibrium involves two states, dissociated and undissociated acid (model A). Consequently, a maximum in K at some temperature requires that the enthalpy of dissociation is dependent on temperature. Model B, described by equation [8.9], provides an alternative explanation in terms of two equilibrium constants which are dependent on temperature. The data can be fitted to the resulting equation in various ways.

Previously¹⁹ the dependence of K on T was fitted about a measured value, $K(\theta)$, at some reference temperature θ . Although this results in an equation with only 3 unknowns, it is statistically less satisfactory because it assumes that the value $K(\theta)$ is without error, i.e. the true value. The procedure described here is more satisfactory from a statistical point of view. The analysis assumes that neither the undissociated acid nor the ion pair contribute to, for example, the overall electrical conductivity of the solution¹¹ or the e.m.f. of the appropriate electrochemical cell.^{8,6,9} Nonetheless, the strength of the acid in solution is determined by K_1 and K_2 . Thus the overall change in Gibbs free energy for acid dissociation is given by

$$\Delta G^\ominus = -RT \ln K_2 + RT \ln (1 + K_1^{-1}) \quad \dots [8.20]$$

Through a series of acids the change in acid strength measured²⁰ by $\delta_R \Delta G^\ominus$ is determined by the substituent effects on K_1 and K_2 . If this is accepted then relationships between substituent effects in related

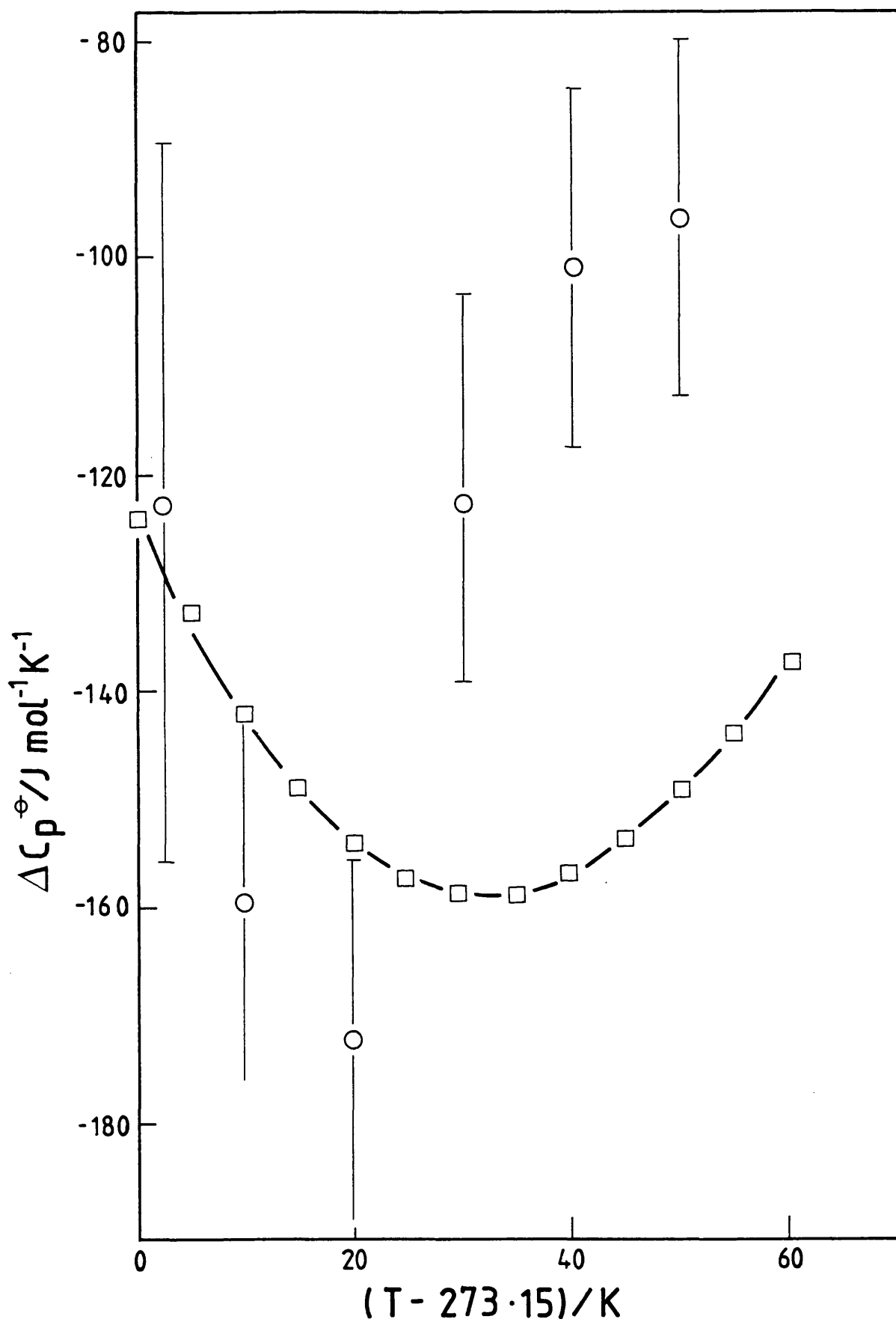


FIGURE (8.3)

Comparison of measured (O) and calculated (□) heat capacities of dissociation for acetic acid in water.

phenomena described by the Hammett equation²¹ are, in these terms, rather complex. Similarly, complexities are introduced in consideration of relationships between ΔH^\ominus and ΔS^\ominus terms under the general heading of iso-equilibria behaviour.²¹

The analysis in terms of model B shows that the overall small value of ΔH^\ominus is a result of two rather marked enthalpy changes associated with the two processes. Indeed the dependence of ΔH^\ominus on temperature generates a sigmoidal curve where ΔH^\ominus is endothermic at low and exothermic at high temperatures [Figure (8.2)]. Consequently, the heat capacity quantity is markedly dependent on temperature being a function of ΔH_1^\ominus , ΔH_2^\ominus and K_1 . The resulting dependence shows a minimum at some temperature which for the acids cited in Table (8.2) is close to the mean of the experimental temperature range. In principle, this dependence for ΔC_p^\ominus obtained from model B should be matched by the dependence of ΔC_p^\ominus obtained from analysis using model A in conjunction with the Clark-Glew⁵ or polynomial¹⁹ equations. However, the latter equations would need at least six terms to identify such a trend in ΔC_p^\ominus . The only direct comparison is with calorimetric data reported by Leung and Grunwald²² who showed that for acetic acid, ΔC_p^\ominus passed through a minimum near 298 K. The two sets of data are compared in Figure (8.3). Although the agreement is not outstanding, the overall trend and magnitudes are sufficiently clear to lend weight to the analysis of the equilibrium data in terms of model B.

If the analysis reported in this section is accepted, the case is made for a detailed examination over an extended temperature range of the heat capacities of acid dissociation, as calculated from thermochemical data.

8.4 SUMMARY

The mathematical approach of this chapter, and Chapter 7, may seem to

be somewhat removed from the type of experiment and discussion in the rest of the thesis. However, most of the chemistry described has its roots in the observation that the intensity of the colour of a solution containing reacting species changes with time, and the mathematics really begins when a differential equation is written down to describe this change in a precise way. The fundamental rôle of thermodynamics is to then relate such properties of a system which can be experimentally measured, e.g. rate and equilibrium constants, solubility, temperature, to the quantities we wish to evaluate, which in this thesis are quantities such as ΔH^\ominus , $\delta_{\text{m}\mu}^\ominus$, ΔG^\ddagger , ΔC_p^\ddagger . As stated in Chapter 1, the use of transition-state theory in the analysis of rate constants means that the principles of reversible thermodynamics can be used to derive activation parameters, ΔX^\ddagger , as well as reaction parameters, ΔX^\ominus .

The Eigen mechanism falls within the realm of two-stage processes, which form the underlying mechanistic basis for most of the systems described throughout the thesis. Indeed, the Eigen mechanism is essentially the reverse of the Eigen-Wilkins mechanism²³ for complex formation. This type of mechanism, involving a pre-equilibrium, was operative in much of the chemistry discussed in previous chapters. Finer differences arise simply from whether the equilibrium is rapidly established with respect to subsequent reactions, or whether the intermediate is present under steady-state conditions.

It may sometimes be possible to demonstrate the presence of the intermediate in kinetic studies, as in Chapter 4 where the rate constant for mercury(II)-catalysed aquation of the $\text{trans-}[\text{Rh}(\text{en})_2\text{Cl}_2]^+$ cation showed a curved dependence on $[\text{Hg}^{2+}]$. This behaviour has been demonstrated²⁴ for Ni^{2+} reacting with trithiocarbonate, CS_3^{2-} , in methanol, where association between the reactants is particularly extensive. Similar

behaviour is also possible for inner-sphere redox reactions, where the precursor or successor complex represents the binuclear intermediate.²⁵

Although an intermediate in the solvolysis of t-butyl chloride has not been detected, the analysis given for this system applies equally well to inorganic examples such as those mentioned above. Once precise kinetic data for such systems are obtained over a wide temperature range, the analysis in Chapter 7 will provide one starting point for the calculation of derived activation parameters.

With regard to solvent effects, detailed quantitative analysis presents a considerable challenge. The ultimate aim is to obtain molecular models for the whole reaction sequence, initial state \rightarrow transition state \rightarrow final state, including changes in both solute and solvent structures. Analysis of the solvent effect along the lines discussed in this thesis contributes to this aim.

APPENDICES

APPENDIX 1

MINICOMPUTER PROGRAM AND OUTPUT

The program is written in Hewlett-Packard BASIC. The key to the arrays set up in lines 5-6 is as follows:

I - control variables I[2] = n^o of cells in run

Q\$ - run details

P - absorbance readings (up to 150 on each cell)

T - time readings

C[I,1] - time of next reading on cell I

C[I,2] - running time for cell I

C[I,3] - time step for cell I

C[I,4] - initial reading on cell I

C[I,5] - final reading on cell I

N[I,1] - n^o of readings on cell I

N[I,2] - n^o of calculations for rate constant for cell I

N[I,3] - n^o of readings before first calculation

N[I,4] - n^o of readings per half-life

N[I,5] - n^o of readings between calculations

N[I,10] - set to 1 when cell I run complete

R[I] - rate constant for cell I

E - calculated absorbances

Y - matrix array for normal equations

X - vector containing Δk , ΔP_0 and ΔP_∞

F - derivatives

G[1] - value of rate constant on entry into 'calc'

G[2] - updated value

Z - workspace

L - error parameters

A - array for parameters to 'solve'

H - loop variable storage

```

0: dsp "hi-have
  a nice day";
  wait 700
1: dsp "your
  friend for toda
  y";wait 700
2: dsp "on-line
  kinetics";wait
  700;flt 5;wtc
  2,2;wtc 2,34
3: dsp "please
  switch JESS to
  HI";wait 1000
4: dsp "mike-
  mod7";wait 700
5: dim I[24],
  Q#[4,15],F[4,
  150],T[4,150],
  C[4,5],N[4,20],
  R[4]
6: dim E[150],
  Y[4,4],X[4],
  F[4],G[2],Z[4],
  L[2],A[4,4],
  H[16]
7: for I=1 to 4;
  for J=1 to 20;
  @+N[I,J];next
  J;next I
8: for J=1 to
  24;@+I[J];next
  J
9: enr "run numb
  er=",I
10: enr "name
  of substrate",
  Q#[1];prt Q#[1]
11: enr "your
  name,please",
  Q#[2]
12: prt "NAME",
  Q#[2];@+I[1];
  enr "solvent",
  Q#[3]
13: enr "tempera
  ture",I[3]
14: wrt 9,"R";
  red 9,Q#[4];
  dsp "time=",
  Q#[4];wait 500;
  prt "date",Q#[4]
15: "mike1":I[1]
  +1+I[1]

```

opening displays

position cell 1 in beam for
start of run

set up arrays

clear arrays

enter run identification details

time and date from internal
clock

```

16: if I[1]>4;
    dsp "no run";
    wait 1000;end
17: enp "number
of cells",I[2]
18: if I[2]<1;
    dsp "try again"
    ;wait 500;eto
    "mike1"
19: if I[2]>4;
    dsp "try again"
    ;wait 500;eto
    "mike1"
20: for K=1 to
4;0+R[K];for
L=1 to 20;0+N[K
,L];next L;next
K
21: 0+I[4]+I[1]
22: dsp "run
details";wait
600;for J=1 to
I[2];ert "for
cell",J;dsp
"cell",J
23: wait 600;
dsp "absorbance
";wait 600
24: enp "est.ini
tial readings";
C[J,4];C[J,4]*
1e4+C[J,4]
25: enp "est.fin
al readings";
C[J,5];C[J,5]*
1e4+C[J,5]
26: enp "guessed
rate constant"
,R[J];if R[J]<1
;eto "les"
27: dsp "too
fast reaction;
reset";wait
600;1e-2+R[J]
28: "les";dsp
"25 readings
per half life";
wait 700
29: enp "if OK,
type 1",I[1]
30: if I[1]=1;
25+N[J,4];eto
"mike3"
31: enp "readings
in half life=
",N[J,4]

```

enter number of cells in run
(error traps if >4 or <1)

clear arrays

set control parameters

enter initial run parameters
for each cell

cell 1

estimated P_0

estimated P_∞

estimated rate constant

if estimate >1.0 reset to 1×10^{-2}

25 readings per half-life

(option to reset)

```

32: "mike3":ln(2
)^(R[IJ]*N[IJ,
41]+C[IJ,3]
33: if I[2]>1;
if C[IJ,3]<10;
10+C[IJ,3]
34: if I[2]=1;
if C[IJ,3]<2;
1+C[IJ,3]
35: dsp "time
step";C[IJ,3];
wait 900
36: end "reading
s before first
calc.=";N[IJ,3]
37: end "reading
s between calc"
;N[IJ,5]
38: if I[2]=1;
sto "mike7"
39: if J>1;sto
"mike5"
40: dsp "are
input values
same for all
cells?";wait
600
41: ent "if yes
type 1";I[1];
if I[1]#1;sto
"mike5"
42: for K=2 to
I[2];C[1,4]+C[K
,4];R[1]+R[K];
N[1,4]+N[K,4]
43: C[1,5]+C[K,
5];N[1,5]+N[K,
5]
44: C[1,3]+C[K,
3];N[1,3]+N[K,
3];next K
45: sto "mike7"
46: "mike5";next
J
47: "mike7":0+I[
1];if I[2]=1;
sto "cale"
48: dsp "please,
set MIKE to M";
wait 1000;sto
"mike6"
49: "cale";dsp
"please switch
MIKE to S";
wait 1000;0+I[1
]

```

calculation of initial time step
for readings

more than 1 cell: at least 10 sec.
1 cell: at least 1 sec.

display time step

enter number of readings prior to
first calculation

number of readings between calcs.

if more than one cell: are
estimates the same for all cells?

if no - enter rest

if yes - rest filled in from
values for cell 1

all cells now set

check setting on MIKE interface
(M or S)

```

50: "mike6":I[1]
+1+I[1]
51: if I[1]>6;
dsp "poor Pract
ice";end
52: ent "ready
to go?-if yes;
type 1";J
53: if J#1;dsp
"try again";
wait 600;I[1]+
1+I[1];eto "mik
e6"
54: wrt 9;"U1=I1
";wrt 9;"U2=I2"
;wrt 9;"U3=I3";
wrt 9;"U4=I4"
55: wrt 9;"A"
56: wrt 9;"U1C";
wrt 9;"U2C";
wrt 9;"U3C";
wrt 9;"U4C";
wrt 9;"F"
57: for K=1 to
I[2];N[K,1]+
1+N[K,1]+J;call
'cell'(K,F[K,
J],T[K,J],C[K,
2])
58: C[K,2]+C[K,
3]+C[K,1];next
K
59: "run":wrt 9;
"U1V";red 9;
C[1,2];if I[2]=
1;jmp 4
60: wrt 9;"U2V";
red 9,C[2,2];
if I[2]=2;jmp 3
61: wrt 9;"U3V";
red 9,C[3,2];
if I[2]=3;jmp 2
62: wrt 9;"U4V";
red 9,C[4,2]
63: dsp "please
do not touch"
64: for K=1 to
I[2];C[K,2]/
1000+C[K,2]
65: if N[K,10]=1
;eto "mike9"
66: if C[K,2]<C[
K,1];eto "mike9"
"

```

READY TO GO? enter 1 - GO
enter #1 - NO
(6 attempts allowed, then run ends)

ports for clocks (peripheral 9)

reset clocks

first reading on each cell

call 'cell': gets and prints
data

calculate time for next reading

clock watching

only watch appropriate number of
clocks for number of cells

clock watching/safety display

LOOP to see which cell to read ...

time elapsed
cell finished - not this one

time for reading not up - not this one

```

67: N[K,1]←I+N[K
,1]←J;call 'cell
'(K,P[K,J],T[K,
J],C[K,2])
68: if N[K,1]<15
0;eto "bert"
69: prt "too
many points on
cell";K
70: prt "alterna
te points dropp
ed";0←S
71: for V=1 to
N[K,1] by 2;1+
S+S;P[K,V]←P[K,
S]
72: T[K,V]←T[K,
S];next V
73: S←N[K,1];S+
2←N[K,3];5←N[K,
5];eto "sask"
74: "bert":if
N[K,3]>J;eto
"mik"
75: "sask":I←H[1
];J←H[2];K←H[3]
;call 'calc'
76: N[K,3]←N[K,
5]+N[K,3];H[1]←
I;H[2]←J;H[3]←K
77: "mik":C[K,
2]←C[K,3]+C[K,
1]
78: "mike9":next
K
79: 0←I[1];for
K=1 to I[2];
I[1]←N[K,10]+I[
1];next K
80: if I[1]<I[2]
;eto "run"
81: for I=1 to
I[2];0←S;prt
"data for cell"
,I;ene "compari
son?-yes enter
1",M
82: if M=1;prt
"summary"
83: for J=1 to
N[I,1];exp(-
R[I]*T[I,J])+B;
C[I,5]←(1-B)+
C[I,4]←B+E[J]

```

if time up, call 'cell': read
the required cell

check number of readings is less
than 150

if >150, alternate points are
dropped

is number of readings required for
calculation attained yet?

if yes: call 'calc'
(store loop variables)

if no: no call

set time for next reading

END LOOP for cell watching

count cells finished

if all finished: data summary
if not: return to line 59 "run"

data summary for cells
start with cell 1

calculated absorbances

$$P_{\infty}(1-e^{-kt}) + P_0 e^{-kt} = P(\text{calc})$$

```

84: E[J]-P[I,
    J]÷H;S+H*H÷S;
    if M#1;ato "sus
    an"
85: prt I,T[I,
    J],P[I,J],E[J],
    H
86: "susan":(C[I
    ,5]-C[I,4])÷
    (C[I,5]-P[I,
    J])÷P[I,J]
87: if P[I,J]>0;
    ato "pip"
88: "swine":prt
    "new values in
    comp";J-1÷N[I,
    1];ato "poke"
89: "pip":ln(P[I
    ,J])÷P[I,J]
90: (C[I,5]-C[I,
    4])÷(C[I,5]-
    E[J])÷E[J]
91: if E[J]>0;
    ato "pep"
92: ato "swine"
93: "pep":ln(E[J
    ])÷E[J];next J
94: "poke":dsp
    "plot the data?
    ";wait 600;0÷I[
    1]
95: enp "if yes-
    enter 1";I[1]
96: if I[1]#1;
    ato "sandy"
97: "fred":if
    I[1]>3;ato "san
    dy"
98: enp "plotter
    ready?if yes
    type 1";M
99: if M#1;I[1]+
    1÷I[1];ato "fre
    d"
100: psc 705;
    pclr;N[I,1]÷V;
    P[I,V]÷Q
101: scl 0,T[I,
    V];0;0
102: T[I,V]÷10÷I
    [1];0÷10÷I[5]
103: fxd 0;pen#
104: xax 0;I[1],
    0;T[I,V];2;pen#

```

choice of listing

calculate data for first-order plot

using observed and calculated
absorbances, generate

$$\ln \left[\frac{(P_{\infty} - P_o)}{(P_{\infty} - P_t)} \right]$$

check for negative argument

choice of plot

no plot - jump on

plotting routine

set up plotter interface

scales: x; 0 to t(max)
y; 0 to kt(max)

```

105: fxd 2;vax
    0,1[5],0,0,2;
    pen#
106: for J=1 to
    N[I,1]
107: plt T[I,J],
    P[I,J],-2;celt
    -.33,-.25
108: lbl "+";
    celt -.67,.25
109: next J
110: pen# ;plt
    T[I,1],E[I];
    line 6
111: for J=2 to
    N[I,1]
112: plt T[I,J],
    E[J],0;next J
113: "sandy":flt
    5;prt "no. of
    points=";N[I,1]
114: prt "rate
    constant=";R[I]
    ;prt "zero valu
    e=";C[I,4]
115: prt "Infini
    ty value=";C[I,
    5];r(8/(N[I,1]-
    3))+8
116: prt "st
    dev on absorban
    ce=";S;next I
117: prt "that
    is all,folks"
118: dsp "run
    complete";wrt
    9,"A";end
119: "calc":dsp
    "cell";K;"point
    s";N[K,1]
120: prt "cell";
    K;prt "range";
    C[K,4],C[K,5]
121: C[K,4]+Z[2]
    ;C[K,5]+Z[3]
122: N[K,2]+1+N[
    K,2];R[K]+G[1];
    1+M;0+L[1];1e30
    +L[2]
123: for J=1 to
    6;prt "cycle ";
    J
124: for Q=1 to
    4;0+X[Q];for
    V=1 to 4;0+Y[Q,
    V]+A[Q,V];next
    V

```

plot all points

straight line drawn $y = k_{\text{calc}} t$

end plotting routine

rate parameter summary

number of data points

calculated rate constant

calculated P_0

calculated P_∞

standard deviation on absorbance

end data summary

RUN COMPLETE - program terminates here

subroutine 'calc': least-squares calculations on required cell

copy and store current

k , P_0 and P_∞

set error parameters

least-squares iteration cycle

clear vectors

```

125: next Q;Q+S
126: for Q=1 to
    N[K,1];exp(-
    G[1]*T[K,Q])+F[
    3]
127: Z[3]*(1-
    F[3])+Z[2]*F[3]
    +H;P[K,Q]-H+E
128: T[K,Q]*(Z[3]
    -Z[2])*F[3]+F[
    1]
129: 1-F[3]+F[2]
    ;S+E*E+S;Y[1,
    4]+E*F[1]+Y[1,
    4]
130: Y[2,4]+E*
    F[2]+Y[2,4];
    Y[3,4]+E*F[3]+Y
    [3,4]
131: Y[1,1]+F[1]
    *F[1]+Y[1,1]
132: Y[2,2]+F[2]
    *F[2]+Y[2,2];
    Y[3,3]+F[3]*
    F[3]+Y[3,3]
133: Y[1,2]+F[1]
    *F[2]+Y[1,2];
    Y[1,3]+F[1]*
    F[3]+Y[1,3]
134: Y[2,3]+F[2]
    *F[3]+Y[2,3];
    next Q
135: Y[1,2]+Y[2,
    1];Y[1,3]+Y[3,
    1];Y[2,3]+Y[3,
    2]
136: for V=1 to
    4;for I=1 to 4;
    Y[V,I]+A[V,I];
    next I;next V
137: S+H[5];I+H[
    11];J+H[12];
    K+H[13];3+N;
    call 'solve'
138: H[11]+I;
    H[12]+J;H[13]+K
139: if f1=4;
    dsp "det=0";
    wait 200;C[K,
    3]+T[K,J]+C[K,
    1];cfa 4;ret
140: X[2]+Z[3]+Z
    [3];X[3]+Z[2]+Z
    [2];G[1]+X[1]+G
    [2]

```

loop through data points,
generating normal equations

calculation of derivative sums
and E_i sums

set up matrix and vector for
normal equations
[equation (2.21)]

normal equations complete

copy Y array to A for 'solve'

store control variables
call 'solve'

error trap (determinant = 0 in
'solve')

calculated updated P_o , P_∞ and k

```

141: if G[2]>0;
    ato "mike10"
142: flt 5;prt
    "neg rate cell"
    ,K;G[2];ret
143: "mike10":H[
    5]→S
144: abs(S-L[2])
    →L[1];S→L[2];
    if JK6;ato "mik
    e20"
145: dsp "not
    enough points
    for analysis";
    wait 500;ret
146: "mike20":G[
    2]→G[1];R[K];
    if L[1]<10;ato
    "sid"
147: next J
148: "sid":Z[2]→
    C[K,4];Z[3]→C[K
    ,5];ln(2)/R[K]→
    F[1]
149: N[K,1]→J;
    2.5*F[1]→F[2];
    T[K,J]-T[K,1]→F
    [1]
150: if F[2]>F[1
    ];ato "harry"
151: flt 5;if
    N[K,2]=1;ato
    "harry"
152: dsp "final
    final final",
    K;wait 500;prt
    "cell finito";
    K;R[K]
153: 1→N[K,10];
    ret
154: "harry":F[2
    ]/N[K,4]→I[24]
155: if 2*I[24]<
    C[K,3];I[24]→C[
    K,3];ato "ox"
156: 2*I[24]→C[K
    ,3]
157: "ox":dsp
    "provisional
    value=";R[K];
    flt 5
158: prt "rate
    constant";R[K];
    ret

```

check k is positive
(if k is negative, exit routine)

error improvement

iteration cycle counter

no minimization: exit routine

reset rate constant

if good fit - jump out

end iteration loop

reset P_0 , P_∞ and new half-life

calculate $2\frac{1}{2}$ half-lives -
is time up?

if yet, print rate constant

if no, jump on

set 'cell finished' flag: exit

reset time step for cell

print provisional rate constant

end subroutine 'calc'

```

159: "cell":fxd
    0;0+I[22]
160: "tony":jmw
    K
161: wtc 2,2;
    wtc 2,34;wrt 9,
    "U1V";eto "buk"
162: wtc 2,1;
    wtc 2,33;wrt 9,
    "U2V";eto "buk"
163: wtc 2,4;
    wtc 2,32;wrt 9,
    "U3V";eto "buk"
164: wtc 2,3;
    wtc 2,35;wrt 9,
    "U4V"
165: "buk":red
    2,P[K,J];red 9,
    T[K,J];T[K,J]/
    1000+T[K,J]+C[K
    ,2]
166: if J=1;eto
    "oke"
167: "tiny":I[22]
    J+1+I[22]
168: if I[22]=3;
    prt "confirmed"
    ;eto "oke"
169: J-1+8;P[K,
    J]-P[K,S]+I[21]
170: 100*abs(I[2
    1])/P[K,S]+I[21
    ]
171: if I[21]>30
    ;prt "check
    30% cell";K;
    eto "tony"
172: "oke":dsp
    "cell",K,T[K,
    J],P[K,J]
173: fxd 0;prt
    "cell",K,J;fxd
    ;prt "time";
    T[K,J]
174: fxd 0;prt
    "readine",P[K,
    J];ret
175: "solve":cfe
    4;0+I
176: if (I+1+I)=
    N;eto +15
177: I-1+K;0+B
178: if (K+1+K)>
    N;eto +3

```

subroutine 'cell': reads
absorbance and time data for
appropriate cell

select cell and clock

read absorbance and time

first reading

subsequent readings

30% absorbance change
check network (eliminate spurious
readings). Reread cell if
necessary.

display data

print data

end subroutine 'cell'

subroutine 'solve'. Solves
normal equations by matrix
inversion.

```

179: if (abs(A[K
, I]) + T) > B; T + B;
K + R
180: sto -2
181: if B = 0; sfa
4; ret
182: I + J; if I = R;
sto +2
183: A[I, J] + T;
A[R, J] + A[I, J];
T + A[R, J]; jmp
(J + 1 + J) > N + 1
184: I + 1 + J; A[I,
I] + B
185: A[I, J] / B + A[
I, J]; jmp (J +
1 + J) > N + 1
186: I + K
187: if (K + 1 + K) >
N; sto -11
188: I + 1 + J
189: A[K, J] - A[K,
I] + A[I, J] + A[K,
J]; jmp (J + 1 + J) >
N + 1
190: sto -3
191: if A[N, N] = 0
; 0 + B; sto -10
192: A[N, N + 1] /
A[N, N] + X[N]; N + I
193: if (I - 1 + I) <
1; ret
194: 0 + S; N + K
195: A[I, K] * X[K] +
S + S; jmp (K - 1 + K)
<= I
196: A[I, N + 1] -
S + X[I]; sto -3
*5130

```

```

run number=
013
fel3
NAME
pad
solvent
aa mech
temperature
25
date
19:07:11:25:35
number of cells
3
for cell
    1.00000e 00
est. initial read
ing
0.25
est. final readin
g
0.05
guessed rate con
stant
5.e-4
if OK, type 1
1
readings before
first calc.=
25
readings between
calc
5
cell          1
time          1
reading      2230
cell          2
time          1
reading      1791
cell          3
time          1
reading      1783
cell          2
time          55.5
reading      2187

cell          1
time          24
reading      1561
cell          2
time          24
reading      1203
cell          3
time          24
reading      1200
cell          1
time          25
reading      1521
cell          1
range        2000
              500
cycle        1
cycle        2
cycle        3
cycle        4
rate constant
              5.27399e-04
cell          2
time          25
reading      1181
cell          2
range        2000
              500
cycle        1
cycle        2
cycle        3
cycle        4
rate constant
              6.13950e-04
cell          3
time          25
reading      1175
cell          3
range        2000
              500
cycle        1
cycle        2
cycle        3
cycle        4
cycle        5
rate constant
              3.55673e-04

```

Important aspects of minicomputer output
for a three-cell kinetic run

```

cell          2
              31
time          2744.4
readings     882
cell          3
              29
time          2940.6
readings     861
cell          1
              31
time          2975.1
readings     1095
cell          2
              32
time          2999.2
readings     871
cell          2
              33
time          3253.9
readings     797
cell          1
              32
time          3289.3
readings     1031
cell          3
              30
time          3330.5
readings     787
cell          3
range        1803
              184
cycle        1
cycle        2
cycle        3
cycle        4
cycle        5
rate constant
              4.97955e-04
cell          3
              31
time          3469.7
readings     799
cell          2
              34
time          3508.7
readings     780
cell          1
              33
time          3603.4
readings     994
cell          3
              32
time          3624.6
readings     786

```

```

cell          2
              35
time          3763.5
readings     759
cell          2
range        1791
              622
cycle        1
cycle        2
cycle        3
cell finito
              2.000000e 00
              5.280007e-04
cell          3
              33
time          3795.5
readings     772
cell          1
              34
time          3917.6
readings     936
cell          3
              34
time          3937.2
readings     754
cell          3
              35
time          4076.5
readings     737
cell          3
range        1812
              553
cycle        1
cycle        2
cycle        3
cycle        4
cell finito
              3.000000e 00
              5.26048e-04
cell          1
              35
time          4231.7
readings     932
cell          1
range        2214
              683
cycle        1
cycle        2
cycle        3
cell finito
              1.000000e 00
              4.38678e-04

```

```

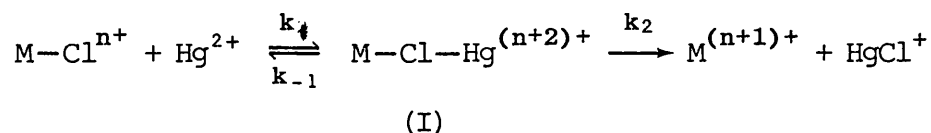
data for cell
              1.000000e 00
comparison?-yes
enter 1
2
if yes-enter 1
1
plotter ready?if
yes type 1
1
no. of points=
              3.500000e 01
rate constant=
              4.38678e-04
zero value=
              2.21359e 03
Infinity value=
              6.76004e 02
st dev on absorbance=
              1.61320e 01
data for cell
              2.000000e 00
comparison?-yes
enter 1
2
if yes-enter 1
2
no. of points=
              3.500000e 01
rate constant=
              5.280007e-04
zero value=
              1.78889e 03
Infinity value=
              6.00624e 02
st dev on absorbance=
              1.50710e 01
data for cell
              3.000000e 00
comparison?-yes
enter 1
2
if yes-enter 1
2
no. of points=
              3.500000e 01
rate constant=
              5.26048e-04
zero value=
              1.81574e 03
Infinity value=
              5.95786e 02
st dev on absorbance=
              1.29255e 01
that is all, folks
s

```

APPENDIX 2

MERCURY (II) -CATALYSED AQUATION

The general mechanism for mercury(II)-catalysed aquation of a chloro-complex is as follows:



The differential equations for this mechanism are:

$$\frac{d}{dt} [\text{I}] = k_1 [\text{M-Cl}^{n+}] [\text{Hg}^{2+}] - k_{-1} [\text{I}] - k_2 [\text{I}] \quad (\text{i})$$

$$-\frac{d}{dt} [\text{M-Cl}^{n+}] = k_1 [\text{M-Cl}^{n+}] [\text{Hg}^{2+}] - k_{-1} [\text{I}] \quad (\text{ii})$$

$$+\frac{d}{dt} [\text{M}^{(n+1)+}] = k_2 [\text{I}] \quad (\text{iii})$$

This set of equations is not soluble in closed form and one has recourse to the steady-state approximation, where it is assumed that [I] is small compared with other species, and that $\frac{d}{dt} [\text{I}] = 0$.

Rearrangement of (i) and substitution into (ii) or (iii) gives

$$+\frac{d}{dt} [\text{M}^{(n+1)+}] = -\frac{d}{dt} [\text{M-Cl}^{n+}] = \frac{k_1 k_2}{k_{-1} + k_2} [\text{M-Cl}^{n+}] [\text{Hg}^{2+}] \quad (\text{iv})$$

Under a large excess of mercury(II), we have

$$k_{\text{obs}} = \frac{k_1 k_2}{k_{-1} + k_2} [\text{Hg}^{2+}] \quad (\text{v})$$

Actually, of course, $d[\text{I}]/dt$ is not zero. If it were, according to (i), $d[\text{M-Cl}^{n+}]/dt$ would also be zero and no reaction would occur. It is a necessary and sufficient[†] condition for the validity of these relations

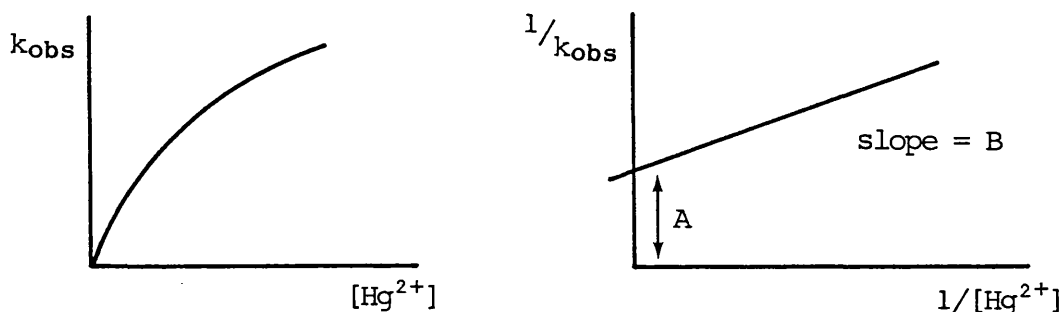
[†] J. H. Espenson, 'Chemical Kinetics and Reaction Mechanisms', McGraw-Hill, New York, 1981, p.72.

that [I] is much less than ($[M-Cl^{n+}] + [M^{(n+1)+}]$), under a large excess of mercury(II).

Three types of behaviour result, depending on the nature of I:

(a) $k_2 \gg k_{-1}$: (I is a transition state), there is no pre-equilibrium formation of I. So $k_{obs} = k_1 [Hg^{2+}]$, and k_1 is the second-order rate constant.

(b) $k_{-1} \gg k_2$: pre-equilibrium conditions for the formation of the intermediate I. $K = k_1/k_{-1}$, and equation (v) reduces to $k_{obs} = k_2 K [Hg^{2+}]$. It can be shown that this expression is really a limiting case when K is small. It describes a linear dependence for k_{obs} on mercury(II) concentration, which is not the case for the rhodium complex in Chapter 4, where the experimentally determined dependence has the following form:



If we write

$$[M]_t = [M-Cl^{n+}] + [I] \quad (vi)$$

Then

$$\begin{aligned} [M-Cl^{n+}] &= [M]_t - [I] \\ &= [M]_t - K[M-Cl^{n+}][Hg^{2+}] \end{aligned}$$

$$\therefore [M-Cl^{n+}] = [M]_t / (1 + K[Hg^{2+}])$$

If [I] is small, $[M-Cl^{n+}] \sim [M]_t$ and the observed first-order rate constant takes the form

$$k_{obs} = \frac{k_2 K [Hg^{2+}]}{1 + K[Hg]} \quad (vii)$$

If $K[\text{Hg}^{2+}] \ll 1$, then equation (vii) reduces to the linear form obtained above. If $K[\text{Hg}^{2+}]$ is significant compared to 1, but $[\text{I}]$ still small, then equation (vii) adequately describes the experimental results. The intermediate is real but transient.

(c) The third case is really an extreme of case (b). If I is a stable, long-lived intermediate, then K is large and equation (vii) reduces to $k_{\text{obs}} = k_2$. The first-order disappearance of I is observed. The rate constant is independent of $[\text{Hg}^{2+}]$.

In case (b), equation (vii) has the following empirical form (see figure):

$$k_{\text{obs}} = \frac{[\text{Hg}^{2+}]}{B + A[\text{Hg}^{2+}]} \quad (\text{viii})$$

This equation was fitted to the experimental data and the empirical constants obtained enabled calculation of K and k_2 .

The data-fitting employed the Newton-Raphson iterative non-linear least squares procedure. In principle, this is the same as the procedure described in Chapter 2 for obtaining rate constants from absorbance data. Thus, applying the condition that

$$\sum_{i=1}^n [k_i^{\text{obs}} - k_i^{\text{calc}}]^2 \rightarrow \text{minimum},$$

the two normal equations are obtained:

$$\sum_{i=1}^n \left(\frac{\partial k}{\partial A}\right)^2 \Delta A + \sum_{i=1}^n \left(\frac{\partial k}{\partial A}\right)\left(\frac{\partial k}{\partial B}\right) \Delta B = \sum_{i=1}^n E_i \left(\frac{\partial k}{\partial A}\right) \quad (\text{ix})$$

$$\sum_{i=1}^n \left(\frac{\partial k}{\partial A}\right)\left(\frac{\partial k}{\partial B}\right) \Delta A + \sum_{i=1}^n \left(\frac{\partial k}{\partial B}\right)^2 \Delta B = \sum_{i=1}^n E_i \left(\frac{\partial k}{\partial B}\right)$$

where n = no. of data points

$$E_i = k_i^{\text{obs}} - k_i^{\text{calc}}$$

The partial derivatives are calculable directly. From equation (viii)

$$\left(\frac{\partial k}{\partial A}\right)_B = - [\text{Hg}^{2+}]^2 (B + A [\text{Hg}^{2+}])^{-2}$$

$$\left(\frac{\partial k}{\partial B}\right)_A = - [\text{Hg}^{2+}] (B + A [\text{Hg}^{2+}])^{-2}$$

Initial estimates for A and B are obtained from the plot of $1/k_{\text{obs}}$ against $1/[\text{Hg}^{2+}]$.

The FORTRAN program written to carry out this procedure is listed here, with a typical output. Initially the main program reads in the data and calculates the slope and intercept of the reciprocal plot. These provide the initial estimates of B and A respectively on entering subroutine NLLS. This subroutine calculates the partial derivatives and the set of k_{calc} values. Equations (ix) are solved by matrix inversion (by calculating the determinant) to yield ΔA and ΔB . The values of A and B are then updated and the process is repeated. The results of each iteration are printed so minimisation could be checked 'visually'. Usually six iterations were sufficient, though in one or two cases up to ten were needed.

Subroutine NLLS returns the least-squares values of A and B with their standard errors to the main program, where the final set of k_{calc} values are generated, and k_{obs} and k_{calc} are listed and plotted. Values of k_2 and K are calculated from A and B, with their appropriate standard errors, and printed.

SOLVENT EFFECTS ON RH-CL HG-CATALYSED AQUATION
 NON-LINEAR LEAST SQUARES ANALYSIS P.0UCS 11.80

10%-MEOH -----

NO. OF DATA POINTS= 8

[HG]	K-OBS
1.0000E-01	2.8034E-04
1.5000E-01	3.8293E-04
2.5000E-01	6.0075E-04
3.5000E-01	7.4990E-04
4.0000E-01	8.0923E-04
5.0000E-01	9.5788E-04
6.0000E-01	1.0169E-03
7.5000E-01	1.1779E-03

INITIAL ESTIMATES: A=4.3422E+02 B=3.1637E+02
 A=INTERCEPT, B=SLOPE OF RECIPROCAL PLOT
 CYCLE... 1 A= 4.34309E+02 B= 3.155780E+02
 CYCLE... 2 A= 4.74382E+02 B= 3.155798E+02
 CYCLE... 3 A= 4.34782E+02 B= 3.155798E+02
 CYCLE... 4 A= 4.34442E+02 B= 3.155798E+02
 CYCLE... 5 A= 4.34282E+02 B= 3.155798E+02
 CYCLE... 6 A= 4.34382E+02 B= 3.155798E+02
 % ERROR A= 3.705712E+00 % ERROR B= 2.540211E+00

[HG]	K-OBS	K-CALC	DIFFERENCE	% DIFF
1.0000E-01	2.8034E-04	2.7854E-04	1.8029E-06	6.4311E-01
1.5000E-01	3.8293E-04	3.9397E-04	-1.1042E-05	-2.8835E+00
2.5000E-01	6.0075E-04	5.8938E-04	1.1373E-05	1.8932E+00
3.5000E-01	7.4990E-04	7.4848E-04	1.4220E-05	1.8953E-01
4.0000E-01	8.0923E-04	8.1744E-04	-8.2058E-06	-1.0140E+00
5.0000E-01	9.5788E-04	9.3848E-04	1.9396E-05	2.0248E+00
6.0000E-01	1.0169E-03	1.0413E-03	-2.4382E-05	-2.3977E+00
7.5000E-01	1.1779E-03	1.1694E-03	8.5299E-06	7.2416E-01

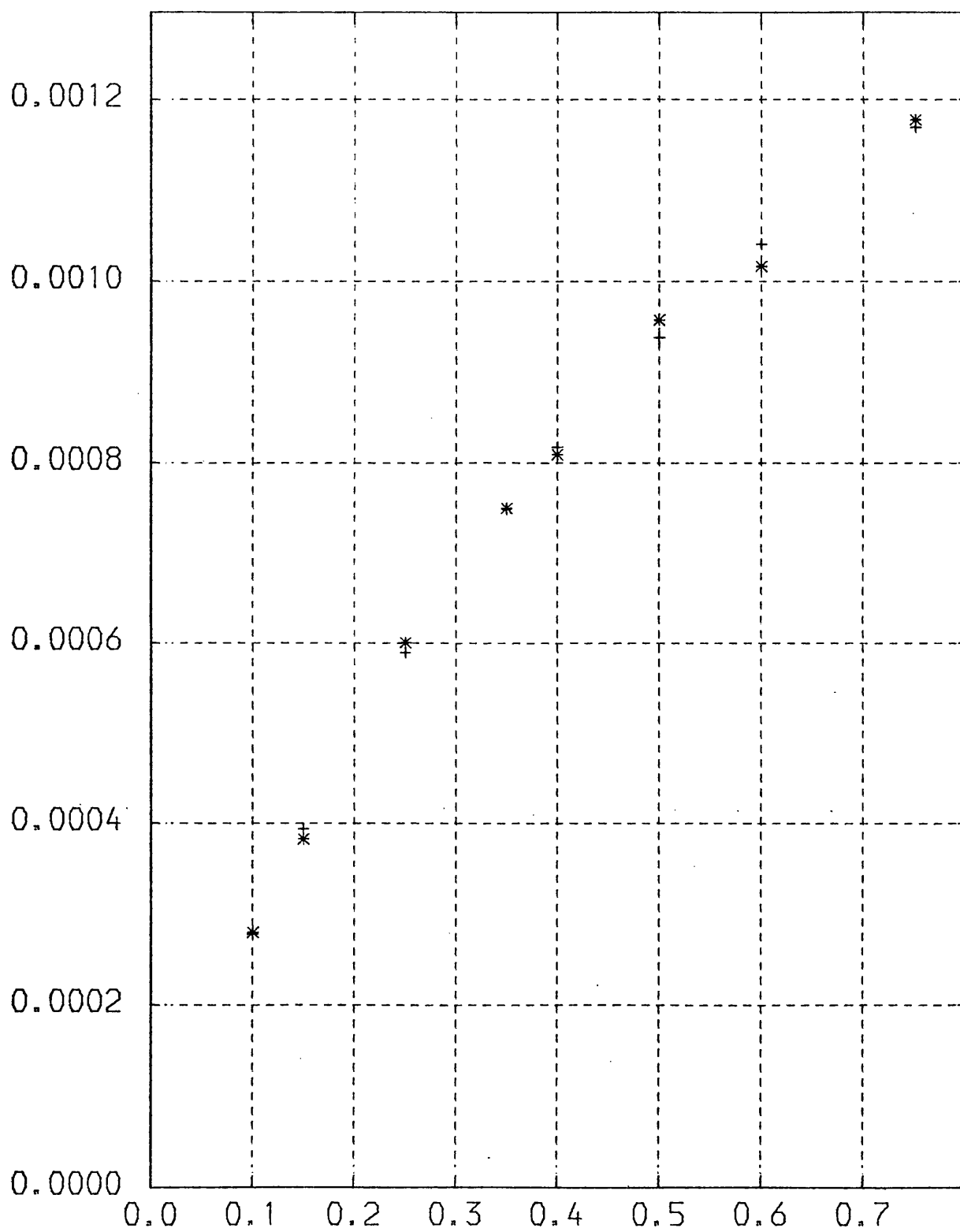
RESIDUAL SUM OF SQUARES= 1.367311E-09

K-OBS-LIMITING= 2.3021E-03 K-EQ=A/B= 1.3765E+00 % ERROR= 3.53438

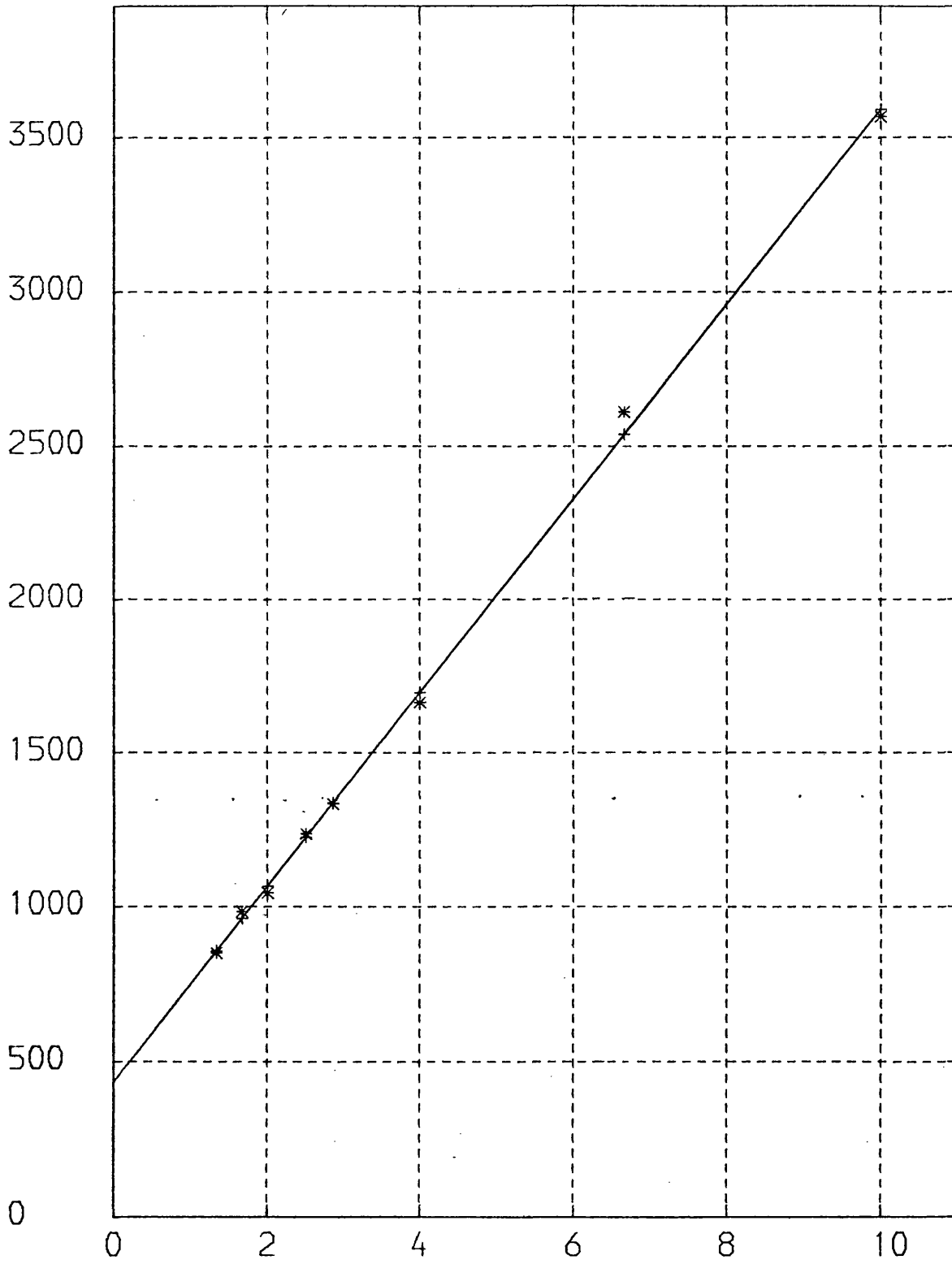
ANALYSIS COMPLETE
 PLOT COMPLETE

K VS. [HG] * = OBS, + = CALC

10%-MEOH



1/K VS 1/[HG] *=OBS, +=CALC 10%-MEOH



```

PROGRAM MERCURY(INPUT,OUTPUT,DATA,TAPE1=DATA,TAPE2=OUTPUT)
COMMON/EINS/ X(20),Y(20),YC(20),YCALC(20),N,A,B,Z1,PEA,PEB
COMMON/ZWEI/RX(20),FKO(20),RYC(20),TITLE
COMMON/MAIN/ DIFF(20),PODIFF(20),P(5)
REAL KLIM

```

```

*****
* THIS PROGRAM FITS DATA FOR KINETIC MECHANISM
* WITH A PRE-EQUILIBRIUM FOLLOWED BY A K2
* DISSOCIATIVE STEP...
* 1/K-OBS VS 1/X IS A STRAIGHT LINE, THEREFORE
* IF 1/K=(B/X)+A, THEN K=X/(B+XA)
* K-LIM=1/A    K-EG=A/B
* THE CURVE IS FITTED USING NON-LINEAR LEAST-SQUARES
* (FIRST-ORDER). A RECIPROCAL PLOT IS ALSO GENERATED.
* WRITTEN BY P.P.DUCE NOV.1980
*****

```

```

10 WRITE(2,10)
   FORMAT(1H1,2X,*SOLVENT EFFECTS ON RH-CL HG-CATALYSED AQUATION*)
11 WRITE(2,11)
   FORMAT(1H ,2X,*NON-LINEAR LEAST SQUARES ANALYSIS  P.DUCE 11.80*)

```

```

   READ(1,25) NP
   READ(1,30) TITLE
   READ(1,20) N
20  FORMAT(I3)
30  FORMAT(A10)
25  FORMAT(I3)

```

```

   N1=N
   Z1=0.0
   DO 2 K=1,N1
     Z1=Z1+1.0
     READ(1,50) X(K),Y(K)
50  FORMAT(F10.0,1PE10.4)
     RKO(K)=1.0/Y(K)
     RX(K)=1.0/X(K)

```

```

2  CONTINUE
   WRITE(2,60) TITLE
60  FORMAT(1HG,10X,A10,75(1H-))
   WRITE(2,65) N
65  FORMAT(1H0,10X,*NO. OF DATA POINTS=*,I3)
   WRITE(2,70)
70  FORMAT(1H0,10X,*[HG]*,10X,*K-OBS*)
   DO 90 J=1,N1
     WRITE(2,80) X(J),Y(J)
80  FORMAT(1HC,7X,1PE10.4,5X,1PE10.4)
90  CONTINUE

```

```

*****
* INITIAL GUESSES OF PARAMETERS FROM
* STRAIGHT LINE RECIPROCAL PLOT
*****

```

```

14 DO 14 M=1,5
   P(M)=0.0
   CONTINUE
   DO 3 K=1,N1
     X1=RX(K)
     Y1=RKO(K)
     P(1)=P(1)+X1
     P(2)=P(2)+Y1
     P(3)=P(3)+X1*Y1
     P(4)=P(4)+X1*X1
3  CONTINUE
   EE=1.0/(Z1*P(4)-P(1)*P(1))
   SLOPE=(Z1*P(3)-P(1)*P(2))*EE
   CEPT=(P(4)*P(2)-P(1)*P(3))*EE
   A=CEPT
   B=SLOPE

```

```

100 WRITE(2,100) A,B
   FORMAT(1H0,10X,*INITIAL ESTIMATES:A=*,1PE10.4,5X,*B=*,
   $1PE10.4)
101 WRITE(2,101)
   FORMAT(1H ,10X,*A=INTERCEPT,B=SLOPE OF RECIPROCAL PLOT*)

```

```

CALL NLLS
*****
* CALCULATE VALUES USING FINAL A,B
*****

```

```

SUMDIFF=0.0
DO 15 J=1,N1
   YCALC(J)=X(J)/(B+A*X(J))
   RYC(J)=1.0/YCALC(J)
   DIFF(J)=Y(J)-YCALC(J)
   PDIFF(J)=DIFF(J)*100.0/Y(J)
   SUMDIFF=SUMDIFF+PDIFF(J)
15  CONTINUE
   WRITE(2,150)
150  FORMAT(1H0,10X,*[HG]*,10X,*K-OBS*,10X,*K-CALC*,11X,
   $*DIFFERENCE*,10X,*% DIFF*)

```

```

DO 29 M=1,N1
WRITE(2,160) X(M),Y(M),YCALC(M),DIFF(M),PODIFF(M)
160 FORMAT(1H0,7X,1PE10.4,5X,1PE10.4,5X,1PE10.4,6X,
31PE12.4,7X,1PE12.4)
29 CONTINUE
WRITE(2,165) SUMDIFF
165 FORMAT(1H0,10X,*CHECK-SUM OF % DIFFERENCES=*,F10.5)
KLIM=1.0/A
EQ=A/B
PEEQ=SQRT(PEA*2+PEB*2)
***** CHECK EQ !!!!!!!!!!!!!!!!!!!!!!!!!!!!!!!!!!!!!!!!!*****
WRITE(2,167) KLIM,EQ,PEEQ
167 FORMAT(1H0,10X,*K-OBS-LIMITING=*,1PE12.4,2X,*K-EQ=A/B=*,
31PE12.4,2X,*% ERROR=*,3PF10.5)
WRITE(2,170)
170 FORMAT(1H0,10X,*ANALYSIS COMPLETE*)
CALL PLOT
WRITE(2,180)
WRITE(2,181)
180 FORMAT(1H ,10X,*PLOT COMPLETE*)
181 FORMAT(1H0,10X,85(1H-))
STOP
END
SUBROUTINE NLLS
COMMON/EINS/ X(20),Y(20),YC(20),YCALC(20),N,A,B,Z1,PEA,PEB
DIMENSION SUM(6),S1(4),Z(2),C(4)
*****
* Y=X/(B+AX) SINCE 1/Y=B/X +A
* THIS SUBROUTINE FITS THE CURVE
*****
ICONT=0
200 CONTINUE
DO 210 II=1,6
SUM(II)=0.0
210 CONTINUE
ICONT=ICONT+1
DO 300 I=1,N
DYBYDA=-X(I)**2/(B+A*X(I))**2
DYBYDB=-X(I)/(B+A*X(I))**2
SUM(1)=SUM(1)+DYBYDA**2
SUM(2)=SUM(2)+DYBYDA*DYBYDB
SUM(3)=SUM(3)+DYBYDB**2
YC(I)=X(I)/(B+A*X(I))
E=Y(I)-YC(I)
SUM(4)=SUM(4)+E*DYBYDA
SUM(5)=SUM(5)+E*DYBYDB
SUM(6)=SUM(6)+E*E
300 CONTINUE
**** SET UP SUM MATRICES ****
S1(1)=SUM(1)
S1(2)=SUM(2)
S1(3)=SUM(2)
S1(4)=SUM(3)
Z(1)=SUM(4)
Z(2)=SUM(5)
*** INVERT S1 MATRIX(4X4) **
DETS1=S1(1)*S1(4)-S1(3)*S1(2)
C(1)=S1(4)/DETS1
C(2)=-S1(2)/DETS1
C(3)=-S1(3)/DETS1
C(4)=S1(1)/DETS1
*** CALCULATE DELTA-A,DELTA-B ***
DELTA A=C(1)*Z(1)+C(2)*Z(2)
DELTA B=C(3)*Z(1)+C(4)*Z(2)
A=A+DELTA A
B=B+DELTA B
WRITE(2,310) ICONT,A,B
310 FORMAT(1H ,10X,*CYCLE...*,I2,5X,*A=*,1PE15.6,2X,*B=*,1PE15.6)
IF(ICONT.EQ.6) GOTO 400
GOTO 200
400 CONTINUE
SEA=SQRT(C(1)*SUM(6)/Z1-2.0)
SEB=SQRT(C(4)*SUM(6)/Z1-2.0)
PEA=SEA*100.0/A
PEB=SEB*100.0/B
WRITE(2,320) PEA,PEB
320 FORMAT(1H ,10X,*% ERROR A=*,1PE15.6,2X,*% ERROR B=*,1PE15.6)
END
SUBROUTINE PLOT
COMMON/EINS/X(20),Y(20),YC(20),YCALC(20),N,A,B,Z1,PEA,PEB
COMMON/ZWEI/RX(20),RKO(20),RYC(20),TITLE
CALL PAPER(1)
N2=N
XMIN=0.0
XMAX=0.8

```

```

YMIN=0.0
YMAX=Y(N2)+Y(N2)/10.0
CALL MAP(XMIN,XMAX,YMIN,YMAX)
CALL CTRMAG(15)
NOCHAR=45
DO 1 I=1,N2
1 CONTINUE
CALL PLOTNC(X(I),Y(I),45)
CALL REDPEN
NOCHAR=43
DO 11 JJ=1,N2
11 CONTINUE
CALL PLOTNC(X(JJ),YCALC(JJ),43)
CALL BLKPEN
CALL CTRMAG(20)
CALL BROKEN(4,4,4,4)
CALL GRATIC
CALL FULL
CALL PLACE(1,1)
CALL TYPECS("K VS. [HG] *=OBS,+=CALC ",28)
CALL TYPECS(TITLE,10)
CALL BORDER
CALL SCALES
CALL FRAME
XMAX=RX(1)+1.0
YMAX=RKO(1)+RKO(1)/10.0
C ***** SMALLEST K LARGEST RECIPROCAL *****
CALL MAP(XMIN,XMAX,YMIN,YMAX)
CALL CTRMAG(15)
NOCHAR=45
DO 2 I=1,N2
2 CONTINUE
CALL PLOTNC(RX(I),RKO(I),45)
CALL REDPEN
NOCHAR=43
DO 21 KK=1,N2
21 CONTINUE
CALL PLOTNC(RX(KK),RYC(KK),43)
CALL POSITN(0.0,A)
DO 22 I=1,N2
22 CONTINUE
CALL JOIN(RX(I),RYC(I))
CALL BLKPEN
CALL CTRMAG(20)
CALL BROKEN(4,4,4,4)
CALL GRATIC
CALL FULL
CALL PLACE(1,1)
CALL TYPECS("1/K VS 1/[HG] *=OBS,+=CALC ",28)
CALL TYPECS(TITLE,10)
CALL BORDER
CALL SCALES
CALL FRAME
CALL GREND
RETURN
END

```

APPENDIX 3

SPECTROPHOTOMETRIC TITRATION

We have

$$A = [(K_c^{-1} + c_o + y) - \{(K_c^{-1} + c_o + y)^2 - 4 c_o y\}^{1/2}] \frac{(c_o \epsilon_{NuL} - A_o) + A_o}{2 c_o} \quad (i)$$

If the molarity of the stock nucleophile solution is m and n microlitres have been added to the cell, then

$$y = (n \cdot 10^{-6} \cdot m) / \text{cellvol}_n \quad \text{mol dm}^{-3}$$

$$c_o^n = c_o \cdot \text{cellvol}_o / \text{cellvol}_n \quad \text{mol dm}^{-3}$$

$$\text{where } \text{cellvol}_n = (10^{-3} \cdot \text{cellvol}_o + 10^{-6} n) \text{ dm}^3$$

Equation (i) contains two unknowns, K_c and ϵ_{NuL} . These may be obtained using an iterative procedure analogous to that described in Appendix 2.

The two normal equations are

$$\sum_{i=1}^N \left(\frac{\partial A}{\partial K} \right)^2 \Delta K + \sum_{i=1}^N \left(\frac{\partial A}{\partial \epsilon} \right) \left(\frac{\partial A}{\partial K} \right) \Delta \epsilon = \sum_{i=1}^N E_i \left(\frac{\partial A}{\partial K} \right) \quad (ii)$$

$$\sum_{i=1}^N \left(\frac{\partial A}{\partial K} \right) \left(\frac{\partial A}{\partial \epsilon} \right) \Delta K + \sum_{i=1}^N \left(\frac{\partial A}{\partial \epsilon} \right)^2 \Delta \epsilon = \sum_{i=1}^N E_i \left(\frac{\partial A}{\partial \epsilon} \right)$$

where $E_i = A_{\text{obs}} - A_{\text{calc}}$, $K = K_c$ and $\epsilon = \epsilon_{NuL}$.

The derivatives are calculated using (i):

$$\left(\frac{\partial A}{\partial K} \right) = -\frac{1}{K_c^2} \frac{(c_o \epsilon_{NuL} - A_o)}{2 c_o} \left[1 - \frac{(y + c_o + K_c^{-1})}{\{(y + c_o + K_c^{-1})^2 - 4 c_o y\}^{1/2}} \right]$$

$$\left(\frac{\partial A}{\partial \epsilon} \right) = \frac{1}{2} [(y + c_o + K_c^{-1}) - \{(y + c_o + K_c^{-1})^2 - 4 c_o y\}^{1/2}]$$

Initial estimates for the values of K_c and ϵ_{NuL} are obtained by:

- (a) estimating A_∞ (ignoring the dilution effect) from a plot of $1/A$ against volume added for the last few data points.
- (b) using the value of ϵ_{NuL} calculated from A_∞ and c_o , with a data point approximately mid-way in the set, to calculate a value for K_c .

In some cases, these estimates were poor and drove the analysis away from minimization, often with disastrous results. In this event, guessed estimates could be overwritten into the program before compilation.

The main program reads in the data, generates the initial estimates and produces a table and a plot of the final results.

Subroutine `KCALC` calculates a value for K_c given a guessed ϵ_{NuL} . Subroutine `NLLS` generates and solves the normal equations. The assignment of variables is best seen in the data-reading sequence. The program is listed with a typical output.

A modified version of the program was written to analyse data for absorbance against initial nucleophile concentration. In this case, the cell volume and associated dilution factors were removed, these usually being inherent in the data themselves.

SPECTROPHOTOMETRIC TITRATION -----
 CALCULATION OF EQUILIBRIUM CONSTANT P.DUCE (2)
 NON-LINEAR LEAST SQUARES...

SYSTEM: 5NO2-PHEN + HYDROXIDE 20% MEQH
 VOL USED IN CELL= 3.20 CC
 STARTING MOLARITY OF SUBSTRATE= 1.35000E-05
 MOLARITY OF STOCK NUCLEOPHILE= 11.2000
 INITIAL OD-UNREACTIONED SUBSTRATE== .3950
 NO. OF ADDITIONS= 10

	VOL NUCL. ADDED	IN-CELL MOLARITY	INITIAL LIGAND CONC	ABSORBANCE
1	10.0000	3.489097E-02	1.34579E-05	.4320
2	20.0000	6.956522E-02	1.3416E-05	.4670
3	30.0000	1.0439848E-01	1.33716E-05	.4930
4	40.0000	1.380716E-01	1.33333E-05	.5200
5	50.0000	1.720777E-01	1.32933E-05	.5430
6	60.0000	2.061759E-01	1.32533E-05	.5680
7	70.0000	2.397594E-01	1.32133E-05	.5850
8	80.0000	2.731707E-01	1.31733E-05	.6080
9	90.0000	3.062839E-01	1.31333E-05	.6200
10	100.0000	3.392939E-01	1.30933E-05	.6380

 ESTIMATE OD-INFINITY FROM OD VS 1/VOL
 USE LAST 4 DATA POINTS: EXTRAPOLATE TO ZERO

EXTRAPOLATED INFINITY= .7560
 ESTIMATED EXTINCTION COEFF. OF PRODUCT= 5.774840E+04

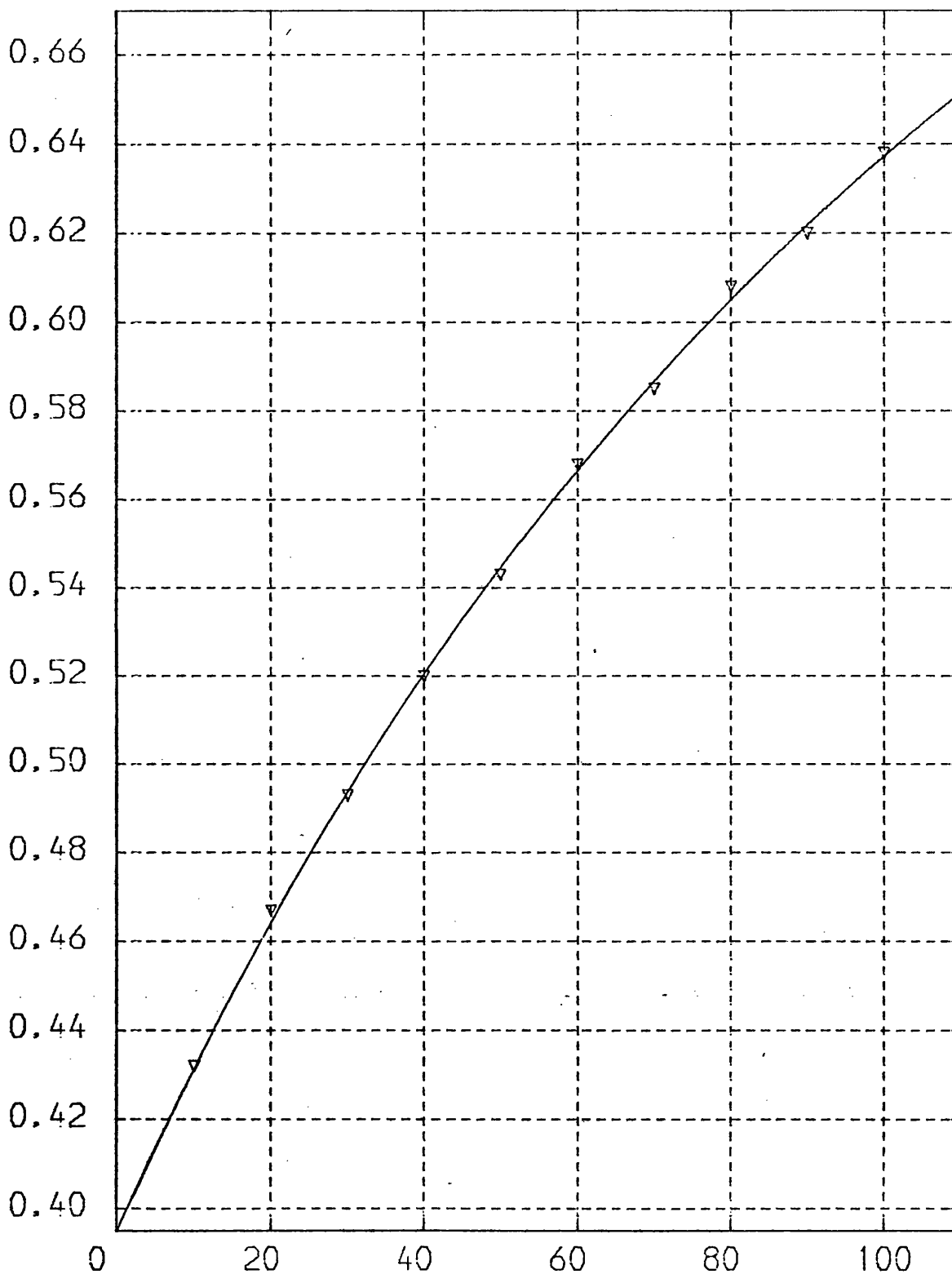
ESTIMATED EQUILM. CONSTANT= 1.000000E+00
 CYCLE... 1 K= 1.95530E+00 -NUL= 8.353237E+04
 CYCLE... 2 K= 1.407538E+00 -NUL= 8.474568E+04
 CYCLE... 3 K= 1.406407E+00 -NUL= 8.738594E+04
 CYCLE... 4 K= 1.407550E+00 -NUL= 8.743131E+04
 CYCLE... 5 K= 1.407550E+00 -NUL= 8.743163E+04
 CYCLE... 6 K= 1.407550E+00 -NUL= 8.743163E+04
 CYCLE... 7 K= 1.407550E+00 -NUL= 8.743163E+04
 CYCLE... 8 K= 1.407550E+00 -NUL= 8.743163E+04
 CYCLE... 9 K= 1.407550E+00 -NUL= 8.743163E+04
 CYCLE... 10 K= 1.407550E+00 -NUL= 8.743163E+04
 CYCLE... 11 K= 1.407550E+00 -NUL= 8.743163E+04
 CYCLE... 12 K= 1.407550E+00 -NUL= 8.743163E+04
 % ERROR K= 3.672729E+00 % ERROR E= 1.891242E+00

EQUILIBRIUM CONSTANT= 1.407538E+00
 EXTINCTION COEFF. OF PRODUCT= 8.743163E+04 (AT THIS WAVELENGTH)
 E-HU: L/E-L= 2.9882

VOL NUCL ADDED	OBS-00	CALC-00
10.0000	.4320	.4316
20.0000	.4670	.4644
30.0000	.4930	.4939
40.0000	.5200	.5206
50.0000	.5430	.5447
60.0000	.5680	.5667
70.0000	.5850	.5868
80.0000	.6080	.6051
90.0000	.6200	.6219
100.0000	.6380	.6373

ST.ERROR ON OBS= 1.884527E-03
 PLOT BEGINS
 PLOT COMPLETE!
 THAT IS ALL, FOLKS

5NO₂-PHEN + HYDROXIDE 20% MEOH
O.D. VS VOL ADDED (MICRO-LITRES)
K= 0.141E01




```

WRITE(2,64)
WRITE(2,65)
WRITE(2,66)
64 FORMAT(1H0,10X,75(1H-))
65 FORMAT(1H0,10X,"ESTIMATE OD-INFINITY FROM OD VS 1/VOL")
*****
* USE LAST 4 DATA POINTS...GENERATE NEW ARRAYS
* CONTAINING OD AND CORRESPONDING 1/VOL...THEN
* DO LEAST SQUARES STRAIGHT LINE:INTERCEPT IS
* THE EXTRAPOLATED OD-INFINITY VALUE
*****
66 FORMAT(1H ,10X,"USE LAST 4 DATA POINTS:EXTRAPOLATE TO ZE
DO 14 I=1,5
P(I)=0.0
14 CONTINUE
IRPLOT=0
N1=N-3
ZZ=4.0
DO 80 II=N1,N
IRPLOT=IRPLOT+1
RVOL(IRPLOT)=1.0/VOLNU(II)
ODR(IRPLOT)=OD(II)
X=RVOL(IRPLOT)
Y=ODR(IRPLOT)
P(1)=P(1)+X
P(2)=P(2)+Y
P(3)=P(3)+X*Y
P(4)=P(4)+X*X
80 CONTINUE
EE=1.0/(ZZ*P(4)-P(1)*P(1))
ODINF=(P(4)*P(2)-P(1)*P(3))*EE
SLOPE=(ZZ*P(3)-P(1)*P(2))*EE
ENUL=ODINF/CLC(N)
WRITE(2,85) ODINF
85 FORMAT(1H0,10X,"EXTRAPOLATED INFINITY=",F10.4)
WRITE(2,87)ENUL
87 FORMAT(1H0,10X,"ESTIMATED EXTINCTION COEFF. OF PRODUCT="
$1PE15.6)
M1=N-2
CALL KCALC
EK=CONST
EK=1.0
C *** SET GUESSED K HERE IF AUTOMATIC GUESS DOESN'T WORK
WRITE(2,90) EK
90 FORMAT(1H0,10X,"ESTIMATED EQUILM. CONSTANT=",1PE15.6)
CALL NLLS
EL=ODO/CL
PPD=ENUL/EL
WRITE(2,160) PPD
160 FORMAT(1H0,10X,"E-NU:L/E-L=",F10.4)
WRITE(2,290)
290 FORMAT(1H0,10X,"VOL NUCL ADDED",7X,"OBS-OD",10X,
$"CALC-OD")
SUMDEV=0.0
DO 300 K=1,N
C1=VOLNU(K)
YY=ODCALC(C1)
ODC(K)=YY
WRITE(2,310) VOLNU(K),OD(K),ODC(K)
310 FORMAT(1H ,10X,F10.4,6X,F10.4,6X,F10.4)
DIFFOD=OD(K)-ODC(K)
SUMDEV=SUMDEV+DIFFOD**2
300 CONTINUE
STEOBS=SQRT(SUMDEV/(Z1-2.0))
WRITE(2,330) STEOBS
330 FORMAT(1H0,10X,"ST.ERROR ON OBS=",1PE15.6)
WRITE(2,350)
350 FORMAT(1H0,10X,"PLOT BEGINS")
*****
* PLOT : OD-OBS WITH CALCULATED
* CURVE BASED ON BEST FIT K AND
* INFINITY VALUES
* SMALLER FRAME/ALL BLACK PLOT
*****
CALL PAPER(1)
XMIN=0.0
XMAX=VOLNU(N)+VOLNU(N)/10.0
YMIN=ODO
YMAX=OD(N)+OD(N)/20.0
CALL PSPACE(0.25,0.70,0.15,C.8)
CALL MAP(XMIN,XMAX,YMIN,YMAX)
CALL CTRMAG(10)
CALL GRAPHF(ODCALC)
CALL CTRSET(4)
DO 365 LL=1,N

```

```

365 CALL PLOTNC(VOLNU(LL),OD(LL),51)
CONTINUE
CALL CTRSET(1)
CALL BROKEN(4,4,4,4)
CALL GRATIC
CALL FULL
CALL BORDER
CALL SCALES
CALL ITALIC(1)
CALL PLACE(30,11)
CALL TYPECS("O.D. VS VOL ADDED(MICRO-LITRES)",31)
CALL PLACE(30,12)
CALL TYPECS("K=",3)
CALL TYPENE(EK,3)
CALL PLACE(30,10)
DO 370 J=1,5
CALL TYPECS(TITLE(J),10)
370 CONTINUE
CALL BLKPEN
CALL ITALIC(0)
CALL GREND
CALL FRAME
WRITE(2,400)
400 FORMAT(1H0,10X,"PLOT COMPLETE!")
WRITE(2,260)
260 FORMAT(1H0,10X,"THAT IS ALL,FOLKS")
STOP
END
SUBROUTINE NLLS
COMMON/ONE/N,CELLVOL,CL,CNU,VCLNU(100),CONCNU(100),OD(100),
$ODINF,TITLE(5),EK,CONST,Z1,ODC,ODC(100),CLC(100),
$ENUL,PEK,PEE,M1
DIMENSION SUM(6),S1(4),Z(2),C(4)
ICONT=0
600 CONTINUE
DO 610 II=1,6
SUM(II)=0.0
610 CONTINUE
ICONT=ICONT+1
DO 640 I=1,N
RK=1.0/EK
V=CONCNU(I)
CL1=CLC(I)
B=(V+CL1+RK)
B1=SQRT(B*B-4.0*CL1*V)
ODINF=CLC(I)*ENUL
A=(ODINF-ODC)/(2.0*CL1)
DYBYDK=-1.0*RK*RK*A*(1.0-(B/B1))
DYBYDE=(B-B1)/2.0
SUM(1)=SUM(1)+DYBYDK**2
SUM(2)=SUM(2)+DYBYDK*DYBYDE
SUM(3)=SUM(3)+DYBYDE**2
VV=VOLNU(I)
E=OD(I)-ODCALC(VV)
SUM(4)=SUM(4)+E*DYBYDK
SUM(5)=SUM(5)+E*DYBYDE
SUM(6)=SUM(6)+E*E
640 CONTINUE
C **** SET UP SUM MATRICES ***
S1(1)=SUM(1)
S1(2)=SUM(2)
S1(3)=SUM(2)
S1(4)=SUM(3)
Z(1)=SUM(4)
Z(2)=SUM(5)
C ** INVERT S1 MATRIX(2X2) **
DETS1=S1(1)*S1(4)-S1(3)*S1(2)
C(1)=S1(4)/DETS1
C(2)=-S1(2)/DETS1
C(3)=-S1(3)/DETS1
C(4)=S1(1)/DETS1
C *** CALCULATE DELTA-K,DELTA-E ***
DELTAK=C(1)*Z(1)+C(2)*Z(2)
DELTAE=C(3)*Z(1)+C(4)*Z(2)
EK=EK+DELTAK
ENUL=ENUL+DELTAE
WRITE(2,650) ICONT,EK,ENUL
650 FORMAT(1H ,10X,"CYCLE...",I2,5X,"K=",1PE15.6,2X,"E-NUL=",1PE15.
IF(ICONT.EQ.12) GOTO 700
GOTO 600
700 CONTINUE
SEK=SQRT(ABS(SUM(6)/SUM(1)*(Z1-2.0)))
SEE=SQRT(ABS(SUM(6)/SUM(3)*(Z1-2.0)))
PEK=SEK*100.0/EK
PEE=SEE*100.0/ENUL

```

```

WRITE(2,670) PEK,PEE
670 FORMAT(1H,10X,"% ERROR K=",1PE15.6,2X,"% ERROR E=",1PE15.6)
WRITE(2,675) EK
675 FORMAT(1H0,10X,"EQUILIBRIUM CONSTANT=",1PE15.6)
WRITE(2,680) ENUL
680 FORMAT(1H0,10X,"EXTINCTION COEFFT. OF PRODUCT=",1PE15.6,
$2X,"(AT THIS WAVELENGTH)")
RETURN
END
SUBROUTINE KCALC
COMMON/ONE/N,CELLVOL,CL,CNU,VCLNU(100),CONCNU(100),OD(100),
$ODINF,TITLE(5),EK,CONST,Z1,ODC,ODC(100),CLC(100),
$ENUL,PEK,PEE,M1
C ***** CALCULATES K FOR A GIVEN DATA POINT,GIVEN ODINF(OR E-NUL
ODINF=CLC(M1)*ENUL
RK=(CONCNU(M1)*(ODINF-OD(M1)))/(OD(M1)-ODC)-
$(CLC(M1)*(ODINF-OD(M1)))/(ODINF-ODC)
CONST=1.0/RK
RETURN
END
FUNCTION ODCALC(VOL)
COMMON/ONE/N,CELLVOL,CL,CNU,VCLNU(100),CONCNU(100),OD(100),
$ODINF,TITLE(5),EK,CONST,Z1,ODC,ODC(100),CLC(100),
$ENUL,PEK,PEE,M1
C *** CALCULATES O.D. FOR A GIVEN VOL ADDED GIVEN K AND E-NUL
RK=1.0/EK
CL2=CL*CELLVOL/(CELLVOL+1.0E-3*VOL)
ODINF=ENUL*CL2
V=1.0E-6*VOL*CNU/(1.0E-3*CELLVOL+1.0E-6*VOL)
B=-1.0*(V+CL2+RK)
C=(ODINF-ODC)*V
A=CL2/(ODINF-ODC)
B2M4AC=B*B-4.0*A*C
ODCALC=-B-SQRT(B2M4AC)
ODCALC=ODCALC/(2.0*A)
ODCALC=ODCALC+ODC
RETURN
END

```

APPENDIX 4

ALBERY-ROBINSON ANALYSIS PROGRAM

The least squares calculation is performed by the NAG library routine EO4HFF. The program calculates the quantities required by this routine.

Subroutine DATA reads in rate constant vs. temperature data, with appropriate headings and reference.

Subroutines XYPLOT, YLIM and XLIM are general purpose plotting routines.

Subroutine CALG is the main subroutine. Initial estimates of the a-parameters are supplied, and routine EO4HFF is entered. On successful exit from this routine, the data has been fitted satisfactorily and the least-squares a-parameters are used to generate calculated rate constants, and derived enthalpy and heat capacity quantities. The temperature dependence of these quantities is displayed by the plotting routines.

Subroutines LSFUN2 and LSHES2 generate arrays required by EO4HFF. LSFUN2 evaluates a vector containing values of the residuals and the Jacobian matrix of their first derivatives. LSHES2 evaluates an array which incorporates the second derivatives.

```

PROGRAM MJ3CG2 (OUTPUT, TAPE5, TAPE6=OUTPUT)
*****
* THE ALBERRY MODEL.
*****
COMMON/MIKE/RK(80),TK(80),TC(80),N
*****
* DATA INPUT FROM DATA FILE :-
*MJ3XXX WHERE XXX IS A THREE DIGIT NUMBER.
*****
COMMON/SID/XDUM(100),ZALPHA(100)
CALL PAPER(1)
CALL GPSTOP(10)
CALL HEAD
CALL DATA
CALL CALG
CALL GRENC
WRITE(6,10)
10  FORMAT(1H0, 10X,*THAT IS ALL FOLK*S*)
END
SUBROUTINE HEAD
WRITE(6,10)
10  FORMAT(1H1,20X,*ANALYSIS OF KINETIC DATA*)
WRITE(6,20)
20  FORMAT(1HC,10X,*MICHAEL J.BLANDAMER*)
WRITE(6,30)
30  FORMAT(1H0,30X,*UNIVERSITY OF LEICESTER,ENGLAND*)
RETURN
END
SUBROUTINE DATA
COMMON/MIKE/RK(80),TK(80),TC(80),N
*****
* READS DATA TAPE=MJ3XXX
* FORMATS ARE :-
* I3=DATA SET
* SA(5)=NAME OF SOLUTE
* SB(5)=NAME OF INVESTIGATOR
* SC(5)=REFERENCE
* IM=0; REACTION IN WATER
* IM=1 : REACTION IN D2O
* IM=2; MIXED SOLVENT SYSTEM.
* SD(5)=NAME OF CO-SOLVENT
* XD=MOLE FRACTION OF CO-SOLVENT:F6.0
* N=NUMBER OF DATA POINTS: I3
* RK( )=RATE CONSTANT
* AT TEMPERATURE=TC /CELSIUS
*****
DIMENSION SA(10)
READ(5,10) ISET
10  FORMAT(I4)
WRITE(6,20) ISET
20  FORMAT(1H ,10X,*DATA SET NUMBER=*,I4)
READ(5,30) (SA(I),I=1,5)
30  FORMAT(5A10)
WRITE(6,40) (SA(I),I=1,5)
40  FORMAT(1H0,10X,*SUBSTRATE:*,5X,5(A10))
READ(5,50) (SA(I),I=1,5)
50  FORMAT(5A10)
WRITE(6,60) (SA(I),I=1,5)
60  FORMAT(1HC,10X,*AUTHOR:*,5X,5(A10))
READ(5,70) (SA(I),I=1,5)
70  FORMAT(5A10)
WRITE(6,80) (SA(I),I=1,5)
80  FORMAT(1H ,10X,*REFERENCE:*,5(A10))
READ(5,90) IM
90  FORMAT(I1)
IF(IM.EQ.0) GOTO 100
IF(IM.EQ.1) WRITE(6,91)
91  FORMAT(1H ,10X,*SOLVENT ---- DEUTERIUM OXIDE*)
IF(IM.EQ.1) GOTO 140
CONTINUE
READ(5,110) (SA(I),I=1,5)
110  FORMAT(5A10)
WRITE(6,120) (SA(I),I=1,5)
120  FORMAT(1H ,10X,*SOLVENT---WATER*,5(A10))
READ(5,130) XD
130  FORMAT(F6.0)
WRITE(6,135) XD
135  FORMAT(1H ,10X,*MOLE FRACTION OF CO-SOLVENT=*,3X,1PE15.6)
GOTO 140
CONTINUE
WRITE(6,150)
150  FORMAT(1H ,10X,*SOLVENT ---- WATER*)
140  CONTINUE
READ(5,161) ICONI
161  FORMAT(I1)

```

```

READ(5,160) N
IF(N.EQ.0) WRITE(6,164)
IF(N.EQ.0) GOTO 201
IF(N.EQ.1) GOTO 201
IF(ICONT.EQ.1) WRITE(6,162)
162 FORMAT(1H,10X,*AVERAGED RATE CONSTANTS*)
IF(ICONT.EQ.0) WRITE(6,163)
163 FORMAT(1H,10X,*INDIVIDUAL RATE CONSTANTS*)
160 FORMAT(I3)
164 FORMAT(1H,5X,*NO RATE CONSTANTS AVAILABLE*)
WRITE(6,170) N
170 FORMAT(1H+,40X,*NUMBER OF DATA POINTS=*,I3)
WRITE(6,180)
180 FORMAT(1H,5X,*INPUT TEMPERATURES IN CELSIUS: CONVERTED TO*
$* KELVIN WHERE TK=TC+273.15*)
WRITE(6,190)
190 FORMAT(1H,26X,*TEMPERATURE*,13X,*RATE CONSTANT*)
WRITE(6,195)
195 FORMAT(1H,18X,*CELSIUS*,10X,*KELVIN*,12X,*S -1*)
DO 200 I=1,N
  READ(5,210) TC(I)
210 FORMAT(F7.0)
  TK(I)=TC(I)+273.15
  READ(5,220) RK(I)
220 FORMAT(F8.0)
  WRITE(6,230) I,TC(I),TK(I),RK(I)
230 FORMAT(1H,10X,I3,2X,1PE14.5,2X,1PE13.5,3X,1PE13.4)
200 CONTINUE
201 CONTINUE
RETURN
END
SUBROUTINE XYPLOT(N,XX,YY,ICONT,Z)
DIMENSION Z(100)
DIMENSION XX(210),YY(210)
K=N
  XMAX=XX(1)
  XMIN=XMAX
  YMAX=YY(1)
  YMIN=YMAX
  DO 40 I=1,K
    IF(XMAX.LT.XX(I)) XMAX=XX(I)
    IF(YMAX.LT.YY(I)) YMAX=YY(I)
    IF(YMIN.GT.YY(I)) YMIN=YY(I)
    IF(XMIN.GT.XX(I)) XMIN=XX(I)
40 CONTINUE
  CALL YLIM(XMAX)
  CALL YLIM(YMAX)
  CALL XLIM(XMIN)
  CALL XLIM(YMIN)
  IF(ICONT.EQ.6) YMIN=0.0
  IF(ICONT.EQ.6) YMAX=1.25*YMAX
  CALL WINDOW(XMIN,XMAX,YMIN,YMAX)
  CALL PSPACE(0.1,0.95,0.1,0.95)
  CALL MAP(XMIN,XMAX,YMIN,YMAX)
  CALL BORDER
  CALL SCALES
  DO 50 M=1,K
    CALL POINT(XX(M),YY(M))
50 CONTINUE
  IF(ICONT.NE.1) GOTO 100
  DO 60 I=1,K
    Y1=YY(I)+Z(I)
    Y2=YY(I)-Z(I)
    CALL POINT(XX(I),Y1)
    CALL JOIN(XX(I),Y2)
60 CONTINUE
100 CONTINUE
RETURN
END
SUBROUTINE YLIM(X)
IF(X.LE.0.0) GOTO 10
X=X+(X/20.0)
GOTO 20
10 X=ABS(X)
X=X-(X/20.0)
X=-X
20 CONTINUE
RETURN
END
SUBROUTINE XLIM(X)
IF(X.LE.0.0) GOTO 10
X=X-(X/20.0)
GOTO 20
10 X=ABS(X)
X=X+(X/20.0)

```

```

20 X=-X
CONTINUE
RETURN
END
SUBROUTINE CALG
COMMON/SIC/XDUM(100),ZALPHA(100)
COMMON/MIKE/RK(80),TK(80),TC(80),N
DIMENSION XX(4),W(3000),IWW(4)
DIMENSION RKC(100),FK1(100),ALPHA(100)
*****
* NON-LINEAR LEAST SQ.
*****
NX=N
ICOUNT=0
IFAIL=1
WRITE(6,5)
5 FORMAT(1H0,25X,*NON-LINEAR LEAST SQ.*)
DO 21 I=1,4
XX(I)=1.0
21 CONTINUE
M=4
WRITE(6,30)
30 FORMAT(1H ,10X,*INITIAL ESTIMATES*)
XX(2)=1.40
XX(3)=3.252
XX(4)=3.476
I=N/2
RKM=RK(I)
TKM=TK(I)
X1=1.0+(1.0E5*XX(3)*EXP(-1.0E3*XX(4)/TKM))
X2=PKM/(1.0E18*EXP(-1.0E4*XX(2)/TKM))
XX(1)=X1*X2
DO 40 I=1,4
WRITE(6,50) I,XX(I)
50 FORMAT(1H ,10X,*NUMBER*,I3,2X,*ESTIMATE=*,1PE15.6)
40 CONTINUE
333 CONTINUE
GOTO 334
CALL EQ4GCF(NX,M,XX,FSUMSQ,IWW,4,W,3000,IFAIL)
GOTO 61
334 CONTINUE
IFAIL=1
CALL EQ4HFF(NX,M,XX,FSUMSQ,IWW,4,W,3000,IFAIL)
ICOUNT=ICOUNT+1
61 CONTINUE
WRITE(6,60) IFAIL
60 FORMAT(1H ,5X,*ERROR TEST=*,I4)
CONTINUE
WRITE(6,70)
70 FORMAT(1H ,20X,*ANALYSIS COMPLETE*)
WRITE(6,737) FSUMSQ
737 FORMAT(1H ,5X,*SUM OF SQUARES=*,1PE15.6)
CONTINUE
DO 80 I=1,4
WRITE(6,90) I,XX(I)
90 FORMAT(1H ,10X,*PARAMETER*,I3,2X,*=*,1PE15.6)
80 CONTINUE
IF(ICOUNT.EQ.16) GOTO 335
IF(IFAIL.NE.0) GOTO 333
335 CONTINUE
RG=8.31434
EA1=1.0E4*RG*XX(2)
EA2=-1.0E3*RG*XX(4)
SUM=0.0
DO 100 I=1,N
RK1(I)=1.0E18*XX(1)*EXP(-1.0E4*XX(2)/TK(I))
ALPHA(I)=XX(3)*1.0E5*EXP(-1.0E+3*XX(4)/TK(I))
RKC(I)=RK1(I)/(1.0+ALPHA(I))
ZALPHA(I)=RK(I)-RKC(I)
SUM=SUM+(ZALPHA(I)**2)
100 CONTINUE
WRITE(6,140)
140 FORMAT(1H ,25X,*COMPARISON OF INPUT AND OUTPUT*)
WRITE(6,210) EA1
210 FORMAT(1H ,5X,*ACTIVATION ENERGY FOR K1=*,1PE15.6)
WRITE(6,202) EA2
202 FORMAT(1H ,5X,*ACTIVATION ENERGY FOR ALPHA=*,1PE15.6)
IF(XX(3).LT.0.0) GOTO 211
AP=1.0E3*XX(4)/ALOG(1.0E5*XX(3))
WRITE(6,209) AP
209 FORMAT(1H ,5X,*ALPHA=1.0 AT T=*,1PE15.6)
211 CONTINUE
WRITE(6,150)
150 FORMAT(1H ,19X,*TEMPERATURE*,5X,*RATE CONSTANT*,6X,
S*CALCULATED*,5X,*DIFFERENCE*,6X,*% DIFF.*)

```

```

DO 160 IW=1,N
XP=100.0*ZALPHA(IW)/RK(IW)
WRITE(6,170) IW,TK(IW),RK(IW),RKC(IW),ZALPHA(IW),
$XP
170 FORMAT(1H ,10X,I3,5(2X,1PE15.6))
160 CONTINUE
SUM=SQRT(SUM/(N-1))
WRITE(6,180) SUM
IF (XX(3).LT.0.0) GOTO 999
180 FORMAT(1H ,10X,*STANDARD DEVIATION ON RATE CONST=*,1PE15.6)
WRITE(6,200)
200 FORMAT(1H ,20X,*CONTRIBUTING PARAMETERS*)
WRITE(6,230)
230 FORMAT(1H ,18X,*TEMPERATURE*,6X,*RATE CONSTANT*,
510X,*K1*,10X,*ALPHA*,10X,*APP. DCP*)
DO 220 IY=1,N
XP=- (EA2**2)*ALPHA(IY)/
#((1.0+ALPHA(IY))**2*RG*TK(IY)**2)
WRITE(6,233) IY,TK(IY),RK(IY),RK1(IY),ALPHA(IY),XP
233 FORMAT(1H ,10X,I3,5(2X,1PE15.6))
RK(IY)=ALOG10(RK(IY))
RK1(IY)=ALOG10(RK1(IY))
ALPHA(IY)=ALOG10(ALPHA(IY))
220 CONTINUE
CALL XYPLOT(N,TK,RK,0,E)
CALL PLACE(1,1)
CALL TYPECS("ALOG10(K-OBS) AGAINST TEMPERATURE",33)
CALL FRAME
CALL XYPLOT(N,TK,RK1,0,E)
CALL PLACE(1,1)
CALL TYPECS("ALOG10(K1) AGAINST TEMPERATURE",30)
CALL FRAME
CALL XYPLOT(N,TK,ALPHA,0,E)
CALL PLACE(1,1)
CALL TYPECS("ALOG10(ALPHA) AGAINST TEMPERATURE",33)
CALL FRAME
CALL XYPLOT(N,TK,ZALPHA,0,E)
CALL PLACE(1,1)
CALL TYPECS("RESIDUALS AGAINST TEMPERATURE",30)
TX=100.0
WRITE(6,701)
701 FORMAT(1H ,16X,*TEMPERATURE*,9X,*ALPHA*,13X,
3*APPARENT DELTA CP*)
DO 700 I=1,100
IX=TX+5.0
ZALPHA(I)=TX
ALPHA(I)=XX(3)*1.0E5*EXP(-1.0E3*XX(4)/TX)
TKM=ALPHA(I)/((1.0+ALPHA(I))**2)
RK(I)=- (EA2**2)*TKM/(RG*TX**2)
WRITE(6,710) I,IX,ALPHA(I),RK(I)
710 FORMAT(1H ,8X,I3,3(2X,1PE15.6))
700 CONTINUE
CALL FRAME
CALL XYPLOT(100,ZALPHA,ALPHA,0,E)
CALL PLACE(1,1)
CALL TYPECS("LOG10(ALPHA) AGAINST TEMPERATURE",40)
CALL FRAME
CALL XYPLOT(100,ZALPHA,RK,0,E)
CALL PLACE(1,1)
CALL TYPECS("APP.DELTA CP AGAINST TEMPERATURE",40)
999 CONTINUE
RETURN
END
SUBROUTINE LSFUN2(M,N,XC,FVECC,FJACC,LJC)
DIMENSION XC(N),FVECC(M),FJACC(LJC,N)
COMMON/SID/XDUM(100),ZALPHA(100)
COMMON/MIKE/RK(80),TK(80),TC(80),NX
DO 10 I=1,M
A2=EXP(-1.0E4*XC(2)/TK(I))
A3=1.0+(XC(3)*1.0E5*EXP(-1.0E3*XC(4)/TK(I)))
A4=EXP(-1.0E3*XC(4)/TK(I))
A23=A2/A3
A43=A4/A3
FVECC(I)=(1.0E18*XC(1)*A23)-RK(I)
FJACC(I,1)=1.0E18*A23
FJACC(I,2)=-1.0E22*XC(1)*A23/TK(I)
FJACC(I,3)=-1.0E23*XC(1)*A23*A43
FJACC(I,4)=+1.0E26*XC(1)*XC(3)*A23*A43/TK(I)
10 CONTINUE
RETURN
END
SUBROUTINE LSHES2(M,N,FVECC,XC,B,LB)
DIMENSION FVECC(M),XC(N),B(LB)
COMMON/SID/XDUM(100),ZALPHA(100)

```

```

COMMON/MIKE/RK(80),TK(80),TC(80),NX
DO 10 I=1,LB
B(I)=0.0
CONTINUE
10 DO 20 I=1,M
A2=EXP(-1.0E4*XC(2)/TK(I))
A3=1.0+(XC(3)*1.0E5*EXP(-1.0E3*XC(4)/TK(I)))
A4=EXP(-1.0E3*XC(4)/TK(I))
A23=A2/A3
A43=A4/A3
B(2)=B(2)-(FVECC(I)*A23*1.0E22/TK(I))
B(3)=B(3)+(FVECC(I)*XC(1)*A23*1.0E26/(TK(I)**2))
B(4)=B(4)-(1.0E23*A23*A43*FVECC(I))
B(5)=B(5)+(FVECC(I)*XC(1)*A23*A43*1.0E27/TK(I))
B(6)=B(6)+(FVECC(I)*2.0*XC(1)*A23*A43*A43*1.0E28)
B(7)=B(7)+(FVECC(I)*XC(3)*A23*A43*1.0E26/TK(I))
B(8)=B(8)-(FVECC(I)*XC(1)*XC(3)*A23*A43*1.0E30/(
$TK(I)**2))
B(9)=B(9)+(FVECC(I)*XC(1)*A23*A43*1.0E26*(1.0-(XC(3)
#*1.0E5*A4))/(A3*TK(I)))
B(10)=B(10)-(FVECC(I)*XC(1)*XC(3)*A23*A43*1.0E29*(1.0
$(XC(3)*1.0E5*A4))/(A3*(TK(I)**2)))
20 CONTINUE
RETURN
END

```

APPENDIX 5

GURNEY EQUATION PROGRAM

As with the Albery-Robinson analysis, the least squares calculation is performed by NAG library routine EO4HFF.

The data is supplied from subroutines which convert temperatures to degrees Kelvin where necessary.

Subroutine GURN supplies initial estimates for the three parameters, and EO4HFF is entered. On successful data-fitting, various contributing parameters are calculated.

Subroutines XYPLOT, XLIM and YLIM are plotting routines. Subroutines LSFUN2 and LSRES2 generate arrays incorporating the residuals with their first and second derivatives, as required by EO4HFF.

```

PROGRAM MJ3EQ2(OUTPUT,TAPE6=OUTPUT,TAPE7)
*****
* ANALYSIS OF EQUILIBRIUM DATA.
*****
COMMON/MIKE/RK(30),TK(30),TC(30),N
COMMON/SIG/DUM(30),ZALPHA(30)
CALL PAPER(1)
CALL HEAD
CALL GPSTOP(300)
  IDATA=3
CALL DATA(IDATA)
CALL GURN(IDATA)
WRITE(6,10)
10  FORMAT(1H0,5X,*THAT IS ALL FOLK*S*)
CALL GREND
END
SUBROUTINE XYPLOT(N,XX,YY,TMD,Z)
DIMENSION Z(50)
DIMENSION XX(30),YY(30)
K=N
  XMAX=XX(1)
  XMIN=XMAX
  YMAX=YY(1)
  YMIN=YMAX
DO 40 I=1,K
  IF(XMAX.LT.XX(I)) XMAX=XX(I)
  IF(YMAX.LT.YY(I)) YMAX=YY(I)
  IF(YMIN.GT.YY(I)) YMIN=YY(I)
  IF(XMIN.GT.XX(I)) XMIN=XX(I)
40  CONTINUE
CALL YLIM(XMAX)
CALL YLIM(YMAX)
CALL XLIM(XMIN)
CALL XLIM(YMIN)
CALL WINDOW(XMIN,XMAX,YMIN,YMAX)
CALL PSPACE(0.1,0.95,0.1,0.95)
CALL MAP(XMIN,XMAX,YMIN,YMAX)
CALL BORDER
CALL SCALES
DO 50 M=1,K
  CALL POINT(XX(M),YY(M))
50  CONTINUE
RETURN
END
SUBROUTINE YLIM(X)
IF(X.LE.0.0) GOTO 10
X=X+(X/20.0)
GOTO 20
10  X=ABS(X)
X=X-(X/20.0)
X=-X
20  CONTINUE
RETURN
END
SUBROUTINE XLIM(X)
IF(X.LE.0.0) GOTO 10
X=X-(X/20.0)
GOTO 20
10  X=ABS(X)
X=X+(X/20.0)
X=-X
20  CONTINUE
RETURN
END
SUBROUTINE GURN(IDATA)
COMMON/MIKE/RK(30),TK(30),TC(30),N
*****
* GURNEY EQUATION.
*****
DIMENSION XX(3),W(3000),IWW(3),ZALPHA(50)
DIMENSION ALPHA(50),YC(50)
DIMENSION WX(50)
WRITE(6,15)
15  FORMAT(1H0,20X,*ANALYSIS USING GURNEY EQUATION*)
NX=N
ICOUNT=0
IFAIL=1
RG=8.31434
  XX(1)=1.0
  XX(2)=1.0
  XX(3)=1.0
  M=3
DO 25 I=1,N
  RK(I)=ALOG(RK(I))
25  CONTINUE

```

```

338 CONTINUE
IFAIL=1
CALL E04HFF(NX,M,XX,FSUMSQ,IWW,3,W,3000,IFAIL)
ICOUNT=ICOUNT+1
WRITE(6,20) IFAIL
20 FORMAT(1H,20X,*IFAIL TEST=*,I4)
DO 30 I=1,3
WRITE(6,40) I,XX(I)
40 FORMAT(1H,5X,*PARAMETER*,I3,*=*,1PE15.6)
30 CONTINUE
IF(ICOUNT.EQ.10) GOTO 337
IF(IFAIL.NE.0) GOTO 338
337 CONTINUE
WRITE(6,50)
50 FORMAT(1H,25X,*ANALYSIS COMPLETE*)
WRITE(6,739) FSUMSQ
739 FORMAT(1H,3X,*SUM OF SQUARES=*,1PE15.6)
THETA=1.0E3/XX(3)
WRITE(6,60) THETA
60 FORMAT(1H,10X,*GURNEY THETA=*,1PE15.6)
WRITE(6,61)
61 FORMAT(1H,10X,*COMPARE GURNEY'S THETA,219 K*)
GC=1.0E3*XX(2)
WRITE(6,70) GC
70 FORMAT(1H,10X,*GURNEY C-VALUE=*,1PE15.6)
GA=XX(1)/XX(2)
WRITE(6,80) GA
80 FORMAT(1H,10X,*GURNEY A-VALUE=*,1PE15.6)
WRITE(6,200)
200 FORMAT(1H,10X,*CONTRIBUTING PARAMETERS*)
WRITE(6,210)
210 FORMAT(1H,11X,*TEMPERATURE*,5X,*LN(K*,
$* OBS*,10X,*LN(K-CALC)*,10X,*DIFF*,10X,*%DIFF*)
S=0.0
DO 220 IY=1,N
YC(IY)=(-XX(1)*1.0E3/TK(IY))-((XX(2)*1.0E3/T
*K(IY))*EXP(TK(IY)*1.0E-3*XX(3)))
ALPHA(IY)=RK(IY)-YC(IY)
WX(IY)=100.0*ALPHA(IY)/RK(IY)
S=S+(ALPHA(IY)**2)
WRITE(6,230) IY,TK(IY),RK(IY),YC(IY),ALPHA(IY),WX(IY)
230 FORMAT(1H,5X,I3,5(2X,1PE15.6))
220 CONTINUE
S=SQRT(S/(N-1))
WRITE(6,8013) S
8013 FORMAT(1H,10X,*ST.DEV.ON LN(K)=*,1PE15.6)
CALL XYPLCT(N,TK,RK,0,E)
CALL PLACE(1,1)
CALL TYPEPCS("LN(K-OBS) AGAINST TEMPERATURE",30)
CALL FRAME
CALL XYPLCT(N,TK,YC,0,E)
CALL PLACE(1,1)
CALL TYPEPCS("LN(K-CALC) AGAINST TEMPERATURE",30)
CALL FRAME
CALL XYPLCT(N,TK,ALPHA,0,E)
CALL PLACE(1,1)
CALL TYPEPCS("RESIDUALS AGAINST TEMPERATURE",30)
CALL FRAME
CALL XYPLCT(N,TK,WX,0,E)
CALL PLACE(1,1)
CALL TYPEPCS("% RESIDUALS AGAINST TEMPERATURE",40)
CALL FRAME
WRITE(6,5005)
5005 FORMAT(1H0,10X,*1ST TERM*,10X,*2ND TERM*,10X,
$* TOTAL *)
DO 5003 I=1,N
ALPHA(I)=-((EXP(TK(I)*1.0E-3*XX(3)))/TK(I)
ALPHA(I)=ALPHA(I)*XX(2)*1.0E3
ZALPHA(I)=-1.0E3*XX(1)/TK(I)
TC(I)=ZALPHA(I)+ALPHA(I)
WRITE(6,5007) I,ZALPHA(I),ALPHA(I),TC(I)
5007 FORMAT(1H,3X,I3,3(2X,1PE15.6))
5003 CONTINUE
CALL XYPLCT(N,TK,ALPHA,0,E)
CALL PLACE(1,1)
CALL TYPEPCS("SECOND TERM ON TEMP",30)
CALL FRAME
CALL XYPLCT(N,TK,ZALPHA,0,E)
CALL PLACE(1,1)
CALL TYPEPCS("1ST TERM ON TEMP",20)
CALL FRAME
CALL XYPLCT(N,TK,TC,0,E)
CALL PLACE(1,1)
CALL TYPEPCS("TOTAL ON TEMP",30)
CALL FRAME

```

```

610 WRITE(6,610)
    FORMAT(1H ,14X,*GIBBS* FUNCTION CONTRIBS.*)
620 WRITE(6,620)
    FORMAT(1H ,10X,*TEMP*,10X,*NON-ELECT.*,10X,*ELECT*)
    DO 630 I=1,N
    XN=RG*GA*GC
    XE=RG*GC*EXP(TK(I)/THETA)
640 WRITE(6,640) TK(I),XN,XE
630 FORMAT(1H ,3(2X,1PE15.6))
CONTINUE
RETURN
END
SUBROUTINE LSFUN2(M,N,XC,FVECC,FJACC,LJC)
COMMON/MIKE/RK(30),TK(30),TC(30),NX
COMMON/SIC/DUM(30),ZALPHA(30)
DIMENSION XC(N),FVECC(M),FJACC(LJC,N)
DO 10 I=1,M
X1=1.0E3/TK(I)
X2=EXP(XC(3)*1.0E-3*TK(I))
FJACC(I,1)=-X1
FJACC(I,2)=-X1*X2
FJACC(I,3)=-XC(2)*X2
FVECC(I)=(-XC(1)*X1)-((XC(2)*X1*X2)-RK(I))
DUM(I)=FVECC(I)
10 CONTINUE
END
SUBROUTINE LSHES2(M,N,FVECC,XC,B,LB)
DIMENSION FVECC(M),XC(N),B(LB)
COMMON/MIKE/RK(30),TK(30),TC(30),NX
COMMON/SIC/DUM(30),ZALPHA(30)
B(1)=0.0
B(2)=0.0
B(3)=0.0
B(4)=0.0
SUM1=0.0
SUM2=0.0
DO 10 I=1,M
X1=FVECC(I)*EXP(XC(3)*1.0E-3*TK(I))
SUM1=SUM1-X1
SUM2=SUM2-(X1*1.0E-3*XC(2)*TK(I))
10 CONTINUE
B(5)=SUM1
B(6)=SUM2
RETURN
END

SUBROUTINE HEAD
*****
* GENERAL HEADING.
*****
10 WRITE(6,10)
    FORMAT(1H1,20X,*ANALYSIS OF DEPENDENCE ON TEMPERATURE*,
    $* OF EQUILIBRIUM CONSTANTS*)
20 WRITE(6,20)
    FORMAT(1H ,10X,*MICHAEL J.BLANDAMER P.P.DUCE *)
30 WRITE(6,30)
    FORMAT(1H ,15X,*UNIVERSITY OF LEICESTER*)
RETURN
END
SUBROUTINE DATA(IDATA)
COMMON/MIKE/RK(30),TK(30),TC(30),N
*****
C * ASSEMBLES DATA FOR ANALYSIS.
C * DATA INPUT ACCORDING TO CODE NUMBER FROM ROUTINE:
C * NOW SEND INPUT INFORMATION TO CORRECT PART OF THIS SUBROUTIN
C *****
10 WRITE(6,10)
    FORMAT(1H0,20X,*DATA*)
IF(IDATA.EQ.1) CALL COVH2O
IF(IDATA.EQ.2) CALL MJBFIVE
IF(IDATA.EQ.3) CALL HAC
IF(IDATA.EQ.4) CALL HAD4
IF(IDATA.EQ.5) CALL D2O
IF(IDATA.EQ.6) CALL FORM
IF(IDATA.EQ.7) CALL DISOP
IF(IDATA.EQ.8) CALL HAD3
IF(IDATA.EQ.9) CALL TRIS
IF(IDATA.EQ.10) CALL TRISB
IF(IDATA.EQ.11) CALL FLHAC
IF(IDATA.EQ.12) CALL BRHA
IF(IDATA.EQ.13) CALL IHAC
IF(IDATA.EQ.14) CALL CLHAC
IF(IDATA.EQ.15) CALL PROP
IF(IDATA.EQ.16) CALL BUTY
IF(IDATA.EQ.17) CALL DMECY

```

```

      IF(IDATA.EQ.18) CALL ISOPCY
      IF(IDATA.EQ.19) CALL HAD20
C *****
C *NOW RETURNED WITH INFORMATION IN ARRAYS EK,TC AND TK.
C *****
      WRITE(6,80)
      WRITE(7,805)
805  FORMAT(1H ,*$READ$*)
80   FORMAT(1H0,16X,*TEMPERATURE*)
      WRITE(6,85)
85   FORMAT(1H ,8X,*CELSIUS*,10X,*KELVIN*,11X,
      $EQUILIBRIUM CONSTANT*,5X,*PK*)
      DO 60 I=1,N
      WRITE(7,801) TK(I)
801  FORMAT(1H ,F10.4)
      WRITE(7,803) RK(I)
803  FORMAT(1H ,F12.9)
      CONTINUE
      ZK=-ALOG10(RK(I))
      WRITE(6,70) I,TC(I),TK(I),RK(I),ZK
70   FORMAT(1H ,I3,2X,1PE15.6,2X,1PE15.6,2X,1PE15.6,8X,1PE15.6)
60   CONTINUE
      WRITE(7,809)
809  FORMAT(1H ,*$RETURN$*)
      RETURN
      END

```

APPENDIX 6

GRUNWALD-WINSTEIN ANALYSIS

This method of relating changes in rate constant of a substitution reaction to changes in solvent composition makes use of the known rate constants for solvolysis of t-butyl chloride in a wide range of pure and mixed solvents.

A given solvent or solvent mixture is characterized by a Y-value, defined as follows:

$$Y = \log \left(\frac{k^{\text{BuCl}}}{k_0^{\text{BuCl}}} \right) \quad (\text{i})$$

k_0^{BuCl} = rate constant for solvolysis at 25°C in
80% ethanol : 20% water.

k^{BuCl} = rate constant for solvolysis at 25°C in
the given solvent.

A plot of the logarithmic values of rate constants of the reaction being studied against the appropriate Y-values give a straight line of the form

$$\log k = mY + \log k_0 \quad (\text{ii})$$

where m and $\log k_0$ are parameters. Deviations from linearity occur if k represents more than one mechanistic pathway. The correlation is best when the reaction under study is a simple dissociation, especially when chloride is the leaving group as in the reference reaction.

The value of m for the reference reaction is 1.00 by definition. The m -values for inorganic substitution reactions are invariably less than 1.00 showing them to be less sensitive to solvent variation than reaction at the carbon centre.

REFERENCES

CHAPTER 1 - REFERENCES

- (1) 'Water - A Comprehensive Treatise', ed. F. Franks, Plenum Press, 1972 - 1981.
- (2) H. S. Frank and W.-Y. Wen, Disc. Faraday Soc., 24, 133 (1957).
- (3) H. Taube and H. Myers, J. Amer. Chem. Soc., 76, 2103 (1954).
- (4) S. Glasstone, K. J. Laidler and H. Eyring, 'The Theory of Rate Processes', McGraw-Hill, New York, 1941;
P. J. Robinson, J. Chem. Ed., 55, 509 (1978).
- (5) A. Ben-Naim, J. Phys. Chem., 82, 792 (1978).
- (6) R. A. Robinson and R. H. Stokes, 'Electrolyte Solutions', Butterworths, London, 1968, 2nd. edn. (revised).
- (7) C. F. Wells, J. Chem. Soc. Faraday I, 69, 984 (1973).
- (8) C. F. Wells, J. Chem. Soc. Faraday I, 74, 636 (1978).
- (9) C. F. Wells, J. Chem. Soc. Faraday I, 70, 694 (1974).
- (10) C. F. Wells, J. Chem. Soc. Faraday I, 72, 601 (1976).
- (11) C. F. Wells, J. Chem. Soc. Faraday I, 71, 1686 (1975).
- (12) C. F. Wells, J. Chem. Soc. Faraday I, 74, 1596 (1978).
- (13) C. F. Wells, J. Chem. Soc. Faraday I, 77, 1515 (1981).
- (14) D. Bax, C. L. de Ligny and M. Alfenaar, Rec. Trav. Chim., 91, 452 (1972).
- (15) M. H. Abraham, J. Chem. Soc. Faraday I, 1375 (1973).
- (16) B. G. Cox, Ann. Rep. Chem. Soc. (A), 249 (1974).
- (17) B. G. Cox, R. Natarjan and W. E. Waghorne, J. Chem. Soc. Faraday I, 75, 1780 (1979).
- (18) O. Popovych and A. J. Dill, Analyt. Chem., 41, 456 (1969).
- (19) H. J. M. Neidermeijer-Denessen and C. L. de Ligny, J. Electroanal. Chem. Interface Electrochem., 57, 265 (1974);
M. Alfenaar, J. Phys. Chem., 79, 2200 (1979) and refs. therein.
- (20) O. Duschek and V. Gutmann, Monatsch. Chem., 104, 1254 (1973) and refs. therein.
- (21) B. Case and R. Parsons, Trans. Faraday Soc., 63, 1224 (1967).
- (22) R. Parsons and B. T. Rufin, J. Chem. Soc. Faraday I, 70, 1636 (1974).
- (23) H. P. Bennetto and D. Feakins in 'Hydrogen-bonded solvent systems', eds. A. K. Covington and P. Jones, Taylor & Francis Ltd., London, 1968.
- (24) H. Schneider, Topics in Current Chemistry, 68, 103 (1976).
- (25) Y. Marcus, E. Pross and J. Hormadaly, J. Phys. Chem., 84, 2708 (1980).
- (26) R. D. Present, J. Chem. Phys., 31, 747 (1959).
- (27) J. Ross and P. Mazur, J. Chem. Phys., 35, 19 (1961).

- (28) R. W. Gurney, 'Ionic Processes in Solution', McGraw-Hill, New York, 1953.
- (29) A. J. Parker, Chem. Rev., 69, 1 (1969).
- (30) W. J. Louw, Inorg. Chem., 16, 2147 (1977).
- (31) I. Prigogine and R. Defay, 'Chemical Thermodynamics', trans. D. H. Everett, Longmans, London.
- (32) C. K. Ingold, 'Structure and Mechanism in Organic Chemistry', G. Bell, London, 1953.
- (33) E. M. Arnett, W. G. Bentrude and P. McC. Duggleby, J. Amer. Chem. Soc., 87, 2048 (1965) and refs. therein.
- (34) S. J. Dickson and J. B. Hyne, Can. J. Chem., 49, 2394 (1971).
- (35) Ref. 29.
- (36) M. H. Abraham, Chem. Comm., 1307 (1969).
- (37) M. H. Abraham, J. Chem. Soc. (A), 1061 (1971).
- (38) M. H. Abraham, J. Chem. Soc. Perkin II, 1343 (1972).
- (39) M. J. Blandamer, J. Burgess and J. G. Chambers, J. Chem. Soc. Dalton, 60 (1977).
- (40) M. J. Blandamer, J. Burgess and S. J. Hamshere, J. Chem. Soc. Dalton, 1539 (1979).
- (41) M. J. Blandamer, J. Burgess and A. J. Duffield, J. Chem. Soc. Dalton, 1 (1980).
- (42) M. J. Blandamer, J. Burgess and R. I. Haines, J. Chem. Soc. Dalton, 607 (1980).
- (43) M. J. Blandamer, J. Burgess, S. J. Hamshere, C. White, R. I. Haines and A. McAuley, submitted to Can. J. Chem.
- (44) M. J. Blandamer, J. Burgess, P. P. Duce and R. I. Haines, J. Chem. Soc. Dalton, 2442 (1980).
- (45) M. J. Blandamer, J. Burgess and R. I. Haines, J. Chem. Soc. Chem. Comm., 963 (1978).

CHAPTER 2 - REFERENCES

- (1) F. Sicilio and M. D. Peterson, J. Chem. Ed., 38, 576 (1961).
- (2) P. G. Wellings, Ph.D. Thesis, University of Leicester, 1981.
- (3) P. Moore, J. Chem. Soc. Faraday I, 68, 1890 (1972).
- (4) E. A. Guggenheim, Phil. Mag., 2, 538 (1926).
- (5) N. W. Alcock, D. J. Benton and P. Moore, Trans. Faraday Soc., 66, 2210 (1970).

CHAPTER 3 - REFERENCES

- (1) M. J. Blandamer, J. Burgess, P. P. Duce and R. I. Haines, J. Chem. Soc. Dalton, 2442 (1980).
- (2) M. J. Blandamer, J. Burgess and R. I. Haines, J. Chem. Soc. Chem. Comm., 963 (1978).
- (3) M. J. Blandamer, J. Burgess, S. J. Hamshere, C. White, R. I. Haines and A. McAuley, submitted to Can. J. Chem.
- (4) L. C. W. Baker and T. P. McCutcheon, J. Amer. Chem. Soc., 78, 4503 (1956).
- (5) Z. Amjad, J.-C. Brodovitch and A. McAuley, Can. J. Chem., 55, 3581 (1977).
- (6) R. A. Marens, J. Phys. Chem., 72, 891 (1968);
E. Pelizzetti, E. Mentaski and E. Pramauro, Inorg. Chem., 15, 2898 (1976).
- (7) J.-C. Brodovitch, R. I. Haines, A. McAuley and J. Sherwood, unpublished results.
- (8) J. Burgess and R. H. Prince, J. Chem. Soc. A, 2111 (1970).
- (9) J. Burgess and A. McAuley (Eds.), 'Inorganic Reaction Mechanisms', Chem. Soc. Specialist Periodical Report, London, 2, 127 (1972); 3, 142 (1974); 5, 158 (1977); 6, 168 (1979).
- (10) D. L. Kepert and J. H. Kyle, J. Chem. Soc. Dalton, 137 (1978).
- (11) J. Burgess, J. Chem. Soc. A, 2571 (1968).
- (12) J. Burgess, J. Chem. Soc. A, 2351 (1970).
- (13) C. F. Wells, J. Chem. Soc. Faraday I, 69, 984 (1973).
- (14) C. L. de Ligny and M. Alfenaar, Rec. Trav. Chim., 84, 81 (1965).
- (15) B. G. Cox, R. Natarajan and W. E. Waghorne, J. Chem. Soc. Faraday I, 75, 86 (1979).
- (16) B. G. Cox, R. Natarajan and W. E. Waghorne, J. Chem. Soc. Faraday I, 75, 1780 (1979).
- (17) B. G. Cox, Ann. Rep. Chem. Soc., 71A, 249 (1974).
- (18) M. T. Beck, Coord. Chem. Rev., 3, 91 (1968).
- (19) M. S. Subhani, Rev. Roum. Chim., 23, 719 (1978).
- (20) E. Grunwald and S. Winstein, J. Amer. Chem. Soc., 70, 846 (1948);
P. R. Wells, 'Linear Free Energy Relationships', Academic Press, London, 1968, Chapter 4; see Appendix 6.
- (21) For example,
J. Burgess, J. Chem. Soc. Dalton, 825 (1973);
L. A. P. Kane-Maguire and G. Thomas, *ibid.*, 1890 (1975);
V. V. Udovenko, L. G. Reiter and I. Beran, Russ. J. Inorg. Chem., 22, 168 (1977).
- (22) H. Taube and H. Myers, J. Amer. Chem. Soc., 76, 2103 (1954).
- (23) J. P. Candlin and J. Halpern, Inorg. Chem., 4, 1086 (1965).

- (24) J. H. Espenson, *Inorg. Chem.*, 4, 121 (1965).
- (25) S. Suvachittanont, *J. Sci. Soc. Thailand*, 3, 118 (1977).
- (26) G. G. Schlessinger, *Inorg. Synth.*, 9, 160 (1967).
- (27) M. J. Blandamer and J. Burgess, *Inorg. Chim. Acta*, 64, L113 (1982).
- (28) M. J. Blandamer, J. Burgess and R. I. Haines, *J. Chem. Soc. Dalton*, 607 (1980).
- (29) M. H. Abraham, personal communication.
- (30) R. Koren, *J. Inorg. Nucl. Chem.*, 36, 2341 (1974).
- (31) B. A. Matthews and D. W. Watts, *Aust. J. Chem.*, 29, 97 (1976).
- (32) K. Ohashi, T. Amano and K. Yamamoto, *Inorg. Chem.*, 16, 3364 (1977).
- (33) J. Barrett and J. H. Baxendale, *Trans. Faraday Soc.*, 52, 210 (1956).

CHAPTER 4 - REFERENCES

- (1) For example,
P. Moore, *Inorg. React. Mechanisms*, 5, 184 (1977); 6, 198 (1979);
7, 179 (1981).
- (2) V. V. Tatarchuk and A. V. Belyaev, *Koord. Khim.*, 4, 1059 (1978).
- (3) M. J. Blandamer, J. Burgess and R. I. Haines, *J. Chem. Soc. Dalton*, 607 (1980).
- (4) J. Burgess and A. J. Duffield, *J. Inorg. Nucl. Chem.*, 42, 1531 (1980).
- (5) R. D. Gillard, personal communication.
- (6) S. N. Anderson and F. Basolo, *Inorg. Synth.*, 7, 217 (1963).
- (7) R. D. Gillard and G. Wilkinson, *J. Chem. Soc.*, 3193 (1963).
- (8) O. T. Christensen, *Z. Anorg. Chem.*, 4, 229 (1893);
M. Mori, *Inorg. Synth.*, 5, 132 (1957).
- (9) J. Springborg and C. E. Schäffer, *Inorg. Synth.*, 18, 75 (1978).
- (10) J. Burgess, K. W. Bowker, E. R. Gardner and F. M. Mekhail,
J. Inorg. Nucl. Chem., 41, 1215 (1979).
- (11) A. Ogard and H. Taube, *J. Amer. Chem. Soc.*, 80, 1084 (1958);
W. A. Levine, T. P. Jones, W. E. Harris and W. J. Wallace, *ibid.*,
83, 2453 (1961);
L. Mønsted and O. Mønsted, *Acta Chem. Scand.*, 28A, 569 (1974).
- (12) D. W. Hoppenjans, J. B. Hunt and C. R. Gregoire, *Inorg. Chem.*, 7,
2506 (1968).
- (13) L. Mønsted and O. Mønsted, *Acta Chem. Scand.*, 28A, 23 (1974).
- (14) W. W. Fee, W. G. Jackson and P. D. Vowles, *Austral. J. Chem.*,
25, 459 (1972).
- (15) For example,
P. R. Adby and M. A. H. Dempster, 'Introduction to Optimization
Methods', Chapman & Hall, London (1974).
- (16) R. I. Haines, Ph.D. Thesis, Leicester University 1977.
- (17) B. G. Cox, R. Natarajan and W. E. Waghorne, *J. Chem. Soc. Faraday I*,
75, 86 (1979).
- (18) For example,
E. Grunwald and S. Winstein, *J. Amer. Chem. Soc.*, 70, 846 (1948);
P. R. Wells, *Chem. Rev.*, 63, 171 (1963).
- (19) J. Burgess and M. G. Price, *J. Chem. Soc. A*, 3108 (1971).
- (20) J. Burgess and A. J. Duffield, unpublished observation.
- (21) D. A. Buckingham, I. I. Olsen and A. M. Sargeson, *Inorg. Chem.*,
6, 1807 (1967).
- (22) For example,
F. Basolo, W. R. Matoush and R. G. Pearson, *J. Amer. Chem. Soc.*,
78, 4833 (1956);
A. E. Gebala and M. M. Jones, *J. Inorg. Nucl. Chem.*, 31, 771 (1969).

- (23) A. Haim, J. Amer. Chem. Soc., 88, 2324 (1966).
- (24) M. J. Blandamer, J. Burgess and S. J. Hamshere, Trans. Met. Chem., 4, 291 (1979).
- (25) E. M. Strel'tsova, N. K. Markova and G. A. Krestov, Russ. J. Phys. Chem., 48, 992 (1974).
- (26) For example,
N. Al-Shatti, T. Ramasami and A. G. Sykes, J. Chem. Soc. Dalton, 74 (1977) and refs. therein.
- (27) D. A. Palmer, R. van Eldik, T. P. Dasgupta and H. Kelm, Inorg. Chim. Acta, 34, 91 (1979).
- (28) J. H. Espenson and S. R. Hubbard, Inorg. Chem., 5, 686 (1966).
- (29) N. Ise, M. Ishikawa, Y. Taniguchi and K. Suzuki, Polymer Lett., 14, 667 (1976).
- (30) O. Popovych and A. J. Dill, Analyt. Chem., 41, 456 (1969).
- (31) C. F. Wells, J. Chem. Soc. Faraday I, 69, 984 (1973).
- (32) M. H. Abraham, personal communication.
- (33) For example,
G. Wittig, G. Keicher, A. Rückert and P. Raff, Annalen, 563, 110 (1949);
J. N. Cooper and R. E. Powell, J. Amer. Chem. Soc., 85, 1590 (1963);
G. Baum, J. Organomet. Chem., 22, 269 (1970).
- (34) A. Seidell, Solubilities of Inorganic and Metal Organic Compounds, 3rd. edn., Vol. 1, Van Nostrand, New York (1940), p.444.
- ³⁶ (35) S. N. Choi and D. W. Carlyle, Inorg. Chem., 11, 1718 (1972).

(15) J. Burgess, J. Chem. Soc. Dalton, 825 (1973)

CHAPTER 5 - REFERENCES

- (1) For example,
'Inorganic Reaction Mechanisms', ed. J. Burgess, Chem. Soc. Specialist Periodical Report, London, Vol. 1, p.176 (1971); Vol. 2, p.168 (1972);
C. H. Langford and V. S. Sastri, 'Reaction Mechanisms in Inorganic Chemistry', ed. M. L. Tobe, M.T.P. Internat. Rev. Sci., Vol. 9, Butterworths, London, Series 1, p.252 (1971) and refs. therein.
- (2) J. Burgess and R. H. Prince, J. Chem. Soc., 4697 (1965).
- (3) R. D. Gillard, Inorg. Chim. Acta, 11, L21 (1974); Coord. Chem. Rev., 16, 67 (1975).
- (4) D. W. Margerum and L. P. Morgenthaler, J. Amer. Chem. Soc., 84, 706 (1962).
- (5) J. Burgess, Inorg. Chim. Acta, 9, 133 (1971).
- (6) R. D. Gillard, L. A. P. Kane-Maguire and P. A. Williams, Transition Metal Chem., 2, 12 (1977).
- (7) J. A. Arce Sagües, R. D. Gillard and P. A. Williams, Inorg. Chim. Acta, 36, L411 (1979) and refs. therein.
- (8) R. D. Gillard, C. T. Hughes and P. A. Williams, Transition Metal Chem., 1, 51 (1976).
- (9) R. D. Gillard, C. T. Hughes, L. A. P. Kane-Maguire and P. A. Williams, Transition Metal Chem., 1, 226 (1976);
R. D. Gillard, L. A. P. Kane-Maguire and P. A. Williams, J. Chem. Soc. Dalton, 1039 (1977).
- (10) J. Burgess and R. I. Haines, J. Chem. Soc. Dalton, 1447 (1978).
- (11) R. D. Gillard and P. A. Williams, Transition Metal Chem., 2, 247 (1977).
- (12) J. Burgess, J. Chem. Soc. A, 431 (1967).
- (13) L. L. Stookey, Analyt. Chem., 42, 779 (1970).
- (14) E. R. Gardner, F. M. Mekhail, J. Burgess and J. M. Rankin, J. Chem. Soc. Dalton, 1340 (1973).
- (15) M. J. Blandamer, J. Burgess and P. G. Wellings, Transition Metal Chem., 4, 95 (1979).
- (16) C. F. Wells, J. Chem. Soc. Faraday I, 69, 984 (1973).
- (17) G. Nord and T. Pizzino, Chem. Comm., 1633 (1970).
- (18) M. J. Blandamer, J. Burgess and P. G. Wellings, Transition Metal Chem., 6, 364 (1981).
- (19) G. Brauer, ed. 'Handbook of Preparative Inorganic Chemistry', Vol. II, 2nd. edn., Academic Press, London (1965), p.1360.
- (20) J. Springborg and C. K. Schäffer, Inorg. Synth., 18; 81; 88 (1978).
- (21) M. J. Blandamer, J. Burgess, M. V. Twigg and P. G. Wellings, Transition Metal Chem., 6, 129 (1981).

- (22) G. L. Traister and A. A. Schilt, *Analyt. Chem.*, 48, 1216 (1976).
- (23) H. A. Bonesi and J. H. Hildebrand, *J. Amer. Chem. Soc.*, 71, 2703 (1949).
- (24) N. J. Rose and R. S. Drago, *J. Amer. Chem. Soc.*, 81, 6138 (1959).
- (25) R. D. Gillard, R. P. Houghton and J. N. Tucker, *J. Chem. Soc. Dalton*, 2102 (1980).

CHAPTER 6 - REFERENCES

- (1) A. D. Pethybridge and J. E. Prue in 'Inorganic Reaction Mechanisms', Part II, ed. J. O. Edwards, Wiley-Interscience, New York (1972).
- (2) H. S. Frank and W.-Y. Wen, Disc. Faraday Soc., 24, 133 (1957); R. A. Robinson and R. H. Stokes, 'Electrolyte Solutions', 2nd. edn. revised, Butterworths (1968), p.15.
- (3) B. Perlmutter-Hayman, Prog. Reaction Kinetics, 6, 239 (1971).
- (4) E. S. Halberstadt and J. E. Prue, J. Chem. Soc., 2234 (1952).
- (5) M. J. Blandamer, J. Burgess and S. H. Morris, J. Chem. Soc. Dalton, 1717 (1974).
- (6) M. J. Blandamer, J. Burgess and S. H. Morris, J. Chem. Soc. Dalton, 2118 (1975).
- (7) N. F. Ashford, M. J. Blandamer, J. Burgess, D. Laycock, M. Waters, P. Wellings, R. Woodhead and F. M. Mekhail, J. Chem. Soc. Dalton, 1 (1979).
- (8) M. J. Blandamer, J. Burgess and D. L. Roberts, J. Chem. Res., (M) 3872, (S) 326 (1977).
- (9) J. Burgess, Annu. Rep. Chem. Soc., 63, 130 (1966); 66, 411 (1969) and refs. therein.
- (10) M. J. Blandamer, J. Burgess and S. J. Hamshere, J. Chem. Soc. Dalton, 1539 (1979).
- (11) W. H. Baddley and F. Basolo, J. Amer. Chem. Soc., 88, 2944 (1966).
- (12) S. J. Hamshere, Ph.D. Thesis, University of Leicester 1980.
- (13) M. J. Blandamer, J. Burgess and S. J. Hamshere, J. Chem. Soc. Dalton, 1539 (1979).
- (14) G. B. Kaufmann, Inorg. Synth., 7, 249 (1963).
- (15) J. Setchenow, Z. Phys. Chem., 4, 117 (1889); Ann. Chim., 25, 226 (1896).
- (16) M. J. Blandamer, J. Burgess and J. C. McGowan, J. Chem. Soc. Dalton, 616 (1980).
- (17) A. I. Vogel, 'A Textbook of Quantitative Inorganic Analysis', 3rd. edn., Longmans, London, pp.462-4, 466 (1962).
- (18) J. Burgess, I. Haigh and R. D. Peacock, J. Chem. Soc. Dalton, 1062 (1974).
- (19) R. Rychly and V. Pekarek, J. Chem. Thermodynamics, 9, 391 (1977).
- (20) G. A. Clarke and R. W. Taft, J. Amer. Chem. Soc., 84, 2295 (1962).
- (21) M. J. Blandamer, J. Burgess, P. P. Duce, A. J. Duffield and S. J. Hamshere, Transition Metal Chem., 6, 368 (1981).
- (22) G. Schlessinger, Inorg. Synth., 6; 182, 191 (1960).

CHAPTER 7 - REFERENCES

- (1) E. A. Moelwyn-Hughes, R. E. Robertson and S. Sugamori, J. Chem. Soc., 1965 (1965).
- (2) R. E. Robertson, Prog. Phys. Org. Chem., 4, 213 (1967).
- (3) S. Valentiner, Z. Phys. Chem., 42, 853 (1907).
- (4) M. J. Blandamer, Adv. Phys. Org. Chem., 14, 203 (1977).
- (5) W. J. Albery and B. H. Robinson, Trans. Faraday Soc., 65, 980 (1969).
- (6) R. E. Robertson and J. M. W. Scott, Can. J. Chem., 50, 167 (1972).
- (7) R. E. Robertson and J. G. Martin, J. Amer. Chem. Soc., 88, 5353 (1966).
- (8) R. E. Robertson and S. E. Sugamori, J. Amer. Chem. Soc., 91, 7254 (1969).
- (9) R. E. Robertson and S. E. Sugamori, Can. J. Chem., 50, 1353 (1972).
- (10) L. Hakka, A. Queen and R. E. Robertson, J. Amer. Chem. Soc., 87, 161 (1965).
- (11) M. J. Blandamer, R. E. Robertson and J. M. W. Scott, Can. J. Chem., 58, 772 (1980).
- (12) M. J. Blandamer, R. E. Robertson, J. M. W. Scott and A. Vrieling, J. Amer. Chem. Soc., 102, 2585 (1980).
- (13) E. M. Arnett, W. G. Bentrude, J. J. Burke and P. McC. Duggleby, J. Amer. Chem. Soc., 87, 1541 (1965).
- (14) P. R. Adby and M. A. H. Dempster, 'Introduction to Optimisation Methods', Chapman & Hall, London (1974).
- (15) N. W. Alcock, D. J. Benton and P. Moore, Trans. Faraday Soc., 66, 2210 (1970).
- (16) A. H. Fainberg and S. Winstein, J. Amer. Chem. Soc., 79, 5937 (1957).

CHAPTER 8 - REFERENCES

- (1) E. J. King, 'Acid-base Equilibria', Academic Press, New York, Chapter 8 (1965).
- (2) R. W. Gurney, 'Ionic Processes in Solution', McGraw-Hill, New York (1953).
- (3) P. R. Adby and M. A. H. Dempster, 'Introduction to Optimisation Methods', Chapman & Hall, London (1974).
- (4) S. Valentiner, Z. Physik. Chem., 42, 853 (1907).
- (5) E. C. W. Clark and D. N. Glew, Trans. Faraday Soc., 64, 539 (1966).
- (6) H. S. Harned and R. W. Ehlers, J. Amer. Chem. Soc., 55, 652 (1933).
- (7) M. Paabo, R. G. Bates and R. A. Robinson, J. Phys. Chem., 70, 540 (1966).
- (8) H. S. Harned and N. D. Embree, J. Amer. Chem. Soc., 56, 1042 (1934).
- (9) H. S. Harned and R. W. Ehlers, J. Amer. Chem. Soc., 55, 2379 (1933).
- (10) D. H. Everett, D. A. Landsman and B. R. W. Pinsent, Proc. Roy. Soc. A, 215, 403 (1952).
- (11) F. A. Feates and D. J. G. Ives, J. Chem. Soc., 2798 (1956).
- (12) D. J. G. Ives and P. G. N. Moseley, J. Chem. Soc. B, 1656 (1970).
- (13) D. J. G. Ives and P. D. Marsden, J. Chem. Soc., 649 (1965).
- (14) D. J. G. Ives and J. H. Pryor, J. Chem. Soc., 2104 (1955).
- (15) A. K. Covington, M. I. A. Ferra and R. A. Robinson, J. Chem. Soc. Faraday I, 73, 1721 (1977).
- (16) R. S. Gary, R. G. Bates and R. A. Robinson, J. Phys. Chem., 70, 2073 (1966).
- (17) A. K. Covington, R. A. Robinson and R. G. Bates, J. Phys. Chem., 70, 3820 (1966).
- (18) M. Eigen, Angew. Chem., Int. Ed. Engl., 3, 1 (1964).
- (19) M. J. Blandamer, R. E. Robertson and J. M. W. Scott, J. Chem. Soc. Perkin II, 447 (1981).
- (20) J. E. Leffler and E. Grunwald, 'Rate and Equilibria of Organic Reactions', Wiley, New York (1963).
- (21) L. P. Hammett, 'Physical Organic Chemistry', McGraw-Hill, New York, 2nd. edn., p.354 (1970).
- (22) C. S. Leung and E. Grunwald, J. Phys. Chem., 74, 687 (1970).
- (23) M. Eigen and K. Tamm, Z. Elektrochem., 66, 93, 107 (1962).
- (24) R. J. Matthews and J. W. Moore, Inorg. Chim. Acta, 6, 359 (1972).
- (25) R. D. Cannon, 'Electron Transfer Reactions', Butterworths, London, pp.124-131 (1980).

KINETICS AND EQUILIBRIA IN AQUEOUS MEDIA

Philip P. Duce

Rate and equilibrium constants for chemical systems involving two-stage processes in aqueous media have been measured and analysed. The major part of this thesis discusses the effect of added organic cosolvents or salts on the reaction kinetics of transition metal complexes in solution. The thesis also includes an analysis of published rate and equilibrium data in order to derive thermodynamic activation and reaction parameters.

The oxidation of iodide by the 12-tungstocobaltate(III) anion by an outer-sphere process, of iron(II) by the chloropentamine cobalt(III) cation by an inner-sphere process, and the mercury(II)-catalysed aquation of some rhodium(III) and chromium(III) chloro-complexes have been studied in binary aqueous mixtures.

The aquation of the N,N,N'',N'' tetraethyldiethylenetriamine-chloro palladium(II) cation and the reaction of cis-bis-(4-cyanopyridine) dichloro platinum(II) with thiourea have been studied in aqueous salt solutions.

For the above reactions, it has been possible to dissect the effects of solvent variation or added salt on the rate constants into their initial state and transition state contributions. This has been done by estimating the change in the chemical potential of the initial state from appropriate solubility measurements. The results obtained are discussed in terms of the solvation characteristics of the species involved.

The reactions of two anionic iron(II) tris-diimine complexes with hydroxide and cyanide in aqueous media have been studied. Kinetic and spectroscopic evidence for intermediates is reported.

With regard to computer-based studies, the temperature dependence of the rate constant for solvolysis of t-butyl chloride in binary aqueous mixtures has been analysed in terms of the two-stage Albery-Robinson mechanism. The derived enthalpies and heat capacities of activation are examined.

The temperature dependence of acid dissociation constants has been analysed using the Gurney equation and the two-stage Eigen mechanism.